OPTIMAL DESIGN AND CONTROL OF THREE-PHASE INDUCTION MOTOR

A THESIS

*Submitted in partial fulfilment of the
requirements for the award of the degree
of*
DOCTOR OF PHILOSOPHY
in
ELECTRICAL ENGINEERING

by

THANGA RAJ C

DEPARTMENT OF ELECTRICAL ENGINEERING
INDIAN INSTITUTE OF TECHNOLOGY ROORKEE
ROORKEE - 247 667 (INDIA)
JULY, 2009

INDIAN INSTITUTE OF TECHNOLOGY ROORKEE
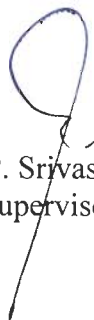## ROORKEE

CANDIDATE'S DECLARATION

I hereby certify that the work which is being presented in this thesis entitled **OPTIMAL DESIGN AND CONTROL OF THREE-PHASE INDUCTION MOTOR** in partial fulfilment of the requirements for the award of *the Degree of Doctor of Philosophy* and submitted in the Department of Electrical Engineering of Indian Institute of Technology Roorkee, Roorkee is an authentic record of my own work carried out during a period from January 2006 to July 2009 under the supervision of Dr. Pramod Agarwal and Dr. S. P Srivastava, Professors, Department of Electrical Engineering, Indian Institute of Technology Roorkee, Roorkee.

The matter presented in this thesis has not been submitted by me for the award of any other degree of this or any other Institution.

(THANGA RAJ C)

This is to certify that the above statement made by the candidate is correct to the best of my knowledge.

Date: July 09, 2009

(S. P. Srivastava)
Supervisor

(Pramod Agarwal)
Supervisor

The Ph.D. Viva-Voce Examination of **Mr. Thanga Raj C**, Research Scholar, has been held on................

Signature of Supervisors

Signature of External Examiner

Abstract

Nowadays, the main concern of policy makers across the world is global warming due to the emission of CO_2 in the atmosphere and researchers have an important role to play in this regard. Furthermore, India is facing severe energy shortage eventhough the installed capacity of Indian power sector is increasing continuously. To mitigate the shortages, Government of India has set a goal "Mission 2012: Power for All' and one of its objectives is optimal utilization of electrical energy. The energy shortage in India is due to the inefficiencies in power generation, distribution and end use system. Economical and more practical method to limit the energy shortage is "energy conservation", particularly for industrial consumers who account for more than 50 percent of the total energy consumption. In end use systems, the induction motor can be considered as one of the largest consumers of electrical energy due to its well known advantageous including robustness, reliability, low price and maintenance free operation. The induction motors are used in both industrial and commercial sectors in a wide range of applications, such as fans, compressors, pumps, conveyors, winders, mills, transports, elevators, home appliances and office equipments. The influence of these motors (in terms of energy consumption) in energy intensive industries is significant in total input cost. A small increment in the efficiency of these motors by providing better control or optimum design can result in substantial saving in the long period.

Induction motor is a high efficiency electrical machine when working closed to its rated torque and speed. However, at light loads, imbalance in copper and iron losses, results considerable reduction in its efficiency. The part-load efficiency and power factor can be improved by making the motor excitation adjustment in accordance with load and speed. To achieve this objective, the induction motor should either be fed through an inverter or redesigned with optimization algorithms. The research in the present work is carried out both in optimal design and control of induction motor to achieve maximum efficiency or minimum operating cost.

The optimization of induction motor design with Artificial Intelligence (AI) and Nature Inspired Algorithms (NIA) has received considerable attention recently. The optimized design of a three-phase induction motor can be obtained by using standard non-linear programming techniques. But these techniques are computationally very expensive and inefficient whereas NIA is competent tool to solve non-linear programming problems. Different NIA based optimization algorithms for induction motor design have been reported in literature. Particle

i

Swarm Optimization (PSO) technique has become very popular since last decade to solve multi dimension non linear programming problems due to its less complexity, fast convergence, etc., than Genetic Algorithm and Evolutionary Programming. Although the rate of convergence of PSO is good due to fast information flow among the solution vectors, its diversity decreases very quickly in the successive iterations resulting in a suboptimal solution. Aiming at this shortcoming of PSO algorithms, many variations have been developed by the researchers to improve its performance. Improved version of PSO called Quadratic Interpolation based Particle Swarm Optimization (QIPSO) is used in the present work which gave better results than reported in the literature in terms of fitness value. SPEED/IMD (Scottish Power Electronics and Electric Drives), a motor design software is used to validate the optimization algorithms in induction motor design.

Moreover, many researchers have focused their research on efficiency optimization of induction motors that are working in industries through optimal flux control. In optimal flux control, there are three main approaches to improve the induction motor efficiency at light loads, namely loss model controller (LMC), search controller and hybrid controller (retain good features of loss model and search control by mixing them). Since the induction motor is a large consumer of electrical energy in the industries and its influence is more in energy intensive industries, it is required to focus industrial loads. Economic analysis of some of the industrial loads such as textile and mining industries are carried out in the present work. To maintain good stability (minimum torque ripples and less overshoots in speed) of the motor during flux adjustment, Fuzzy Pre-compensated Proportional Integral (FPPI) controller is used.

A comprehensive literature survey on the induction motor drives, design of materials during construction and efficient control of part-load machine, is carried out in the present work. Common sources affecting induction motor efficiency and their solutions to improve it are discussed in brief. An experimental study is investigated on induction motor with unbalance voltages to study the negative effects of it on motor's efficiency. Economic losses due to voltage unbalance are determined and the available potential of efficiency improvement opportunities in the industrial sectors is discussed.

Induction motor design optimization is carried out in the present work with the help of QIPSO algorithms and explored its superiority in comparison with normal design, Rosenbrock, basic PSO and Simulated Annealing (SA) methods. The design of the induction motors includes determination of geometry and data required for manufacturing the machine so as to satisfy the vector of performance variables together with a set of constraints. Optimal design of

motors refers to ways of doing efficiently synthesis by repeated analysis such that the objective function is maximized or minimized while all constraints are satisfied. There are large number of design parameters involved in the design of the induction machine. Selection of objective functions, variables and constraints are the main steps. The proper optimization of induction motor design is achieved by intelligent selection of objective function and constraints according to the requirement, and further selection of variables which affect the objective function and the constraints. Material cost, efficiency, starting torque, temperature rise and operating cost are taken as objective functions and nine performance indices as constraints. The design variables which are most sensitive to the objective functions have been judiciously chosen. They are: ampere conductors, ratio of stack length to pole pitch, stator slot depth to width ratio, stator core depth, average air gap flux densities, stator winding current density, and rotor winding current density. The objective functions and constraints are expressed in terms of the above variables.

The effectiveness of PSO and QIPSO in terms of variable and constraint values selection is realized by using SPEED software. By using the ranging function of SPEED, effect of various design parameters are plotted against the objective function and some of the constraints. The performance based optimal design of induction motor is also carried out to reduce the required number of variables to design the motor. To achieve this, motor design is carried out by QIPSO algorithm with seven variables. The design realization is then done by SPEED software and selects minimum variables which are affecting the performance of the motor in depth. Again the motor is optimized by QIPSO with reduced variables.

In practice, induction motors experience unbalanced terminal voltage when fed from power supply and subjected to harmonics when fed through inverter. It results increased losses due to time harmonics/negative sequence currents. These losses reduce motor's life and hence, derating must be applied to avoid the damages. Moreover, to ensure consistent, efficient and reliable operation of motors, accounting unbalanced stator voltage and harmonics in supply, optimized design of the motor receives considerable attention from industry. The present work investigates the performance and design of the induction motor under both unbalance and harmonics in the supply. For unbalance voltage consideration, positive and negative sequence currents are derived and incorporated in the motor design. For inverter supply, harmonic currents are derived from the equivalent circuit and use them as additional constraint so that motor design is carried out with limited harmonics.

For optimal energy control of induction motor, flux level in a machine is adjusted to give minimum operating cost for the industrial load. The flux controller improves the economics in terms of operating cost (energy cost and demand charge cost) and the test results show that the flux level in the most economic motor is adjusted according to load and speed, particularly at light load. PSO is utilized to calculate optimal flux when LMC is considered and ramp search method is used to decrement the flux when search controller is considered. Hybrid controller is designed by mixing both LMC and search controller.

At any operating point of induction motor characterized by the speed and torque, an optimal flux (in other words, optimal ratio of voltage and frequency) can be found that meets the requirement of the operating point and minimizes the overall losses. To implement LMC, induction motor loss model is developed and optimal value of flux is obtained to give maximum efficiency of the motor. Maximum and minimum levels of flux and stator currents are forced as constraints in the algorithm. In search control method, which does not require the knowledge of the motor loss model, DC link or input power of the machine drive is measured regularly at fixed interval and optimal flux producing current or flux value is searched which results in minimum power input or stator current of the motor for the given values of speed and torque. Once the DC link power is minimized the adjustment of flux is stopped and the current flux is maintained. Hybrid controller is also used to retain good features of individual controllers, while eliminating their major drawbacks. By this hybrid controller, slow convergence (drawback of search control) and parameter variation (drawback of LMC) due to saturation and temperature variations are eliminated and good results are obtained with rough knowledge of parameters. To increase the stability of the motor drive during flux changes at variable speed and load operation, Fuzzy Pre-compensated Proportional Integral Controller is used and compared its results with conventional Proportional Integral (PI) controller. Fuzzy pre-compensation means that the reference speed signal is altered in advance using Fuzzy Logic in accordance with the rotor speed, so that a new reference speed signal is obtained which helps to improve dynamic performance of the motor. The combination of PSO and FPPI results in improved performance of the motor compared with conventional controllers. In order to illustrate the importance of efficiency optimized controllers in industries, a medium scale textile industry is considered for economic analysis.

To summarize, the loss models of scalar and vector controlled induction motor are derived with the consideration of saturation effects. The broad approaches of induction motor loss minimization, namely loss model, search and hybrid controller are discussed with the special

attention of their advantages and drawbacks. Design improvements of induction motor by selecting optimal values of variables and constraints using Particle Swarm Optimization and its variant, called QIPSO, are given. Optimized results given by PSO and QIPSO are validated by one of the electrical motor design software named SPEED/IMD and some benchmark problems. The performance based optimal design of induction motor is also carried out and achieved reduction in number of required design variables. Supply voltage unbalance and harmonics are taken into account while designing the motor. A detailed study along with simulation results of induction motor optimization though NIA based efficient control is presented. FPPI controller is used to maintain good stability of the drive when the flux is adjusted. Case study in a medium scale textile industry for economical analysis is also presented. The results of both optimal design and control show excellent performance of the motor with proposed optimization algorithm, in terms of efficiency, operating cost, manufacturing cost, starting torque and temperature rise.

Acknowledgements

(THANGA RAJ C)

CONTENTS

List of Figures

List of Tables

List of Symbols

ω, ω_r	Rotor speed
$\omega_r{}^*$	Speed command or reference speed
ω_b	Base speed
ω_e	Angular frequency of supply voltage
ρ_c	specific resistivity of stator winding material
δ_c	stator winding material density, kg/m^3
δ_i	stamping material density, kg/m^3
θ_{mr}	full load rotor temperature rise, $^\circ C$
θ_{ms}	full load stator temperature rise, $^\circ C$
δ	pre-compensated reference speed
δ_r	rotor winding material density, kg/m^3
ρ_r	specific resistivity of rotor winding material
$\Delta\omega_{re}$	change in speed error
ΔE	difference in objective function values
μ_o	permeability of free space = $4\pi \times 10^{-7}$ Henry/m
μs	Micro second
a	per-unit frequency
a_b	rotor bar area, mm^2
a_e	end ring cross section, mm^2
as	Slip frequency
a_{sc}	total area occupied by the conductors in stator slot, mm^2
a_{sr}	area of rotor slot, mm^2
a_{ss}	area of stator slot, mm^2
AT	total ampere turns
$B_{t(max)}$	maximum tooth flux density, wb/m^2
C_{fw}	Mechanical loss coefficients
D	stator bore diameter, m
D_e	end ring diameter, m
d_{sr}	depth of rotor slot, mm

d_{ss}	depth of stator slot, mm
E	Air-gap voltage
E_m	Peak amplitude of supply phase voltage
E_{ph}	voltage per phase, volts
f	Frequency
f_{rated}	rated frequency
I_d^*	flux producing current command
I_q^*	Current command for torque component
i_{as}, i_{bs}, i_{cs}	Three-phase stator winding currents
I_b	rotr bar current, A
I_c	core loss component of no load current per phase, A
I_D	rotor inner diameter, m
I_e	end ring current, A
I_m	magnetizing current per phase, A
I_o	no load current per phase, A
I_{ph}	rated full load current per phase, A
i_{qs}, i_{ds}	d-axis and q-axis currents respectively
I_r	rotor current
I_s	Stator current
K_1, K_2	switching loss coefficients
K_c	Core coefficient
K_e, K_h	Eddy current and hysteresis coefficients
K_I	Integral gain of PI speed controller
K_P	Proportional gain of PI speed controller
K_{str}	Stray loss coefficient at fundamental frequency
K_w	winding factor
L	gross stack length, m
I_g	radial air gap length, mm
L_i	net core length, m
L_m	magnetizing inductance
L_{mt}	mean length of stator winding turn, m
L_r	rotor inductance

L_s	stator inductance
n_d	number of ventilating ducts
OD	outside diameter of stator core, m
P	number of poles
P_{rs}'	specific rotor slot permeance referred to stator,
P_{loss}	Total losses
P_o	power output, kW
P_{ss}	specific stator slot permeance
R_r'	Rotor resistance
R_m	Core loss resistance
R_{mb}	Core loss resistance at rated frequency and flux
R_s	Stator resistance
S	KVA rating of motor
s	Slip
S_a, S_b, S_c	Magnetizing curve coefficients
S_1	number of stator slots
S_2	number of rotor slots
SCL	full load stator copper loss, W
S_d	cooling surface of two ends of ventilating ducts, m^2
S_f	stator slot fullness factor
S_{fr}	rotor slot fullness factor
S_i	stator inside cylindrical surface area, m^2
SIL	total stator iron loss, W
S_o	stator outside cylindrical surface, m^2
S_s	effective cooling area, m^2
T_{fl}	full load torque
Temp	temperature
T_e^*	Electrical torque command
t_{13}	stator tooth width at one third tooth height from the narrow end, mm
TC_c	cost of winding material
TC_i	total cost of iron
T_e	Developed electrical torque

T_{max}	maximum torque
T_{ph}	stator winding turns per phase
TRT_1	starting to full load torque ratio
TRT_2	maximum to full load torque ratio
t_s	mean stator tooth width
T_{st}	starting torque
V	voltage
V_{as}, V_{bs}, V_{cs}	Three-phase source voltages
V_c	DC link voltage
w	inertia weight
W_c	weight of the stator core, kg
W_d	width of ventilating duct, mm
W_F	friction-windage loss, W
W_r	weight of the rotor iron, kg
W_{RCL}	total copper loss, W
W_{rw}	weight of rotor winding, kg
W_{sw}	weight of stator winding, kg
X'_r	rotor leakage reactance per phase referred to stator, ohm
X_1	total reactance per phase referred to stator side, ohm
X_{ls}	Stator leakage reactance, ohm
X_m	magnetizing reactance per phase, ohm
X_o	overhang leakage reactance per phase, ohm
X_{rs}	rotor slot leakage per phase, ohm
X_s	stator leakage reactance, ohm
X_{ss}	stator slot leakage reactance per phase, ohm
X_z	Zigzag leakage reactance per phase, ohm
Y	pole pitch, m
η	Efficiency
Φ	air-gap flux
Φ_m	maximum air-gap flux
Φ_{rated}	Rated flux
ω_{re}	Sped error

ABBREVIATIONS

AI	Artificial Intelligence
ANN	Artificial Neural Network
ASD	Adjustable Speed Drives
CO_2	Carbon di-oxide
CR	No-load to full load current ratio
EA	Evolutionary Algorithm
EP	Evolutionary Programming
ET	Evolutionary Techniques
FL	Fuzzy Logic
FPPI	Fuzzy Pre-compensated Proportional Integral
GA	Genetic Algorithm
IEC	International Electrotehnical Commission
IEEE	Institution of Electrical and Electronics Engineers
IGBT	Insulated Gate Bi-polar Transistor
IM	Induction Motor
IMD	Induction Motor Drives
ITE	Iteration
IS	Indian Standard
JEC	Japanese Electric Code
kW	Kilo Watt
kWh	Kilo Watt-hour
LMC	Loss Model Control
MMF	Magneto Motive Force
NIAs	Nature Inspired Algorithms
NLP	Non Linear Programming
NTC	No Tooling Cost
PC	Personal Computer
PF	Power Factor
PI	Proportional Integral
PSO	Particle Swarm Optimization
SA	Simulated Annealing

SC	Search Control
SPEED	Scottish Power Electronics and Electric Drives
SPWM	Sinusoidal Pulse Width Modulation
SRF	Stationary Reference Frame
SSRF	Synchronously Rotating Reference Frame
TC	Total active material cost
TC_c	Total Cost of Copper
TC_i	Total Cost of Iron
THD	Total Harmonic Distortion
VSI	Voltage Source Inverter

Introduction and Literature Review

Edison, a famous inventor and industrialist has said that only rich people can use candles in the future which is still a distant reality. Nowadays, the main concern of policy makers across the world is global warming due to the emission of CO_2 in the atmosphere and researchers have an important role to play in this regard. Kyoto protocol, an international agreement between more than 170 countries, has been created to bring down the level of emission of greenhouse gasses (include carbon dioxide, methane and nitrous oxide) to the levels of early 1990s. This agreement provides an opportunity to developing countries like India, China for setting up new eco friendly technologies, thereby earn carbon credits. In the year 2007, the contribution of India to carbon trading was around 20%.

Even though the installed capacity of Indian power sector is increasing continuously, the country is still facing severe energy shortages. To mitigate the shortages, Government of India has set a goal "Mission 2012: Power for All" and its objectives [74] are as follows,

- Sufficient power to achieve GDP growth rate of 8%.
- Reliable of power
- Quality power
- Optimal utilization of electrical energy
- Commercial viability of power industry
- Power for all

The Bureau of Energy Efficiency (BEE) created under the Energy Conservation Act in India which is responsible for taking up both promotional and regulatory function required for successful implementation of energy conservation measures. Bridging the demand-supply gap through capacity addition alone is an expensive option. Therefore, cheaper and more practical solution is the "energy conservation", particularly for industrial consumers who account for more than 50 per cent of the total energy consumption.

The Induction Motor (IM) can be considered the largest consumer of electrical energy due to its well known advantageous including robustness, reliability, low price, maintenance free operation. It is used in both industrial and commercial sectors over a wide range of applications, such as: fans, compressors, pumps, conveyors, winders, mills, transports, elevators, home appliances and office equipments. Pumping systems account for nearly 20% of the world's electrical energy demand and range from 25-50% of the energy usage in

certain industrial applications. The influence of these motors (in terms of energy consumption) in energy intensive industries is significant in total input cost

Induction motors consume around 70% of the electricity used in industries and hence, a small increment in the efficiency of these motors by providing better control or optimum design can result in substantial saving in the long period. Furthermore, increasing oil prices on which electricity and other public utility rates are highly dependent are rapidly increasing. It, therefore, becomes imperative that major attention be paid to the efficiency of induction motors [183].

Induction motor is a high efficiency electrical machine when working closed to its rated torque and speed. However, at light loads, no balance in between copper and iron losses, results considerable reduction in the efficiency. The part-load efficiency and power factor can be improved by adjusting the motor excitation in accordance with load and speed. To implement the above goal, the induction motor should either be fed through an inverter or redesigned with optimization algorithms.

To conserve electrical energy in the industrial sector through a reduction in losses of induction motor, it is particularly interesting to deal with energy intensive industries like textile industry and mine industry. Because textile industries are found to be energy intensive (4% energy cost in total input cost) compared to other industries like chemical, food, computer manufacturing, etc. [122], and hence such industries are considered in the present work to reduce the energy cost and the total input cost.

Apart from optimal control, the induction motor efficiency can also be improved by modifying materials and construction with the help of advanced optimization techniques. Optimum design of induction motor is a non-linear multi dimension problem whereas optimal control is a single or two dimension problems. Therefore the role of optimization techniques is more important in design than control of IM to get global optimum.

This dissertation deals with both the techniques (optimal control and design) to achieve minimum energy losses or maximum efficiency of the induction motor in a wide range of load and speed variations. To complete this goal, induction motor loss model and the load diagrams of textile and mineral industries are collected for optimal control of induction motor. One of the Nature Inspired Algorithms (NIAs), Particle Swarm Optimization (PSO) and its improved version have been developed for optimal design of induction motor with careful selection of variables and constraints.

1.1 Design Optimization of Induction Motor

The optimization of induction motor design with AI and NIA has received considerable attention recently. The design optimization of a three-phase induction motor can be

formulated as a general non-linear programming problem and standard non-linear programming (NLP) techniques can be used to solve it. But these NLP techniques are computationally very expensive and inefficient whereas NIA is competent tool to solve NLP. Extensive work has also been reported in the past on inverter-fed induction motor design in order to minimize torque ripples and harmonic currents.

The digital computer has made this task much simpler than the old techniques (using previous experience of the engineer to select variables and constraints), but even so the number of possible designs is too large that it is not practical to check all the alternatives [152]. Furthermore, optimal control of IM is also essential one because it is not possible to optimize the motor efficiency for every operating point by optimizing machine design.

1.2 Energy Efficient Control of Induction Motor

The first principle of electrical energy conservation through optimal control is: don't need electrical energy in the form of light, heat and others turn it off. The next option is that use energy efficiently in consumer appliances. One of the most common practices contributing to sub-optimal induction motor efficiency is that of partial loading. Under-loading of induction motor is common for several reasons. Original equipment manufacturers tend to use a large safety factor in motors they select. Under-loading of the motor may also occur from under utilization of the equipment. For example, machine tool equipment manufacturers provide for a motor rated for the full capacity load of the equipment example, depth of cut in a lathe machine. The user may need this full capacity rarely, resulting in under-loaded operation most of the time. Another common reason for under loading is selection of a larger motor to enable the output to be maintained at the desired level even when input voltages are abnormally low. Finally, under-loading also results from selecting a large motor for an application requiring high starting torque where a special motor, designed for high torque, would have been suitable [26].

Some industrial examples of induction motor drive with partial load are spinning drive in textile industry, mine-hoist load in mineral industry and pumps in all types of process industries. In these applications, induction motor should operate at reduced flux causes a balance in between iron losses and copper losses results efficiency improvement.

a) Spinning Drive in Textile Industry

A ring spinning frame manufactures the cotton into yarn that is wound on spindles (Fig. 1.1) and used to feed cone winding machine. After that it can be used to make end products such as clothing with the help of weaving machine.
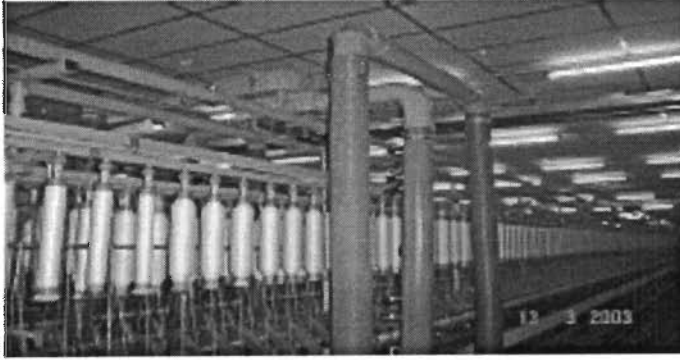
Fig. 1.1 Textile spinning ring frame

The induction motor is employed as main drive with a power rating in the range of 25 kW to 75 kW. The shaft load of motor is depending on the quantity of yarn in the spindles. The quantity of the yarn in the spindles varies from zero (when the process starts) to full (when process completes), hence the motor shaft load varies from zero to rated. Discrete nature of load points is considered for ease of analysis, shown in Fig.1.2. Energy saving potential is mainly available in the motor up to time t_3 from start.
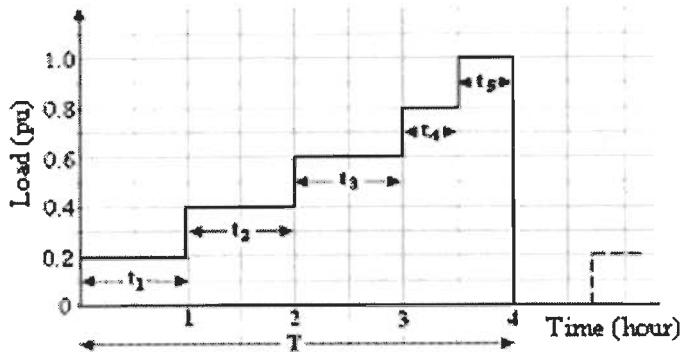
Fig.1.2 Average load diagram of a typical spinning ring frame drive motor

b) Mine Hoist Load

The load diagram of mine hoist in a mineral industry is shown in Fig.1.3 [32]. Region 't_3' of this load diagram offers light load (0.14 pu) and half rated speed of the motor. This dissertation focuses this region for optimal energy control using PSO because the adjustment of flux level is mainly required at lightly loaded condition.
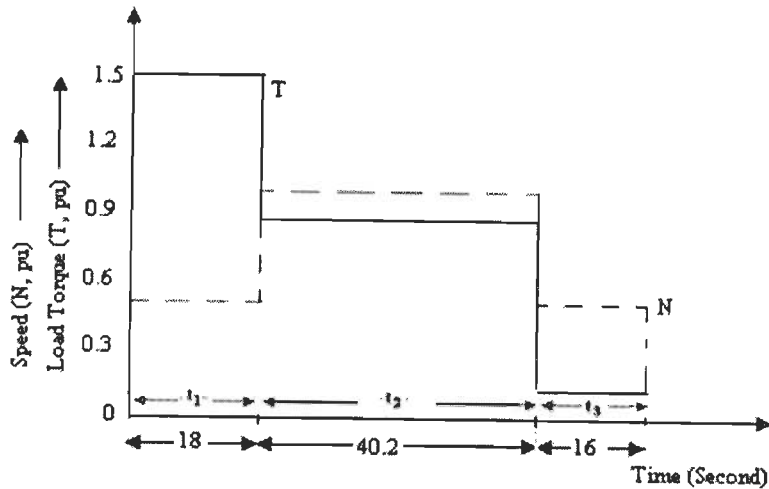
Fig. 1.3 Mine hoist load diagram

c) Energy Saving in Pumps

Pump drives have applications in all the industries and their importance is more in chemical plants, refineries and boilers. Earlier the pumps were run at a constant speed by induction motor and control the fluid flow was obtained by mechanical arrangements such as throttling valve.

Fig. 1.4 [43] shows pump and load characteristics by controlling fluid flow (a) throttling valve and (b) pump speed with the help of Adjustable Speed Drives (ASD). Load curve has two components: one to lift the fluid to the required height and other to overcome friction. The steady state operating point is obtained where the two curves are intersected. The operating point P corresponds to maximum opening of the valve, and therefore, provides maximum flow of fluid.
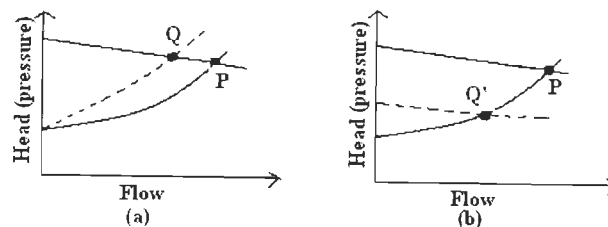
Fig. 1.4 Control of flow in a pump by control of: (a) Valve opening (b) pump speed.

If the fluid flow is controlled by adjusting throttling valve, which added extra resistance in the tube, the friction component is increased and load characteristic is changed from P to Q (shown in Fig. 1.4 (a)). This change in operating point clearly indicates the reduction in fluid flow but the pump head has increased. It is noted that the power consumption by the pump remains same (or somewhat higher due to increase in head) even lower fluid flow.

If the pump is fed through ASD, no need to adjust valve to control the fluid flow and kept the valve at maximum opening. To control the fluid flow in this case, simply reduce the speed of the drive and hence the operating point is shifted from P to Q' (shown in Fig. 1.4 (b)). Here, pump head is largely reduced and the fluid flow is same as point Q. Since output power of pump is the product of head and fluid flow the power to be supplied by ASD is significantly lower. Thus energy conservation is taking place and the saving is much large if the pumps have ratings in megawatt range.

1.3   Literature Review

Efficiency optimization is very much essential not only to electrical systems, but also helpful in reduction of global warming. This section presents a review of the developments in the field of efficiency optimization of three-phase induction motor through optimal control and design techniques. Optimal control covers both the broad approaches namely, loss model control (LMC) and search control (SC). Optimal design covers the design modifications of materials and construction in order to optimize efficiency of the motor. The use of Artificial Intelligence (AI) techniques such as Artificial Neural Network (ANN), fuzzy logic, expert systems and NIAs in optimization of induction motor design and control are also included.

Since engineering problems require global optima academic as well as industrial experts are giving more attention to evolutionary search techniques such as genetic algorithm, PSO, simulated annealing (SA), differential evolution, etc. Some of the design optimization results using conventional algorithms [8], [15], [19], [34], [51], [52], [55], [56], [58], [68], [72], [75], [83], [96], [110], [113], [114], [138], [144], [151], [152], and AI and nature inspired algorithm based techniques [16], [37], [84], [121], [156], [170], [181] are available in the literature. In optimal control, there are two main approaches to improve the induction motor efficiency at light loads, namely loss model controller (LMC) [1] - [4], [13], [25], [28], [30], [39], [48], [60], [61], [66], [67], [76], [80], [85], [86], [88], [94], [97], [98], [115], [129], [130], [133], [134], [136], [145], [146], [157] - [161], [165], [171], [172], [177], [180], [182] and search controller (SC) [22], [35], [47], [59], [81], [86], [89], [104], [109], [111], [119], [154], [161] for minimum power input. References [29], [63], [178] described both LMC and SC. References [6], [27], [42], [61], [64], [123] described some other controls of IM efficiency optimization and [18], [24], [41], [117], [141], [184] described soft starting to improve motor performance. LMC determines the optimal air gap flux through the motor loss model. In case of search control, it measures the input power of the drive and searches for optimum flux or excitation current of the motor.

1.3.1 Optimal Design of Induction Motor

a) Conventional Algorithms

Statistical method [68], Monto Corlo [8], Sequential Unconstraint Minimization Technique (SUMT) [113], [138], [151], Hook Jeeves (HJ), [52], modified Hook Jeeves [56], [96], Han Powel method [58], modified Han Powel method [144] are the few methods which have been applied successfully in induction motor design in the past.

In [58], Modified Hook Jeeves (MHJ) search method was applied to an induction motor design based on efficiency optimization and its results were compared with Han Powel method and simple HJ method. Same authors in Ref. [56] have used HJ method to optimize a new motor and their results were compared with conventional industrial motors. Efficiency, efficiency-cost and cost are considered as objective functions. Authors analyzed the effects of supply voltage variation in the motor performance and concluded that higher efficiency can be obtained by increasing the voltage. Optimal design of induction motor for the application of electric vehicles was performed in [55] using MHJ method with the objective of a weighted summation of motor losses. Voltage and current harmonics were considered in their work. Service condition has been considered in [110] before taking the design optimization of IM. Authors of above paper concluded that the following modifications have helped to consume minimum energy in pump load systems, (i) stator core length increased up to 130%, (ii) number of stator winding turns decreased up to 10%.

Hydraulic pump in aerospace applications have been considered in [34] for design optimization. Supply frequency, environment and inrush current are considered as constraints in addition with normal constraints. Induction motor design with two objective functions was carried out in [75], one was of material cost and other was of operating cost. A global optimization approach has been introduced in [72]. Here error is taken as an objective function (for efficiency maximization, calculate efficiency in each step and find error (100-efficiency)). If error is more, large step size was used for adjusting variables.

Sequential unconstraint minimization technique (SUMT) was successfully applied to optimize IM in [113], [138], [151]. Torque pulsation has been considered in [151] as an additional constraint for an inverter fed IM design. Authors suggested that the flux and higher order harmonic currents should be as low as possible to have least pulsation. Reactance should be maintained at least 4 times greater than normal machine. Stack length and stator and rotor current densities to be decreased. Also to have a least pulsation, select stator core depth greater, rotor slot depth deeper and larger stator bore dia. Energy efficient irrigation pump was designed using SUMT with interior penalty function approach in [113].

In [14], constraint Rosenbrock method (Hill Algorithm) used to optimize the motor. Material cost was considered as an objective function and concluded that higher value of current densities required for getting optimum value. Six to four pole machines are to be selected for adjustable speed applications even upto 3600 rpm speed required, suggested in [51].

Sequential Quadratic Programming (SQP) for non-linear constraint optimization technique was successfully implemented to IM design in [152]. In this paper, authors have included practical considerations to reduce the computation time. The following are the practical considerations,

- Effects of different starting vectors:

Here the starting values of variables are taking their lower limit, upper limit and intermediate values. Then the analysis was carried out in the objective function value iteration by iteration. The values of the variables available in the literature were also considered for analysis. Out of four combination of variables, the upper limit value of variation offered poor results at starting but good results at final iteration.

- Effect of different step size

Authors have observed that the step size for increasing variable values is either too small (less than 10^{-3}) or too big (greater than 0.1) deteriorates the result in 30 kW IM and recommended to set the value 0.005 as step size to get good results.

- Effect of constraints:

Authors reported that there was no distinct difference between different sets of constraints considered for analysis.

- Effect of changing objective function:

Authors considered various types of objective function like efficiency, power factor and torque and observed that efficiency was slightly affected when torque was considered as an objective function.

- Change of variables and performance parameters with iteration:

Authors set the entire variables to upper limits and analyzed the performance related parameters with iteration. From the observation, efficiency and power factor were almost same from second iteration onwards.

Stator copper losses and core losses including harmonic losses are reduced by optimal selection of stator slot design in [83]. Authors used finite element method (FEM) to design the same and reduced core and winding losses by 2.22%. IM efficiency has been improved in Ref. [19] by modifying production technological process and is called as no tooling cost (NTC). It does not require a complete redesign of laminations. Authors modified the following in a totally enclosed fan cooled standard induction motor, (i) the rotor with copper

bar included in the slot before the aluminium die cast of the cage, (ii) increase of the core axial length, (iii) Annealing of the stator core. Authors finally concluded that the production cost for higher efficiency motors in considerably reduced by NTC.

b) AI and NIA Based Algorithms

Most of the NIA have been considered in [121] for IM efficiency maximization. GA was applied to IM design and achieved 25% reduction of the total cost [37]. In Ref. [181], genetic algorithm was used and good results were achieved in terms of convergence time/global convergence and the ability to handle discrete variables. In Ref. [170], GA was used to the design of permanent magnet brushless DC motor with the focus of efficiency optimization and achieved improvement by 1.5% than computer aided design. Hybridization of evolutionary programming (EP) and simulated annealing (SA) also proposed and applied to IM design [121]. Authors used EP to search the optimum point where as SA assists EP to converge towards the optimum point. Authors concluded that EPSA (hybrid) performed well for the design of induction motor.

Improved evolution strategy (ES) (hybrid of SA and GA) has been considered in [84] for the motor design serving to electric vehicle. Shaking technique was included to avoid local minima which appear in conventional ES. In Ref. [16], authors used SA to design three-phase induction motor and concluded that SA performed better than conventional methods. In Ref. [156], fuzzy logic was used as expert system to design the electromagnetic systems.

1.3.2 Optimal Control of Induction Motor

Optimum control of IM is essential one because it is not possible to optimize the motor efficiency for every operating point by optimizing machine design. In many applications of constant speed operation, induction motors operate under partial load for prolong periods, such as spinning drive in textile industry, mine hoist load, drill presses and wood saw. A simplest method to improve efficiency of induction motor operate at light load is to keep the motor connection in star results reduced power consumption. In the operation of motor at star mode, however, the developed torque and temperature rise are to be measured and keep at normal. Even though this method is not suitable for wide range of partial loads, still it is working at many textile industries in India.

1.3.2.1 Loss Model Based Controllers

The role of loss model controller is to measure the speed and stator current and determines optimal air gap flux through the loss model of the motor. The inner part of the control algorithm may be in scalar [1], [3], [4], [25], [61], [76], [85], [86], [94], [115], [129],

[134], [145], [146], [157], [158], [180], [182] or vector [2], [13, [28], [30], [39], [48], [60], [66], [67], [80], [97], [98], [130], [133], [136], [159] –[161], [165], [171], [172], [177]. In scalar control technique, variables are controlled in magnitude only whereas in vector control, variables are controlled in magnitude and phase. The complex induction motor can be modelled as DC motor by performing simple transformation in the vector control scheme. One advantage of loss model controller is that there is no delay in calculation of optimal flux and drive performances but time delay occurs in case of search control due to the search.

Artificial intelligence controllers like artificial neural network, fuzzy, PSO, GA can also be used for finding optimal flux level with minimum time. The exact values of machine parameters including their variations due to core losses and main inductance flux saturation are required in this approach. Many researchers have reported several strategies using different variables to minimize losses in IM. Some algorithms use slip speed [66], [67], [134], [158], rotor flux [39], [60], [85], excitation current [177], voltage [146], [159] – [161] etc. as variables.

a) *Scalar Controlled Drives*

The behaviour of an ac induction motor drive is described by three independent variables- the speed, the terminal voltage, the terminal frequency- and the parameters of the motor and its power supply [94]. At any operating point characterized by the speed and torque, an optimal flux (in other words, optimal ratio of voltage and frequency) can be found that meets the requirement of the operating point and minimizes the overall losses. Losses of the IM are represented by resistances in the equivalent circuit [85]. The stray load losses are represented by the additional resistance in the stator side. The power losses in the resistances depend on stator current and should be measured to calculate optimal air gap flux as well as to avoid over current flow in the motor [86].

(i) **Conventional Controllers**

In Ref. [85], a loss model controller with detailed analysis for minimizing the losses in scalar controlled induction motor is presented and suggested that the air gap flux is always kept greater than 0.3 pu independently on LMC command. This is because very low flux creates more motor currents and disturbs torque, and finally losses will be more. Authors of the above paper have concluded that rated flux operation essential during transient (starting) to maintain good dynamics. The detailed study on efficiency optimization of scalar controlled IM is available in [88].

The procedure described in Ref. [158] is based on optimal slip control of current source inverter fed induction motor. First, the optimal slip is searched by trial and error with the help

of loss model and the results are tabulated in the microprocessor memory. Then the motor is operated at optimal efficiency by simply tracking the optimal slip given in the table. Optimization was carried out successfully at centrifugal pump drives and is available in [34].

The variables, input voltage and frequency are considered to optimize the motor efficiency in [146]. Authors achieved 10-15% of efficiency improvement in a 2 hp induction motor at 0.4 pu load. Core saturation, source harmonics and skin effects are included in their research.

The flux level of the motor can be adjusted to get maximum efficiency without considering inverter losses in small drives less than 10 kW; but the effect of inverter losses in medium size (10-1000 kW) drives is significant [4]. Authors concluded from their experiments that there was no critical issues in the drive operation when the converter losses are neglected but the robustness decreases when disturbance occurs. More studies on efficiency optimization of scalar controlled IM was carried out in [1], [3], [25], [61], [76], [87], [115], [129], [145], [182].

(ii) AI and NIA Based Controllers

Many recent developments in science, economics and engineering, demand numerical techniques for searching global optima to corresponding optimization problems [180]. As discussed earlier, the effect of motor parameter variations has been focused in [157] and GA is used to search motor parameter to avoid error in the loss model. Then optimum values of voltage and frequency were arranged in a table for the energy saving controller. A 3-3-1 feed forward neural network (NN) was used in [136] to implement loss model controller. The inputs to the NN are torque, speed and rotor resistance of the IM and the output is the optimum rotor flux to minimize total losses. In Ref. [159], [160] authors used offline NN to find optimal voltage values to attain the best efficiency of the IM in a short time with only two step changes in the voltages, irrespective of load, to settle at the desired speed or torque.

In Ref. [48], [66], [67] authors used particle swarm optimization (PSO) as a searching tool to find the optimal value of variables for which the objective is maximum/minimum. Slip speed is considered in [66], [67] and the values of flux and hysteresis bands are considered in a direct torque controlled IM [48] as a variable to minimize losses. ANN is used for implementing optimum variables in the controllers. PSO is used to adjust proportional integral differential controller gains in [25] and get less torque and speed ripples in the drive.

b) *Vector Controlled Drives*

In vector control, the variables are considered in magnitude and phase. This technique of control needs more calculation than scalar control. The field oriented controller (FOC) generates the required reference currents based on the reference torque.

(i) Conventional Controller

Generalized d-q loss (vector) model including core saturation effects is presented in [13] and optimized IM, permanent magnet synchronous motor, direct current motor, synchronous reluctance motor through optimal excitation current (ids). Authors took optimal i_{ds} calculation less than 7µs in an experimental set up and concluded that minimum losses are reached when d-axis power losses equal to q-axis power losses. Induction motor equivalent circuits in d-q coordinates with stator and rotor core loss resistances are given in [171]. Parameter variations effects during losses minimization in induction motor through the simple IM loss models including iron losses are studied in [60] and achieved minimum electromagnetic losses by proper adjustment of magnetic flux. The procedures to get minimum energy in [39] are: (i) derive the study state values of currents and fluxes for the given load, (ii) design the steady state feedback control based on lyapunov, and (iii) implement the steady state values in real time and finally got good torque stability when minimum energy operation of induction motor.

In Ref [98], Loss Minimization Algorithm (LMA) has been simplified with a voltage dependant source and loss resistance. Authors considered current and voltage constraints when searching the optimal flux level and suggested that the model without leakage reactance yield a higher loss than the actual one.

The modified equivalent circuit of IM in d-q coordinates is presented in [165] with the consideration of inverter switching losses. The newly defined parameters R_{ls}, R_{lr} are stator and rotor resistances respectively. Stray load losses are associated with stator and rotor leakage fluxes. Authors of Ref [165] determined harmonic iron losses in laminated iron cores under non-sinusoidal excitation. Minimum time- minimum loss speed control of IM is described in [30].

Two common problems on lightly loaded motor are highlighted in [177] that are: (i) large speed drop when increasing sudden load torque, and (ii) slow acceleration. Authors proposed one algorithm which distributed stator current optimally into the flux producing current and torque producing current during a sudden load torque impact occurring at light load. The algorithm was accounted for main flux saturation effects in the machine and was shown the dynamics of the flux variation.

(ii) AI Based Controller

A hybrid technique, GA-PSO based vector control of induction motor for loss minimization as well as torque control is presented in [80]. PSO was used for mutation process of GA to improve the learning efficiency of GA. Floating point GA is applied in [130] for minimizing IM losses through flux adjustment. Basic GA is used in [172] to identify rotor time constant from the error between motor and commanded stator currents, which helped in on-line adjustment of slip angular speed. Optimum flux producing current and corresponding efficiency are focused in [2], [130] by using neural network. Change in core loss resistance (R_m) due to flux and frequency have taken into account. The variation in the iron loss resistance can be found from the equation (1.1) [2], where R_{mb} is the value of R_m at rated frequency and flux.

$$R_m = R_{mb}(f/f_{rated})^{1.1}(\Phi/\Phi_{rated})^2 \tag{1.1}$$

1.3.2.2 Search Controller

Search Control (SC) does not require the knowledge of the motor loss model for implementing optimization controllers. This controller measures the input power of the machine drive regularly at fixed interval and searches optimal flux value which results in minimum power input or stator current for the given values of speed and torque. Torque ripple is always present in SC due to the oscillations in the air gap flux.

Induction Motor efficiency optimization through search control was successfully carried out in [22], [35], [47], [59], [81], [86], [89], [104], [109], [111], [119], [154], [161] for minimum power input. The advantages of search control in induction motor efficiency optimization are as follows [89],

- If the power input is measured on the source side of the rectifier, the minimization is not restricted to the motors but affects the entire system and thus reduces the total amount of energy consumed.
- Since the source voltage and current waveforms have a much smaller harmonic content than the corresponding motor waveforms, the power measurement is more accurate and easier to obtain.
- Insensitive to parameter variation in the motor due to thermal and core saturation effects.

a) Scalar Controllers

In Ref. [57], the authors described the problems that arise while considering input power instead of stator current as the controlled variable to optimize the efficiency of IM. When stator current is used as variable, its minimum can be more easily detected than the input power. Stator current leads to more loss reduction and less torque ripple due to the absence of oscillation in the air gap flux. In Ref. [86], the authors presented the loss minimization process in the 1 hp drive when both the controlled variables are considered and it is revealed that power input to the drive is smaller in stator current minimization than the power input minimization.

Minimum power input to the drive is achieved by adjusting inverter input frequency in [86]. Authors have shown a significant efficiency improvement as compared to v/f control and concluded that large energy saving potentials available in pump and fan drives. In Ref [35], three controllers, first controller carried out voltage adjustment according to losses for minimum power input. The second controller changed the frequency to correct rotor speed losses caused by voltage drops. The third controller produced an initial commanded frequency which compensates the variation in slip with changing load and speed.

b) Vector Controllers

Smooth variation instead of step change in control variable to minimize input power of IM was proposed in [171]. Flux producing current (i_{ds}) was considered as variable. Torque producing current (i_{qs}) also adjusted in accordance with ids to avoid deterioration in the torque. From the experience of the authors in [89], a 7.5 hp motor took 7 seconds for completing minimization program (reduces flux step by step until input power is minimized) and the minimization process depends on the motor time constant. Thus longer is the time for high rated motor and shorter is the time for larger rated slip. Moreover fast convergence produce more ripples in the torque. The squared rotor flux was adjusted in [81] until the measured input power reached to minimum. Since the controller depends on rotor resistance its variations were also taken into account. Three indirect vector control schemes namely, stator flux field orientation, rotor flux field orientation and air gap flux field orientation were used in [119] for optimizing IM torque and efficiency and it concluded that rotor flux field orientation offers best optimal efficiency.

c) AI and NIA Based Controllers

Fuzzy logic based search control for optimizing IM efficiency is described in [47], [109], [154], [161]. Loss minimization during transient state by adjusting flux level using fuzzy logic has been proposed in [47]. Voltage was considered as a controlling variable in [161]. For

both steady state and transient state, fuzzy logic was used to optimize motor efficiency in [154]. In [109], fuzzy logic was used to decrement flux till the drives settled down to minimum input power. But the speed or torque command changes, the efficiency optimization using fuzzy abandoned and the rated flux was established to get the best transient performance. Feed forward torque compensator was used to reduce torque pulsation.

1.3.2.3 Combination of Loss Model and Search Based Controllers

Ref. [29], [63], [178], use both LMC and SC to analyze induction motor efficiency optimization. The controller developed in [178] ensures to retain good features of both the LMC and SC, while eliminating their major drawbacks. Authors used input power in order to identify on-line the loss function parameters and optimize flux value. Therefore slow convergence (drawback of SC) and parameter variation (drawback of LMC) were eliminated. Hybridization of LMC and search control was performed in [27] and it achieved good results with rough knowledge of parameters. LMC compared with SC in [63] and concluded that the LMC is more appropriate in FOC because optimal flux can be imposed in a short time where as search control varies the flux continuously and produces more oscillation in the torque.

A new approach to IM efficiency optimization using natural variables is presented in [42]. Core loss resistance and saturation dependent magnetizing inductance were used as variables to find optimal rotor flux and corresponding minimum losses. The controller was implemented in stationary reference frame through input-output linearization with decoupling technique.

Optimal slip control has been used to implement maximum torque per ampere control of IM in [27]. The specialty of this technique is that it can be implemented in the same drive which is already having v/f control. Torque command of the torque loop in IM drive is set based on the optimal slip control in [61].

Ref. [64] explained how energy saving work can be applied in IM through proper ventilation. Authors compared the properties of a machine with its own and outside ventilations. In a 3 hp motor with foreign ventilation, the lowering of temperature is the most significant for a supply voltage frequency near the rated one. In case of own ventilation, low temperature is obtained when the supply frequency is much less than the rated one. Own ventilation helped to decrease the winding temperature.

Ref. [6] presented terminal impedance control for energy saving in induction motor and it is good for practical applications because no speed transducer is required. Authors

suggested that this controller is effective up to 35% load and can save up to 10% of total energy consumed by the motor.

Intermittent disconnection of the supply is one method to conserve energy which is described in [123]. It is applicable only to low hp motors due to transient problems during switching. Authors achieved up to 50% energy saving in the motor and suggested that the switching off one phase of three phase supply during partial load of motor does not contribute any savings.

Performance optimization of IM during soft starting by eliminating supply frequency torque pulsation and keeping line current constant was presented in [184]. Starting torque pulsation is eliminated by triggering back to back connected thyristors at power points at the first cycle of the supply voltage. This technique is not suitable for the motors which require more starting torque.

1.4 Scope of Work and Author's Contribution

Induction motor is a large consumer of electrical energy in the industries and that its influence is more in energy intensive industries like textile and mine industries. It is a high efficiency electrical machine when working close to its rated torque and speed. However, the influence of many factors like partial load, rewinding, time and space harmonics and power quality disturbances, results in considerable reduction in the efficiency. A small increment in the efficiency of these motors by providing better control or optimum design can result in substantial saving in the long period. In general, there are two broad approaches to improve the induction motor efficiency, namely optimal design and optimal control.

After exhaustively review of the existing literature in the field of optimal design and control of induction motor, it is found that extensive efforts are being made to improve the performance of these motors, particularly for industrial motors where partial loading occur, with the help of advanced energy optimal controllers. Furthermore, efforts are also being made to improve the motor design with the consideration of non-ideal supply voltages (unbalanced and non-sinusoidal voltages).

Spinning drive motor in textile industry and hoist-load in mineral industry are identified as partially loaded motors which suffer from poor efficiency and more operating cost in the plant as well. These loads are concentrated to focus in the present work with NIA based optimal control of induction motor fed with Pulse width Modulated (PWM) Voltage Source Inverter (VSI). In this control, the flux level in a machine has been adjusted to give minimum operating cost for the industrial load. The flux controller improves the economics in terms of operating cost (energy cost and demand charge cost) and the test results (presented in

chapter 6) show that the flux level in the most economic motor will be adjusted according to load and speed, particularly at light load. To increase the stability of the motor drive during flux changes at variable speed and load operation, Fuzzy Pre-compensated Proportional Integral (FPPI) Controller is used and its results have been compared with conventional Proportional Integral (PI) controller.

Apart from optimal control, induction motor design optimization has also been concentrated with the help of PSO algorithm, which is very familiar since last decade to solve multi dimension non linear programming problems. Variant of PSO, called Quadratic Interpolation based Particle Swarm Optimization (QIPSO) is also used and explored its superiority in comparison with normal PSO, Simulated Annealing (SA) and constrained Resenbrock method. To realize the importance of PSO in terms of variable and constraint values selection, SPEED (Scottish Power Electronics and Electric Drives) - IMD (Induction Motor Drives) software is used and the results are analyzed in detail.

The variables required to design induction motor are reduced based on the motor performance which was carried out by SPEED/IMD and much reduction in computation time without compromising optimum design results was observed. Harmonic current is derived from the harmonic equivalent circuit and it has been forced as an additional constraint so that motor design is carried out with limited harmonics when fed from inverter supply.

In practice, induction machines experience over-voltages and under-voltages, depending on the location of the motor and the length of the feeder used. Furthermore, the supply voltage is not always balanced. Therefore, the motor will experience a combination of over- or under-voltages with unbalance voltages [132]. Moreover, consistent, efficient and reliable operation of motors, accounting unbalanced voltage in the stator terminals and its optimized design will receive considerable attention from industry. Effects of unbalanced stator voltage in the design variables, motor torque, temperature rise and efficiency are also analyzed.

Thus the main contributions of the author can be summarized as follows:

1. Optimal control of industrial motors by adjusting the flux level during variable load and speed operation-

    - A complete mathematical modeling of the drive is carried out with the special attention of their losses.

    - Data of industrial loads such as spinning drive motor in textile industry and mine-hoist in mineral industry are collected.

    - Simulation model of the induction motor drive with loss model control, search control and their hybridization is developed. Fuzzy Pre-Compensated

Controller is designed to achieve better dynamic performances of the motor during flux adjustment.

- Exhaustive simulations are carried out to evaluate the performance of the motor operating with given load diagram.

- Various performance indices such as input power, operating cost, speed and torque are evaluated.

- Case study in a medium scale textile industry for economical analysis is presented.

2. Optimal design of induction motor using Particle Swarm Optimization (PSO) and its improved version called Quadratic Interpolation based Particle Swarm Optimization (QIPSO) algorithm-

- Formulated the induction motor design problem with seven variables, nine constraints and five objective functions.

- Developed PSO and QIPSO algorithms to solve induction motor design problem.

- Supply voltage unbalance and harmonics are taken into account while designing the motor.

- Optimized results given by PSO and QIPSO are validated by SPEED software.

- The performance based optimal design of induction motor using SPEED is carried out and achieved reduction in number of required design variables.

1.5   Thesis Organization

The thesis is divided into seven chapters and are organized as follows,

Chapter 1, which reports the methodologies to optimize the induction motor drives, design of materials during construction and also efficient control when the motor is operated in part load. The potential of efficiency improvement opportunities available in the industrial sectors are presented. Furthermore, a comprehensive literature survey on improvement of efficiency of induction motor through optimum design and control with conventional, AI and NIA based controllers or algorithms are presented.

Chapter 2, which presents the common sources affecting induction motor efficiency and their solutions to improve it are briefly discussed. An experimental study on the induction motor operation under unbalance voltages is conducted to see the negative effects of it on

motor's efficiency. The broad approaches of induction motor loss minimization, namely loss model controller and search controller are discussed. Finally the design aspects of induction motor and the role of SPEED software used in design optimization are discussed.

Chapter 3, which deals with the mathematical model of vector controlled induction motor drive. The complete induction motor drive scheme is explained in detail. The drive model consists of a front end diode converter, Pulse Width Modulation (PWM) inverter, induction motor, energy optimal controller, current control and a speed controller. Stator reference frame induction motor model equations are derived. Optimal energy controller is designed through the loss models of entire variable speed drive systems to adjust the flux in accordance with the load. Fuzzy Pre-Compenstaed Proportinal Integral (FPPI) controller is designed to solve stability problems in the drive during flux adjustment.

Chapter 4, which investigates the design improvements of induction motor by selecting optimal values of variables and constraints using Particle Swarm Optimization (PSO). How the improved version of basic PSO called Quadratic Interpolation based PSO (QIPSO) is effective in design optimization of induction motor is also shown. Five objective functions namely, material cost minimization, efficiency maximization, starting torque maximization, temperature rise minimization and operating cost minimization are focused in this chapter. The design is also performed for the motor under unbalance and harmonics in the supply.

Chapter 5, realises the induction motor design results of chapter 4 which are obtained by Particle Swarm Optimization (PSO) and Quadratic Interpolation based Particle Swarm Optimization (QIPSO) via SPEED (Scottish Power Electronics and Electric Drives) software. The effects of variables (width of the stator slot, depth of the rotor slot and length of the stator stack), which are more dominant to give good design, in the performance indices are plotted by the help of ranging function in the SPEED. The number of required variables to get optimum design results of motor is reduced. Performance based optimal design of induction motor using SPEED is carried out and its results are analyzed. Theoretical justification is also given for the design with minimum material cost.

Chapter 6, presents simulation studies on the energy optimal control of an inverter-fed three-phase induction motor. The first part gives an overview of various controllers example: loss model controller, search controller and their hybridization. Second part considers mine hoist drive of a mineral industry and the implementation of efficiency optimization controllers with the help of Particle Swarm Optimization (PSO) and fuzzy logic. Fourth part analyzes the efficiency improvement of spinning drive of textile industry along with a case study in a medium scale industry. Fuzzy Pre-Compenstaed Proportinal Integral (FPPI) is used to improve motor's dynamic performances during the activation of energy optimal control.

Motor is also simulated for the possible wide ranges of speed and torque in addition with industrial loads.

Chapter 7, concludes on the whole thesis and gives its future scopes.

Appendices (design expressions, test motor specifications, MATLAB/SIMULINK models and the various standards involved induction motor efficiency measurement) are given in the end.

Efficiency Improvements in Induction Motor Drive

[The factors affecting induction motor efficiency are discussed in this chapter. Energy optimal control and design techniques of induction motor are described. An experimental study on operation on induction motor with unbalanced supply voltage is carried out. How nature inspired algorithms based algorithms are utilized in optimal control and design of induction motor are presented. Finally the design aspects of induction motor are discussed.]

2.1 Introduction

Electrical energy, measured in kWh, represents more than 30% of all used energy and it is on the rise. Part of the electrical energy is used directly to produce heat or light. The larger part of electrical energy is converted into mechanical energy in electrical motors. Among electric motors, induction motors are most used both for home appliances and various industries [20]. Motors rarely operate at or even close to their name-plate conditions because [179]: (a) operation at exact rated load is unusual, as industrial users are generally very conservative in their applications; hence, most motors operate well below their rating; (b) the consequences of under-voltage on motor performance are generally known to be serious; hence, many users deliberately set plant voltages higher than the rated value; (c) although over-voltage is most common, under-voltage operation is also possible; (d) there is a frequent necessity to connect single-phase loads to three-phase supplies, which can cause unavoidable unbalances of supply system equipment; hence, motor terminal voltages are rarely perfectly balanced.

Among the above practical situations, efficiency of induction motor is more affected at the part load operating conditions and hence researchers are focusing their research on the optimal control techniques like loss model controller and search controller for the industrial motors already in use. For newly designed motor, efficiency can be improved by using quality of materials and choosing optimal values of design variables with the help of advanced optimization algorithms. Various energy optimal controllers of induction motor at part-load and design optimization techniques are discussed in section 2.4 and 2.5 respectively.

2.2 Factors Affecting Induction Motor Efficiency

As mentioned earlier induction motor is a high efficiency electrical machine when working closed to its rated torque and speed. However, the influence of many factors like partial load, rewinding, time and space harmonics and power quality disturbances, results considerable reduction in the efficiency.

a) Partial Loading

Partial loading in induction motor is common for several reasons and are following,

- Motor manufacturer may use a large safety factor
- Under utilization of the motor by the industrial/domestic customers
- Due to under voltage in the remote areas, customers tend to use larger motor to maintain desired torque
- The applications which require large starting torque so the customer tends to use special designed motor with higher starting torque.

The Table 2.1 [163] shows the impacts of partial loading in the performances (efficiency and power factor) of induction motors. From the Table 2.1, it is seen that the motor which are operating at 75% load there is no significant difference in the efficiency and power factor in comparison with the motor operate at 100% load. Therefore, replacement of motor which operate at 75% load or above by a lower ratting one is not recommended.

b) Rewinding Effect

Normally there are two options in front of motor users when it fails, they must be repaired or replaced quickly to avoid production loss. Careful rewinding by using good quality of materials and workmanship can sometimes maintain motor efficiency at previous level, but the poor rewind results in greater energy consumption and shorter life due to higher operating temperatures.

The impact of rewinding on motor efficiency and power factor can be easily assessed if the no-load losses of a motor are known before and after rewinding. Maintaining documentation of no-load losses and no-load speed from the time of purchase of each motor can facilitate assessing this impact [26].

It is economically attractive to replace failed motors rather than spending the expenses of rewinding. Though common practice is to replace failed motors below 20 hp and repair those above 20 hp, replacing all failed motors up to 50 hp is almost always economical [120].

Table 2.1 Efficiency and Power Factor of the Induction motor with Different Load

HP	kW	Pole	Efficiency			Power factor		
			100% load	75% load	50% load	100% load	75% load	50% load
5.0	3.7	2	83.1	81.2	77.3	0.84	0.80	0.70
		4	82.0	82.0	80.0	0.88	0.84	0.75
		6	85.0	84.3	81.3	0.78	0.69	0.53
10.0	7.5	2	84.3	83.2	79.4	0.91	0.88	0,80
		4	85.5	84.6	81.3	0.85	0.77	0.64
		6	87.0	85.5	82.5	0.76	0.68	0.53
25.0	18.5	2	88.5	87.7	85.0	0.95	0.93	0.86
		4	89.5	89.4	87.9	0.89	0.85	0.75
		6	89.8	90.0	89.0	0.82	0.78	0.67
50.0	37.0	2	38.5	87.5	85.0	0.92	0.90	0.86
		4	91.3	91.0	89.5	0.84	0.81	0.73
		6	91.3	91.2	90.2	0.86	0.83	0.77
75.0	55.0	2	-	-	-	-	-	-
		4	92.7	92.5	91.0	0.85	0.81	0.69
		6	93.7	93.9	93.4	0.80	0.74	0.67
100	75.0	2	-	-	-	-	-	-
		4	92.9	92.6	91.2	0.91	0.89	0.36
		6	92.7	92.6	91.4	0.80	0.75	0.64

c) Time and Space Harmonics Effect

Induction motors constitute the most popular traction devices and are sensitive to harmonic voltages. Induction motors, even under normal operating conditions, involving perfectly sinusoidal voltage supply produce a relatively limited amount of current harmonics due to the winding arrangement and nonlinear behaviour of the iron core. The most important effect of such phenomena is reduction of motor efficiency, especially under important loading, and the associated losses are usually referenced as stray losses [173].

When induction motors are connected to an inverter supply, the losses increase due to time harmonics. The increased losses reduce motor's life and derating must be applied to avoid the damages.

Space harmonic fields are produced by the distributed type of windings, slotting of stator and rotor, magnetic saturation and inequalities in air gap length [153]. The space harmonics

caused by the variation of air gap reluctance are called slot harmonics. The effect of these harmonics in the air gap flux wave is to give birth to unwanted parasitic torques, vibration and noise [153]. These torques are responsible for generation of asynchronous crawling and synchronous crawling or cogging, respectively, in induction machine particularly cage type.

d) Power Quality Disturbances

Nowadays, Induction Motors (IMs) are mostly working on the non-ideal supply voltage environments like, non-sinusoidal (inverter supply), under, over and unbalanced sinusoidal voltages. This leads to more power losses and increases the interest in studying power quality (PQ) issues in the industrial equipments. Some of the PQ problems are as follows [11]:

- Short interruptions
- Voltage dips
- Voltage swells
- Voltage and current transients
- Voltage and current harmonics distortion
- Voltage flicker
- Voltage unbalance
- Phase angle imbalance and/or jump

One case study on the effects of voltage swell in the industrial equipments such as induction motor is explained here. In 1999, two 5 HP induction motors in the pirn winding section, which is one of the preparatory sections of the weaving process, were burnt out at the same instant in a medium scale textile processing industry (Haitima Textiles Limited, Coimbatore), resulting in a fire accident. The plant engineer found that the connections and the input supply voltages to the motors were correct. Further investigations with the insitu personnel revealed that there was a big sound from the motor followed by a brightening of the tube lights. Then the engineer thought that the problem was due to the excess of supply voltage at a short duration but he didn't confirm because no facility was available in his plant for the storage of on-line voltage monitoring. However, he contacted with the electricity supplier (Somanur sub-station, Tamil Nadu Electricity Board) through telephone and validated that it was voltage swell (over voltage) due to the fault occurred in the distribution system near by plant. It is one of the Power Quality (PQ) disturbances in the electrical supply used to consumer appliances.

Among the above mentioned PQ problems voltage unbalance effects in the induction motor is more severe in terms of reduction in efficiency and increase in temperature rise.

An experimental study is conducted to see the effects of the same and is presented in the next section.

2.3 Effects of Voltage Unbalance

Supplying a three-phase induction motor with unbalanced voltages has many negative effects on its performance. These effects include increased losses due to more negative sequence current and, consequently, temperature rise, a reduction in efficiency, torque and insulation life of the motors. Some of the studies on the effects of voltage unbalance in the performance of induction motor are available in [54], [55], [131]. [132], [179], [33], [149]. An experimental study is performed in the present work which investigates the negative effects of a small quantity of unbalanced sinusoidal voltage (0.96% unbalance and 2.9% THD) over balanced (inverter supply) non-sinusoidal voltage (23.7% THD) on the performance of induction motor in terms of line currents, power factor and efficiency. Performance of a 5 HP three-phase squirrel cage induction motor under the above stated supply conditions was measured through a real load test. This study has given an idea as to how the unbalanced voltage affects the performance of induction motor even sinusoidal one.

The testing of the 4 pole, 400V, 5 HP (parameters: R_s = 2.42, R_r = 2.05, L_m = 0.23 mH, Ls = L_r = 0. 237mH, R_m = 95.5 Ω) squirrel-cage induction motor covered stator and rotor copper losses, slip, power factor and iron losses were measured. The experimental set up for testing induction motor is shown in Fig. 2.1. This experimental set-up is capable to handle non-sinusoidal quantities experienced by inverter supplied drives. The input power, input voltages and currents are measured using voltage and non-contacting current probes, and the signals are digitally processed by the power quality (PQ) analyzer (Fluke 434). A DC generator is used as variable load to the motor.
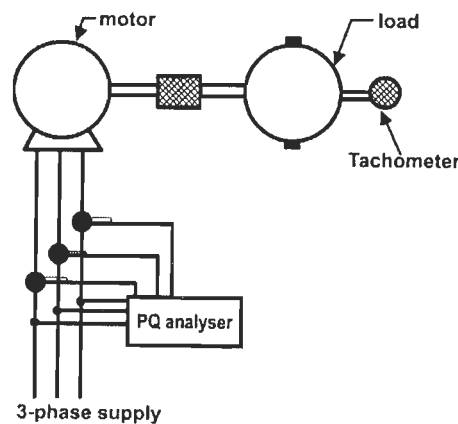
Fig. 2.1. Test bench layout

One common reason for occurrence of voltage unbalance in the industry is uneven load sharing of single phase loads like tube lights, single phase motors (mostly cooling fans), computer systems, etc. Apart form this, unbalanced transformer banks, malfunction of automatic power factor correction equipments and the faults in the equipments and the lines are the main contributors of voltage unbalance. Quantification of voltage unbalance levels is based on the following three definitions,

(1) Line Voltage Unbalance Rate (LVUR) as defined by National Electrical Manufactures Association (NEMA), the ratio of maximum voltage deviation from the average line voltage magnitude to the average line voltage magnitude [33]:

$$LVUR = \frac{\max \left[|V_{ab} - V_{avg}| |V_{bc} - V_{avg}| |V_{ca} - V_{avg}| \right]}{V_{avg}} * 100 \qquad (2.1)$$

where $V_{avg} = \dfrac{V_{ab} + V_{bc} + V_{ca}}{3}$

V_{ab}, V_{bc}, V_{ca} are line-to-line voltages

(2) Phase Voltage Unbalance Rate (PVUR) as defined in IEEE std 141, the ratio of maximum voltage deviation from average phase voltage magnitude to the average phase voltage magnitude [33]:

$$PVUR = \frac{\max \left[|V_a - V_{avg}| |V_b - V_{avg}| |V_c - V_{avg}| \right]}{V_{avg}} * 100 \qquad (2.2)$$

where $V_{avg} = \dfrac{V_a + V_b + V_c}{3}$

V_a, V_b, V_c are phase voltages.

(3) Voltage Unbalance Factor (VUF) has been given by the IEC as follows [62],

$$VUF = \frac{V_-}{V_+} \qquad (2.3)$$

where V_+ and V_- represent the voltages of the positive and negative sequence components, respectively.

2.3.1 Performance Investigation

At the time of testing, a 5.5 kW voltage source inverter is used for setting balanced non-sinusoidal voltage. In order to match the frequency of both supplies (sinusoidal and non-sinusoidal), set the voltages nearly to 425 V which is somewhat higher than rated voltage of the motor. If the three-phase voltages are higher than the rated value and are not equal, it is known as three-phase over-voltage unbalance (3ΦOV). Equation 2.1 is used for calculating voltage and current unbalance since only the magnitude of the line voltages was collected at the time of testing. Summation of losses method, as stipulated in IEC 34-2, is used for

efficiency determination of the motor. Additional load losses are assumed to be equal to an estimated 0.5% of the power input of the motor and to vary as the square of the stator current. The rotor Joule losses are evaluated as the product of the rotor slip for the air gap transmitted power. The waveform and phasor diagram of both unbalanced sinusoidal and non-sinusoidal supply voltages applied to the test motor are shown in Fig. 2.2 and 2.3. The percentage of Total Harmonic Distortion (THD) in the supply voltages and currents are shown in Fig.2.4. THD (23.7%) is much higher in non-sinusoidal supply whereas only 2.9 % THD presents in the unbalanced sinusoidal supply

a) No-Load Test

The motor was first operated in the unbalanced sinusoidal voltage no load condition to establish the baseline for normal performance. Tests were then performed at no load for the non-sinusoidal balanced condition. Table 2.2 gives a summary of the performance of the motor characteristics during no load testing for the 0.96% unbalanced sinusoidal voltage condition and balanced non sinusoidal voltage. In Table 2.2, the voltage unbalance is 0.96% which creates the current unbalance is 6.58%. The no-load losses have increased at unbalanced voltage by 12.82% from 0.195 kW to 0.22 kW.

Table 2.2. No- Load Performance of Motor

Parameters	096% unbalanced sinusoidal voltage	Balanced non-sinusoidal voltage
Line voltage, Volts	425.5, 425.4, 419.3	425
Line current, Amps	2.2, 2.7, 2,.5	2.1
Input power, kW	0.22	0.195
Power factor	0.13	0.14
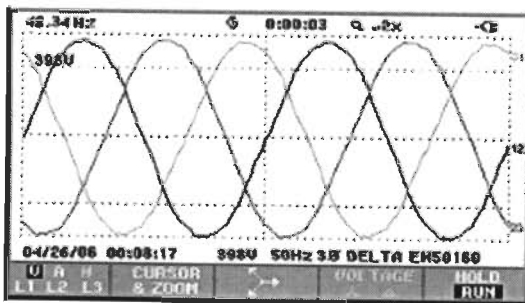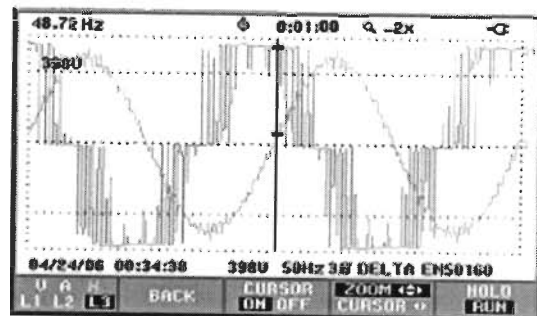
(a)   (b)

Fig. 2.2. Input supply waveforms of the test motor: (a) Sinusoidal (b) non sinusoidal
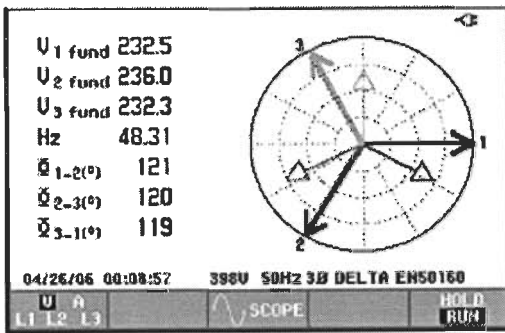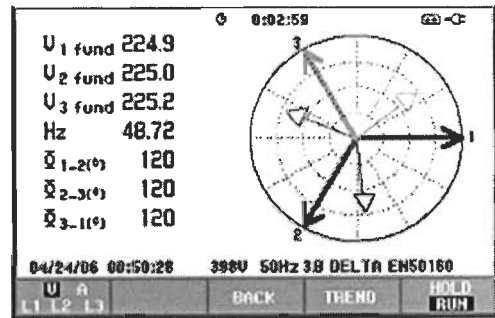
(a)   (b)

Fig. 2.3. Phasor diagram of input supply: (a) Sinusoidal (b) non sinusoidal
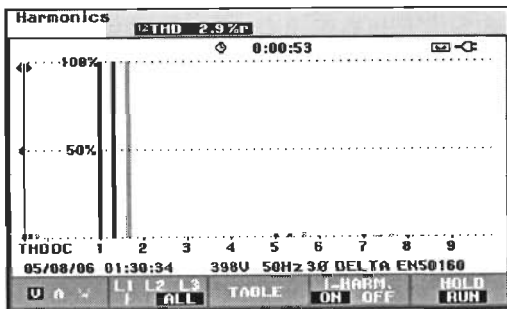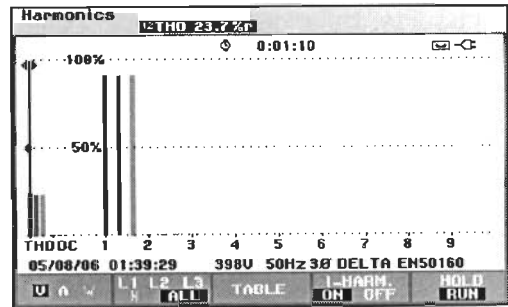
(i)   (ii)

(a) Voltage THD: (i) Sinusoidal supply, (ii) Non sinusoidal supply
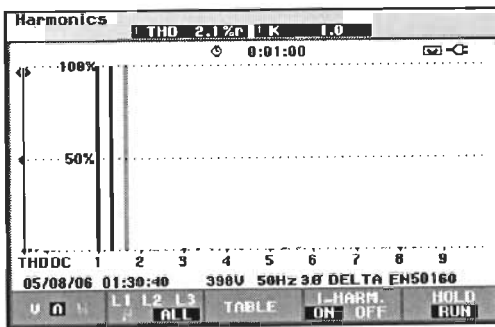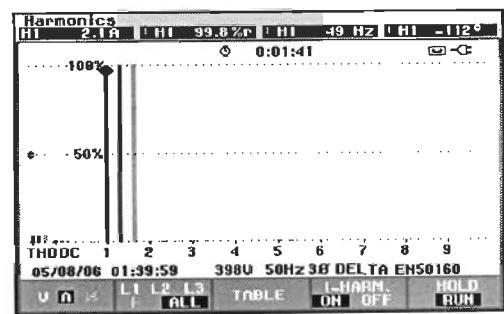
(i)   (ii)

(b) Current THD: (i) Sinusoidal supply, (ii) Non sinusoidal supply

Fig. 2.4 Harmonic spectrum of input supply (a) Voltage, (b) Current

b) Load Test

Motor is indirectly loaded with the help of DC generator and lamp load. Measurements were taken for the entire range of loading i.e. from no-load to full load. The summary of the load tests is tabulated in Table 2.3 and 2.4.

Table 2.3. Load Test under Unbalanced Sinusoidal Voltage

Power input (kW)	Line currents (Amps)	Total losses (kW)	Efficiency (%)	Power factor (%)
0.72	2.8, 3, 2.6	0.27	62.5	35
1.46	3.5, 3.6, 3.2	0.31	78.8	58
2.1	4.2, 4.3, 3.8	0.35	83.2	70
3.09	5.3. 5.6, 5.1	0.49	84.3	80
3.9	6.5, 6.7, 6.1	0.61	84.5	84
4.66	7.5, 7.8, 7.3	0.74	84.0	85

Table 2.4. Load Test under Balanced Non-sinusoidal Voltage

Power input (kW)	Line currents (Amps)	Total losses (kW)	Efficiency (%)	Power factor (%)
0.6	2.3	0.23	59.4	33
1.26	3.0	0.26	79.4	58
2.25	4.3	0.35	84.6	72
2.76	5.1	0.40	85.4	75
3.74	6.5	0.57	84.7	78
4.39	7.5	0.68	84.5	79

2.3.2 Results and Discussion

Fig. 2.5 - 2.7 shows the experimental results for a 5HP, 400V, three-phase squirrel-cage induction motor supplied by both unbalanced sinusoidal and balanced non-sinusoidal supply voltages. Efficiency of the tested motor under unbalanced sinusoidal voltage is slightly smaller than the motor operated with balanced non-sinusoidal (inverter) voltage shown in Fig. 2.5. Line currents drawn by the motor under both operating conditions is shown in Fig. 2.6. This figure shows that the current drawn by the motor under unbalance supply is higher than the current under balanced supply at low loads and this situation reverses at high loads. Also, improved power factor is obtained by use of non-sinusoidal balanced supply at low loads and unbalanced sinusoidal voltage at high loads. Lower power factor is obtained by use of unbalanced sinusoidal voltage at low loads and non-sinusoidal voltage at high loads shown in Fig. 2.7. Overall, this study reveals that the motor offers

more negative effects even small amount of voltage unbalance is present in the supply voltages.
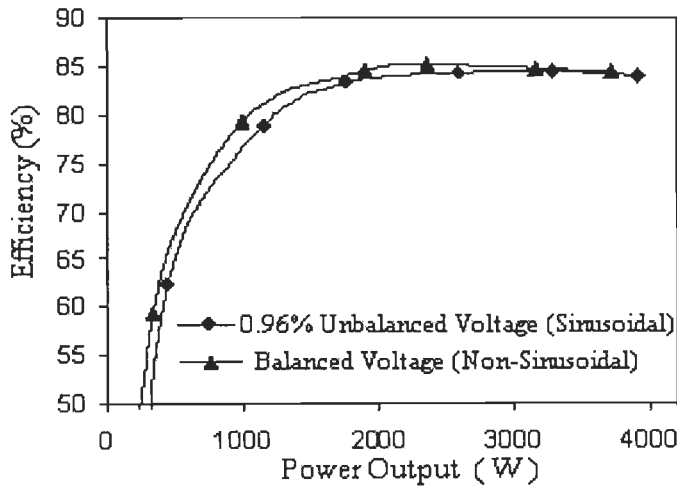
Fig. 2.5. Efficiency of motor at different load.
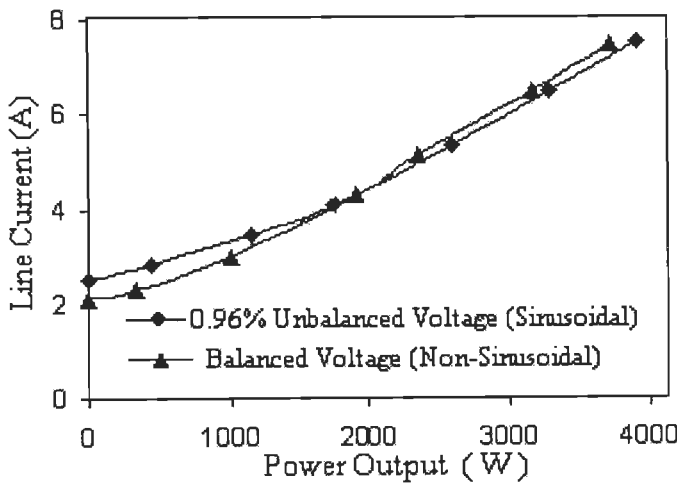
Fig. 2.6. Line current of motor at different load.
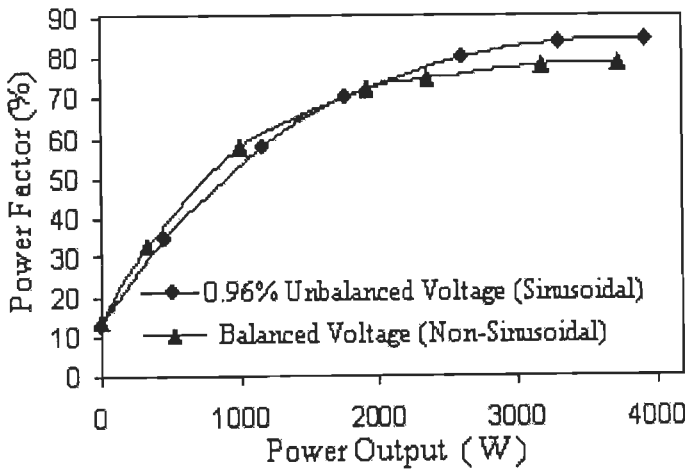
Fig. 2.7. Power factor of motor at different load

a) Economical Analysis

From the consumer's point of view, efficiency reduction means paying more for energy as a result of unbalanced voltage supplies. From the power system point of view, operation of motor with lower efficiency implies an increase of the system load and a reduction of the power plant reserves [54].

An analysis of a 5 HP motor operating under small unbalanced sinusoidal voltage (0.96%) compared with balanced non-sinusoidal voltage at the following electricity tariff (TNEB, HT tariff I for the industries situated in Non-Metropolitan localities) and assuming 8000 hours of operation/year is summarized in Table 2.5. Extra KW consumption by the motor due to unbalanced voltage is 0.27 KW (4.66 - 4.39). US $ 188 additionally paid per year to the electricity supplier due to 0.96% voltage unbalance in one motor compared to non-sinusoidal supply.

Maximum demand (KVA) charges: US $ 6.66/month

Energy (kWh) charges: US $ 0.077/kWh

(1 US $= IRS 45 approximately)

Table 2.5 Economic Losses due to 0.96% Voltage Unbalance in a 5 HP Motor

Extra kW consumption at full load	Extra consumed energy (kWh/year)	Extra demand charge (US$/year)	Extra payment (US$/year)
0.27	2160	21.5	187.8

b) Simulation Results up to 5% Unbalance

For theoretical analysis of the same test motor, MATLAB SIMULINK model of three-phase induction motor with stationary reference frame has been created for getting different parameters (stator and rotor copper losses, torque and temperature rise) of the motor under different PVUR.

The rotor and stator copper losses, torque and temperature rise of the motor are shown in Fig. 2.8 for balanced voltages and in Fig. 2.9-2.11 for unbalanced voltages, 1%, 2.5% and 5% respectively. Simulation results show that torque ripple, losses and temperature rise are increased when unbalanced voltage level is increased. It is seen that there is no oscillation in the torque of the motor under balanced voltage shown in Fig 2.8, but in case of unbalanced (5%) voltage, there is much oscillation in the torque and temperature rise increased by 3°C. Stator and rotor losses also increased by 1.4 times and 1.73 times respectively and are shown in Fig.2.11.
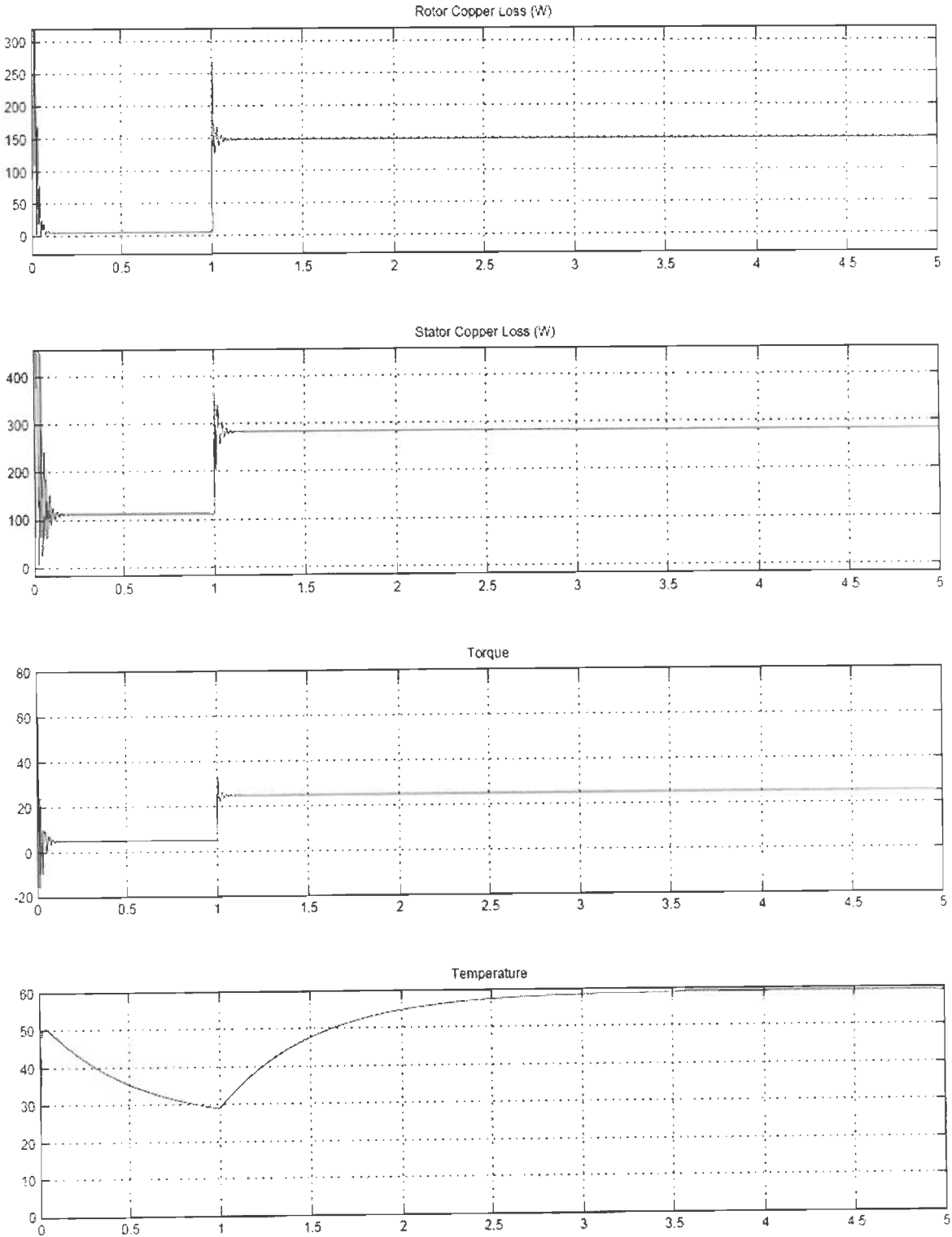
Fig.2.8. Simulation results of the motor under balanced voltages: 1) rotor copper loss, 2) stator copper loss, 3) torque, and 4) temperature rise
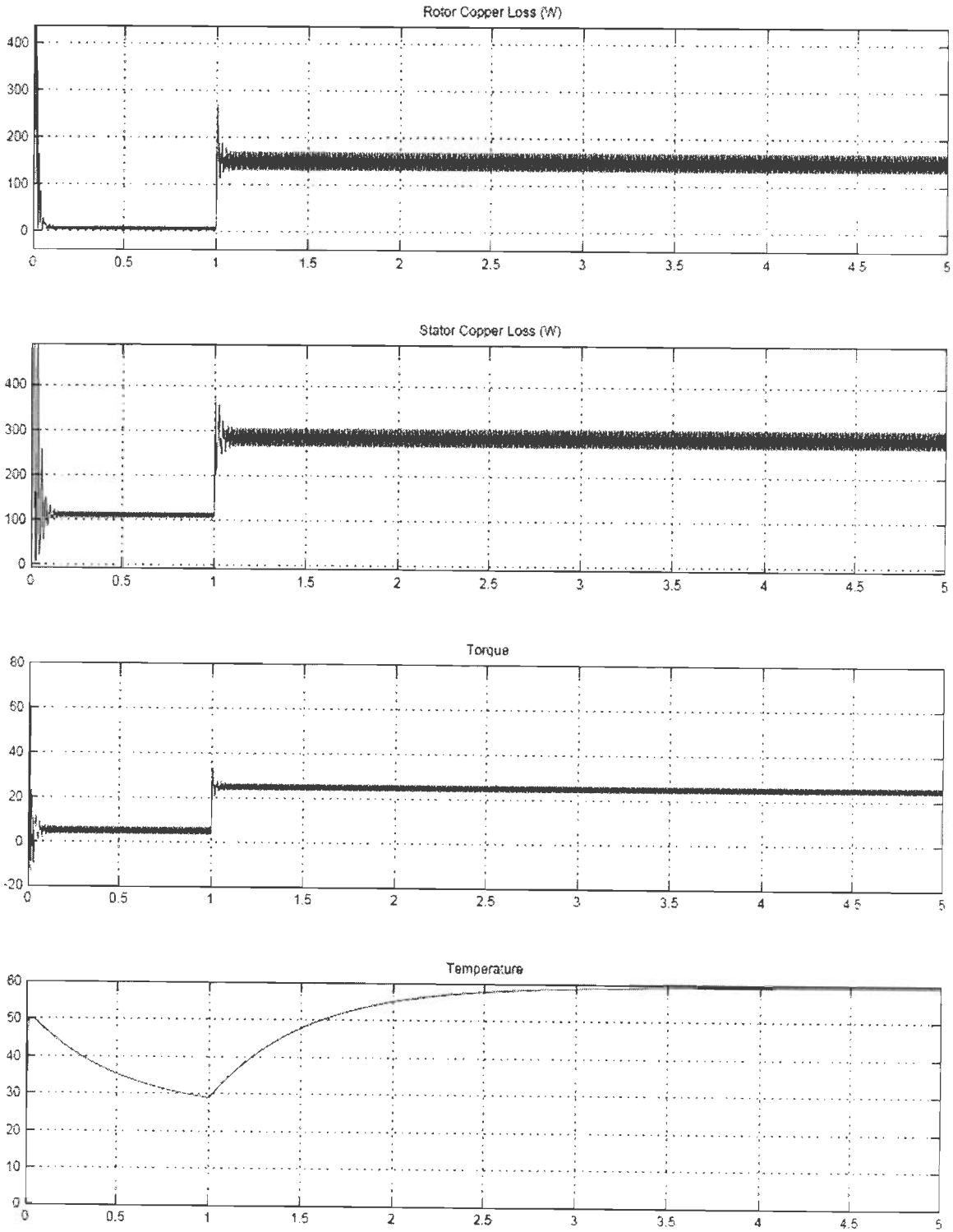
Fig.2.9. Simulation results of the motor under 1% unbalanced voltage: 1) rotor copper loss, 2) stator copper loss, 3) torque, and 4) temperature rise
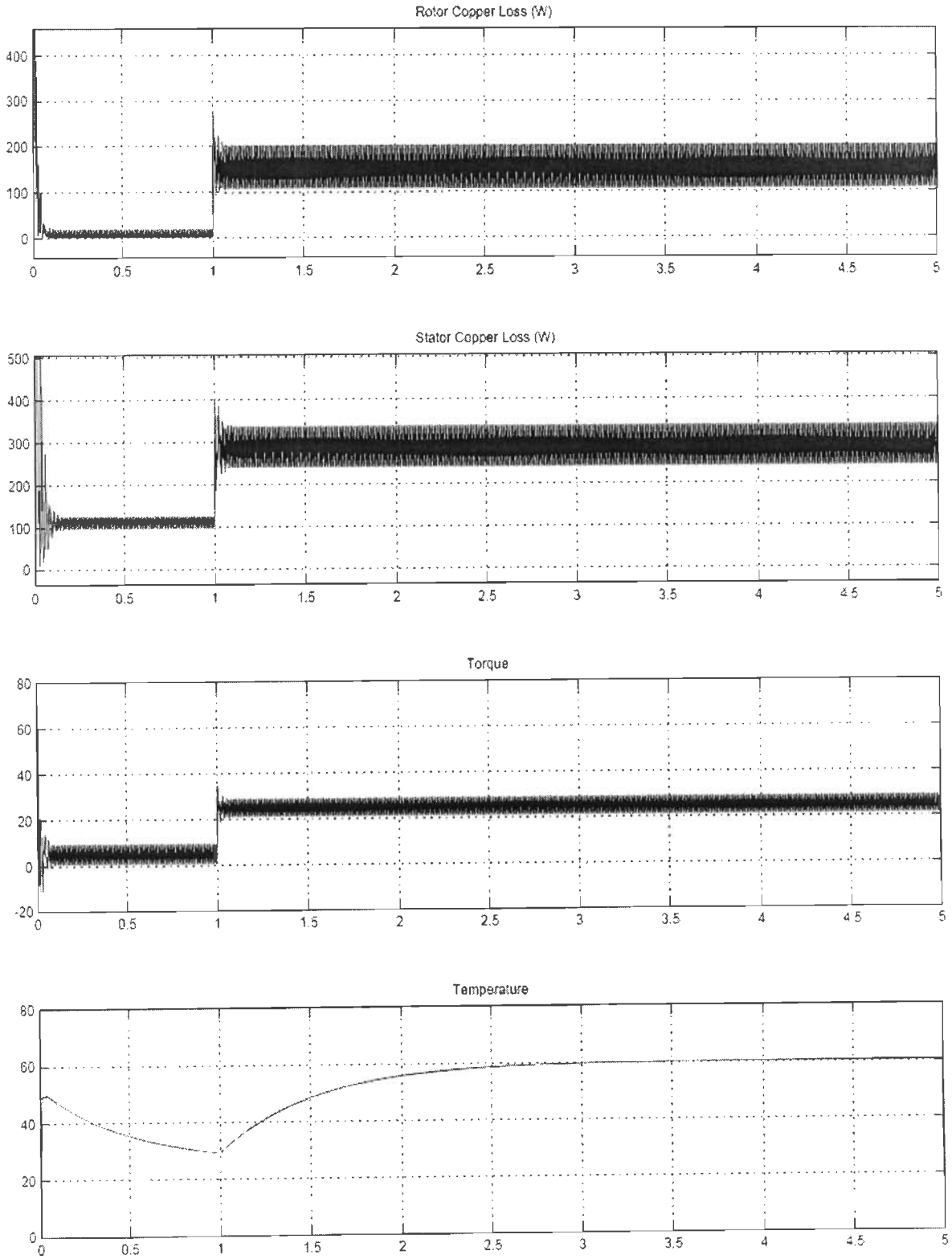
Fig.2.10. Simulation results of the motor under 2.5% unbalanced voltages:1) rotor copper loss, 2) stator copper loss, 3) torque, and 4) temperature rise
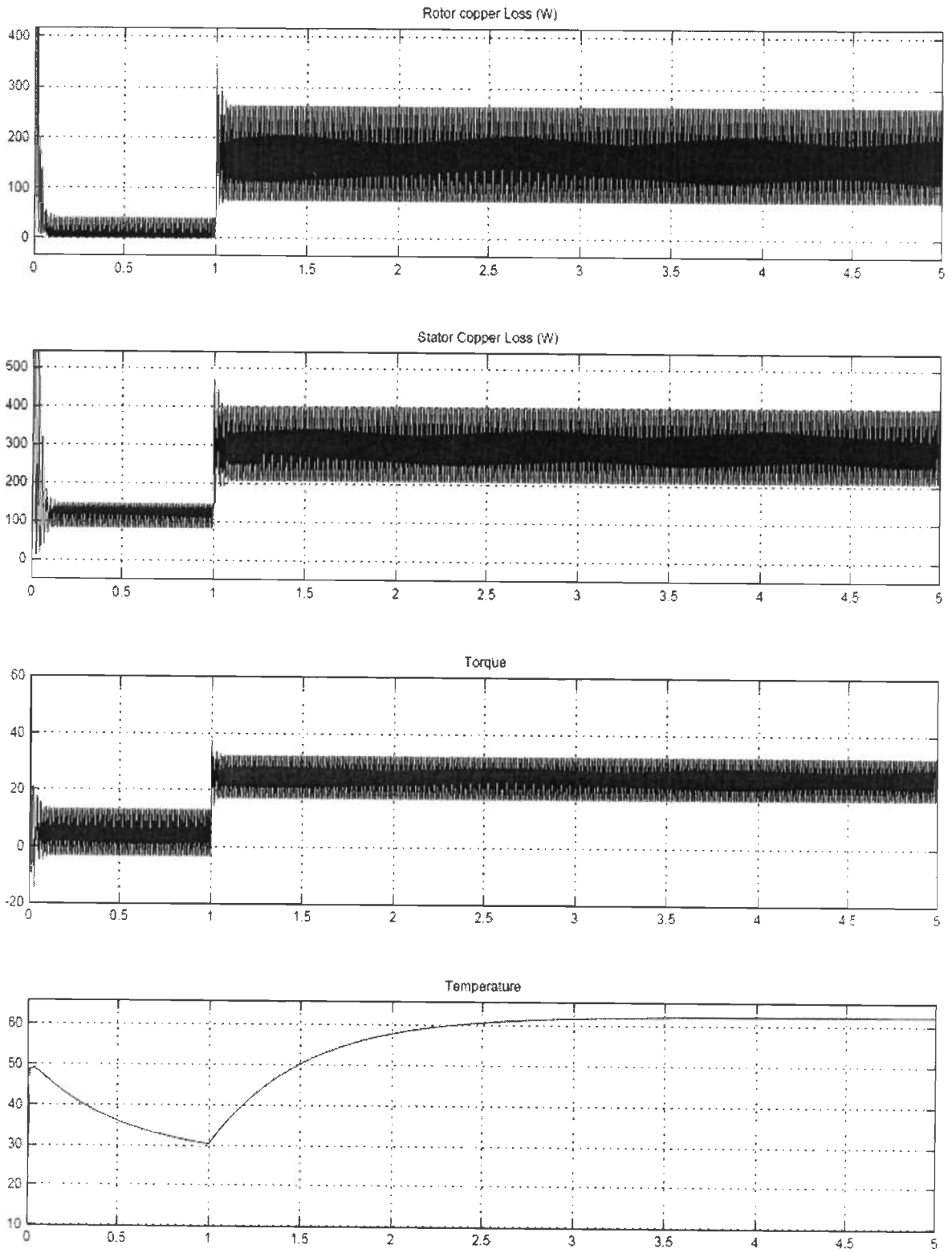
Fig.2.11. Simulation results of the motor under 5% unbalanced voltages: 1) rotor copper loss, 2) stator copper loss, 3) torque, and 4) temperature rise.

The experimental study leads to the following conclusions:

- Despite sinusoidal supply, unbalanced voltages affected the efficiency of induction motor very much.
- Although balanced non-sinusoidal supply has more THD, it gave superior performance.
- Additional payment of US $ 188 per year, to the electricity supplier, due to a small amount of voltage unbalance (nearly 1%) in a 5 HP motor.
- Industry personnel should not ignore voltage unbalance even its value is very less.
- Increase of rotor copper loss is more than stator copper in the motor under unbalanced stator voltages.

2.4   Optimal Energy Control of Induction Motor

The losses in the IM drive system are divided into a number of loss terms, connected with specific parts of the machine. The total losses shown in Fig. 2.12 comprises of copper losses in stator and rotor, iron losses due to eddy current and hysteresis, stray losses arise on the copper and iron of the motor, friction losses, converter losses due to the resistance offered by the solid state switches and finally the cable losses due to the resistance offered by the cable. Power output is the product of shaft load and its speed.
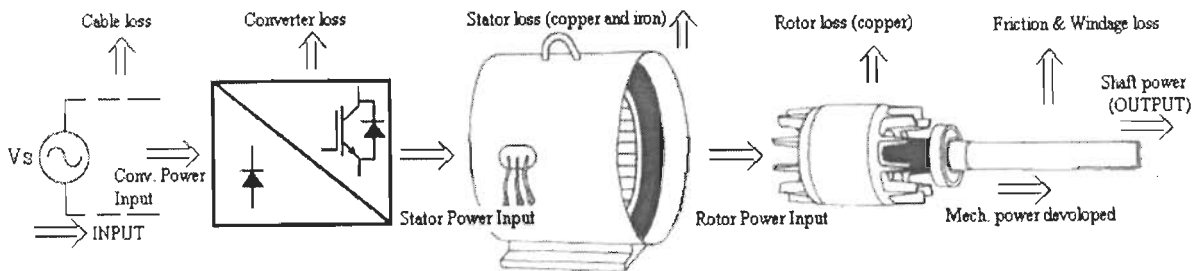
Fig. 2.12. Losses in the induction motor drive system

The induction machine should operate with the rated flux for the rated value of load torque, where as for load torque less than rated, the reduction of flux causes a reduction in iron losses and magnetizing current. For a very low load torque (up to about 15% of the rated value), energy saving work can reduce power loss by even 70-90% [64]. In this section, various controllers which are used to operate the motor with higher efficiency or reduced operating cost at partial load are discussed.

a) Star Connected Winding of Motor

Induction motors operation at light load, require less torque. Motor connection in star results reduced power consumption. When the motor run in star mode, the voltage applied to stator phase winding is reduced by the factor $\sqrt{3}$. Since the torque developed in the motor is directly proportional to square of the voltage, the developed torque in star mode is

also reduced by the factor 3. Therefore, the motor can be operated in star mode up to 0.33 p.u loads. In this case, the developed torque and temperature rise of the motor are to be measured and keep them normal. This method is not suitable for wide range of partial loads. This controller saves converter losses due to the absence of power electronic circuits and is shown in Fig. 2.13.
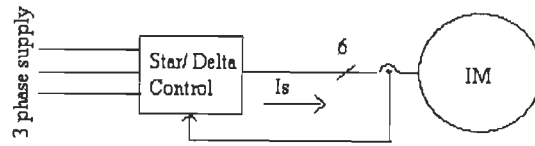
Fig. 2.13 Efficiency optimization by star/delta starter

b) *Variable Voltage and Fixed Frequency (VVFF) Control*

Three-phase induction motors have very large starting current, which can go up to eight times the current rated. This fact causes other energy users to be disturbed during such a start period, as it will cause a voltage drop on the electrical energy mains supply. In order to minimize this undesirable effect, soft start method is very recent electronic method [139] and it has been frequently used in industry. It consists in applying a voltage to the motor, which is gradually increased in a ramp wise manner, thus enabling the motor to start. Three-phase voltage controller is used which consists of two thyristors per phase in anti parallel connection, where the input is connected to the respective phase of the mains supply and the output to each motor phase. Soft starter is aimed at the application of a reduced voltage to the motor for its start and reduction of voltage at motor is low load. In this case the iron losses are decreased which results in energy conservation.

c) *Variable Voltage and Variable Frequency (VVVF) Control*

Constant V/f control is the scalar (variables are controlled in magnitude only) type control shown in Fig. 2.14 for minimizing the losses of induction motor at light load. The idea is to calculate, for specific operating point, the optimal V/f ratio (in other words the optimal flux), that assures minimum losses still allowing the required speed and torque [27]. Most of the industrial drives the dc link voltage and two or three phase currents are measured. In servo drives the speed may be measured in addition with these quantities [5].
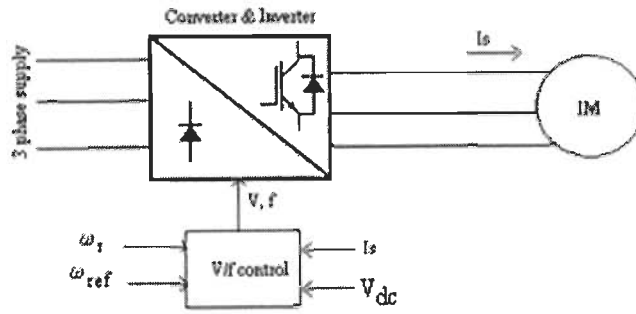
Fig. 2.14 Efficiency optimization by VVVF control

d) Displacement Power Factor Control

Variation in slip of induction motor causes variations in the motor terminal impedance and hence power factor, current and efficiency. While maintaining constant optimal slip by using automatic voltage controller the terminal impedance and hence power factor and efficiency remain constant at optimal values irrespective of load [76]. Even though power factor control implementation is so simple because of not requiring speed information, it is only valid for one specific motor [5].

e) Rotor Slip Frequency Control

In this control, optimum rotor slip frequency is calculated for a wide range of speed and torque of given motor and a look up table is constructed, shown in Fig. 2.15. The optimal efficiency slip can be calculated by using the equivalent circuit parameters of an induction motor. Presence of harmonics in inverter supply optimal slip calculation may not be accurate. The optimal slip frequency can also be calculated from the measurement of input power, output power of the motor, inverter frequency and slip frequency [129]. Stochastic algorithms can be used to find optimal value of slip from the loss model of the motor in accordance with load and speed with the objective of efficiency maximization or minimum input power. These calculation can be done offline and accommodate them in a table. In no case the constraints (line current and flux) should exceed than rated.
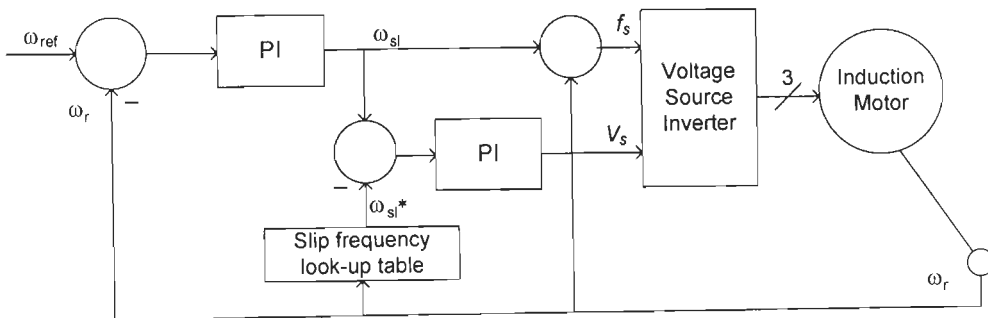
Fig. 2.15 Efficiency optimization by rotor slip frequency control

f) *Loss Model Control*

The loss model controller measures the speed and stator current and through the motor loss model determines the optimal air-gap flux [136]. The main problem of this approach is that it requires the exact values of machine parameters which include core losses and saturation of main inductance flux [66]. The inner part of control algorithm may be scalar or vector. NIA algorithms like differential evolution, particle swarm optimization, and genetic algorithm can be used for searching optimal flux/frequency level.

(i) Scalar Control

Scalar control technique is somewhat simple to implement, but the inherent coupling effect results in instability of the drive. At any operating point characterized by the speed ω_r and torque T, a combination of the voltage and frequency can be calculated to run the motor with minimum loss [94]. In loss model, formulation of total controllable losses in terms of frequency should be carried out first and then find its optimum point in which losses in the motor are minimum. The block diagram of this type of control is shown in Fig. 2.16.
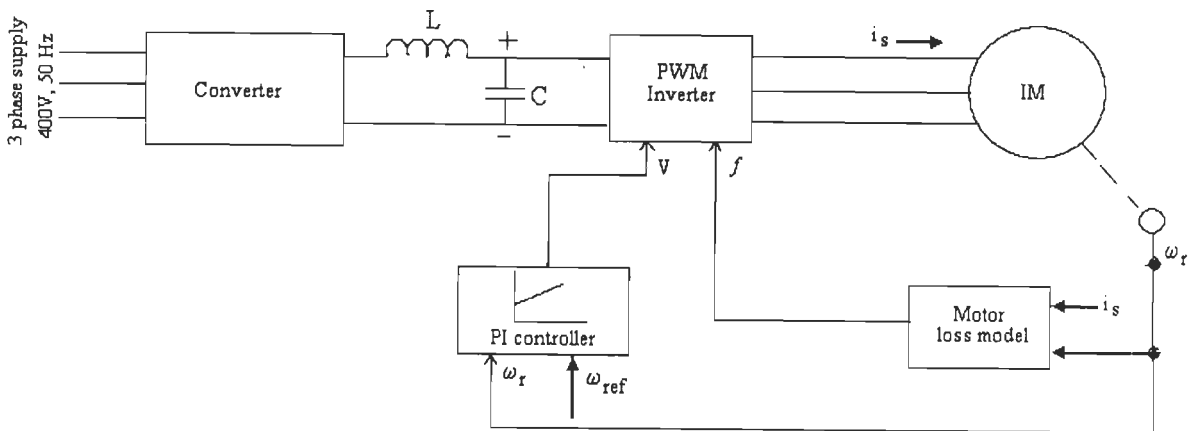
Fig. 2.16 Efficiency optimization in scalar controlled IM drive

(ii) Vector Control

In vector control, the variables are controlled in magnitude and phase. This technique of control needs more calculations than the standard V/f control [105]. In this control, the complex induction motor can be modeled as a DC motor by performing simple transformations. The field oriented controller generates the required reference currents to drive the motor. These currents are based on the reference torque. Torque producing current (i_{qs}) is generated by proportional-integral controller and flux producing current (i_{ds}) is generated by energy controller and are converted into three phase quantities. PWM current controller generates the pulses for inverter triggering circuits according to the error in the

currents between reference and actual values. The block diagram of vector control for IM efficiency optimization is shown in Fig. 2.17.
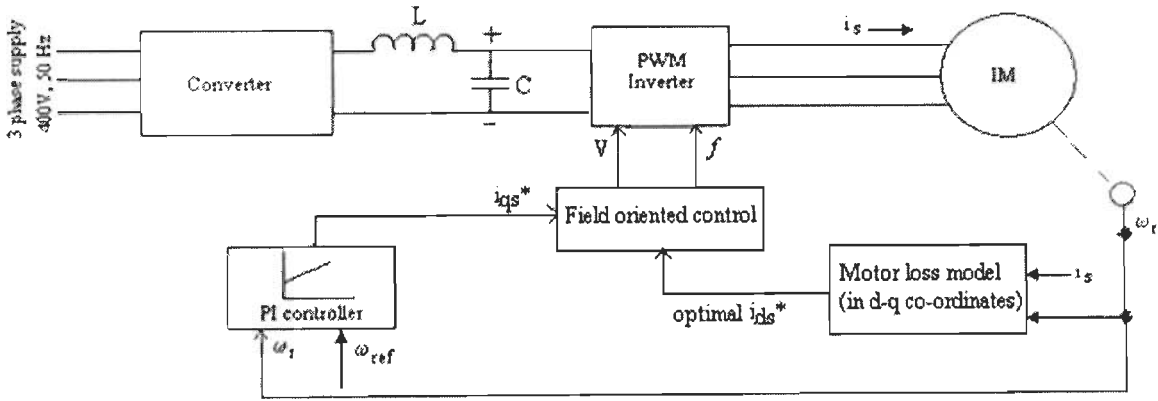
Fig. 2.17. Efficiency optimization in vector controlled IM drive

g) Search Control

This controller measures the input power or dc link power of the machine drive continuously and searches for an optimal flux value which results in minimum power input to the motor for given values of speed and torque. This technique is slow for reaching the optimum value and a ripple in steady state torque is always present. Minimum power input to the drive is achieved by adjusting inverter input frequency (scalar control) [86] or flux producing current (ids) (vector control) [171]. Based on the analysis in [119], rotor flux field orientation offers best optimal efficiency in comparison with other two vector control schemes namely, stator flux field orientation and air gap flux field orientation. The block diagram of search control for IM efficiency optimization is shown in Fig. 2.18.
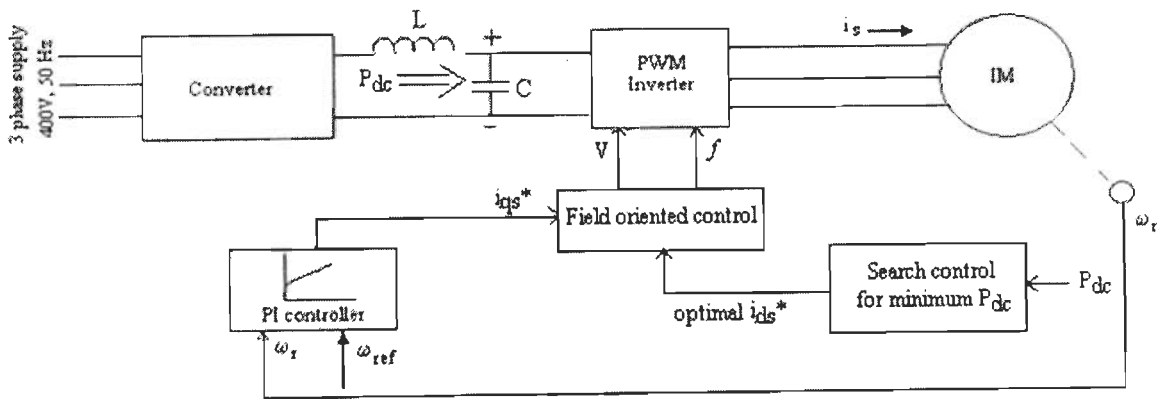
Fig. 2.18. Efficiency optimization through search control in IM drive

2.5 Optimal Design of Induction Motor

The design optimization consists of some proper optimization technique. There are various optimization techniques available and are discussed in chapter 4. But machine design optimization is not only running of a mathematical optimization an iterative procedure. There are some other important steps which are required to be followed before the implementation of the optimization technique. These steps are:

a) Selection of Objective Function

First of all for the design of the induction motor, some aim is to be set. The objective function to be maximized (minimized) should be chosen. The objective function is mostly chosen keeping in mind the customers demand and the profit of manufacturer. Objective functions may be the following:

- Active materials (production) cost
- Efficiency
- Starting torque
- Temperature rise
- Operating cost (energy cost)
- Harmonic current (incase of inverter fed supply)
- Torque ripple (incase of inverter fed supply)

b) Selection of Variables

After the selection of the objective function, the next important step is to select the variables. There are a number of variables available which affect the machine design. A very important problem in the IM design is to select the independent variables and the problem becomes very much complicated using too many variables [138]. Therefore variables selection is important in the motor design optimization and minimum possible number of variables is convenient to design the motor.

c) Selection of Constraints

To make a motor practically feasible and acceptable, the constraints have a big role in it. There are so many parameters which decide the good or bad performance of the motor. Just by optimizing one of the performance characteristics does not make a good design of the motor. Also it is not possible to obtain best performance in terms of all the performance parameters. Thus, it is necessary to check that the factors which affect the motor's performance are well within the limits, so that the motor could give a satisfactory and

reliable performance. These constraints play the most important role in the machine design. Hence the selection of constraints is an important issue. The constraint which gets most effected with the variation in the objective function should be considered with special care.

d) *Realisation of Design Results*

Once the motor's design results are obtained from the optimization algorithm, it is better to realize or justify the results before start of production. One of the motor computer aided design softwares, Scottish Power Electronics and Electrical Drives (SPEED) is used in the present work. This software is also used to minimize number of variables which are required to design the motor by performance evaluation before starting design optimization. Realisation of motor design results, using SPEED software, is presented in chapter 5.

2.6 Conclusion

An overview of the factors which are affecting induction motor losses along with experimental studies was presented initially and briefly explained how the efficiency of induction motor can be increased by providing efficient controllers and optimal design using advanced algorithms. Among many factors affecting motor efficiency, partial loading is the main potential for energy conservation. From the experimental study, it was observed as to how a small unbalanced supply voltage affects induction motor in terms of efficiency and operating cost. The steps involved in optimal design of induction motor are discussed. A brief introduction about the SPEED software is given.

Even though energy saving is obtained when the motor operate in star connection at low loads, it is not well suited for energy optimization over a wide range of loads. VVFF technique is not suitable for the motor that require high starting torque. The main advantage of search control is that it does not require the knowledge of the motor loss model for implementing optimization controllers. But the problem is that it requires ripple free dc link or input power measurement and more convergence time. Nowadays, researchers are concentrating more on search control with AI techniques than loss model control.

Mathematical Modeling of Induction Motor Drive for Optimal Energy Control

---

[This chapter deals with the mathematical model of the vector controlled induction motor drive. The complete induction motor drive scheme is explained in detail. The drive model consists of a front end diode converter, Pulse Width Modulation (PWM) inverter, induction motor, energy optimal controller and a speed controller. Stator reference frame induction motor model equations are derived. The motor-load system is represented by a set of first order non-linear differential equations. The switching models of the PWM inverter are described in order to emphasize their behaviour with respective loads. Optimal energy controller is designed through the loss models of entire variable speed drive systems to adjust the flux in accordance with the load. Fuzzy Pre-Compensated Proportional Integral (FPPI) controller is designed to solve stability problems in the drive during flux adjustment.]

3.1 Introduction

The induction motor (IM) drive receives power from three-phase ac supply and runs a mechanical load at desired speed. The drive model is developed so that it consumes minimum power from the utility supply system for the given values torque and speed. The model of the complete drive system is an integrated model of its constituents like front-end diode converter, PWM inverter, induction motor, resolver, load and controllers. The developed model of the drive system is used for current, speed and optimal energy controllers. The drive model is simulated on digital computer along with the designed controllers.

The model of the drive is developed using equivalent circuit representations of magnetically coupled circuits. The equivalent circuit of the induction motor is similar to that of a transformer. In the motor model, the expression of electromagnetic torque is established in terms of machines variables such as the current and the displacement of the mechanical system [92]. Induction motor is represented with a set of first order non-linear equations to analyze the drive.

In inverter models, one of the simple and preferred pulse width modulation (PWM) strategies, named Sinusoidal Pulse Width Modulation (SPWM) is used. SPWM is more popular

in inverters serving to industries. Inverter models are represented with different possible switching patterns and their corresponding output voltages.

Loss models of motor and converter for fundamental and harmonic frequencies are developed for optimal energy control. Loss model, search controllers and hybrid controllers are considered. The model based on calculation of optimal flux or flux producing current with respect to given load and speed and hence maximum efficiency / minimum power consumption is achieved in the drive systems. The conventional Proportional Integral (PI) controller and Fuzzy Pre-Compensated Proportional Integral (FPPI) are used as speed controllers. Few assumptions are made in developing the model of the drive. These assumptions make the analysis simple without loss of significant accuracy.

3.2 Induction Motor Drive

Fig. 3.1 shows the complete drive scheme. The drive scheme consists of three controlled parts, these are: front end diode converter, PWM inverter and induction motor. Others are optimal energy control and speed control. Converter and inverter are linked with a dc link capacitor. The front-end diode converter converts three-phase ac supply into dc supply. Source resistance (R) and inductance (L) are included and are connected in series with the input supply voltages (E_a, E_b, E_c). The PWM inverter fed induction motor drive draws power from the dc output of the front end diode converter. The PWM inverter feeds three-phase variable frequency and variable amplitude ac currents to the induction motor. The three-phase currents required by the induction motor are also controlled to be nearly sinusoidal by PWM current controller of the drive. The sinusoidal motor and supply currents are achieved by fast switching actions of IGBT power switches of the inverter and the converter. In PWM inverters, the output voltage and frequency are controlled within the inverter by varying the width of the output pulses. Hence at the front end, instead of a phase-controlled thyristor converter, a diode bridge rectifier can be used. A very popular and simple method of controlling the voltage and frequency is by sinusoidal pulse width modulation.
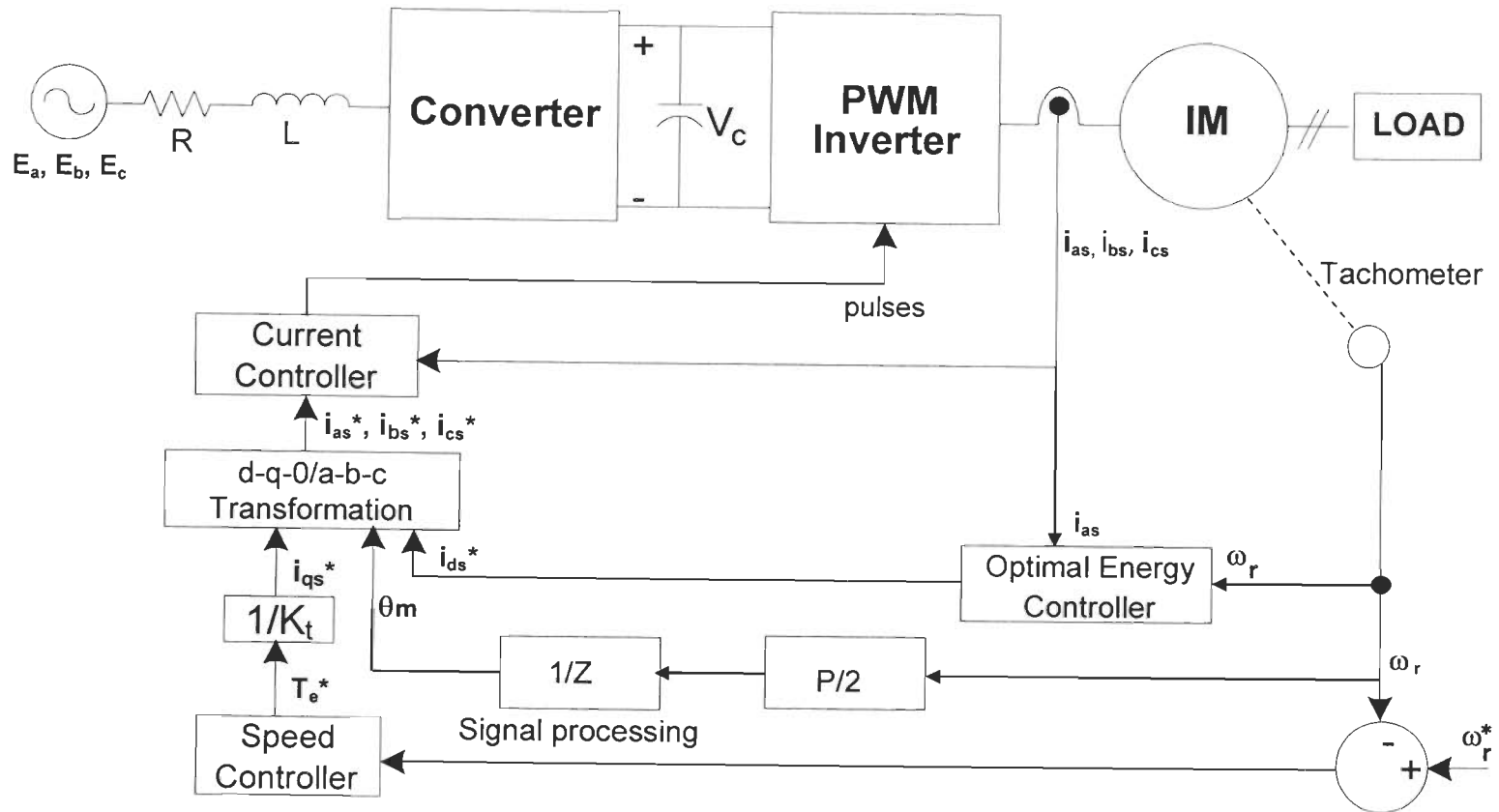
Fig. 3.1. Schematic block diagram of Induction motor drive scheme

The speed and stator currents are given to energy optimal controller of the induction motor drive, which generates flux producing current command. Particle Swarm Optimization (PSO) is used to find the optimal flux producing current of motor through its loss model. Continuous measurement of input power or dc link power is done when search control is incorporated in the optimal energy control block. Reference and actual motor speeds are given to speed controller of the IM drive, which generates torque command. Torque component of the current is obtained by dividing the torque command with the IM torque constant. The rotor position is calculated through digital signal processing for obtaining two phase (dq0-axis) to three phase (abc-axis) reference currents transformation. The PWM current controller of the IM drive compares the three-phase reference currents with the actual currents and generates switching signals for IGBT switching of the PWM inverter. The controlled switchings of the PWM inverter generates variable frequency variable magnitude three-phase sinusoidal motor currents to achieve desired speed with optimal efficiency (minimum loss).

3.2.1 Control Scheme of Induction Motor Drive

The inverter converts the dc link voltage into variable frequency and variable magnitude currents for the induction motor. To operate the inverter, only two stator currents are sensed and third current is negative sum of the two currents as shown in Fig. 3.2. Three phase reference currents are generated, which produce desired torque to accelerate and decelerate the motor for the desired speed regulation. The three-phase actual stator currents are compared with respective three-phase reference currents and current errors are produced. One PWM current controller is used for each phase. The three-phase current errors are sent to respective phase PWM current controllers. The current controller of phase 'a' provides switching signals for devices T_1 and T_4, current controller of phase 'b' provides switching signals for devices T_3 and T_6, and current controller of phase 'c' provides switching signals for devices T_5 and T_2 to regulate phase 'a', phase 'b' and phase 'c' currents respectively. The switching devices are IGBTs with inbuilt anti-parallel diodes for freewheeling action. The switching actions apply the dc link voltage across three-phase line-to-line terminals of the motor. The three phase currents are independently controlled in the stator reference frame and care is taken to avoid unbalancing of the currents. Variable frequency and regulated current are obtained through the PWM inverter as needed for the induction motor. PWM technique, flux angle calculation, inner current controller and outer speed controller of the drive are briefly explained in following section.

A number of control strategies have been successfully applied in the past to three phase converters and inverters, some of which include sinusoidal pulse width modulation (SPWM), hysteresis current control, indirect current control, SPWM with instantaneous current control, space vector modulation (SVM). The main aim of any modulation technique is to obtain variable output (voltage) having a maximum fundamental component with minimum harmonics. The SPWM technique is a simple and popular for industrial converters, which is used in the present work. The basic principle of the PWM technique involves the comparison of triangular carrier wave frequency with the fundamental frequency sinusoidal modulating wave.

The induction motor receives three-phase sinusoidal voltages at the stator terminals and produce rotating magnetic flux. This stator flux should be sinusoidal to obtain ripple free torque. Hence, the motor needs three-phase sinusoidal current to produce ripple free torque. As mentioned earlier the speed controller gives torque command. Using the torque command q-axis current command is calculated. Accurate position of the rotor is required to transform the rotor reference q-d axis currents into stator reference a-b-c axis currents. The reference slip frequency of the rotor is added to the sensed rotor speed and then a discrete integration is carried out to calculate the flux angle and hence rotor position. The rotor positions are sampled at a fixed time interval to obtain the speed of the motor. The speed controller utilizes rotor speed and current controller makes use of the rotor position to perform respective control actions.

The drive is controlled with two control loops i.e., inner PWM current control loop and outer speed control loop. Reference or command speed is compared with actual speed of the drive and speed error is processed through the speed controller. The output of the speed controller is torque command for the drive. The electrical torque of the drive is directly proportional to the q-axis current component (i_{qs}) of the induction motor. Dividing the torque command by torque constant, the q-axis current command is obtained.
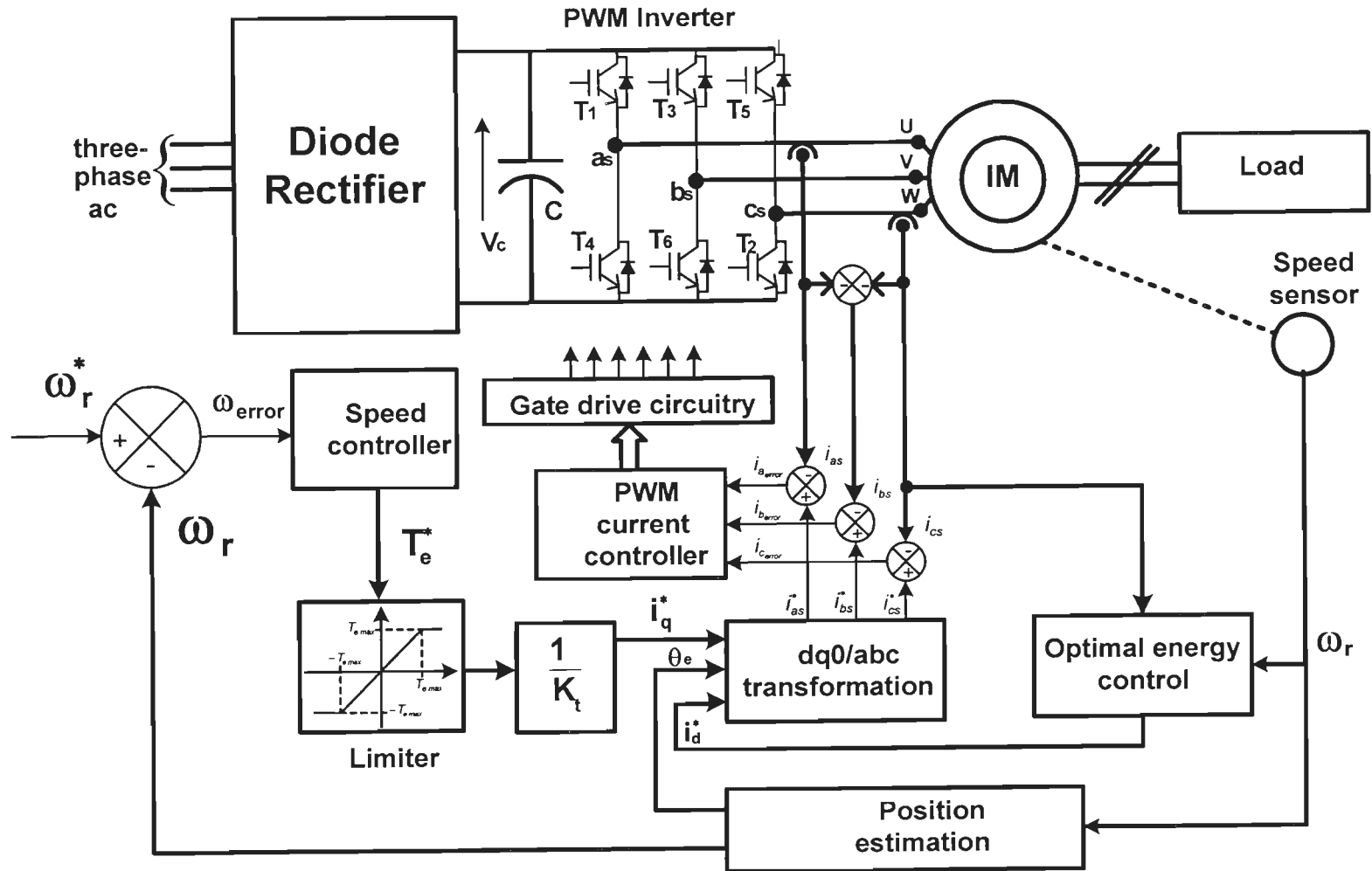
Fig. 3.2 Induction motor drive control scheme.

To get optimal efficiency of motor, energy controller produces optimal flux producing current (i_{ds}) command for the desired speed and load torque. Flux adjustment in the motor in accordance with the given load and speed results in loss minimization of the motor or entire drive systems. The reference values of the q-axis, d-axis currents and rotor position (angle) are used to calculate three-phase reference currents i_{as}^*, i_{bs}^* and i_{cs}^* using Park's transformation. Actual stator currents i_{as} and i_{cs} are sensed and the third current i_{bs} is calculated as the negative sum of the two sensed currents as shown in Fig. 3.2. The actual currents are compared with the reference currents and current errors are sent to respective PWM current controllers. Outputs of the current controllers are the desired switching pulses of the inverter switching transistors. The switching pulses are applied to the switching devices through the gate drive circuitry. The switching pulses generated by current errors i_{aerror}, i_{berror} and i_{cerror}, are applied to devices of inverter legs of phase-a, phase-b and phase-c respectively. Due to controlled switchings of the inverter devices PWM phase voltages are applied across the motor phase windings to obtain actual currents almost equal to the reference currents. Once the actual currents follow the reference currents, the desired torque is developed to track the reference speed of outer loop.

3.3 Mathematical Model of the Drive

The mathematical model of the drive scheme includes model of the induction motor, model of the PWM inverter, PI speed controller and detailed loss models of both motor and inverter. The assumptions made for the modeling of the drive scheme are as follows;

- The three phase stator windings of the induction motor are balanced and produce sinusoidally distributed Magneto Motive Force (MMF) in the space.
- The DC link voltage available at the input terminals of inverter are assumed ripple free.
- The three-phase sinusoidal currents flowing into the motor are also assumed ripple free.
- Switching transients in the inverter and converter are neglected.
- Switching transition times of the switching devices are negligible.
- Three-phase input currents to the converter are sinusoidal.

3.3.1 Induction Motor Model

The winding arrangement for a 2-pole, 3-phase, star connected, symmetrical induction machine is shown in Fig. 3.3 [93]. The stator winding are identical, sinusoidally distributed,

displaced 120^0 with resistance R_s. The rotor windings are also considered as three identical sinusoidally distributed windings, displaced 120^0 with resistance R_r. the dynamic model of the induction motor is derived by using a two phase motor in direct and quadratic axes. The *qd* reference frames are usually selected on the basis of convenience. The relationship of *abc* and *dq* axes are shown in Fig. 3.4. There are three reference frames used for the analysis of induction motor. They are: stationary, rotor and synchronously rotating reference frames. In the stationary rotating reference, the *qd* variables of the machine are in the same frame as those normally used for the supply network, used in the present work.
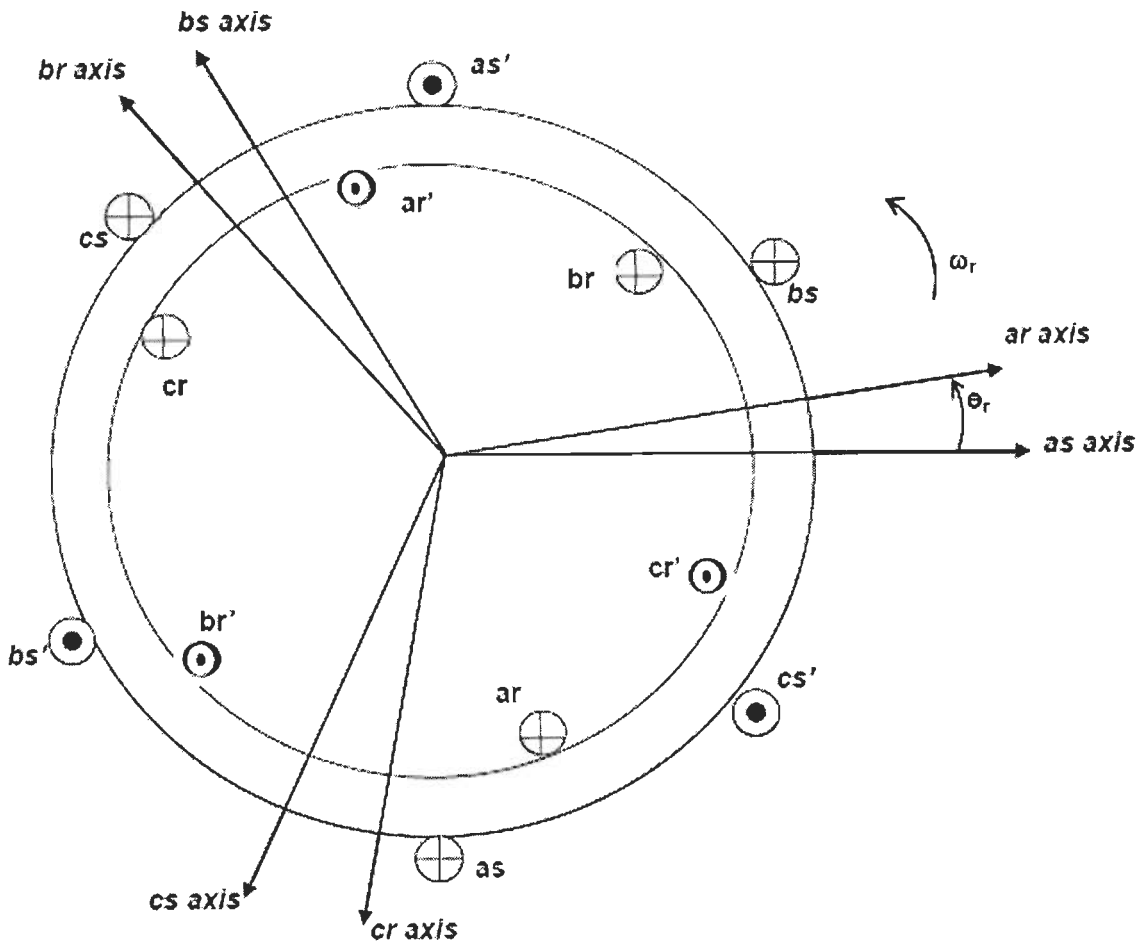
Fig. 3.3. Two-pole, three-phase, star connected symmetrical induction machine
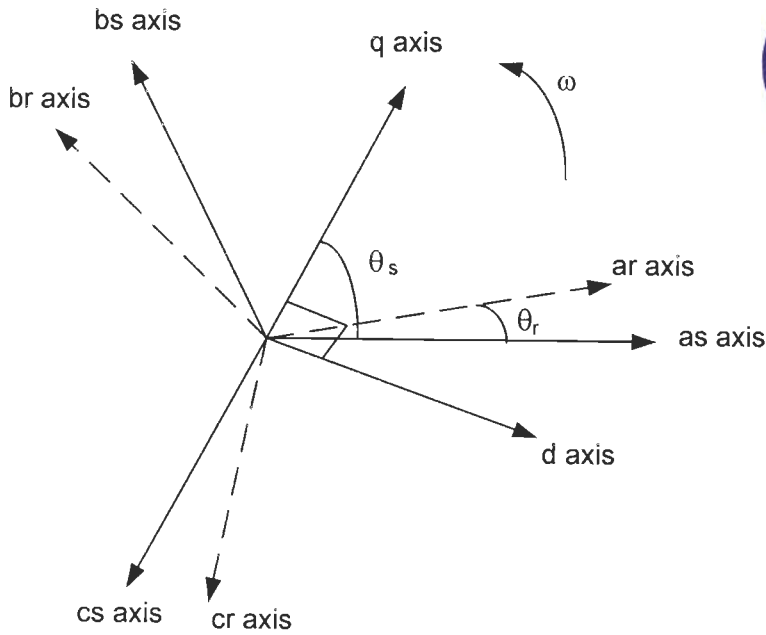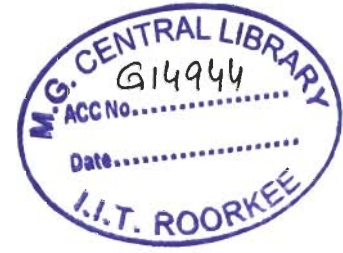
Fig.3. 4. Two-pole, three-phase symmetrical induction machine

The squirrel cage induction motor is modelled using *dq* theory in the stationary reference frame which needs fewer variables and hence analysis becomes easy. The voltage-current relationship in the stationary reference frame of the induction motor in terms of the d-q variable is expressed as [92]:

$$V = [R]i + [L]pi + [G]\omega_r i + [F]\omega_c i \qquad (3.1)$$

where the [R] matrix consists of resistive elements, the [L] matrix consists of the coefficients of the derivative operator *p,* the [G] matrix has elements that are the coefficients of the electrical rotor speed ω_r, and the [F] matrix is the frame matrix which has the coefficients of the reference frame speed ω_c. In the stationary reference frame the term $[F]\omega_c i$ is found to be identically zero, hence the Eq. (3.1) can be rewritten as:

$$[v] = [R][i] + [L]p[i] + \omega_r [G][i] \qquad (3.2)$$

Rearranging the Eq. (3.2), the current derivative vector can be expressed as follows:

$$p[i] = [L]^{-1}\{[v] - [R][i] - \omega_r [G][i]\} \qquad (3.3)$$

where '*p*' is the differential operator (d/dt) and 'ω_r' is the rotor speed in electrical 'rad/sec'. Three-phase induction motor is assumed to have balanced windings and connected with

balance supply voltages, thus the zero sequence components are zero and eliminate the zero sequence equations from the present analysis. Current and Voltage vectors are given as follows:

$$[i] = \begin{bmatrix} i_{qss} & i_{ds} & i_{qr} & i_{dr} \end{bmatrix}^T \tag{3.4}$$

$$[v] = \begin{bmatrix} v_{qs} & v_{ds} & v_{qr} & v_{dr} \end{bmatrix}^T \tag{3.5}$$

where v_{qs} and v_{ds} are the q- and d-axis voltages are applied across the stator windings and v_{qr} and v_{dr} are the q- and d-axis voltages across the rotor windings. As the rotor bars are short circuited in a squirrel cage induction motor, the voltages v_{qr} and v_{dr} are zero. Similarly the currents are also defined.

The three phase to two phase currents and voltages transformations are achieved by using the following equations:

$$\begin{bmatrix} i_{qs} \\ i_{ds} \end{bmatrix} = [T_{abc}] \begin{bmatrix} i_{as} \\ i_{bs} \\ i_{cs} \end{bmatrix} \text{ and } \begin{bmatrix} v_{qs} \\ v_{ds} \end{bmatrix} = [T_{abc}] \begin{bmatrix} v_{as} \\ v_{bs} \\ v_{cs} \end{bmatrix} \tag{3.6}$$

The transformation from two phase to three phase currents and voltages can be obtained as:

$$\begin{bmatrix} i_{as} \\ i_{bs} \\ i_{cs} \end{bmatrix} = [T_{abc}]^{-1} \begin{bmatrix} v_{qs} \\ v_{ds} \end{bmatrix} \text{ and } \begin{bmatrix} v_{as} \\ v_{bs} \\ v_{cs} \end{bmatrix} = [T_{abc}]^{-1} \begin{bmatrix} v_{qs} \\ v_{ds} \end{bmatrix} \tag{3.7}$$

$$\text{where, } [T_{abc}] = \frac{2}{3} \begin{bmatrix} \cos\theta_s & \cos\left(\theta_s - \frac{2\pi}{3}\right) & \cos\left(\theta_s + \frac{2\pi}{3}\right) \\ \sin\theta_s & \sin\left(\theta_s - \frac{2\pi}{3}\right) & \sin\left(\theta_s + \frac{2\pi}{3}\right) \end{bmatrix}$$

In the stator reference frame, q-axis usually aligns with the phase-a winding; this implies that the *qd* frames are fixed to the stator. In that case, $\theta_s=0$ (angle between stator axis and q axis, shown in Fig. 3. 4), and the relationship of *abc* to *dq* variables are given as:

$$[T_{abc}] = \frac{2}{3} \begin{bmatrix} 1 & -\frac{1}{2} & -\frac{1}{2} \\ 0 & -\frac{\sqrt{3}}{2} & \frac{\sqrt{3}}{2} \end{bmatrix}$$

The resulting induction motor equations with stationary reference frame is

$$\begin{bmatrix} v_{qs} \\ v_{ds} \\ v_{qr} \\ v_{dr} \end{bmatrix} = \begin{bmatrix} R_s + L_s p & 0 & L_m p & 0 \\ 0 & R_s + L_s p & 0 & L_m p \\ L_m p & -L_m \omega_r & R_r + L_r p & -L_r \omega_r \\ L_m \omega_r & L_m p & L_r \omega_r & R_r + L_r p \end{bmatrix} \begin{bmatrix} i_{qs} \\ i_{ds} \\ i_{qr} \\ i_{dr} \end{bmatrix} . \qquad (3.8)$$

The electromagnetic torque is obtained by:

$$T_e = \frac{3}{2} \frac{P}{2} L_m \left(i_{qs} i_{dr} - i_{ds} i_{qr} \right) \qquad (3.9)$$

At the steady state condition of the motor, Eq. (3.9) can be rewritten as

$$T_e = K_t i_{qs} \qquad (3.10)$$

where, $K_t = \frac{3}{2} \frac{P}{2} L_m^2 i_{ds}$ is a torque constant which depends on air gap flux. In the present study, air gap flux is also adjusted to run the motor at optimal efficiency. Hence this constant is valid only for steady state operation. P is the number of poles in the motor.

3.3.2 PWM Inverter Model

Fig. 3.5 shows a circuit diagram of the PWM inverter fed induction motor. The three-terminal voltages of the induction motor are denoted by 'a$_s$', 'b$_s$' and 'c$_s$' to represent the three phases of stator windings and these are connected to three legs of the inverter. DC link voltage is represented by a dc voltage source V$_c$ and three voltages E$_{Ba}$, E$_{Bb}$, and E$_{Bc}$ represent back emfs of induction motor windings. There are six transistor switches in the inverter (180° conduction mode) with inbuilt anti-parallel diode in parallel to each transistor switches to provide for freewheeling path. Gate signals of transistors are denoted as *a, b, c, a', b', c'*. A device is in 'ON' state if a high gate pulse is applied or the antiparallel diode across it is conducting. Similarly, the device is defined in the 'OFF' state if a low gate pulse is present and it's anti parallel diode is not freewheeling. In the inverter legs, at any instant; if upper transistor switch or it's parallel diode is 'ON' then lower switch and it's parallel diode of the corresponding leg is 'OFF' and vice-versa. It is assumed that T$_1$ and T$_4$, T$_3$ and T$_6$ as

well as T_5 and T_2 are switched in complementary way. Thus there are 8 possible switching vectors presented in Table 3.1 and their equivalent circuits are shown in Figs. 3.6(a) to 3.6(h). If all the upper switches of the three legs are simultaneously 'ON', the magnitude of voltages applied across the phase windings is zero as shown in Fig. 3.6(g). Similarly, when the three switches of the lower legs are simultaneously 'ON', the voltage applied across the three-phase windings is zero, i.e., the terminals of the induction motor are short-circuited as shown in Fig. 3.6(h). The transformed values of the stator phase and line voltages of the motor for each switch position are also given in the Table 3.1.
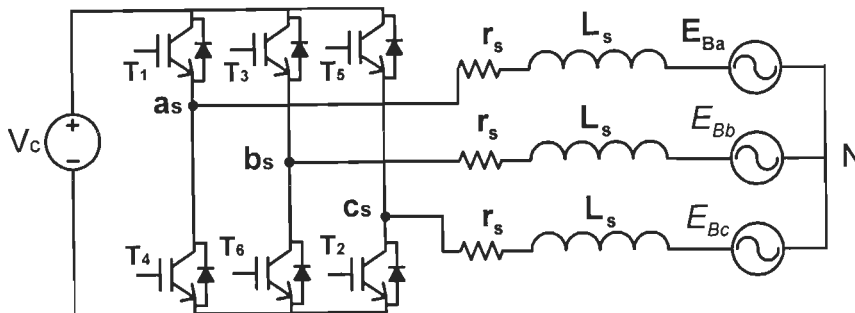
Fig. 3.5 Schematic diagram of PWM Inverter and equivalent circuit of IM.

Table 3.1 Switching Vectors of PWM Inverter and the Corresponding Output Voltages

SI. No	Switching States (1 = ON, 0 = OFF)	Line-Neutral Voltage			Line-Line Voltage		
	$(T_1,T_2,T_3,T_4,T_5,T_6)$	V_{as}	V_{bs}	V_{cs}	V_{ab}	V_{bc}	V_{ca}
1	(1,1,1,0,0,0)	$\dfrac{V_c}{3}$	$\dfrac{V_c}{3}$	$-\dfrac{2V_c}{3}$	0	1	-1
2	(0,1,1,1,0,0)	$-\dfrac{V_c}{3}$	$\dfrac{2V_c}{3}$	$-\dfrac{V_c}{3}$	-1	1	0
3	(0,0,1,1,1,0)	$-\dfrac{2V_c}{3}$	$\dfrac{V_c}{3}$	$\dfrac{V_c}{3}$	-1	0	1
4	(0,0,0,1,1,1)	$-\dfrac{V_c}{3}$	$-\dfrac{V_c}{3}$	$\dfrac{2V_c}{3}$	0	-1	1
5	(1,0,0,0,1,1)	$\dfrac{V_c}{3}$	$-\dfrac{2V_c}{3}$	$\dfrac{V_c}{3}$	1	-1	0
6	(1,1,0,0,0,1)	$\dfrac{2V_c}{3}$	$-\dfrac{V_c}{3}$	$-\dfrac{V_c}{3}$	1	0	-1
7	(1,0,1,0,1,0)	0	0	0	0	0	0
8	(0,1,0,1,0,1)	0	0	0	0	0	0
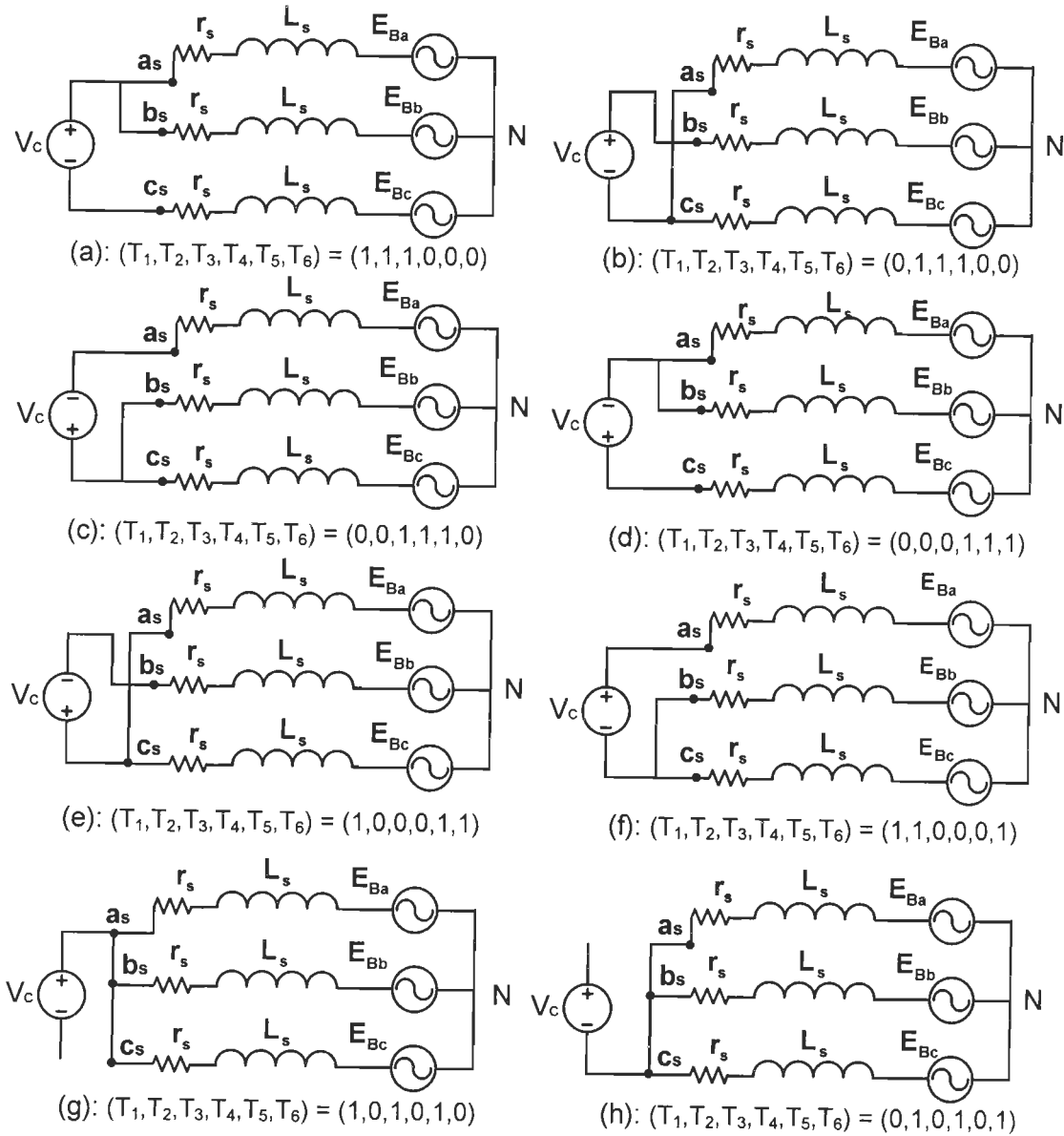
Fig. 3.6 Motor winding connections with respect to different switching vectors

3.4 Speed Controller

Proportional Integral (PI) controller can be used to control the speed of induction motor. The Proportional Integral and Differential (PID) controller is normally avoided because differentiation can be problematic when input command is a step. Generally the speed error, which is the different of reference speed ($\omega_{r(n)}{}^{*}$) and actual speed ($\omega_{r(n)}$), is given as input to the controllers. These speed controllers process the speed error and give torque value as an input. Then the torque value is fed to the limiter which gives the final value of reference torque. The speed error and change in speed error at n^{th} instant of time are given as;

$$\omega_{r\,e(n)} = \omega_{r(n)}^{\textstyle *} - \omega_{r(n)} \tag{3.11}$$

$$\Delta\omega_{r\,e(n)} = \omega_{re(n)} - \omega_{re(n-1)} \tag{3.12}$$

Two speed controllers are used in the present work. They are: PI controller and Fuzzy Pre-Compenstaed PI (FPPI) controller.

3.4.1 PI Speed Controller

The PI speed controller is the simplest speed controller as compared to any other speed controller. The general block diagram of the PI speed controller is shown in Fig 3.7. The output of the speed controller (torque command) at n^{th} instant is expressed as follows:

$$T_{e(n)} = T_{e(n-1)} + K_p \Delta\omega_{re(n)} + K_i \omega_{re(n)} \tag{3.13}$$

Where, $T_{e(n)}$ – torque output of the controller at the nth instant

K_p, K_i – are proportional and integral gain constants respectively

A limit of the torque command is imposed as

$$T_{e(n+1)} = \begin{cases} T_{e\,max} & for \quad T_{e(n+1)} \geq T_{e\,max} \\ -T_{e\,max} & for \quad T_{e(n+1)} \leq -T_{e\,max} \end{cases} \tag{3.14}$$

The gains of PI controller shown in Eq. (3.13) can be selected by many methods like trial and error method, Ziegler-Nichols method and evolutionary techniques based searching. Trial and error method is used in the present work. The numerical values of these controller gains depend on the ratings of the motor.
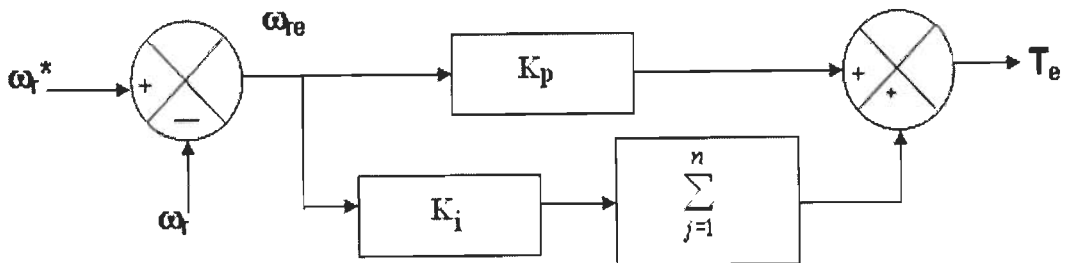
Fig. 3.7 Block diagram of PI speed controller

3.4.2 Fuzzy Pre-Compensated PI Speed Controller

The PI speed controller which is discussed in the previous section is simple in operation and zero steady state error when operating on load. But, the disadvantages of this PI controller is the occurrence of overshoot while starting, undershoot while load application and overshoot while load removal. Furthermore, it requires motor model to determine its gains and is more sensitive to parameter variations, load disturbances and suffer from poor performance when applied directly to systems with significant nonlinearities [82], [95]. These disadvantages of PI controller can be eliminated with the help of a Fuzzy Logic (FL) controller which need not require model of the drive and can handle nonlinearity of arbitrary complexity. But the disadvantage of FL speed controller is the occurrence of steady state speed error.

Hence to derive the advantages present in both PI and FL controllers, Fuzzy Pre-Compensated PI (FPPI) controller is used in which both PI and FL controllers are used. Fuzzy pre-compensation means that the reference speed signal (ω_r^*) is altered in advance using fuzzy logic in accordance with the rotor speed (ω_r), so that a new reference speed signal (ω_{r1}^*) is obtained and the main control action is performed by PI controller. Some specific features such as overshoot and undershoot occurring in the speed response which are obtained with PI controller can be eliminated [150] and this controller much useful to present work, mine hoist load, where torque/speed of the motor varies very frequently.

As usual, the inputs to the FL are speed error ($\omega_{re(n)}^*$) and the change in speed error ($\Delta\omega_{e(n)}$) and the output of the FL controller is added to the reference speed to generate a pre-compensated reference speed (δ), which is to be used as a reference speed signal by the PI controller shown in Fig. 3. 8.The fuzzy pre-compensator can be mathematically modeled as follows [28]:
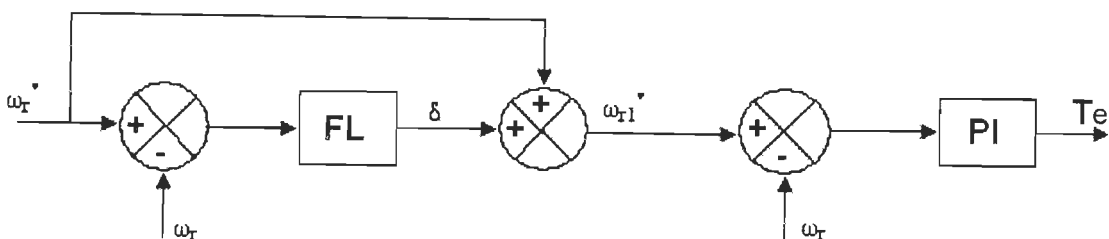
Fig. 3.8 Block diagram of FPPI speed controller

Referring to the Eqs. 3.11 and 3.12 for speed error and change in speed error, Pre-compensated speed reference (δ) and updated new reference speed ($\omega_{r1}^{\cdot}$) can be calculated as

$$\delta_{(n)} = F[\omega_{re\,(n)}, \Delta\omega_{re(n)}] \tag{3.15}$$

$$\omega_{r1}^{\cdot} = \delta_{(n)} + \omega_{r(n)}^{*} \tag{3.16}$$

where F is fuzzy logic mapping

Fuzzy rules of this controller are shown in Fig. 3.9 where the fuzzy variables are: NB stands for negative-big, NM for negative-medium, NS for negative-small, ZE for zero, PB for positive-big, PM for positive-medium and PS for positive small. The corresponding fuzzy rule table is shown in Table 3.2.

Table 3.2 Logic Rules for Fuzzy Logic (FL) Speed Controller

ω_{re} / $\Delta\omega_{re}$	NB	NM	NS	ZE	PS	PM	PL
NB				NB	NB		
NM	NB			NB	NB		
NS	NB			NM	NM	NM	PM
ZE	NB	NM	NS	ZE	PS	PM	PB
PS	NM		PS	PS	PM		
PM				PM	PB	PB	
PL			PM	PM	PB		
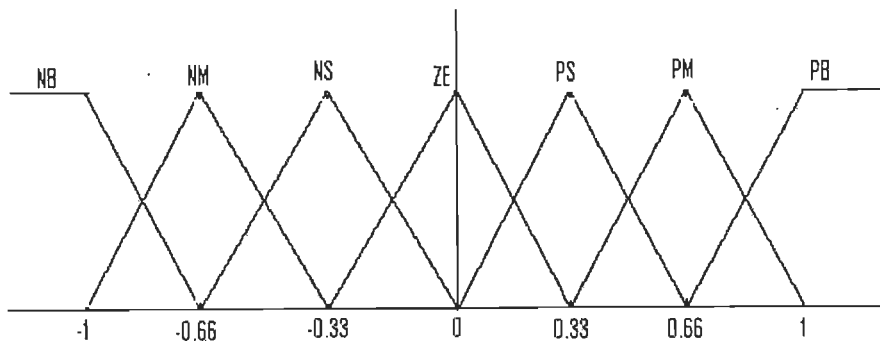
Fig. 3.9. Fuzzy sets considered for speed control

3.5 Loss Model for Induction Motor Drive

Variable speed electrical motor drive technology has advanced dramatically in the last two decades with the advancement of power electronic devices and magnetic materials [147]. The variable speed induction motor drive system consists of three distinguish elements such as controllable power converter, an electric motor which drives a load (mechanical) at controllable speed and also driver controllers such as speed, current and optimal energy controller [112]. Fig. 3.10 [5] shows the power flow through an electrical motor drive systems form the power station to the load (pump, hoist, etc). In every parts of the chain there are losses associated with transportation of energy.
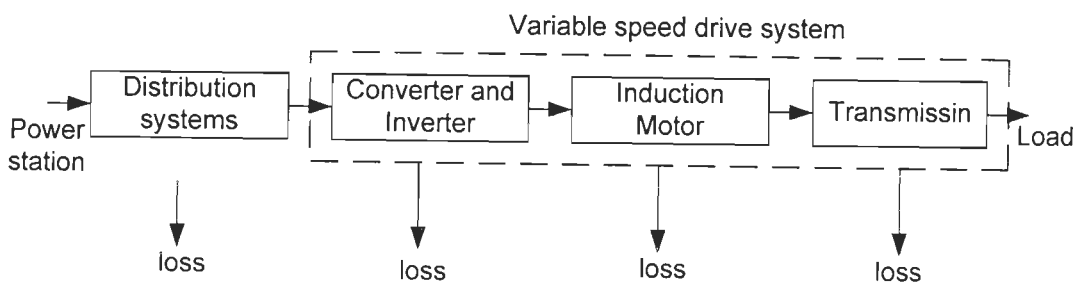
Fig. 3.10 Power flow in variable speed drives

Distribution system: Transmission lines, distribution transformer and distribution lines. Copper loss (I^2R) is significant in the distribution systems.

Converter: Power electronic unit controls the stator voltage and frequency of the motor in accordance with the desired operation. The losses in the power electronic unit consist mainly of semiconductor switching losses and conduction losses in the chokes.

Motor: The losses in the induction motor are divided into a number of loss terms, connected with specific parts of the machine which comprises copper loss in the stator and rotor, iron losses due to eddy current and hysteresis, stray loss arise on the copper and iron of the motor and friction losses.

Transmission: Losses due to the contact of motor shaft gear and belts.

The present work considers motor and converter losses to develop loss minimization algorithm.

3.5.1 Induction Motor losses

The equation of efficiency in any system is given by

$$\eta = \frac{output}{input} \tag{3.17}$$

In case of induction motor drive, the output is the power supplied by the motor to drive the load (product of shaft load and its speed) and the input is the power consumed by the total system including motor, converter circuits and cables. Since the efficiency of induction motor or any system depends on the total losses associated with it, Eq. 3.17 is rewritten as

$$\eta = \frac{output}{output + losses} \tag{3.18}$$

The losses in the IM drive system are divided into a number of loss terms, connected with specific parts of the machine. The power losses in the induction motor are portions of the input power that eventually transform to heat rather than driving load. The fundamental frequency losses can be classified as below [60] and are illustrated in the model shown in Fig. 3.11.

1. Power losses in the stator windings due to stator currents and stator resistance R_s.
2. Power losses in the rotor bars and end rings due to rotor currents
3. Iron core losses due to magnetic losses in the laminations, inductance and eddy current losses.
4. Stray losses due to stator and rotor slotting, distributed stator and rotor MMFs and slot and overhang leakages. This loss is more in the high frequency inverter fed supply voltages.
5. Winding and friction losses due to mechanical drag in bearings and cooling fan.

In addition to the fundamental frequency losses in induction motor, it also offers harmonic losses due to voltage- time harmonics when it is connected to static converter. These losses depend on the type of converter and the pulse width modulation used with it. [20].
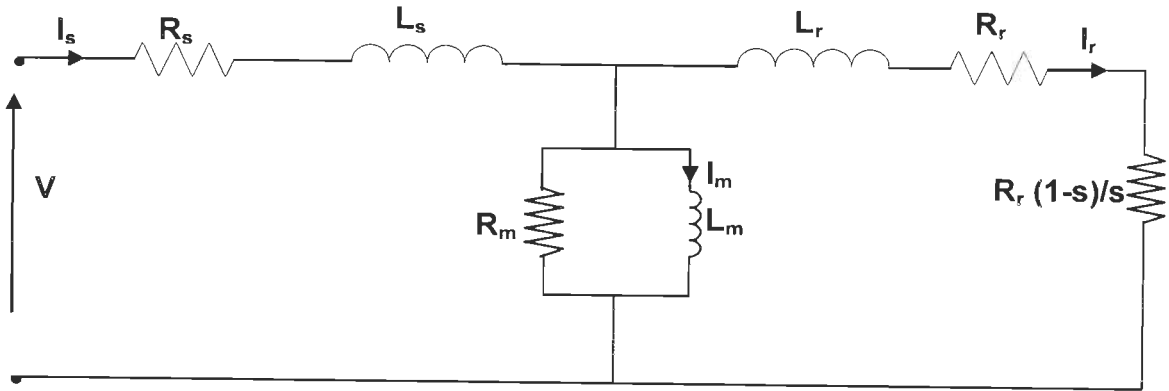
Fig. 3.11 Simple equivalent circuit of induction motor

a) Stator Resistance Loss

The resistance R_s in the equivalent circuit model, shown in Fig. 3.11, will generate heat in the stator winding of the motor which is proportional to the square of the current. The stator copper loss per phase, P_{cus} in watts is calculated by

$$P_{cus} = I_s^2 R_s$$

(3.19)

where, Rs – stator resistance per phase and I_s – stator current

It is known that the stator resistance will vary in accordance to the temperature and the adjustment is needed to get correct value of stator resistance. With the winding resistance value, R_{so}, available at a known temperature T_o, the resistance, R_{st}, at any other temperature T, can be determined [73] by.

$$R_{st} = R_{so} \frac{(T + K_{cu})}{T_o + K_{cu}}$$

(3.20)

where, R_{so} – stator resistance at known temperature T_o

K_{cu} – temperature coefficient for copper

b) Rotor Resistanc Loss

The rotor copper loss per phase, P_{cur}, is calculated by

$$P_{cur} = I_r^2 R_r$$

(3.21)

where, R_r – rotor resistance per phase

I_r – rotor current

Similar to stator resistance, rotor resistance corrected for any temperature (T) and is determined using Eq. (3.22):

$$R_{rt} = R_{ro} \frac{(T + K_{al})}{T_o + K_{al}}$$ (3.22)

where, R_{ro} – rotor resistance at known temperature T_o

K_{al} – temperature coefficient for aluminium

c) Core Losses

In general, core losses arise both due to the induced currents in the core as well as the hysteresis characteristics of the core material. If the magnetic field set up in a ferromagnetic core is time varying, the field will induce a voltage in the core and thus cause current flow within the core itself. Due to the finite resistance of the core material, a resulting power loss occurs [167]. These losses can be modelled in terms of hysteresis and eddy current losses [154] and are given by

$$P_h = K_h f \Phi_m^2$$ (3.23)

$$P_e = K_e f^2 \Phi_m^2$$ (3.24)

Where, P_h – hysteresis loss

P_e – eddy current loss

K_h – hysteresis coefficient given by material and design of motor

K_e – eddy current coefficient given by material and design of motor

f – fundamental frequency of stator voltage

Φ_m – mutual flux or air-gap flux

The total stator core loss, P_{cs}, is determined by

$$P_{cs} = P_h + P_e = P_{cs} = K_h f \Phi_m^2 + K_e f^2 \Phi_m^2$$ (3.25)

The rotor core loss, P_{cr}, is calculated by using the Eq. (3.25) but with slip frequency instead of stator frequency

$$P_{cr} = K_h (sf) \Phi_m^2 + K_e (sf^2) \Phi_m^2$$ (3.26)

where s – slip

Total core loss at fundamental frequency is

$$P_c = P_{cs} + P_{cr} = \left[K_h \left(\frac{1+s}{f} \right) + K_e (1+s^2) \right] f^2 \Phi_m^2 \qquad (3.27)$$

where, P_c - Total core losses of the motor.

As the mutual flux Φ_m is related to air-gap voltage V_m and core coefficient K_c

$$\Phi_m = \sqrt{K_c} \, \frac{V_m}{f} \qquad (3.28)$$

Equation (3.27) can be rewritten as

$$P_c = K_c \left[K_h \left(\frac{1+s}{f} \right) + K_e (1+s^2) \right] V_m^2 \qquad (3.29)$$

The equivalent core loss resistance, R_m can be determined by

$$R_m = \frac{1}{K_c \left[K_h \left(\frac{1+s}{f} \right) + K_e (1+s^2) \right]} \qquad (3.30)$$

With the consideration of harmonics, assuming the coefficients K_h and K_e remain same at harmonic frequency, and since harmonic slip $s_n=1$, the equivalent core loss resistance R_{mn} at harmonic frequency f_n can be obtained by

$$R_{mn} = \frac{0.5}{K_c \left(\frac{K_h}{f_n} + K_e \right)} \qquad (3.31)$$

The simplified expression for the core losses in the induction motor by neglecting rotor iron losses is given by [86]

$$P_c = (K_e f^2 + K_h f) \Phi_m^2 \qquad (3.32)$$

d) Stray Load Loss

The stray losses are high frequency losses in the induction motor caused by space harmonics in the air-gap flux. Magneto Motive Forces (MMF) of the motor-load currents, which divert some of the no-load magnetic flux into leakage paths, thereby creating flux

pulsations and eddy currents losses in the laminations, conductors and adjacent metal parts [7]. Stray losses can be represented by a group of losses and empirical equations can be used to evaluate them which require the knowledge of machine dimensions, type of core material, lamination thickness, winding geometry, etc. [154]. These losses can be divided into six components [7],

1. The eddy current losses in the stator copper due to slot leakage flux.
2. The losses in the motor end structure due to end leakage flux
3. The high frequency rotor and stator surface losses due to the zigzag leakage flux
4. The high frequency tooth pulsation and rotor I^2R losses due to zigzag leakage flux
5. The six times frequency rotor I^2R losses due to circulating currents induced by the stator belt leakage flux.
6. The extra iron losses in motors with skew leakage flux.

The stray losses can be modelled in a way similar to that used for core loss modelling. The stator stray loss per phase at harmonics frequency f_n can be given as (3.33) [154].

$$P_{strn} = K_{strn}\left[\frac{K_h}{f_n} + K_e\right]V_{sn}^2 \qquad (3.33)$$

Where P_{strn} – stray load loss at harmonic frequency

K_{strn} – stray loss constant at n^{th} harmonic frequency

V_{sn} – voltage across the stator leakage inductance at harmonic frequency

The losses at harmonic frequency can be represented by an equivalent resistance R_{strn} in parallel with leakage inductance as (3.34).

$$R_{strn} = \frac{1}{K_{strn}\left[\dfrac{K_h}{f_n} + K_e\right]} \qquad (3.34)$$

The expression of voltage across the stator leakage inductance, V_s is

$$V_s = 2\pi L_s I_s \qquad (3.35)$$

For the fundamental frequency, stray loss can be modelled as Eq. (3.36) by substituting the Eq. (3.35) in Eq. (3.33). Since the rotor current in a squirrel cage induction motor is not

measurable it is common practice to express the stray load losses as function of stator current.

$$P_{str} = K_{str} \left[K_h f + K_e f^2 \right] I_s^2$$ (3.36)

where P_{str} – stray load loss at fundamental frequency

K_{str} – stray loss constant at fundamental frequency

V_s – voltage across the stator leakage inductance at fundamental frequency

I_s – stator fundamental current

f - fundamental frequency

The equivalent resistance R_{str} can be represented in series with the stator leakage reactance as given in Eq. (3.37).

$$R_{str} = K_{str} \left[K_h f + K_e f^2 \right]$$ (3.37)

The simplified equation for the stray load losses is given by [86]

$$P_{str} = K_{str} f^2 I_r'^2$$ (3.38)

where, $I_r'^2$ – rotor current referred to stator

e) Mechanical Losses

The main reasons of mechanical losses appearing in the induction motor are friction and windage losses. These losses are relatively a small percentage of the total motor losses are separated by the four components [38]. These are: friction loss in the bearing, windage loss of outside fan, friction air losses of rotor and windage losses of internal fans and finally friction power loss of V-ring seals. Normally, total mechanical losses are approximated by the researchers [147], [86] which is given by:

$$P_{mech} = C_{fw} \omega^2$$ (3.39)

where, ω - speed of the rotor

C_{fw} – mechanical loss coefficient

P_{mech} – mechanical power loss

f) Harmonic Motor Losses

The concept of operating a converter fed induction motor at significantly higher frequency than conventional 50-60 Hz range results high frequency harmonic losses. Fig. 3.12 [118] illustrates the frequency dependent losses. The conductor losses tend to decrease with the increasing in value of frequency. On the other hand core losses increase slowly as the frequency increases. This implies there is some time harmonic frequency when the total losses are a minimum. The location of this minimum is design dependent, the ratio of low frequency core and copper losses being an important parameter.
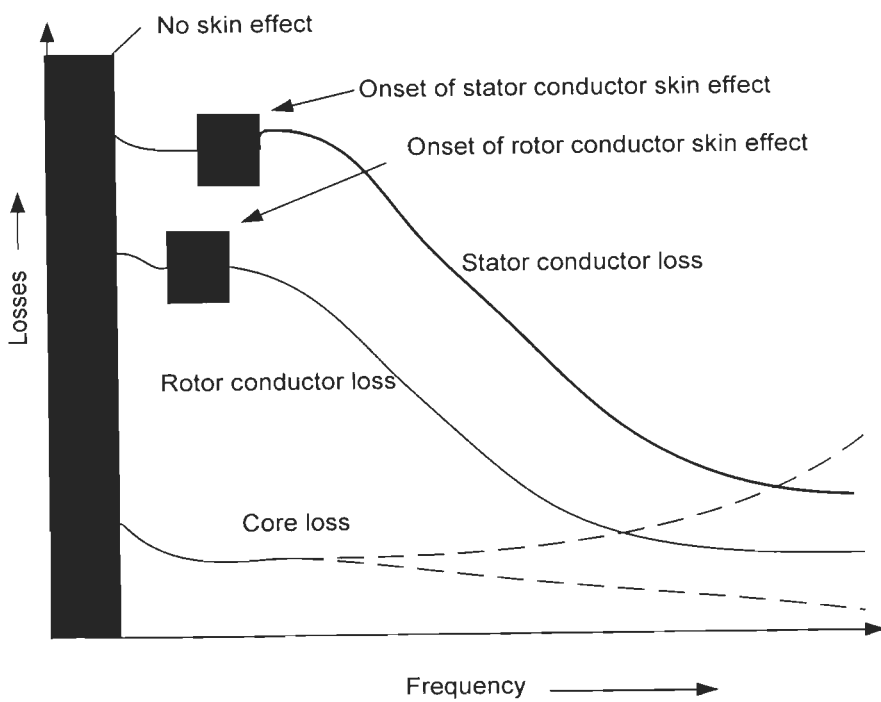
Fig. 3.12 Variation of time harmonic losses with frequency

Total high frequency conductor losses (stator and rotor) per phase can be calculated as in Eq. (3.40) [118].

$$P_{cuh} = I_h^2 (R_s + R_r) \qquad (3.40)$$

Where, P_{cuh} – harmonic conductor losses per phase

I_h – harmonic current which depends on harmonic frequency and leakage reactance

R_s, R_r – stator and rotor resistances respectively which are also frequency dependent.

3.5.2   Loss model of Converter and Inverter Systems

Fig. 3.13 shows the variable speed drive system which consists of diode rectifier and IGBT (Insulated Gate Bi-polar Transistor) inverter. Snubber circuits of inverter are ignored for the ease of illustration of the system. Loss models of converter and inverter have been derived in this section. These losses can be classified as follows [5]. In a diode rectifier, the switching loss can be neglected and the conduction loss needs to be considered [154].

1. Rectifier conduction loss
2. Losses in the power supply unit
3. Choke conduction losses
4. Inverter losses
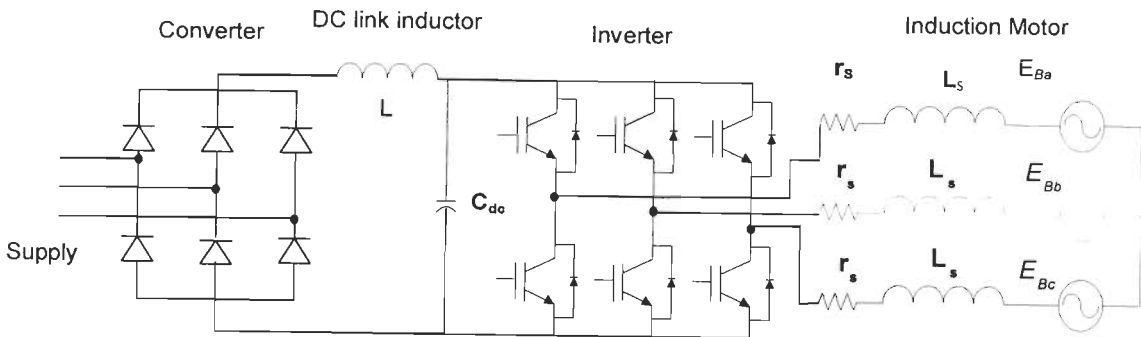
Fig. 3.13 PWM inverter fed induction motor drive

The loss of the three-phase diode rectifier is calculated knowing that two diodes are conducting at a time:

$$P_{rect} = 2V_D I_{dc} = 2V_D \frac{P_{outdc}}{V_{dc}}$$

(3.41)

where, V_{dc} – diode forward voltage

P_{rect} – rectifier loss

P_{outdc} – diode rectifier output power

V_{dc} – dc link votage

Due to internal resistance of the power supply (transformer), it offers power loss which depends on the size (rating) of power supply unit. The power supply can be modelled as constant load and its power consumption is determined as the power input to the converter when the inverter is switching, but without a motor connected to the output.

The approximate conduction losses in the dc link chokes, P_{choke}, are calculated as:

$$P_{choke} = R_{choke} \left(\frac{P_{in_{inv}}}{V_{dc}} \right)^2 \qquad (3.42)$$

where, R_{choke} – total dc resistance in the dc link inductor

$P_{in_{inv}}$ - rectifier output or inverter input power

V_{dc} - dc link voltage

Inverter switching losses can be calculated by measuring the transistor turn-on loss, the transistor turn-off loss and th diode turn-off loss. The total inverter losses (both conducting and switching) can be calculated as function of stator current and switching frequency [5].

$$P_{inv} = f\left(I_s, f_{sw}, \varphi, m_i \right) \qquad (3.43)$$

where, P_{inv} – total inverter losses

I_s – stator current

F_{sw} – swithing frequency

φ – phase shift angle

M_i – modulation index varying from 0 to1

These losses can be approximated as Eq. (3.44) [66].

$$P_{inv} = K_{inv1} I_s + K_{inv2} I_s^2 \qquad (3.44)$$

where, K_{inv1} and K_{inv2} are the switching constant.

3.6 Model Based on Optimal Energy Control

The part load efficiency of induction motor can be improved by adjusting the flux level of the motor with the help of optimal energy controllers. Different types of optimal energy controllers for induction motor have discussed in the section 2.3 (chapter 2). In the present work, three methods are used to optimize the energy consumption (in other words efficiency improvement) of the motor for a given load and speed, namely: loss model control (LMC), search control (SC) and hybrid of LMC and SC controllers. It is noted that the LMC approach requires the exact values of machine parameters which includes core losses and

main inductance flux saturation. Loss model equations are derived from the equivalent circuit of the motor and are expressed in the next section.

3.6.1 Loss Model Controller

Fig. 3.14 [86] shows the modified per phase equivalent circuit of induction motor which includes stray losses in terms of stray resistance R_{str} connected in series with stator leakage reactance:
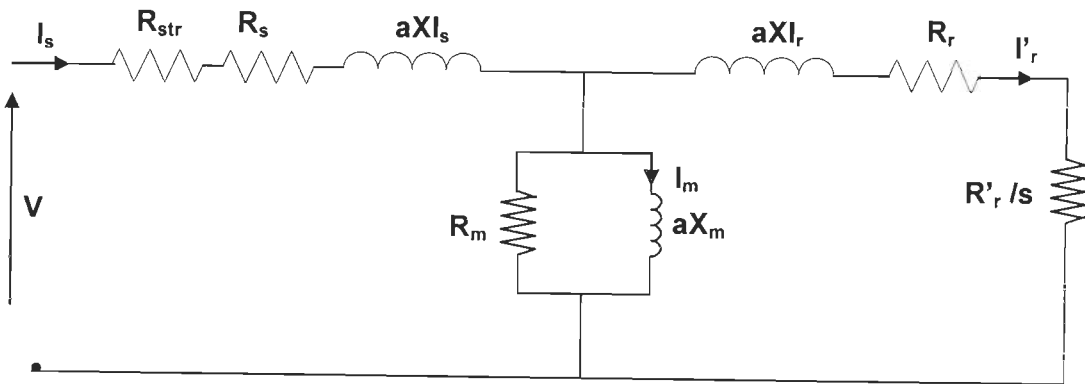
Fig. 3. 14 Modified equivalent circuit of induction motor with stray resistance

Motor parameters (R_s, X_{ls}, X_{lr}, R_r) are derived from the no-load and blocked rotor tests and are represented by per-unit quantities. Stator and rotor circuits have been merged by adjusting the rotor parameters in accordance with the effective turns ratio. Referring the Fig. 3.14, motor equations (3.45) – (3.54) are given in the per-unit systems [86]. The per-unit frequency

$$a = \frac{\omega_e}{\omega_b} = \frac{\omega}{1 - s} \qquad (3.45)$$

The magnetizing current in terms of the air-gap flux and the magnetizing reactance is given by

$$I_m = \frac{E/a}{X_m} = \frac{\Phi_m}{X_m} \qquad (3.46)$$

The rotor current reflected in to the stator in terms of the air gap flux is given by

$$I'_r = \frac{\Phi_m}{\sqrt{(\frac{R'_r}{sa})^2 + X'^2_{lr}}}$$ (3.47)

From Eq. (3.47), the air gap flux can be expressed as

$$\Phi_m = I'_r \sqrt{(\frac{R'_r}{sa})^2 + X'^2_{lr}}$$ (3.48)

The electromagnetic torque is given by

$$T_e = I'^2_r \frac{R'_r}{sa}$$ (3.49)

Substituting Eq. (3.47) into Eq. (3.49), the electromagnetic torque is rewritten as

$$T_e = \frac{R'_r / sa}{\left(R'_r / sa\right)^2 + X'^2_{lr}} \Phi^2_m$$ (3.50)

Usually, the induction motor operates with a small slip and the condition $R'_r / sa \gg X'_{lr}$ holds. In this case, Eqs. (3.43) and (3.45), air-gap flux and electromagnetic torque respectively, become

$$\Phi_m \cong \frac{R'_r I'_r}{sa}$$ (3.51)

$$T_e \cong \frac{sa}{r'_r} \Phi^2_m = \Phi_m I'_r$$ (3.52)

Stator current of the motor is calculated by

$$I^2_s = I^2_m + c_L I'^2_r : \text{ where, } c_L = 1 + 2\frac{X'_{lr}}{X_m}$$ (3.53)

Equation (3.46) can also be written including magnetic saturation effects as

$$I_m = S_a \Phi_m + S_b \Phi_m{}^3 + S_c \Phi_m{}^5 \tag{3.54}$$

From the Eqs. (3.19) to (3.44), the total losses at both fundamental and harmonic frequency, P_{loss}, in the induction motor drive considering conductor losses, iron losses, stray losses, mechanical losses and converter losses are given by

$$P_{loss} = R_s I_s^2 + R_r' I_r'^2 + \left[K_e \left(1 + s^2 \right) a^2 + K_h (1 + s) a \right] \Phi_m^2 + K_{str} \omega^2 I_r'^2$$

$$+ C_{fw} \omega^2 + I_h^2 (R_s + R_r') + K_{inv1} I_s + K_{inv2} I_s^2 \tag{3.55}$$

As discussed earlier, rotor current in squirrel cage induction motor is not measurable and the total losses can be expressed as in Eq. (4.51).

$$P_{loss} = R_s I_s^2 + \left(R_r' + K_{str} \omega^2 \right) \frac{T_e^2}{\Phi_m^2} + \left[K_e \left(1 + s^2 \right) a^2 + K_h (1 + s) a \right] \Phi_m^2 + C_{fw} \omega^2$$

$$+ R_s \left(S_a \Phi_m + S_b \Phi_m{}^3 + S_c \Phi_m{}^5 \right) + I_h^2 (R_s + R_r') + K_{inv1} I_s + K_{inv2} I_s^2 \tag{3.56}$$

Loss model controller (LMC) calculates the optimal value of flux in the Eq. (3.56) for the given value of load torque and speed so that losses in the drive are minimum (or maximum efficiency). Stochastic techniques like Particle Swarm Optimization (PSO) or genetic algorithm can be used as the inner part of LMC for finding optimal flux level. PSO is used in the present work to find the optimal flux with the consideration of its maximum and minimum limits. The loss minimization problem of induction motor can be formulated as

$$\text{Minimize } P_{loss} (T_e, \omega, \Phi_m) \tag{3.57}$$

3.6.2 Search and Hybrid Controllers

Unlike LMC for finding optimal flux from loss models, search control adjusts (decrease) flux or flux producing current step by step with small value and watch the dc link power at every adjustment. Once the dc link power is minimized the adjustment will be stopped and maintain the current flux. This technique is slow for reaching the optimum value and a ripple in steady state torque is always present but the loss minimization in the total system can be achieved without the knowledge of motor and converter parameters. Ramp search method can be used as search control and specific model is not required to implement this type of controllers.

Hybrid controller (which consists both LMC and search control) is used to retain good features of individual controllers, while eliminating their major drawbacks. By this hybrid controller, slow convergence (drawback of search control) and parameter variation (drawback of LMC) due to saturation and temperature variations can be eliminated and good results can be achieved with rough knowledge of parameters.

3.7 Conclusion

The drive scheme considered for investigation is presented. Mathematical model of the induction motor is presented in stator reference frame. PWM inverter model is explained for every possible switching state. The current controllers used in the drive are sinusoidal pulse width modulation controllers; these controllers are modelled. Optimal energy controller is designed through the loss models of entire variable speed drive systems. The PI controller equations for speed controller are described in detail. FPPI controller is designed to solve stability problems in the drive during flux adjustment. The drive model is obtained for the vector control scheme. Using the PWM inverter, induction motor and associated controller models, the complete drive can be simulated to study its performance.

Design Optimization of Induction Motor

[In this chapter the design improvements of induction motor by selecting optimal values of variables and constraints using Particle Swarm Optimization (PSO) and its variants are discussed. The classification of optimization problems and their solving techniques are presented. The formulation of motor design problems with the detailed explanations of variables, constraints and objective functions are given. Effects of variables on the performance indices and the objective functions of the motor are analyzed. The nature of optimization techniques used in this thesis i.e. Rosenbrock method, Simulated Annealing, basic PSO and the improved version of PSO, called Quadratic Interpolation based Particle Swarm Optimization (QIPSO) are explained in detail. Results obtained by each method for the objective functions, material cost, efficiency, starting torque, temperature rise and operating cost are given. Optimized motor design with the consideration of voltage unbalance and limited harmonic current (in case of inverter supply) is also carried out.]

4.1   Introduction

Optimization is one of the most important areas in engineering and applied research. Many engineering problems can be formulated as optimization problems. Electrical engineering problems like motor design, economic dispatch problem, pressure vessel design, VLSI design etc. can be formulated as optimization problems. These problems when subjected to a suitable optimization algorithm help in improving the quality of solution. This is the reason that electrical engineering community has shown a significant interest in digital computer based optimization algorithms and development of software on motor design to obtain the global optimum solution of the problems.

In particular there has been a focus on Evolutionary Algorithms (EA) for obtaining the global optimum solution to the problem, because in many cases it is not only desirable but also necessary to obtain the global optimal solution. Evolutionary algorithms have also become popular because of their advantages over the traditional optimization techniques (decent method, quadratic programming approach, etc). A detailed description of various traditional optimization techniques can be found in [69]. Some important differences of EAs over classical optimization techniques are as follows:

- Evolutionary algorithms start with a population of points whereas the classical

optimization techniques start with a single point.

- No initial guess is needed for EAs, however, a suitable initial guess is needed in most of the classical optimization techniques.

- EAs do not require an auxiliary knowledge like differentiability or continuity of the problem on the other hand classical optimization techniques depend on the auxiliary knowledge of the problem.

- The generic nature of EAs makes them applicable to a wider variety of problems where as classical optimization techniques are problem specific.

Some common EAs are Genetic Algorithms (GA), Evolutionary Programming (EP), Particle Swarm Optimization (PSO), Differential Evolution (DE) etc. These algorithms have been successfully applied for solving induction motor design problems [37], [121], [181], [84], [16], etc. Some improved versions of PSO based on Quadratic Interpolation proposed by Pant et al. [124] – [127] have applied successfully in unconstrained and constrained test problems and real life applications. PSO and its variant (QIPSO) are used in the present work for designing the induction motor.

4.2   General Optimization Problem

The system while designing, fabricating or maintaining it, engineers are required to take many technological and managerial decisions at several stages. It is expected that the decisions taken should lead to either minimize the efforts or maximize the gain. In any practical situation the ultimate goal can be defined as a function of certain decision variables. Thus the optimization can be defined as the process of investigating the conditions that give the maximum or minimum value of function under given circumstances. There is no unique method available for solving all optimization problems with the same efficiency, and hence several optimization methods have been propounded to handle specific type of problems. The optimum seeking methods are commonly known as mathematical programming techniques. These techniques provide a means for finding the minimum or maximum of a function of several variables under a prescribed set of constraints [15]. The design process for an induction motor involves many steps. The general flow of design optimization of induction motor is shown in Fig. 4.1.
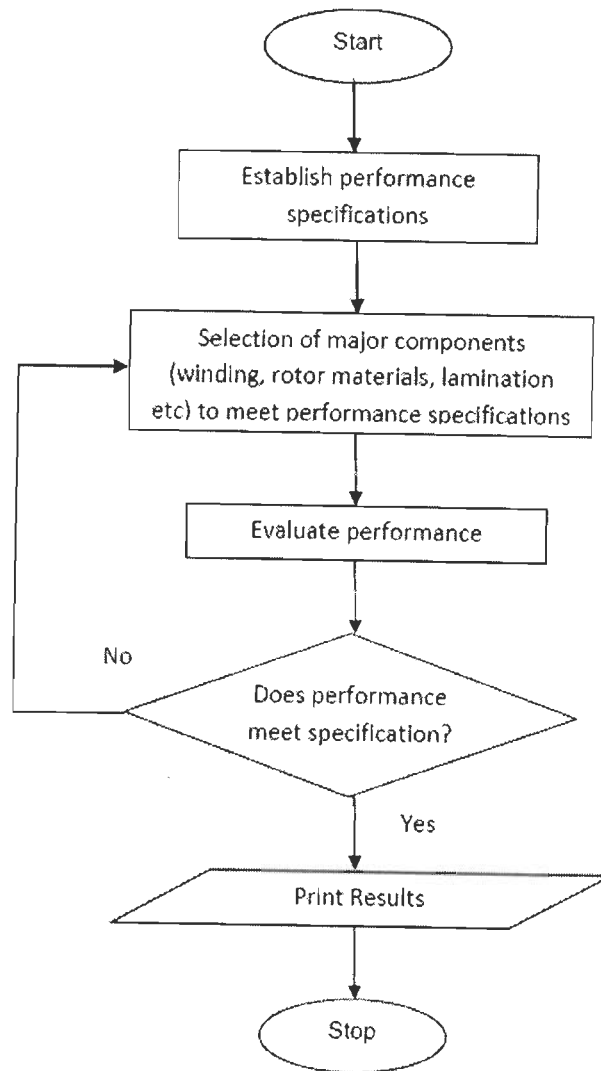
Fig. 4.1. General flow chart for motor design

A general nonlinear programming problem can be stated in mathematical terms as follows;

Find X= (x_1, x_2.....x_n) such that

To optimize F(X) i.e minimum or maximum

Subject to $g_i(X) \geq 0$, i=1, 2,....,m

and $l_j(X) = 0$,   j = m + 1,.......p

where X is an N-dimensional vector termed as the design vector, F(X) is called the objective function and $g_j(X)$ and $l_j(X)$ are respectively the inequality and equality constraints. The problem can be said to be unconstrained when p=0, and when p is greater than m the problem is said to have both equality and inequality constraints. In some problems only

inequality or equality constraints may be present. The following terminologies are important in any optimization problem [15].

a) *Design Vector*

In any engineering system the design is controlled by several parameters and they are termed as design variables or decision variables. In some of the problems the number of variables are too large and it is unwieldy to deal with such a large number of variables. Fortunately, in most of the designs certain quantities can be fixed at the outset and such parameters are called as assigned or pre-assigned parameters. Seven design variables which are given in section 4.5.1 and thirteen assigned parameters (details available in Appendix A) are used in induction motor design problem of this chapter.

b) *Design Constraints*

In order to produce an acceptable design certain restrictions are to be satisfied. The restrictions put on the design are collectively called as design constraints. They can further be classified into two types, i.e. functional constraints and size constraints, depending upon whether the restrictions refers to performance or some other physical limitations. More constraints are available in the motor designs which decide the good or bad performance. Nine constraints forced into the induction motor design in the present work which are available in section 4.5.2.

c) *Objective Function*

In any design procedure under given circumstances several acceptable designs can be produced for different sets of design variables. The optimization process enables to select the best design on the basis of certain criterion with respect to which the design is to be optimized. This criterion, when expressed in terms of design variables is termed as objective function. In most of the cases the optimized design of one criterion may not necessarily be optimized design for some other criterion and hence selection of suitable objective function is one of the most important decisions in whole of the optimum design process. Five objective functions related to cost and performances are considered in the present work and are available in section 4.5.3.

Several factors have to be considered in deciding upon a particular method to solve a nonlinear programming problem. Some of them are [15]:

> Nature of problem to be solved and required accuracy.

> The time necessary for preparation of the program. Available programs, if any, for direct use and improvement

> The generality of program, necessity of derivatives, previous knowledge of the methods and their efficiency etc.
> The ease with which the program can be used and its output interpreted
> Computation facilities- time taken for convergence

Considering the one dimensional method, the use of analytical method for this design optimization problem is difficult since the functions are not directly differentiable and hence numerical methods are to be employed for differentiating the objective function and the constraint. Interpolation methods are efficient than the elimination methods but, they fail to converge at global minimum if the function is a multimodal one. The simplest method which can give reasonably accurate results by approximately fixing the step size is unrestricted search or incremental search method. In this method an ordered search from a given point considering each variable in turn is conducted using fixed step size. It is inefficient for the optimization.

The constrained minimization techniques for nonlinear function and constraints are more justified to select. In this category amongst the direct methods, cutting plane method requires convex programming problem with objective function and constraints as nearly linear functions and hence cannot be used. Feasible directions methods are more effective for the problem using linear constraints or for linear programming problems. Heuristic search method (Box method) and Rosenbrock's method (Hill algorithm) were conveniently applied for the induction machine optimization problem. Nowadays Nature Inspired Algorithms (NIA) are the efficient alternatives of Box and Rosenbrock methods and hence particle swarm optimization (one of the nature inspired algorithms) and its variant are used in the present work.

4.3 Induction Motor Design Optimization

Optimum design of Induction Motor (IM) is a non-linear multi dimension problem and therefore the role of optimization techniques is more important in design of IM to get global optimum. Detailed literature survey on induction motor design using conventional and artificial intelligence based techniques has been given in the chapter 1.

4.3.1 Conventional Methods

The classical methods of differential calculus can be used to find the maxima or minima of a function of several variables and without any constraint. Another requirement with such methods is the demand for continuous differentiable functions with respect to design

variables. In most of the engineering problems the analytical differentiation of functions is a difficult task and hence such methods have limited scope in the applications. The various types of conventional (non-NIA based) non linear optimization methods for constrained and unconstrained problems are shown in Fig. 4.2 - 4.4 [15].
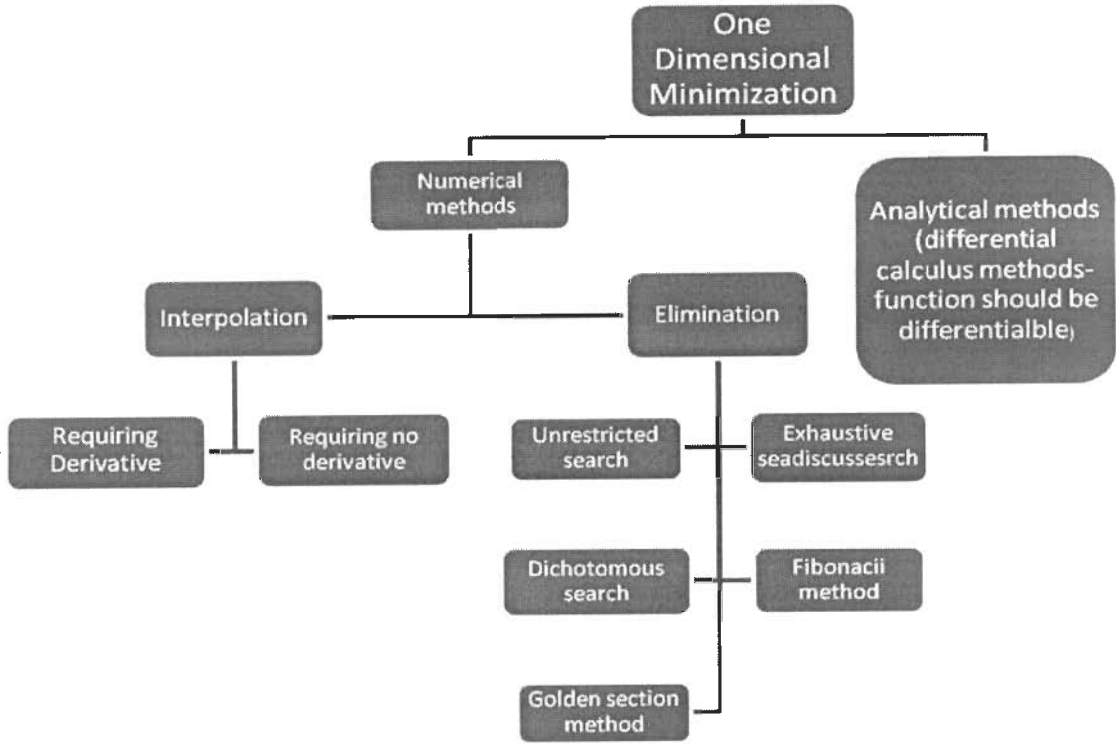
Fig. 4. 2. One dimensional minimization techniques
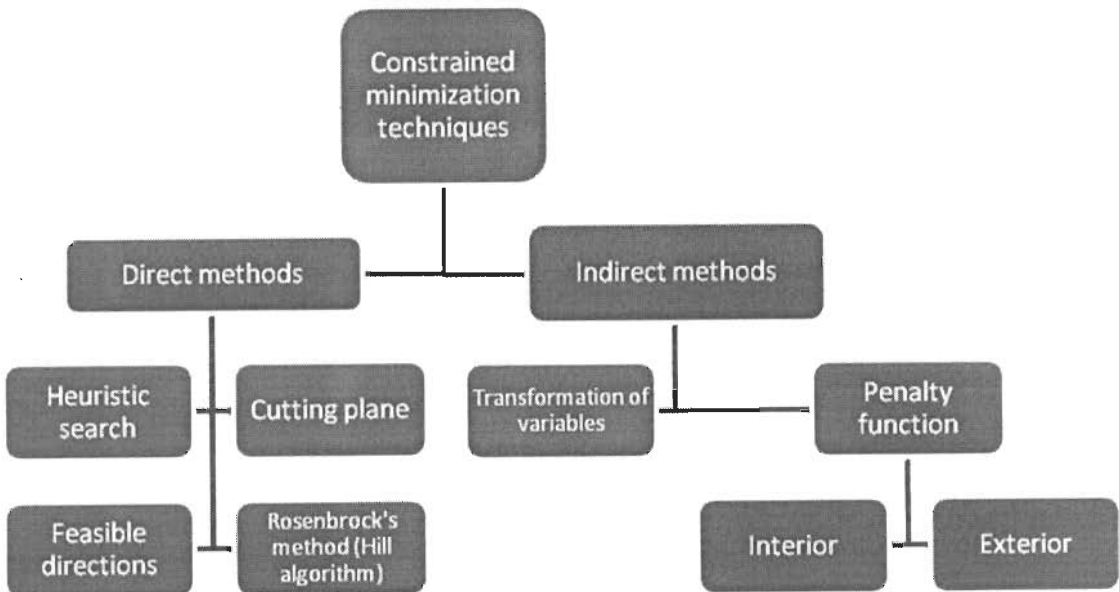
Fig.4.3. Various constrained minimization methods
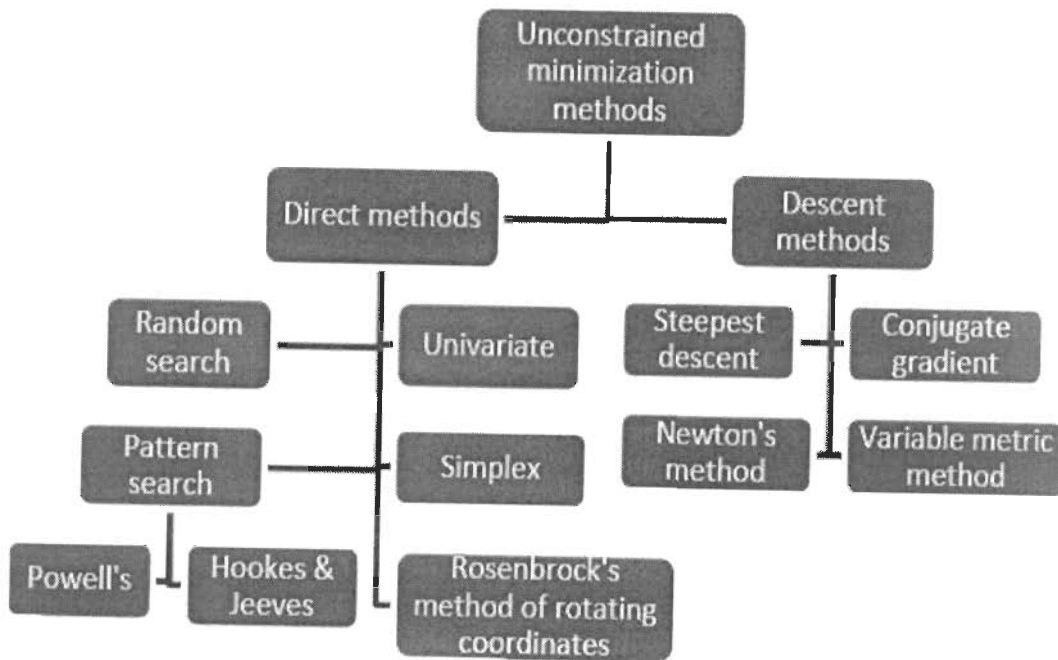
Fig.4.4. Various unconstrained minimization methods

4.3.2 NIA Based Methods

The design optimization of a three-phase induction motor can be formulated as a general constrained non-linear programming and the standard Non Linear Programming (NLP) techniques can be used to solve it. But these techniques are computationally very expensive and inefficient whereas NIA is a competent tool to solve non-linear programming problems. There are many traditional methods in the literature for solving non linear programming problems as said above. However, most of the traditional methods require certain auxiliary properties (like convexity, continuity etc.) of the problem and also most of the traditional techniques are suitable only for a particular type of problem (for example Quadratic Programming Problems, Geometric Programming Problems etc). Keeping in view the limitations of traditional techniques researchers have proposed the use of stochastic optimization methods and intelligent algorithms for solving NLP which may be constrained or unconstrained. Some examples are: Genetic Algorithms (GA) [37], [170], [181], Simulated Annealing (SA) [16] [121], and Particle Swarm Optimization [121], Improved evolution strategy (hybrid of SA and GA) [83], hybrid of evolutionary programming and SA [121].

4.4 Formulation of Induction Motor Design Problem

The design of the induction motors means determining the geometry and all data required for manufacturing so as to satisfy a vector of performance variables together with a

set of constraints. Design optimization refers to ways of doing efficiently synthesis by repeated analysis such that some single or multiple objective functions are maximized or minimized while all constraints are fulfilled. There are large number of design parameters involved in the design of the induction machine. Selection of objective functions, variables and constraints are the main steps. The proper optimization requires an intelligent selection of objective function, and constraints according to the drive's requirement, and further selection of variables which affect the objective function and the constraints. A problem in the selection of variables is that the design problem of IM would have been very much complicated using too many variables [138]. In the present work, seven variables $(x_1......x_7)$ and nine constraints $(C_1...C_9)$ are considered.

a) Variables

ampere conductors/m, x_1

ratio of stack length to pole pitch, x_2

stator slot depth to width ratio, x_3

stator core depth (mm), x_4

average air gap flux densities (wb/m^2), x_5

stator winding current densities (A/mm^2), x_6

Rotor winding current densities (A/mm^2), x_7

b) Constraints

To make a motor practically feasible and acceptable, the constraints have a big role in it. The constraint which gets most effected with the variation in the objective function should be considered with special care. The constraints $(C_1...C_9)$ are forced into the induction motor design and are expressed in terms of variables.

maximum stator tooth flux density, wb/m^2 ≤ 2, C_1

stator temperature rise, °C ≤ 70, C_2

full load efficiency, pu ≥ 0.8, C_3

no load current, pu ≤ 0.5, C_4

starting torque, pu ≥ 1.5, C_5

maximum torque, pu ≥ 2.2, C_6

slip, pu ≤ 0.05, C_7

full load power factor ≥ 0.8, C_8

rotor temperature rise, °C ≤ 70, C_9

(i) Maximum Stator Tooth Flux Density

The expression for maximum tooth flux density is given below (detailed expressions are available in Appendix A)

$$B_{t(max)} = \frac{1.57\pi DLx_5 * 10^3}{S_1 t_{13} L_i} \tag{4.1}$$

The maximum permissible tooth flux density in the present case has been taken as 2.0 wb/m^2. This limitation of stator flux density depends upon the stamping materials used.

(ii) Stator Temperature Rise

The permissible value of temperature rise depends upon the type of insulating material. Moreover the industrial situation for which the motor is to be used is also a controlling factor of a motor to fix its thermal rating. For example, in textile mills the motor with higher permissible temperature rise cannot be used due to danger of fire. In the presented work, the motor is designed with Class B insulation and maximum permissible temperature is forced as one of the constraints which value is considered as 70°C. The equation for temperature rise (θ_{ms}) in terms of copper and iron losses is given below,

$$\theta_{ms} = \frac{\tau_c(SCL + SCL)}{S_s} \tag{4.2}$$

(iii) Full Load Efficiency

Efficiency improvement in motor design helps to reduce the energy consumption/operating cost of energy intensive industries which results reduced environmental pollutions. Therefore industrial customers will be more interested in having efficient motors. In the present work, the efficiency (η) has been restricted to a minimum of 80% and the corresponding equation is given below,

$$\eta = \frac{1000P_o}{1000P_o + SCL + W_{RCL} + SIL + W_F} * 100 \tag{4.3}$$

(iv) No-Load to Full Load Current Ratio

Motors, in industrial applications, frequently run at part load and no load. In order to reduce the no load losses a low value of no load current is justified. The expression for no load to full load current ratio (CR) is given in (4.4) and its maximum value is restricted as 0.5.

$$CR = \frac{I_o}{I_{ph}} \; ; \; I_o = \sqrt{I_m^2 + I_c^2} \qquad (4.4)$$

(v) Full Load Slip

The value of slip at full load depends on the rotor resistance. A very high value of slip makes a motor to draw more stator current causing more heating of motor. In the present work, maximum limit put on the full load slip is 0.05 p.u and the expression for slip is given in Eq. (4.5).

$$s = \frac{W_{RCL}}{1000 P_o + W_{RCL} + W_F} \qquad (4.5)$$

(vi) Starting to Full Load Torque Ratio

Starting torque requirement is varied from motor to motor depends on the job, for example, more starting torque is required in the mine hoist load. The ratio of starting torque to full load torque (TRT_1) in this work is restricted to a minimum of 1.5. Detailed expressions of T_{st} and T_{fl} are given in Eqs. (A.59) and (A.60).

$$TRT_1 = \frac{T_{st}}{T_{fl}} \qquad (4.6)$$

(vii)   Maximum to Full Load Torque Ratio

Standard organizations impose restriction on the ratio of maximum to full load torque (TRT_2) depending upon the purpose for which the motor is to be used. It is restricted to not smaller than 2.2 in this work. A detailed expression of T_{max} is given in Eq. (A.63).

$$TRT_2 = \frac{T_{max}}{T_{fl}} \qquad (4.7)$$

(viii)   Full Load Power Factor

Induction motors are characterized by power factors less than unity, leading to lower overall efficiency (and higher overall operating cost) associated with a plant's electrical system. Therefore, it is necessary to improve the power factor in induction motor. The minimum value of the power factor prescribed in the present optimized design is 0.8 at full load. The expression of power factor is given in Eq. (4.8).

$$PF = \frac{R_s + G_4}{\sqrt{\left\{ (R_s + G_4)^2 + (X_s + G_5)^2 \right\}}} \qquad (4.8)$$

(ix) Full Load Rotor Temperature Rise

Similar to stator temperature rise, rotor temperature is also an important constraint to the design of induction motor. It is restricted to the value of less than 70°C. The expression for full load rotor temperature rise can be written as Eq. (4.9).

$$\theta_{mr} = \frac{\tau_c W_{RCL}}{S_r} \qquad (4.9)$$

c) Objective Functions

The objective function is mostly chosen keeping in mind the customers demand and the profit of manufacturer. The following objective functions are considered in this work while designing the machine using optimization algorithms (detailed expressions are given in Appendix A). The objective functions are,

F(X) = A; Active material cost minimization

F(X) = B; Maximization of Efficiency

F(x) = C; Maximization of Starting torque

F(x) = D; Minimization of temperature rise in the stator circuit of the motor

F(x) = E; Operating cost minimization

d) Optimization Tool

PSO and QIPSO algorithms are used in the present work for optimizing induction motor design. Constrained Rosenbrock and Simulated Annealing (SA) are considered for comparing PSO and QIPSO results. The results of Rosenbrock method and SA are referred from the existing literature.

4.5 Effect of Design Variables

The effect of above design variables on objective functions and other performance indices are investigated by using the equations given in Appendix A.4. Vary the value of one variable in a wide range for studying its effects in performance indices, other variables are assigned the normal values used in the standard design procedure. The computer flow chart for iterative method is shown in Fig. 4.5. Computer program is stopped at maximum iteration (ITE) is reached.
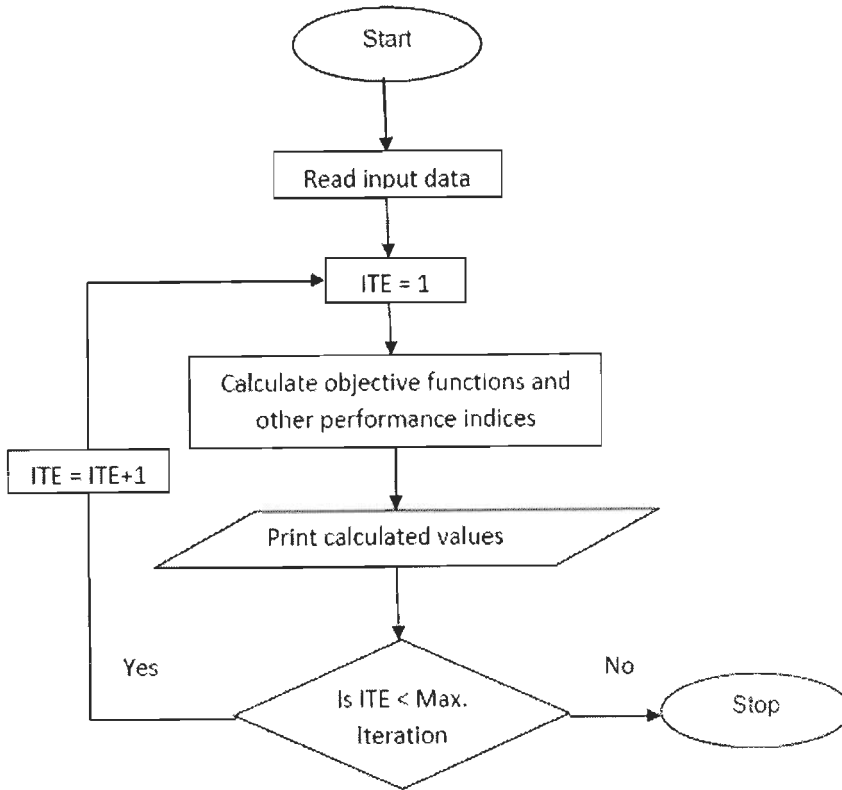
Fig. 4.5. Computer flow chart for investigating the effect of variables

a) *Effects of Ampere Conductors*

Ampere conductors (ac), in other words electric loading, affects copper losses and armature reaction. The losses must be dissipated by ventilation so that the designer has several restrictions on his choice of specific loading. The effects of ac on the performance indices are shown in Fig. 4.6 and Fig. 4.7. With the higher value of ac the stator tooth flux density increases but not much whereas, with the increased value of ac the starting and full load torque have reduced. Efficiency, power factor and slip are almost constant through out the variations in ampere conductor. Higher values of ac offer slight reduction in no-load to full load current ratio. The full load stator and rotor temperature are more with the higher value of ampere conductor per metre, shown in Fig. 4.7.
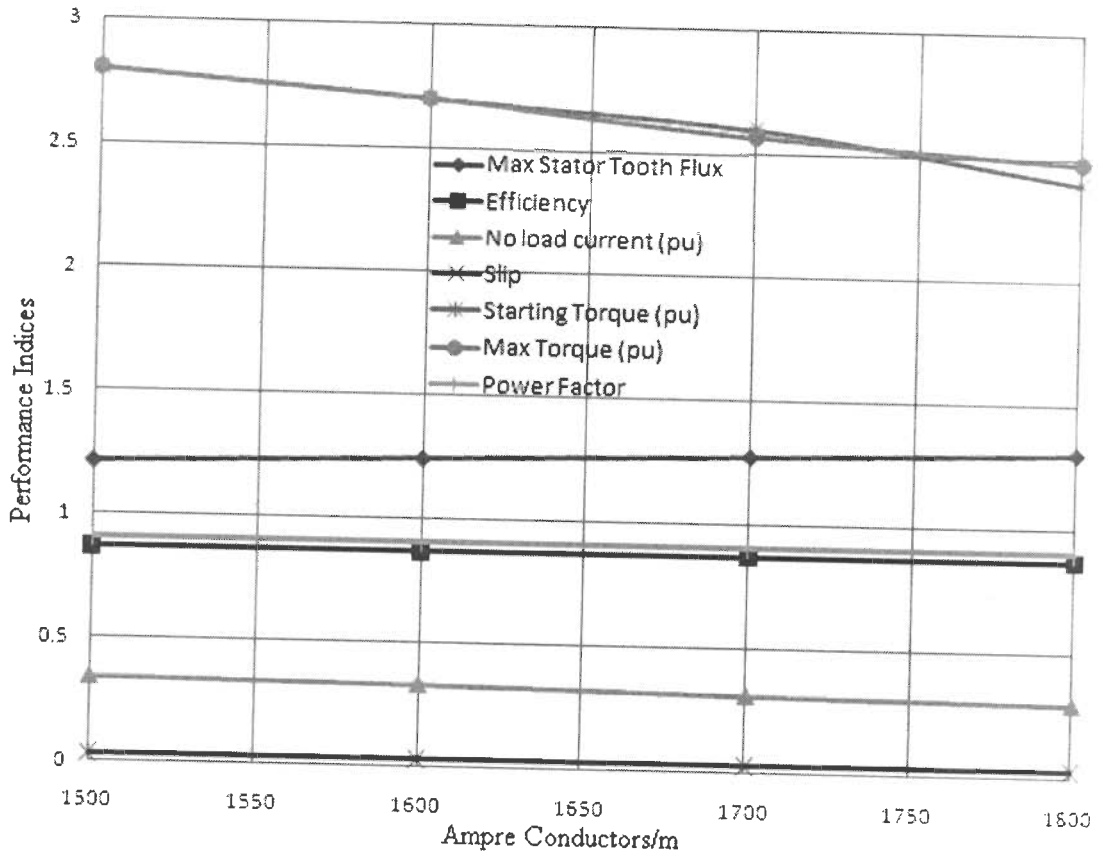
Fig. 4.6. Effects of ampere conductors/m in performance indices of the motor
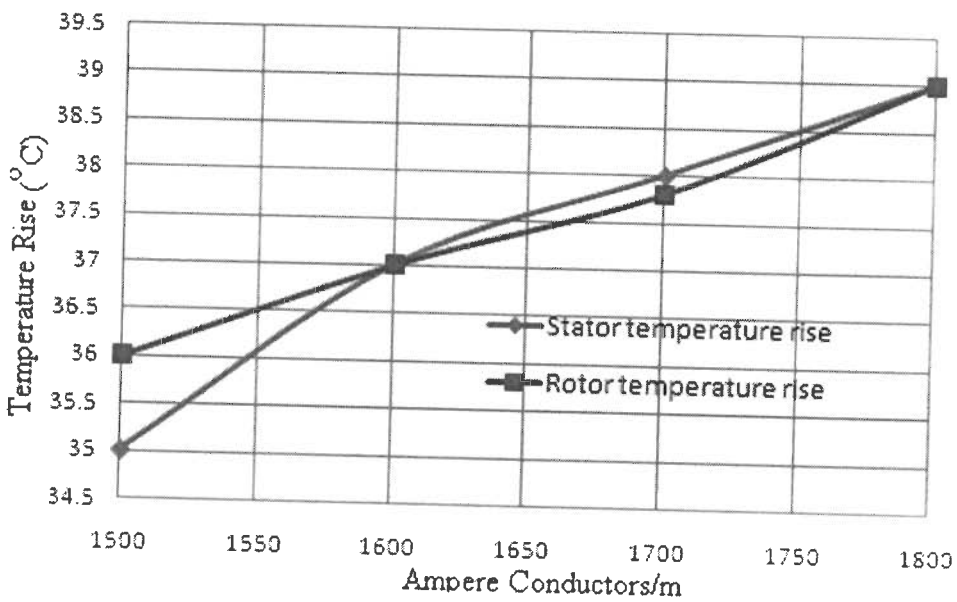
Fig. 4.7. Effects of ampere conductors/m in temperature rise of the motor

b) Effects of Ratio of Stack Length to Pole Pitch

Similar to ampere conductors, effect of ratio of stack length to pole pitch (L/τ) in stator tooth flux density is low. With the higher value of L/τ the stator tooth flux density slightly decreases. No-load to full load current ratio lightly increases with higher value of L/τ. More per-unit starting and maximum torques can be obtained by using higher value L/τ. The variations in these torque with respect to L/τ are almost same. Efficiency and slip increase with the higher value of L/τ. There is no effect of this variable on the power factor and stator temperature rise but the full load rotor temperature rise is less with high value of L/τ. In general, the following range of values of stack length to pole pitch ratio is recommended to achieve good performances [143]. Fig. 4.8 and 4.9 show the effects of L/τ on the performance indices of the motor.

For minimum material cost: the range of L/τ is 1.5 to 2.

For good power factor: the range of L/τ is 1.0 to 1.25.

For good efficiency: the value of L/τ is 1.5

For good overall design: the value of L/τ is 1.0
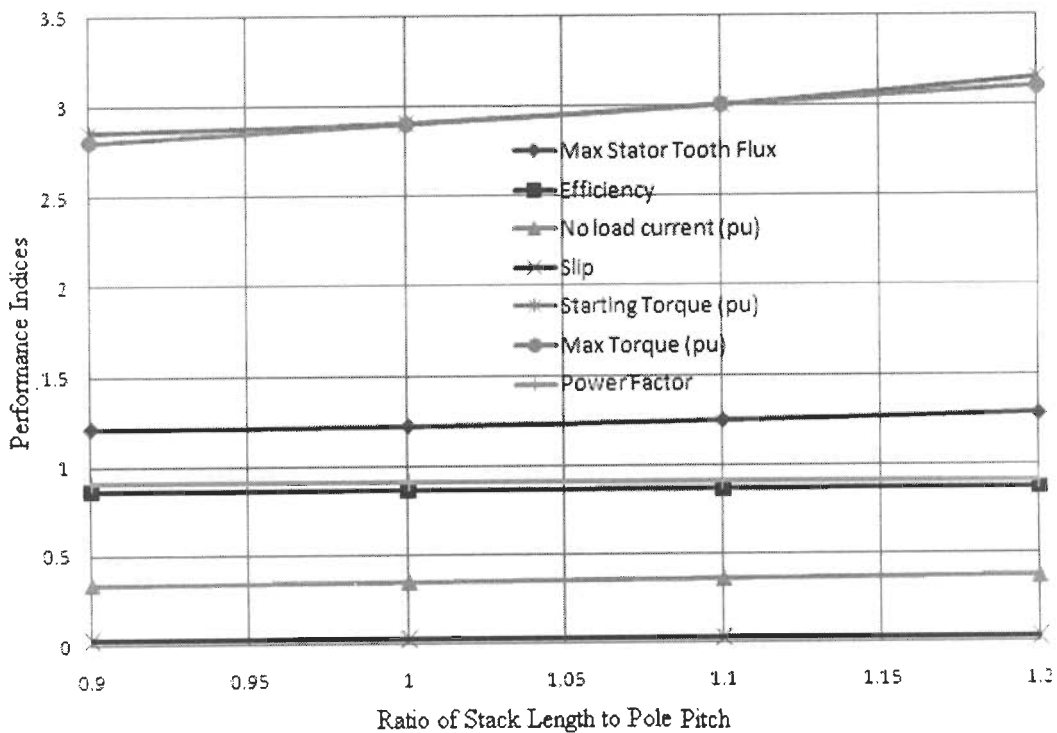
Fig. 4.8. Effects of ratio of stack length to pole pitch in the motor's performance indices
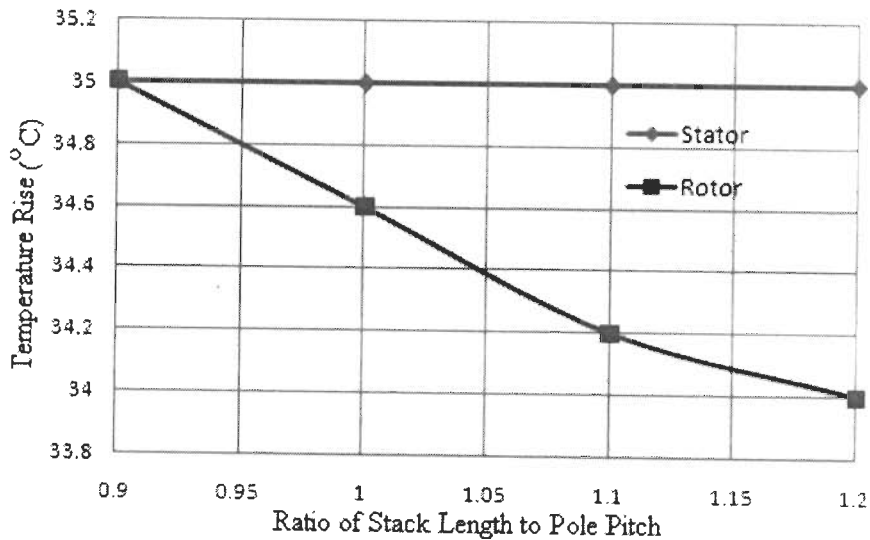
4.9. Effects of ratio of stack length to pole pitch in the motor's temperature rise

c) *Effects of ratio of Stator Slot Depth to Width*

With the increased value of stator slot depth to width ratio the tooth flux density reduces considerably where as efficiency and per-unit no-load current are increased with the higher value of stator slot depth to width ratio. The effect of this variable in slip is almost negligible. Lower values of stator slot depth to width ratio give higher value of per-unit maximum torque. The effect of this variable in starting torque is significant. Lower value of this variable offers higher starting torque and this torque value decreases with increase in slot depth to width ratio upto a certain value and then increases with the increase in slot depth to width ratio, shown in Fig. 4.10. Almost no and less effects of this variable in stator and rotor temperature rise respectively, shown in Fig. 4.11.

d) *Effects of Core Depth*

The effects of core depth in the performances indices of the motor are shown in Fig. 4.12 and 4.13. The stator core depth has practically no effect on the stator tooth flux density and slip. Also, the effects of this variable on stator and rotor temperature rise are almost same. Lower value of core depth offers higher value of per-unit starting and maximum torques. Similarly, efficiency and power factor are more with the higher value of this variable. The effect of core depth in power factor is significant such that power factor is very low at lower value of core depth. Full load stator temperature rise is less with higher value of core depth whereas; with the increased value of core depth the full load rotor temperature rise increases.
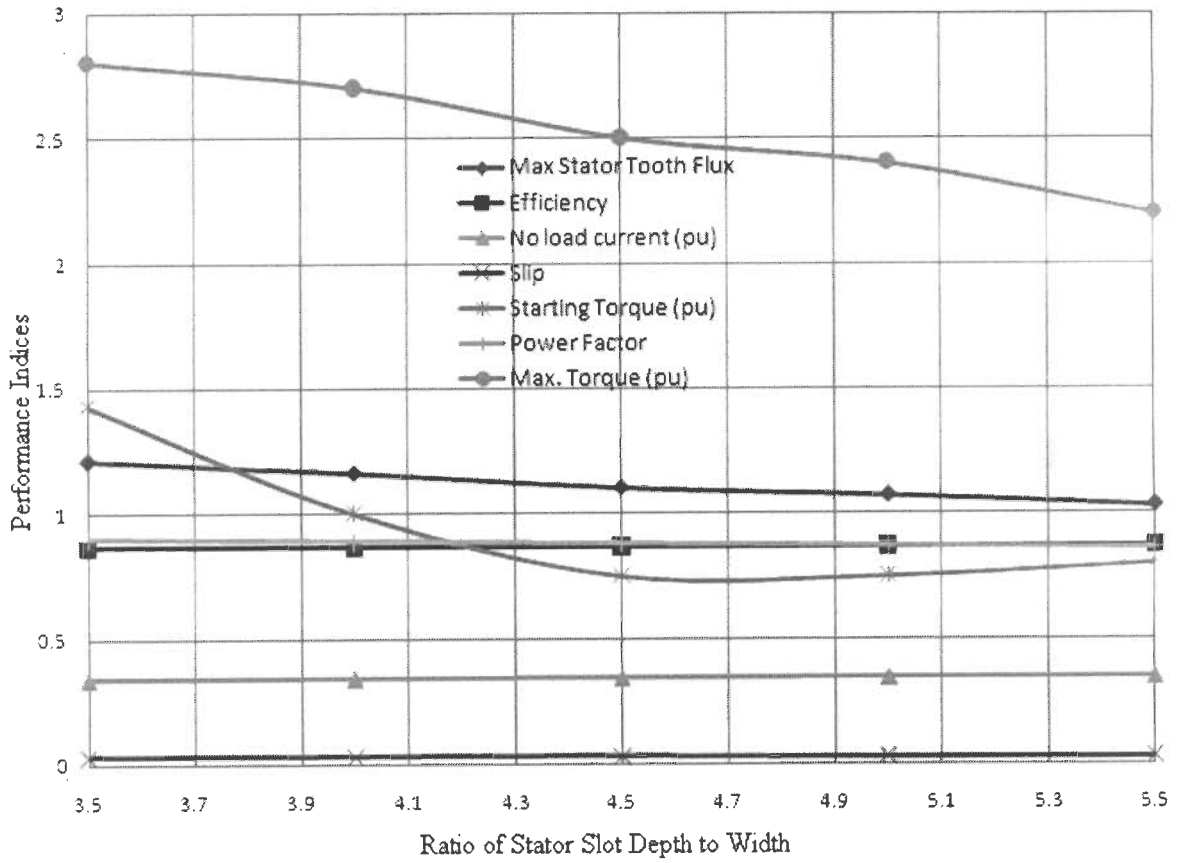
4.10. Effects of ratio of stator slot depth to width in the motor's performance indices
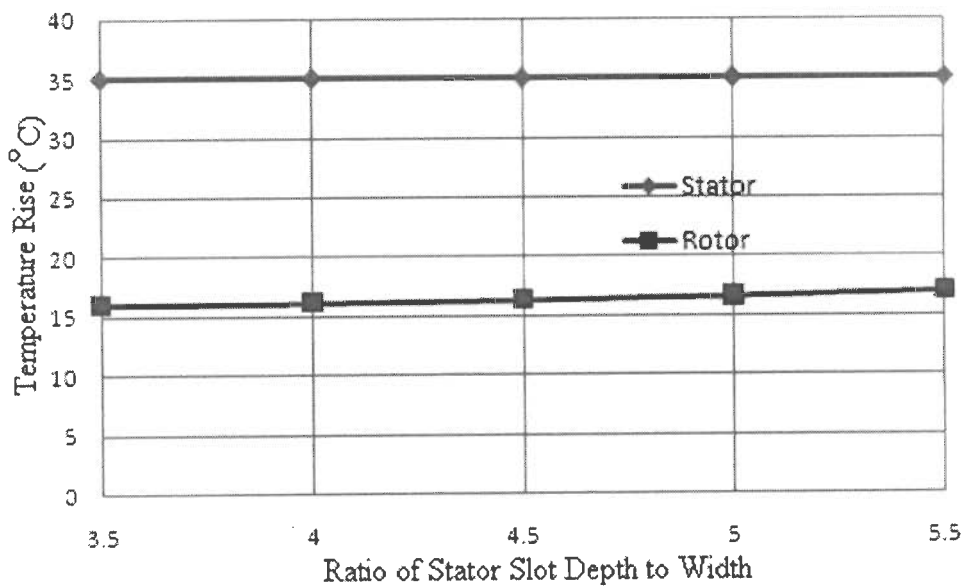
4.11. Effects of ratio of stator slot depth to width in the motor's temperature rise
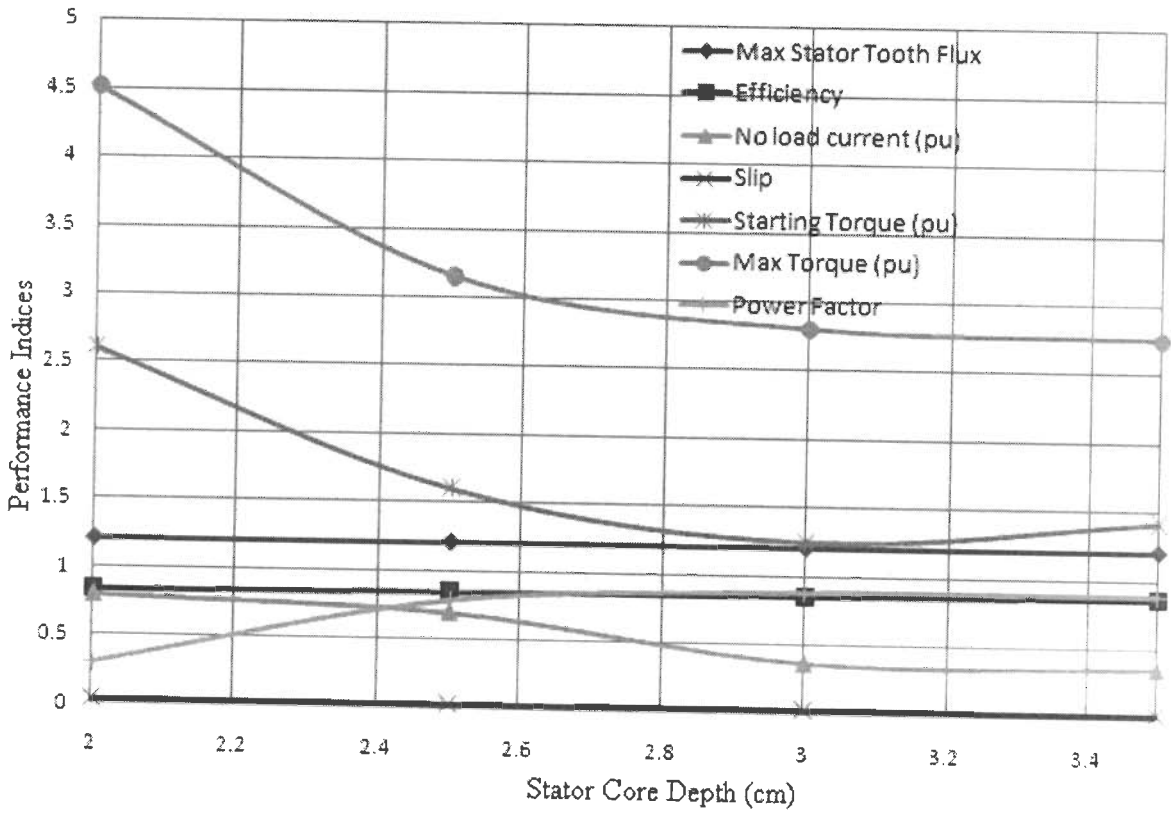
4.12. Effects of stator core depth in the motor's performance indices
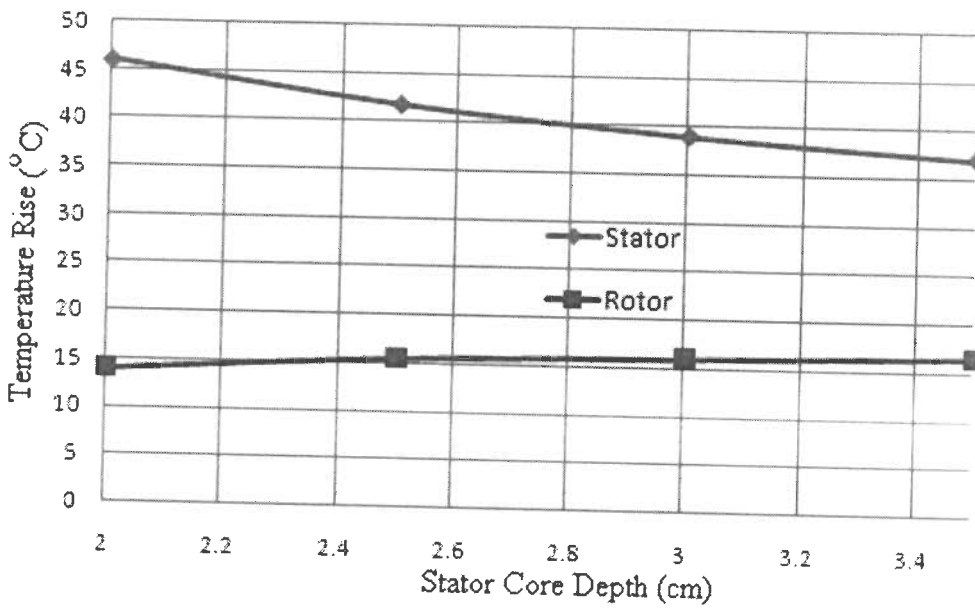
4.13. Effects of stator core depth in the motor's temperature rise

e) Effects of Average Air-gap Flux Density

The effect of air-gap flux density (shown in Fig. 4.14) on maximum stator tooth flux density is very significant. Higher the air-gap flux density results higher tooth flux density. Lower value of this variable helps to get higher efficiency, power factor and starting torque whereas, maximum torque and no-load current are higher when the value of air-gap flux density increased. The effect this variable in the slip is very low. Stator temperature rise is significantly higher with the higher value of air-gap flux density whereas, the effect of this variable in the rotor temperature rise is almost negligible, shown in Fig. 4.15.
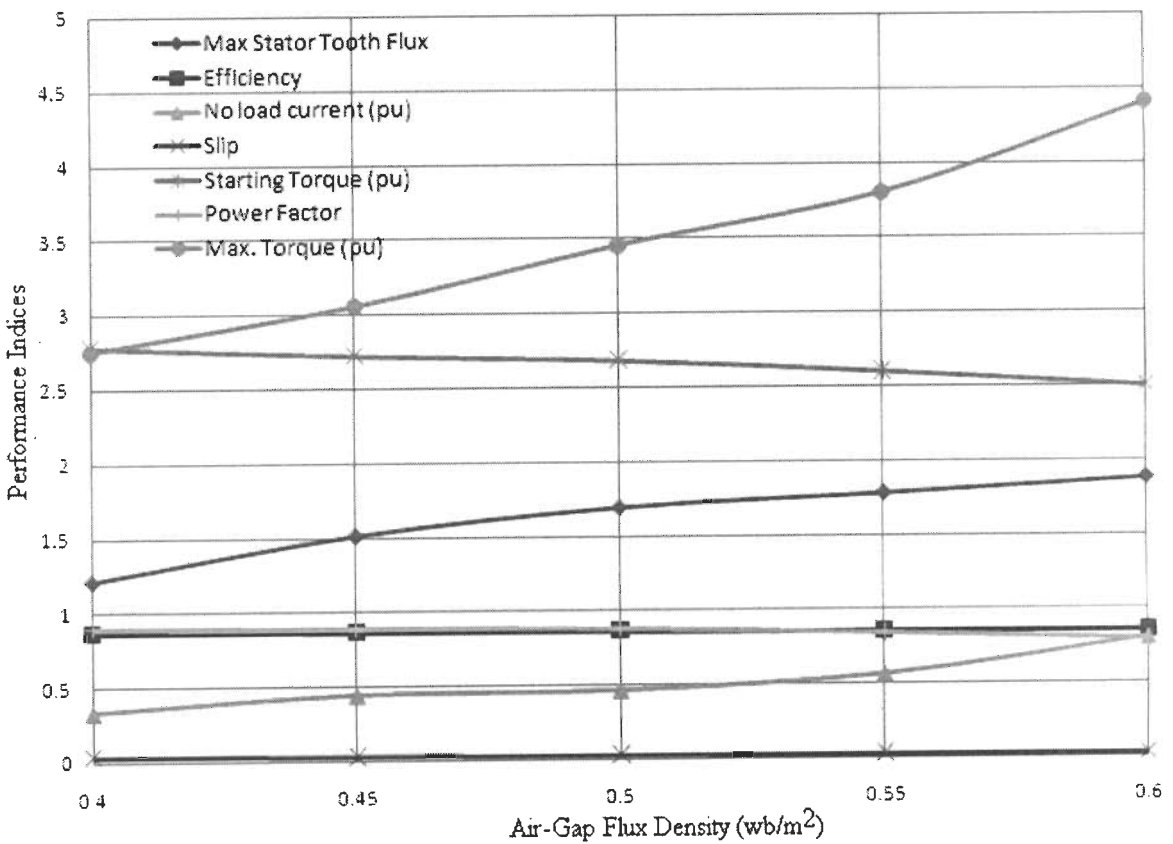
Fig. 4.14. Effects of air-gap flux density in the motor's performance indices
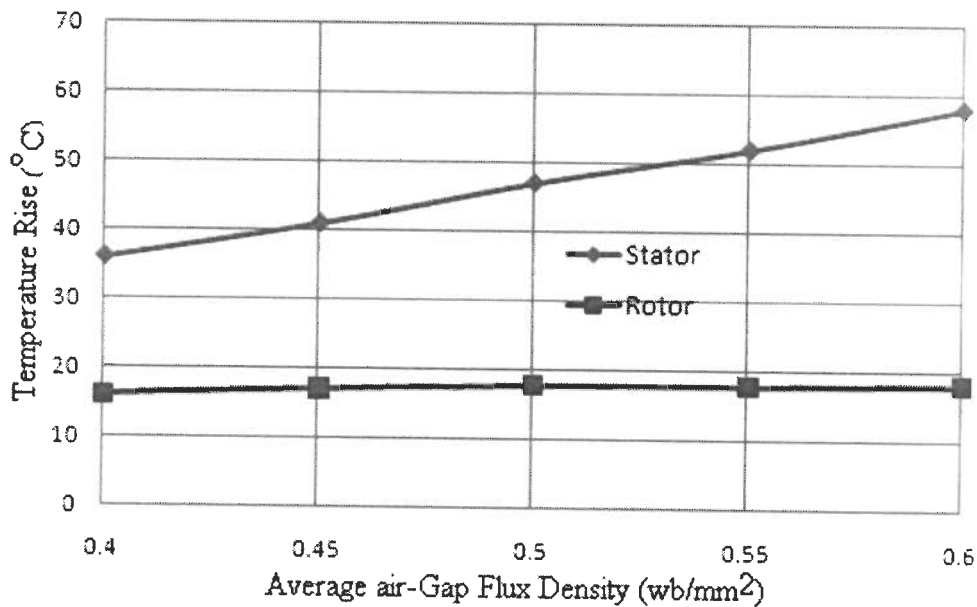
Fig. 4.15. Effects of air-gap flux density in the motor's temperature rise

f) Effects of Stator Winding Current Density

The effects of stator winding current density on the performances of the motor are shown in Fig. 4.16 and 4.17. Starting and maximum torque have decrease with the increase of stator winding current density. The stator tooth flux density decreases with the increasing value of stator winding current density up to a certain value and then increases with the increase in stator winding current density. Higher stator temperature rise with the higher value of stator winding current density and the effect of this variable in the rotor temperature rise is very low. Remaining performance indices such as efficiency, power factor, no-load current and slip have higher value with the lower value of stator winding current density

g) Effects of Rotor Winding Current Density

Fig. 4.18 and 4.19 show the effects of rotor winding current density in the motor performance related items. The effect of this variable is almost negligible in the stator tooth flux density, power factor, no-load current and stator temperature rise. Starting and maximum torques have higher values with the higher value of rotor winding current density. Stator tooth flux density has higher value at the higher value of rotor winding current density. Efficiency is lower with the higher value of rotor winding current density whereas, the value of slip is higher with the higher value of rotor winding current density. Full load rotor temperature rise is significantly higher at the higher value of this variable, shown in Fig. 4.19.
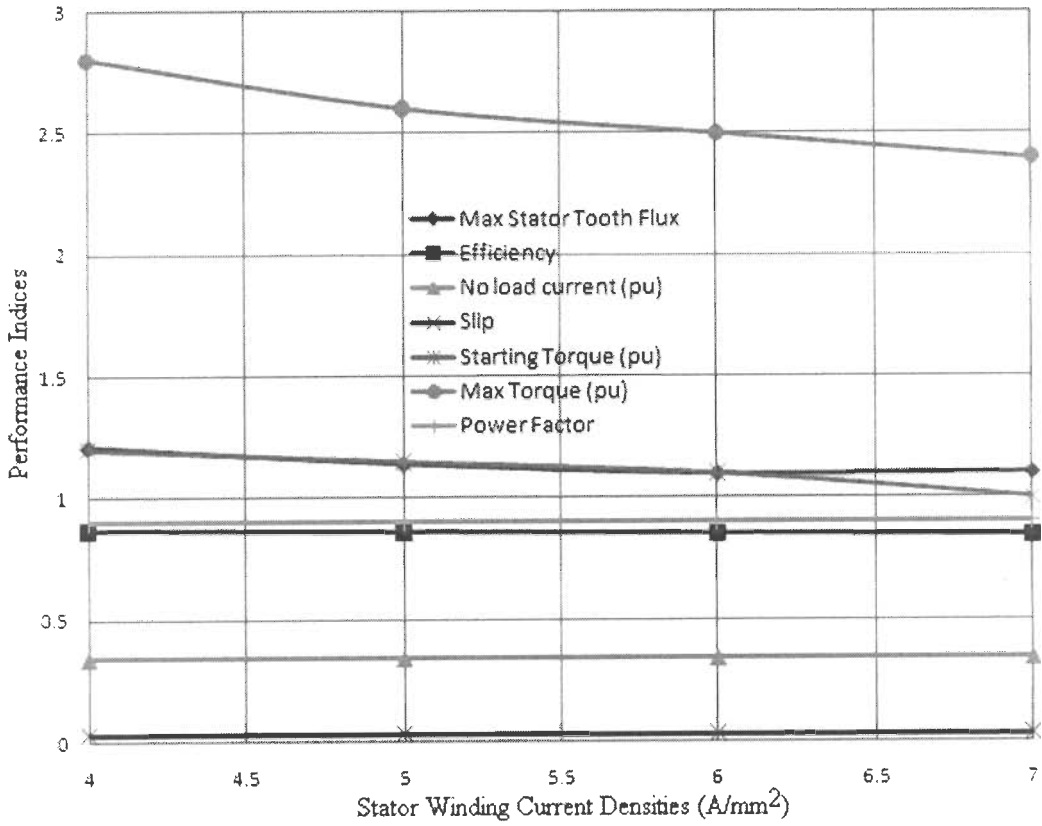
Fig. 4.16. Effects of stator winding current density in the motor's performance indices
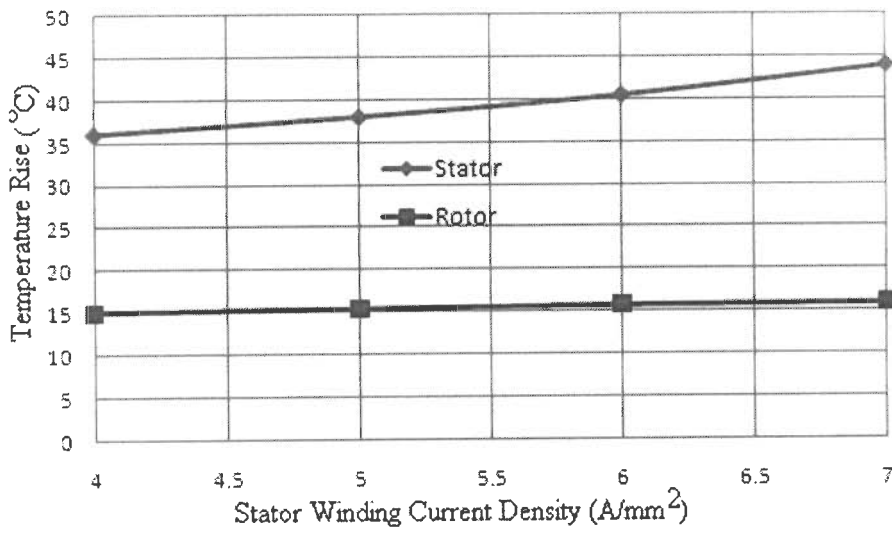
Fig. 4.17. Effects of stator winding current density in the motor's temperature rise
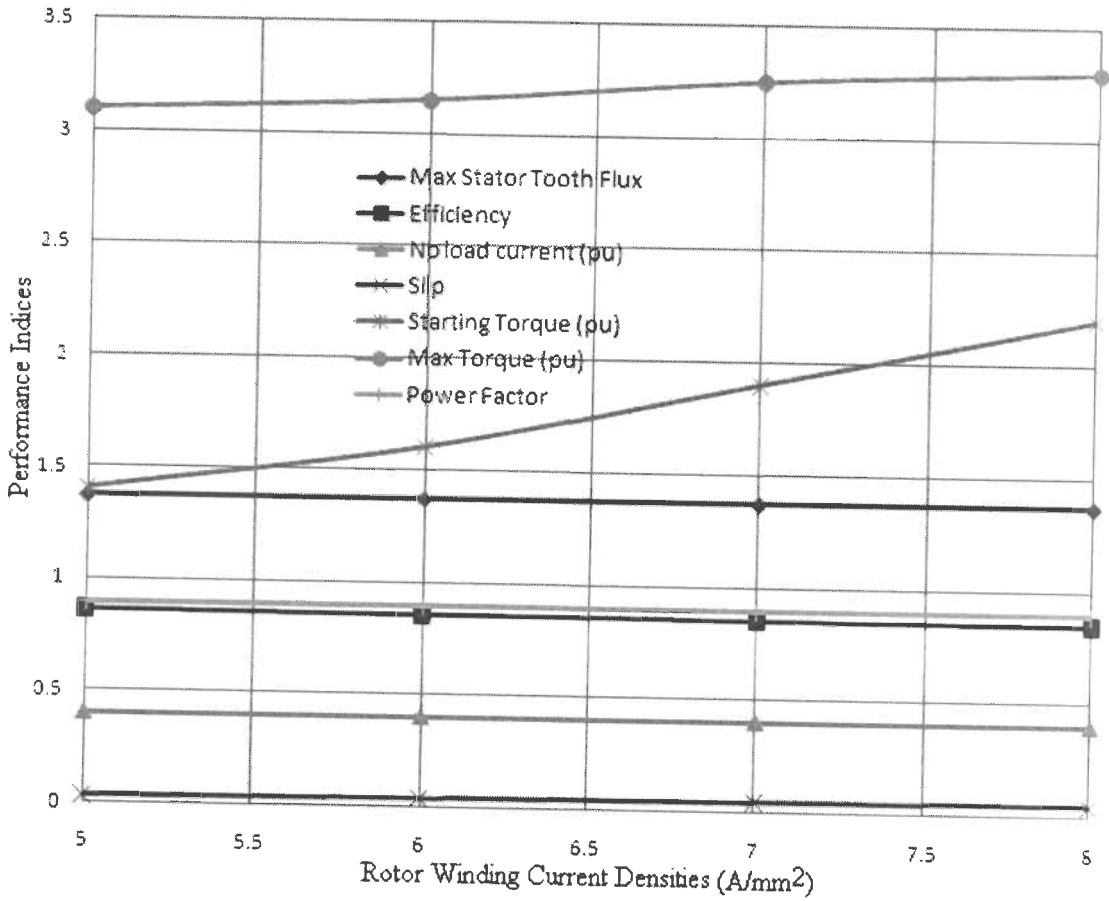
Fig. 4.18. Effects of rotor winding current density in the motor's performance indices
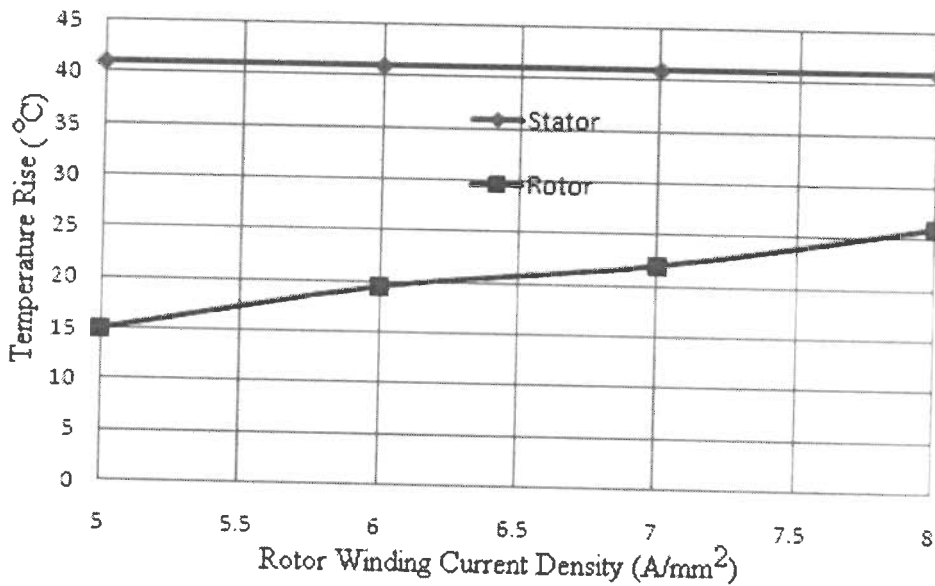
Fig. 4.19. Effects of rotor winding current density in the motor's temperature rise

4.6 Optimization Techniques for Induction Motor Design

Induction motor design optimization is carried out in the present work with the help of PSO and QIPSO algorithms and its superiority has been explored in comparison with Constrained Rosenbrock, and Simulated Annealing (SA) methods. The detailed description of all methods is given below.

4.6.1 Rosenbrock Method

This method is an iterative procedure that bears some correspondence to the exploratory search of Hooke & Jeeves, in which small steps are taken during the search in orthogonal coordinates. Instead of continually searching the coordinates corresponding to the directions of independent variables, an improvement can be made after one cycle- of coordinate search by lining the search directions in an orthogonal system, with the overall step on the previous stage as the first building block for the new search coordinates [69]. Rosenbrock [140] applied this improvement to optimize nonlinear unconstrained problems with several variables. Constrained Rosenbrock method (Hill algorithm) is successfully applied in the induction motor by Bhardwaj, et al., [14] with the further improvement of this method that it does not necessarily require a starting feasible point. The steps involved in this algorithm are given below;

Step 1)- Read n, m (explicit plus implicit constraints) and number of stages (nn)

Select starting point X_i and initial step size λ_i, i=1,2 ,..............., n.

Step 2)- Calculate objective function and constraints

Step 3)- Check constraints. If satisfied, go to step 4, otherwise select another starting point using the iterative method and go to step 2. Continue the procedure till feasible point is obtained and then go to step 4. If in a preselected range no feasible design exists, then print the error message and terminate the program.

Step 4)- Set i=1

Step 5)- Increment the variable X_i with a discrete λ_i parallel to the axis and evaluate the function.

Step 6)- Check the feasibility of the point. This is done as follows-

Define F_0, the current best objective function value for a point where the constraints are satisfied, and F^*, the current best objective function value for a

point where the constraints are satisfied and in addition the boundary zones are not violated. Initially set $F_0 = F^* =$ feasible starting point objective function. If the current point objective function, F, is worse than F_0 or if constraints are violated the trial is a failure, go to step 7.

If there is an improvement in the objective function and in addition the constraints and boundary zones are violated, set $F^*=F_0$ and go to step 8.

Step 7)- Record the failure and set λ_i(new)= $-\beta$ λ_i(old), The recommended value of β by Rosenbrock is 0.5.

Step 8)- Record the success and set λ_i(new)=α λ_i(old), The recommended value of α by Rosenbrock is 3.0

Step 9)- Check whether all the variables are considered. If not set i= i+1 and go to step 5

Step 10)-Check convergence. If the number of stages prescribed exceeds the prescribed limit or if the change in the objective function or the vector components is smaller than the preselected value, go to step 15

Step 11)- Check for the success and failure.

If at least one success and failure have been encountered in all directions, the stage ends. If so, go to next step. If success and failure are not encountered in each direction, go to step 4.

Step 12)- Rotate the axes. Each rotation of axes is termed- a stage. The axes are rotated by the following procedure.

$$S_{i,j}^{(K+1)} = \frac{D_{i,j}^{(K)}}{\sqrt{\sum_{m=1}^{N}(D_{m,j}^{K})^2}} \qquad (4.10)$$

where $D_{i,1}^{(K)} = A_{i,1}^{(K)}$

$$D_{i,j}^{(K)} = A_{i,j}^{(K)} - \sum_{e=1}^{j-1}[(\sum_{n=1}^{j} M_{n,e}^{K+1} A_{n,j}^{(K)}).M_{i,e}^{K+1}]$$

$$j = 2, 3,........N$$

$$A_{i,j}^{(K)} = \sum_{e=j}^{N} d_e^{(K)} M_{i,e}^{(K)}$$

where *i= variable index=1,2,................n*

j=direction index=1,2,....................n

K=stage index

d$_i$= sum of distances moved in the I direction since last rotation of axes

M$_{i,j}$= normalized direction vector component

For easy to understand, this method is illustrated in Fig. 4.20.

Let P_1 be the initial point.

An exploratory search along the coordinate axes leads to point P_2.

Construction of a new orthonormal frame with a first direction along P_1P_2.

Starting from P_2, another exploratory search along the new coordinates leads to P_3.

This iterative process is repeated until the error test meets the requirements
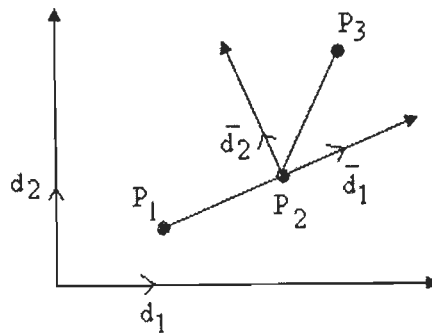
Fig. 4.20 Illustration of Rosenbrock search method

Step 13)- Make a search in all the directions using the new coordinate axes.

$$X_i^{(K)}(new) = X_i^{(K)}(old) + \lambda_j^{(K)} M_{i,j}^{(K)} \qquad (4.11)$$

Go to step 4

Step 14)- Print results of optimum design

Step 15)- Stop.

4.6.2 Simulated- Annealing Method

Simulated Annealing (SA) is a meta-heuristic algorithm and can be applied to global optimization problems. This method was developed based on the analogy between the annealing process of solids and the process of solving combinatorial optimisation problems [87]. The procedure [102] of simulated annealing starts from an initial solution to the problem. It then generates a new trial solution from the neighbourhood of the current solution. If the new solution is better than the current solution, it is accepted and used as the new current solution. Otherwise, it may be accepted or rejected depending on an acceptance probability which is determined by the difference between objective functions of the two solutions and by a control parameter called temperature following the convention in thermodynamics. This process then continues from the new current solution. Initially, the temperature is set at a high level so that almost all moves will be accepted. It is then decreased slowly during the procedure until almost no moves will be accepted. SA is successfully applied in the induction motor design and the computational steps of this algorithm are as follows [16].

Step 1: Initialization

Choose an initial point $x^{(0)}$, a termination criterion ε. Set *Temp*, temperature at a sufficiently high value, number of iterations (n) to be performed at a particular temperature, and set t=0.

Step 2: Calculate a neighboring point $x^{(t+1)} = N(x^{(t)})$, usually a random point in the neighborhood is created.

Step 3: If $\Delta E = E(x^{(t+1)} - E(x^{(t)}) \leq 0$, set $t = t+1$; or else create a random (r) number in the range (0,1). If $r \leq \exp(\Delta E / Temp)$ set $t = t +1$; or go to step 2.

Step 4: If $|x^{(t+1)} - x^{(t)}| \leq \varepsilon$ and *Temp* is small, terminate; or else if (t mod n) = 0, then lower T according to a cooling schedule. Go to step 2; or go to step 3.

Here, *Temp* is the temperature, ΔE is the difference in the objective function values.

4.6.3 Particle Swarm Optimization (PSO)

The concept of Particle Swarm Optimization (PSO) was first suggested by Kennedy and Eberhart [79]. Since its development in 1995, PSO has emerged as one of the most promising optimizing technique for solving global optimization problems. Its mechanism is inspired by the social and cooperative behavior displayed by various species like birds, fish etc including human beings. The PSO system consists of a population (swarm) of potential solutions called particles. These particles move through the search domain with a specified velocity in search of optimal solution. Each particle maintains a memory which helps it in

keeping the track of its previous best position. The positions of the particles are distinguished as personal best and global best. The working of the classical Particle Swarm Optimization (PSO) may be described as:

In a D-dimensional search space the position of the ith particle is represented as $X_i = (x_{i1}, x_{i2}, \ldots x_{iD})$. Each particle maintains a memory of its previous best position $P_{besti} = (p_{i1}, p_{i2} \ldots p_{iD})$. The best one among all the particles in the population is represented as $P_{gbest} = (p_{g1}, p_{g2} \ldots p_{gD})$. The velocity of each particle is represented as $V_i = (v_{i1}, v_{i2}, \ldots v_{iD})$. In each iteration, the P vector of the particle with best fitness in the local neighborhood, designated g, and with this P vector of the current particle is combined to adjust the velocity along each dimension and a new position of the particle is determined using that velocity. The two basic equations which govern the working of PSO are that of velocity vector and position vector given by:

$$v_{id} = wv_{id} + c_1 r_1 (p_{id} - x_{id}) + c_2 r_2 (p_{gd} - x_{id}) \qquad (4.12)$$

$$x_{id} = x_{id} + v_{id} \qquad (413)$$

Acceleration constants c_1, c_2 [46] and inertia weight w are the predefined by the user and r_1, r_2 are the uniformly generated random numbers in the range of [0, 1], p_i and p_g are the particle's previous best position and the swarm's previous best position, and x_i is the current position of the ith particle.

The first part of Eq. (4.12) (i.e. wv_{id}) represents the inertia of the previous velocity, which serves as a memory of the previous flight direction. This memory term can be seen as a momentum, which prevents the particle from drastically changing direction, and to bias towards the current direction. The concept of inertia weight w was introduced by Shi and Eberhart [148] as a mechanism to control the exploration and exploitation skills of the swarm. The inertia weight controls the momentum of the swarm by weighing the contribution of the previous velocity. The value of inertia weight is very significant in order to ensure an optimal tradeoff between exploration and exploitation mechanisms of the swarm population. Larger values of w enhance the exploration by locating promising regions in the search space whereas a smaller value helps to endorse the local exploitation. Initially the inertia weight was kept static during the entire search duration for every particle and dimension. With the due course of time inertia weights with dynamic weights were introduced.
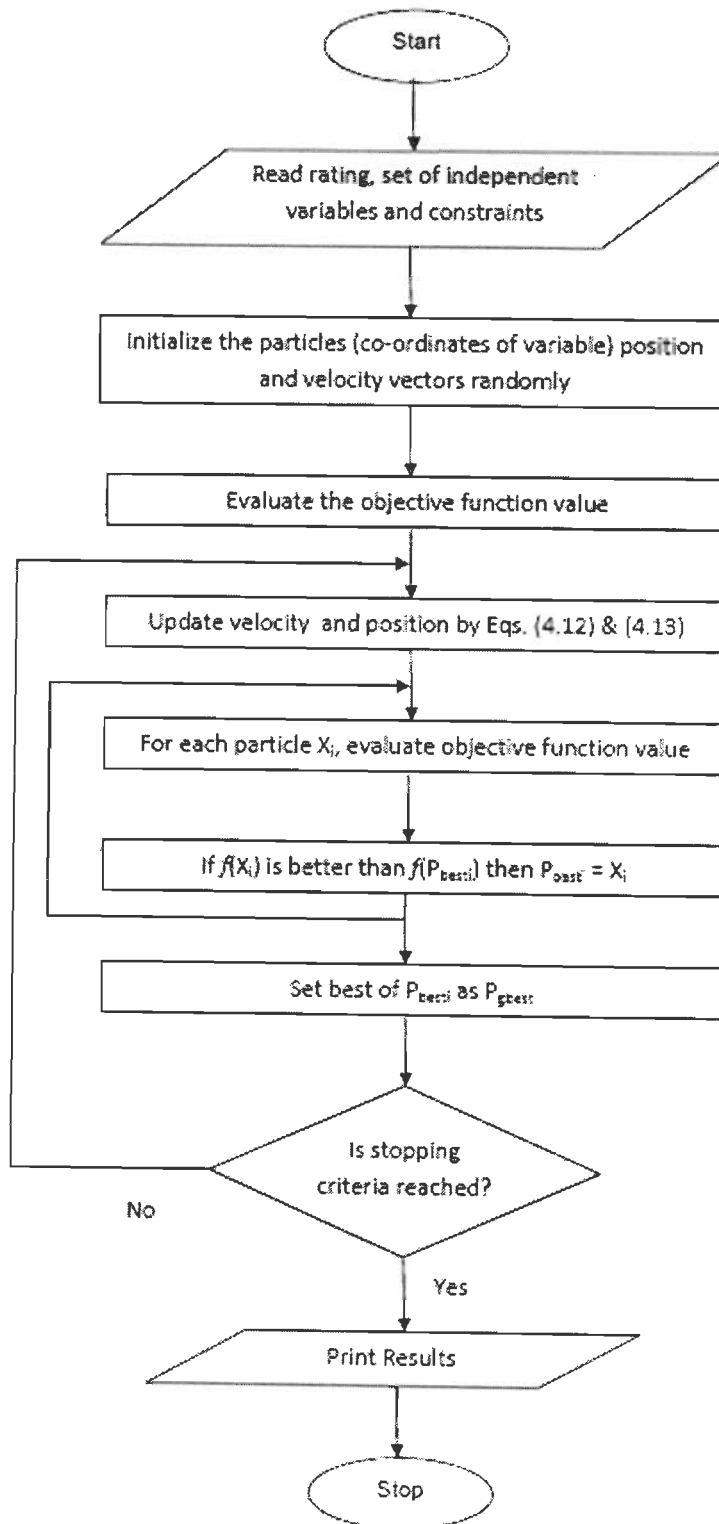
Fig. 4.21. Flowchart of Particle Swarm Optimization technique

The second part (i.e. $c_1 r_1 (p_{id} - x_{id})$) is the cognition part and it tells us about the personal experience of the particle. In a sense, this cognition part resembles individual memory of the position that was the best for the particle. The effect of this term is that particles are drawn back to their own best positions, resembling the tendency of individuals to return to

situations or places that was most satisfied in the past.

The third part (i.e. $c_2 r_2 (p_{gd} - x_{id})$) represents the cooperation among particles and is therefore named as the social component [79]. This term resembles a group norm or standard which individuals seek to attain. The effect of this term is that each particle is also drawn towards the best position found by the particle's neighbourhood. The computational steps of PSO are shown below and the corresponding flow chart is shown in Fig. 4.21.

Step1: Initialization

For each particle i in the population,

Step1.1: Initialize X[i] with Uniform distribution.

Step1.2: Initialize V[i] randomly.

Step1.3: Evaluate the objective function of X[i],and assigned the value to fitness[i].

Step1.4: Initialize P_{best}[i] with a copy of X[i].

Step1.5: Initialize Pbest_fitness[i] with a copy of fitness[i].

Step1.6: Initialize P_{gbest} with the index of the particle with the least fitness.

Step 2: Repeat until stopping criterion is reached:

For each particle i:

Step 2.1: Update V[i] and X[i] according to Eqs. (4.12) and (4.13).

Step 2.2: Evaluate fitness[i].

Step 2.3: If fitness[i] < Pbest_fitness[i] then P_{best}[i] =X[i], Pbest_fitness[i] =fitness[i].

Step 2.4: Update P_{gbest} by the particle with current least fitness among the Population.

4.6.4 Improved Particle Swarm Optimization

Although the rate of convergence of PSO is good due to fast information flow among the solution vectors, its diversity decreases very quickly in the successive iterations resulting in a suboptimal solution [100]. Aiming at this shortcoming of PSO algorithms, many variations have been developed by the researchers to improve its performance. The Particle Swarm Optimization with Quadratic Interpolation (QIPSO) algorithm proposed by Pant, et.al [144] which works initially like basic PSO and does crossover to find new particle and it is accepted in the swarm only if it is better than the worst particle present in the swarm. The process is repeated iteratively until a better solution is obtained. It uses a = X_{min}, (the

leader having minimum function value) and two other randomly selected particles {b, c} (a, b and c are different particles i.e. a ≠ b ≠ c) from the swarm (tribe) to determine the coordinates of the new particle $\tilde{x} = (\tilde{x}^1, \tilde{x}^2, ..., \tilde{x}^n)$, where

$$\tilde{x}^i = \frac{1}{2} \frac{(b^{i^2} - c^{i^2})*f(a) + (c^{i^2} - a^{i^2})*f(b) + (a^{i^2} - b^{i^2})*f(c)}{(b^i - c^i)*f(a) + (c^i - a^i)*f(b) + (a^i - b^i)*f(c)} \qquad (4.14)$$

The flow of QIPSO algorithm is shown in Fig. 4. 22, where $f(x)$ represents the objective function value of x, and the computational steps are given below.

Step 1: Initialization.

>   For each particle i in the population:

>   **Step1.1**: Initialize the particles (X[i]) with Uniform distributed random numbers.

>   **Step1.2**: Initialize particle's velocity V[i].

>   **Step1.3**: Evaluate the objective function of X[i], and assigned the value to fitness[i].

Step 2: Position and Velocity updation,

>   For each particle i:

>   **Step 2.1**: Update V[i] and X[i] according to Eqs. (4.12) and (4.13)

>   **Step 2.2**: Evaluate fitness[i].

>   **Step 2.3**: If fitness[i] < Pbest_fitness[i] then P_{best}[i] =X[i], Pbest_fitness[i] =fitness[i].

>   **Step2.4**: Update P_{gbest} by the particle with current least fitness among the population.

Step 3: Find the new particle using Eq. (4.14)

>   If new particle is better than worst particle in the swarm, replace worst particle by the new particle

Step 4: Go to step 2 until stopping criterion is reached.

```
                          ┌──────────┐
                          │  Start   │
                          └────┬─────┘
                               │
                ╱──────────────────────────────╲
               ╱  Read rating, set of independent ╲
               ╲   variables and constraints      ╱
                ╲──────────────────────────────╱
                               │
         ┌─────────────────────────────────────────────┐
         │ Initialize the particles (co-ordinates of    │
         │ variable) position and velocity vectors      │
         │ randomly                                     │
         └──────────────────┬──────────────────────────┘
                            │
         ┌─────────────────────────────────────────────┐
         │     Evaluate the objective function value    │
         └──────────────────┬──────────────────────────┘
                            │
         ┌─────────────────────────────────────────────┐
         │ Update velocity and position by Eqs.         │
         │ (4.12) & (4.13)                              │
         └──────────────────┬──────────────────────────┘
                            │
         ┌─────────────────────────────────────────────┐
         │ For each particle Xₗ, evaluate objective     │
         │ function value                               │
         └──────────────────┬──────────────────────────┘
                            │
         ┌─────────────────────────────────────────────┐
         │ If f(Xᵢ) is better than f(Pbest) then        │
         │ Pbest = Xᵢ                                   │
         └──────────────────┬──────────────────────────┘
                            │
         ┌─────────────────────────────────────────────┐
         │        Set best of Pbest as Pgbest           │
         └──────────────────┬──────────────────────────┘
                            │
         ┌─────────────────────────────────────────────┐
         │  Find a new particle (temp) using Eqn.(4.14) │
         └──────────────────┬──────────────────────────┘
                            │
         ┌─────────────────────────────────────────────┐
         │ Calculate the fitness value of particle temp │
         └──────────────────┬──────────────────────────┘
```

Update velocity and position by Eqs. (4.12) & (4.13)

For each particle X_i, evaluate objective function value

If $f(X_i)$ is better than $f(P_{best})$ then $P_{best} = X_i$

Set best of P_{best} as P_{gbest}

Find a new particle (temp) using Eqn. (4.14)

Calculate the fitness value of particle temp

If f (temp) is better than f (worst particle) — No

Yes

Replace the worst particle by the new one

Is stopping criteria reached?   No   Yes

Print

Stop

Fig. 4.22. Flowchart of QIPSO technique

4.7 Results and Discussion

The main parameters of PSO and QIPSO algorithms are inertia weight w and acceleration constants c_1 and c_2. After performing a number of experiments and going through various PSO versions available in literature, the present work considered the following experimental settings: the inertial weight w is taken to be linearly decreasing from 0.9 to 0.5. Acceleration constants c_1 and c_2 are taken as 2.0 each and r_1, r_2 are taken as the uniformly distributed random numbers between 0 and 1. Both the algorithms were implemented using Turbo C++ on a PC compatible with Pentium IV, a 3.2 GHz processor and 2 GB of RAM.

Particle Swarm Optimization and its variant, QIPSO with their parameters settings mentioned above have been applied to optimize poly-phase induction motor design. The programs have been tested with some standard benchmark problems (Appendix A) having different dimensions and then applied to the motor design. Results have been presented for three different capacity motors, i.e. 2.2 kW, 7.5 kW and 110 kW.

The results of fresh design of induction motor obtained from different optimization techniques and their comparative study is presented. The salient features of the optimized design are discussed. In view of the results presented in Tables 4.1 – 4.13 discussions have been extended to investigate the usefulness of the methods employed for optimization of design of induction motor.

4.7.1 Material Cost

The results of two optimized induction motors, sample motor 1 (7.5 kW, 440 V) and sample motor 2 (110 kW, 3.3 kV) whose specifications are available in Appendix 4, using Particle Swarm Optimization (PSO) and its variant, Quadratic Interpolation based Particle Swarm Optimization (QIPSO) algorithms are shown in Tables 4.1 and 4.2. Results of conventional method (constrained Rosenbrock and normal design) have also been tabulated for the ease comparison. It is noted that the limits of variables chosen for all the optimization techniques have been the same throughout. The results obtained by PSO and QIPSO are better than the other methods and their percentage improvements are shown in Table 4.3. The analysis of the results, obtained design, are given below;

The permissible limit for maximum stator tooth flux density has been taken as 2.0 wb/m^2 and this value in optimized design is much below the saturation limit. Average flux density value offered by PSO and QIPSO are higher than the Rosenbrock and normal methods and hence lower material cost. Since the cost of copper is more than the iron, minimum copper is used in the PSO and QIPSO based design in comparison with Rosenbrock method. As a result of this, the winding current densities used in the PSO and QIPSO based design have

comparatively of much higher values. Use of such a high current density requires much less slot dimensions and provide more tooth width, thus reducing the saturation in the teeth portion. Since the temperature rise of the motor depends on the product of ampere conductors/m and stator current density the PSO and its variant have chosen lower value of ampere conductors/m than Rosenbrock to manage limited temperature rise in the motor. Tabulated results show that the PSO and its variant based optimizations make use of lower specific electric loading thus permitting the use of high winding current density.

Table 4.1 Optimum Design Results in Sample Motor 1 for Material Cost Minimization

Items	Normal Design [15]	Rosenbrock Method [15]	PSO	QIPSO
ampere conductor/m	16000	20000	19260	19457
stack length / pole pitch	1.00	1.1877	0.937	1.069
stator slot depth to width	4.00	3.7315	4.61	4.343
Stator core depth	30.00	27.316	30.795	27.242
Air gap flux density	0.50	0.4938	0.7171	0.697
stator current density	6.00	8.193	10.08	9.092
rotor current density	8.00	8.713	8.95	8.721
Stator tooth flux density	1.0928	1.2464	1.68	1.746
Stator temperature rise, °C	47.3115	69.99	40.66	41.171
Full load efficiency, pu	0.8402	0.824	0.86	0.8640
No load current, pu	0.3870	0.4078	0.5	0.500
Starting torque, pu	1.6774	1.596	1.9	1.666
Maximum torque, pu	2.7468	2.5	2.811	2.634
Full load Power factor	0.8924	0.8867	0.9	0.917
Full load slip	0.0454	0.0497	0.042	0.041
Rotor temperature rise, °C	27.7774	40.32	28	32.3
Material cost[a] (Rs)	1131.35	847.7	644.5	604.68
Stator bore diameter (m)	0.1895	0.161	0.1636	0.146
Stack length (m)	0.1489	0.1502	0.1204	0.122

[a] For comparison purpose, Rs. 14/kg for iron cost and Rs 42/kg for winding materials cost are considered as in [15].

Table 4.2 Optimum Design Results in Sample Motor 2 for Material Cost Minimization

Items	Normal Design [15]	Rosenbrock Method [15]	PSO	QIPSO
ampere conductor/m	23500	27499	18572.8	20162.4
stack length / pole pitch	1.20	0.9833	0.961	0.9801
stator slot depth to width	3.60	3.3347	4.5379	4.201
Stator core depth	55.00	44.38	31.466	31.244
Air gap flux density	0.42	0.4643	0.4684	0.4712
stator current density	5.00	7.2171	11.841	10.72
rotor current density	9.00	14.3413	13.2519	15.326
Stator tooth flux density	1.3359	1.4206	1.0889	1.275
Stator temperature rise, °C	46.00	69.99	38.5812	40.08
Full load efficiency, pu	90.87	88.09	0.8991	0.900
No load current, pu	0.2421	0.3016	0. 5	0. 5
Starting torque, pu	1.5665	1.9903	2.299	2.109
Maximum torque, pu	3.5147	3.2015	3.521	3.205
Full load Power factor	0.9409	0.9201	0.9554	0.96
Full load slip	0.0279	0.04387	0.0446	0.0442
Rotor temperature rise, °C	24.83	49.19	35.562	38.435
Material cost [a] (Rs)	9554.83	6459.66	5340.37	5128.0
Stator bore diameter (m)	0.5148	0.5040	0.39364	0.3901
Stack length (m)	0.3236	0.2609	0.41855	0.4191

[a] For comparison purpose, Rs. 14/kg for iron cost and Rs 42/kg for winding materials cost are considered as in [15].

Table 4.3 Percentage Improvement of PSO and QIPSO Algorithms in comparison with normal design and Rosenbrock method

Algorithm	Sample Motor 1		Sample Motor 2	
	Normal Design	Rosenbrock's Method	Normal Design	Rosenbrock Method
PSO	43.0	23.9	44.1	17.3
QIPSO	46.5	28.6	46.3	20.6

The core depth in QIPSO based optimal design decreases considerably causing more flux concentration in core and hence requires more ampere turns thus increasing the no load current (shown in Table 4.1 and 4.2). The ratio of stator slot depth to width is mainly responsible for controlling the torque ratio. In the PSO and QIPSO based optimized design, this ratio is higher than Rosenbrock techniques and hence comparatively higher torque ratio has been obtained. The starting torque ratio, however, is well above the limiting value due to use of higher current density.

The power factor is slightly higher in optimized design than Rosenbrock and the full load rotor temperature rise is much lower than the specified limit. The core length to pole pitch ratio is mainly responsible for cost reduction and higher values are preferred. On the other hand the performance of the motor is controlled to a greater extent by the stator slot depth to width ratio. Both these ratios adjust themselves in the PSO and QIPSO based design to obtain the minimum cost of motor.

In general, for minimum material cost, the tendency of the variable in obtaining an optimized design has been to have:

1. lower specific electric loading
2. lower stator core depth
3. lower value of stator slot depth to width ratio
4. higher values of stator and rotor winding current densities.

The values of ampere conductors/m, stator and rotor current densities in sample motor 1 chosen by all the algorithms with their material costs are shown in Fig 4.23 - 4.25. PSO and QIPSO have chosen lower value of ampere conductors/m and higher values of stator and rotor current densities than Rosenbrock which results low material cost of the motor.
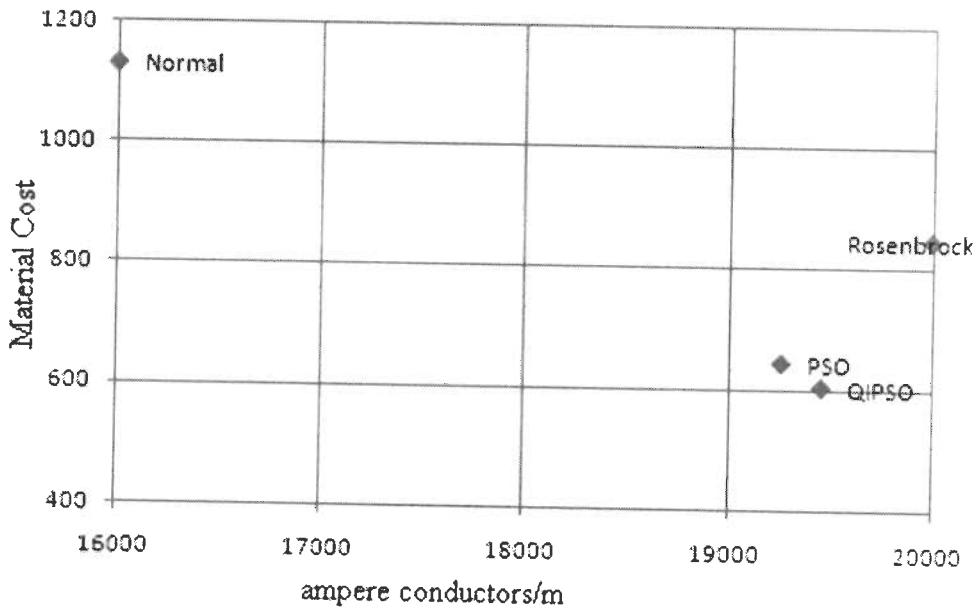
Fig. 4. 23. Optimal values of ampere conductors at material cost minimization.
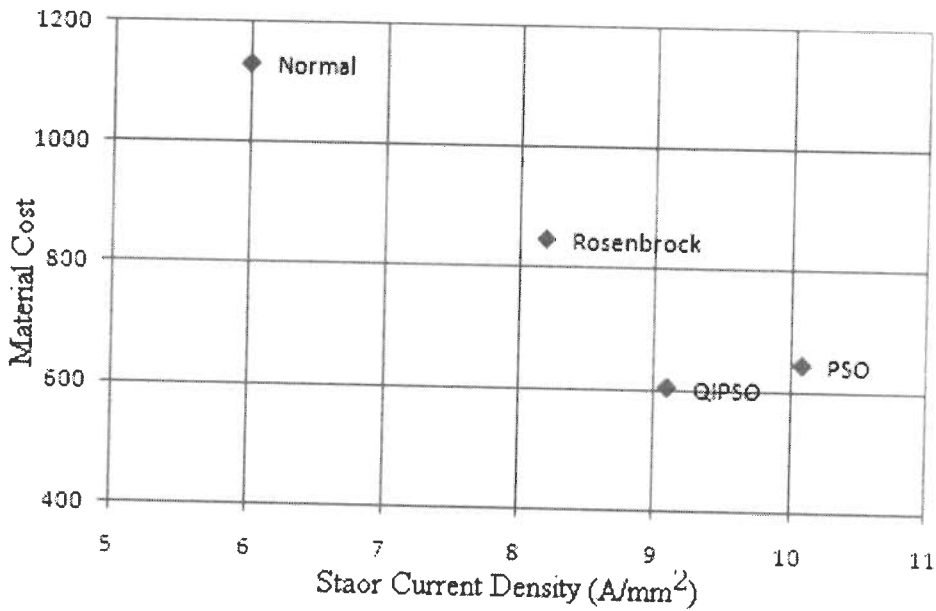
Fig. 4. 24. Optimal values of stator current density at material cost minimization.
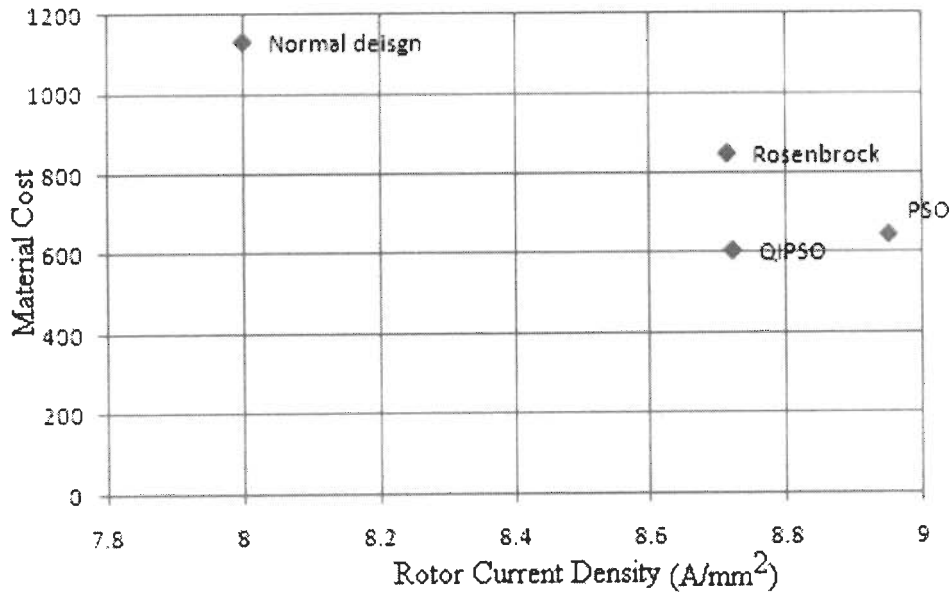
Fig. 4. 25 Optimal values of rotor current density at material cost minimization.

4.7.2 Efficiency, Starting Torque and Temperature Rise Optimization

The results of PSO and QIPSO based optimal deign of a 3 hp, 400V, three-phase induction motor (sample motor 3, specifications available in Appendix A.1) for the objective functions, efficiency, starting torque and temperature rise are given in Tables 4.4 – 4.6. The results obtained by PSO and QIPSO have been compared with the available literature i.e. Simulated Annealing (SA) technique and normal design.

If the motor is designed with respect to optimizing its efficiency, the QIPSO gave considerably better results than normal design and also quite better than SA and PSO.

Temperature rise and slip are lower in QIPSO but main dimensions are slightly higher than SA which results higher volume. Width of stator slot in the PSO and QIPSO based optimized design is much higher than normal design and SA. The values of depth of the stator slot, width and depth of rotor slots are lower in the PSO and QIPSO based design. Percentage improvement in the objective functions by the help of QIPSO in comparison with other methods is shown in Table 4.7.

If the motor is designed with respect to its starting torque maximization, QIPSO offers better results than others significantly. In this case, main dimensions are higher but temperature rise considerably reduced. Full load slip in QIPSO is smaller than normal design and SA but more than PSO. Similar to efficiency optimization, required air-gap flux density is more in QIPSO compared with other methods but within the limiting value.

Table 4.4 Optimum Design Results in Sample Motor 3 for Efficiency Maximization

Items	Optimization algorithms			
	Normal [16]	SA [16]	PSO	QIPSO
Width of the stator slot (m)	0.00132	0.0011	0.00487	0.00433
Depth of the stator slot (m)	0.021	0.0159	0.01962	0.01515
Width of the rotor slot (m)	0.0068	0.005	0.00399	0.00355
Depth of the rotor slot (m)	0.0093	0.0091	0.00634	0.00660
Air gap flux density (wb/m^2)	0.6	0.521	2.000	2.00
Air-gap length (m)	0.0003	0.0003	0.0005	0.0005
Full load slip	0.0699	0.056	0.0488	0.0416
Stator bore diameter (m)	0.105	0.102	0.0902	0.0890
Stator outer diameter (m)	0.181	0.177	0.208	0.1913
Stack length (m)	0.125	0.097	0.1269	0.109
Temperature rise, °C	46.8178	41.391	44.463	39.83
Efficiency	**0.80309**	**0.82848**	**0.833**	**0.8356**
Starting torque, pu.	1.2027	1.3444	1.426	1.730
Power factor	0.8041	0.8333	0.840	0.800

In temperature rise minimization, again QIPSO performed well with an improvement percentage of 18.37%, 4.57% and 10.03% compared to normal design, SA and PSO respectively. Here main dimensions are lower and efficiency is slightly better than others. For overall performance, QIPSO gave better results than others and it is more suitable to the optimization of design of induction motor.

From the design results presented in Tables 4.4 – 4.6, particularly the following variable show dominance in the PSO and QIPSO based designs to achieve good performances in all the objective functions.

1. Width of the stator slot
2. Depth of the rotor slot
3. Length of the stator stack

The value of above variables obtained from the different optimization algorithms and the corresponding objective function values are shown in Fig. 4.26 – 4.34. The effects of these variables in the performance indices (efficiency, starting torque and temperature rise) and how the optimization algorithms have carefully chosen these values are realized in the next chapter with the help of SPEED software.

Table 4.5 Optimum Design Results in Sample Motor 3 for Starting Torque Maximization

Items	Optimization algorithms			
	Normal [16]	SA [16]	PSO	QIPSO
Width of the stator slot (m)	0.00132	0.0012	0.00464	0.00555
Depth of the stator slot (m)	0.021	0.0187	0.02272	0.02118
Width of the rotor slot (m)	0.0068	0.0056	0.00379	0.00454
Depth of the rotor slot (m)	0.0093	0.0071	0.00537	0.00291
Air gap flux density (wb/m^2)	0.6	0.4713	1.1805	2.00
Air-gap length (m)	0.0003	0.0004	0.0005	0.0005
Full load slip	0.0699	0.0645	0.046	0.050
Stator bore diameter (m)	0.105	0.1028	0.111	0.0999
Stator outer diameter (m)	0.181	0.1733	0.252	0.2179
Stack length (m)	0.125	0.1162	0.164	0.114
Temperature rise, °C	46.8178	64.475	53.11	41.810
Efficiency	0.8030	0.79179	0.813	0.825
Starting torque, pu.	**1.2027**	**1.3776**	**1.668**	**1.966**
Power factor	0.8041	0.7938	0.863	0.813
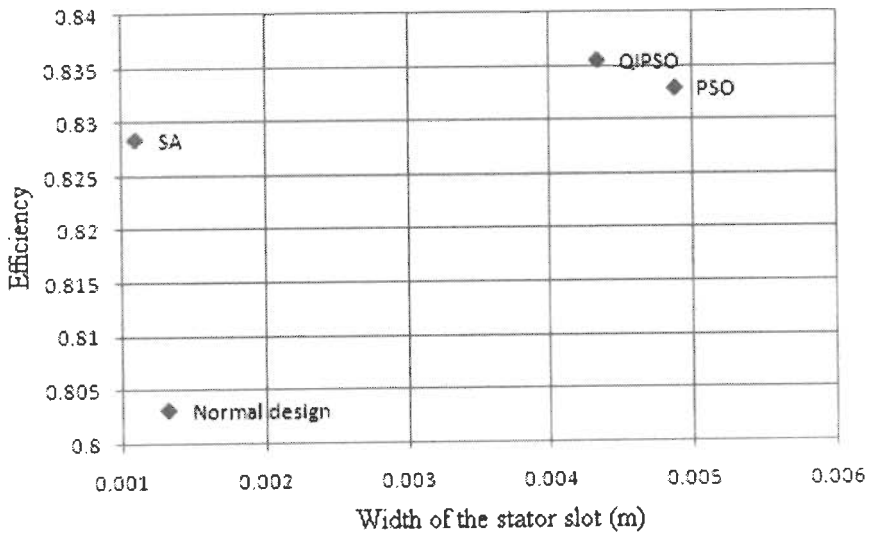
Fig. 4. 26. Optimum values of width of stator slot for maximum efficiency

4.6 Table Optimum Design Results in Sample Motor 3 for Temperature Rise Minimization

Items	Optimization algorithms			
	Normal [16]	SA [16]	PSO	QIPSO
Width of the stator slot (m)	0.00132	0.0013	0.00444	0.00457
Depth of the stator slot (m)	0.021	0.0236	0.01919	0.02258
Width of the rotor slot (m)	0.0068	0.005	0.00363	0.00374
Depth of the rotor slot (m)	0.0093	0.0093	0.00652	0.00499
Air gap flux density (wb/m^2)	0.6	0.439	2.000	1.632
Air-gap length (m)	0.0003	0.0004	0.0005	0.0005
Full load slip	0.0699	0.0684	0.05	0.05
Stator bore diameter (m)	0.105	0.101	0.085	0.189
Stator outer diameter (m)	0.181	0.171	0.1919	0.099
Stack length (m)	0.125	0.1216	0.124	0.114
Temperature rise, °C	**46.817**	**40.039**	**42.470**	**38.20**
Efficiency	0.80309	0.803748	0.827	0.814
Starting torque, pu.	1.2027	1.117	1.098	1.133
Power factor	0.8041	0.7814	0.830	0.858
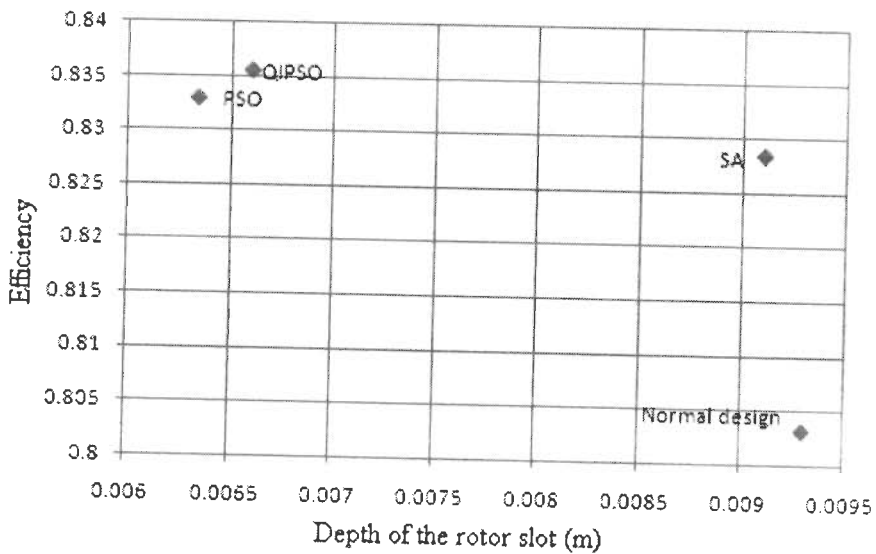
Fig. 4. 27. Optimum values of depth of rotor slot for maximum efficiency
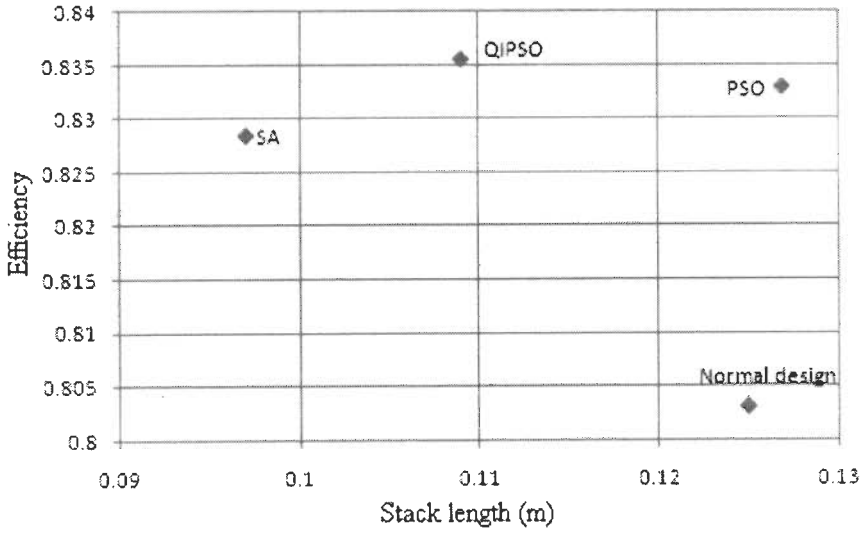
Fig. 4. 28. Optimum values of stack length for maximum efficiency
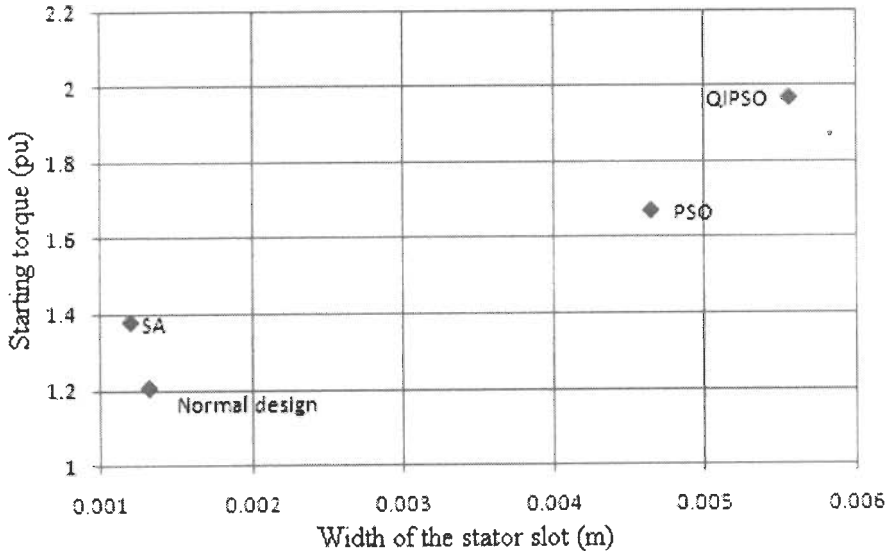
Fig. 4. 29. Optimum values of width of stator slot for maximum starting torque
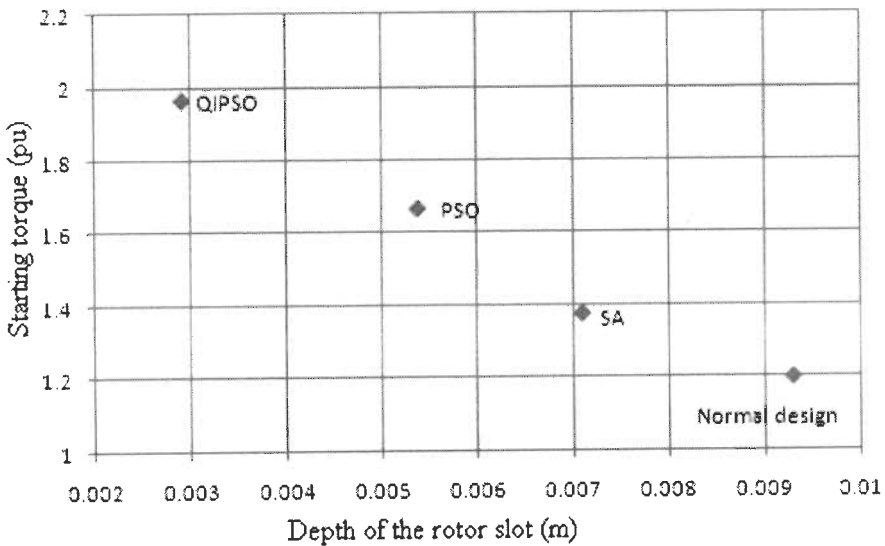
Fig. 4. 30. Optimum values of depth of rotor slot for maximum starting torque
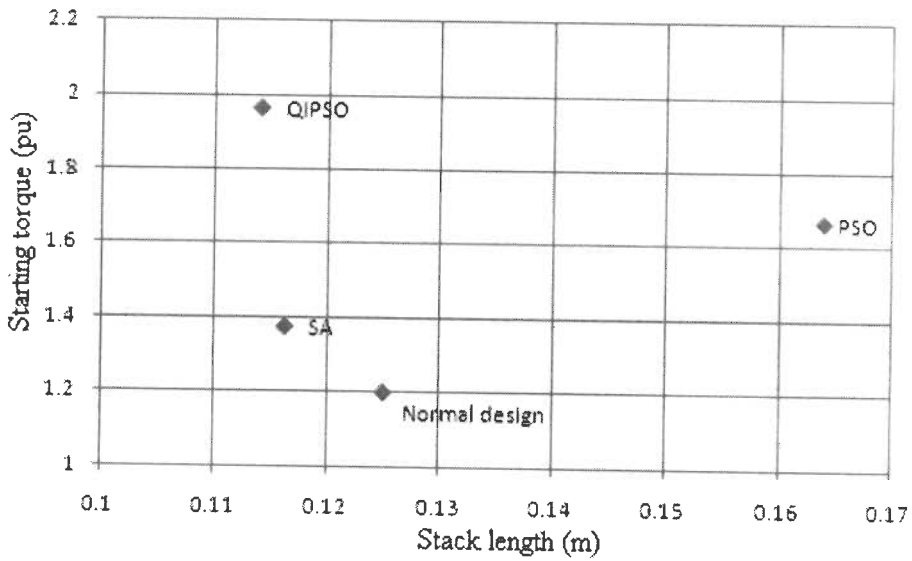
Fig. 4. 31. Optimum values of stack lenth for maximum starting torque
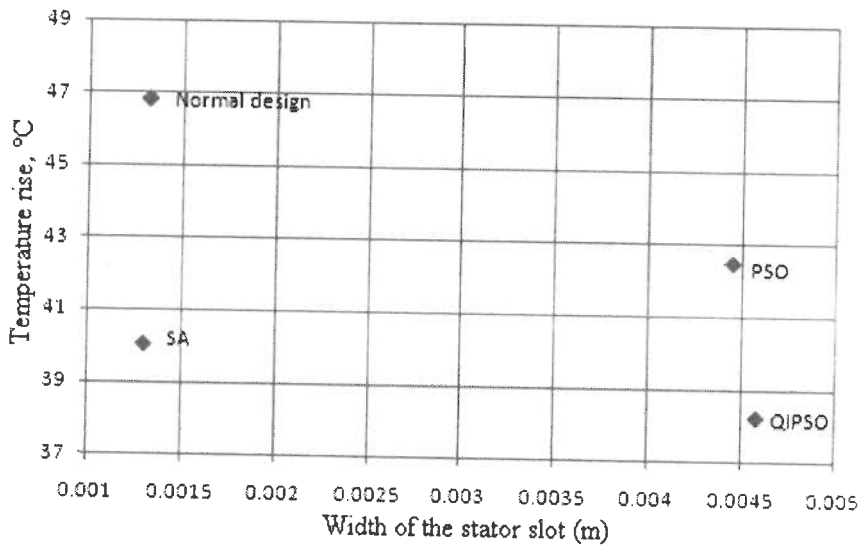
Fig. 4. 32. Optimum values of width of stator slot for minimum temperature rise
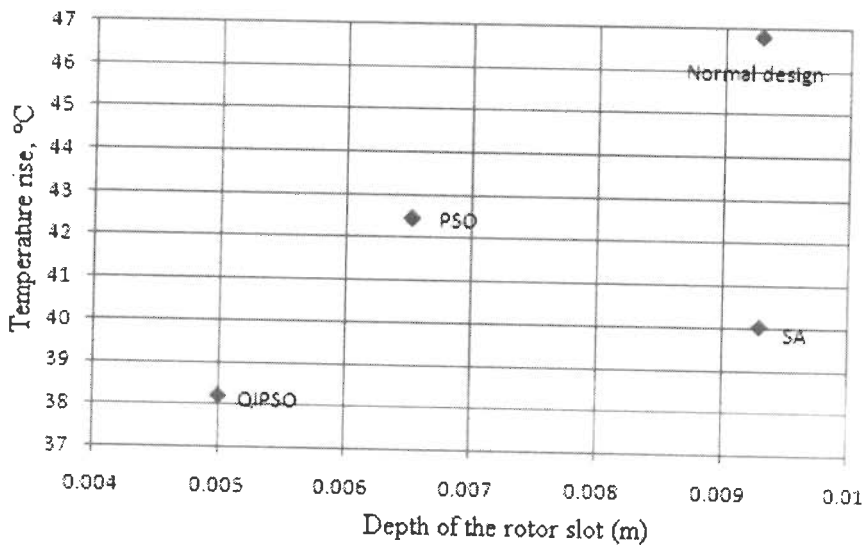
Fig. 4. 33. Optimum values of depth of rotor slot for minimum temperature rise
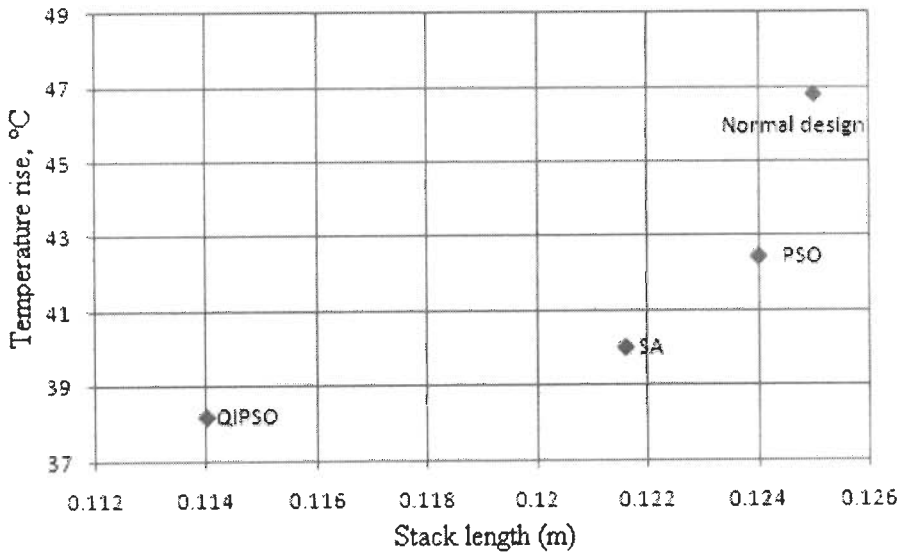
Fig. 4. 34. Optimum values of stack length for minimum temperature rise

Table 4.7 Improvement Percentage using QIPSO in Comparison with Normal Design, PSO and SA

Objective Function	Sample motor 3		
	Normal	SA	PSO
Efficiency	4.05	0.85	0.31
Starting Torque	63.46	42.71	19.66
Temperature rise	18.38	4.57	10.03

4.7.3 Operating Cost

Total energy cost (TEC) or operating cost of a motor is an important issue in the industry. On an average standard motors consume electricity equivalent to 60-100 times its purchasing price during its working life. A motor consumes electricity equivalent to its capital cost in just three weeks of continuous use. Indian electricity service providers have two parts of tariff for industrial consumers: (i) energy charge, (ii) fixed demand charge. PSO is used to design the motors of minimum operating cost and optimized design results are shown in Table 4.8.

a) Energy cost calculation

The energy cost of the induction motor can be calculated over the whole life cycle of the motor and is given below. Power factor penalty is not considered in this paper because almost all the industries have centralized power factor correction equipments.

$$S = C_e * T * N * P_{in} \qquad (4.15)$$

where   S   Energy cost for life periods

           C_e Energy cost (US $/KWH)

           T   Total operating hour/year

           N   Motor's evaluation life in years

           P_{in} Input power of the motor (KW)

b) Demand cost calculation

Demand charge cost (D) consumed by the motor over the whole life of the motor can be calculated by using the equation (4.4) and is given below

$$D = C_d * 12 * N * P_{in} \qquad (4.16)$$

where, C_d - Demand cost per month (US $)

The total energy cost (TEC) of the motor for the complete life is the summation of two individual energy costs and is given by

$$TEC = P_{in} * N * \{(C_e * T) + (C_d * 12)\} \qquad (4.17)$$

When total energy cost minimization is considered as an objective function in PSO based design, efficiency and torque are considerably higher than Rosenbrock algorithm. Higher ampere conductors, stack length to pole pitch ratio, stator slot depth to width, stator core depth and average air gap flux density are required to achieve optimum operating cost or energy cost of the motor. But the lower values of stator and rotor winding current densities are required to have a motor with minimum operating cost. Stator and rotor resistances are less in the optimized design. The active material costs rise by 36% and 15.4% for the sample motor 1 and sample motor 2 respectively, if optimization is done on the basis of energy cost. But, the energy cost or operating cost is reduced by 6.5% and 4.4% for the sample motor 1 and sample motor 2 respectively.

Table 4.8 Optimum design results for energy cost minimization using PSO

Items	Objective function (Sample Motor 1)		Objective function (Sample Motor 2)	
	Material cost	Energy cost	Material cost	Energy cost
ampere conductor/m	19260	23847	18572.8	16216.1
stack length / pole pitch	0.937	1.32	0.961	1.5534
Stator slot depth to width	4.61	5.04	4.5379	4.8914
Stator core depth	30.795	35.19	31.466	45.490
air gap flux density	0.7171	0.75	0.4684	0.7858
Stator current density	10.08	5.47	11.841	6.6228
rotor current density	8.95	5.2	13.2519	7.8297
Stator tooth flux density	1.68	2.0	1.0889	2.000
Stator temperature rise, °C	40.66	48.4	38.5812	40.276
Full load efficiency, pu	0.86	0.91	0.8991	0.9525
No load current, pu	0.5	0.5	0. 5	0.1942
Starting torque, pu	1.9	2..05	2.299	2.311
Maximum torque, pu	2.811	3.0	3.321	3.614
Full load Power factor	0.9	0.87	0.9554	0.9578
Full load slip	0.042	0.03	0.0446	0.0242
Rotor temperature rise, °C	28	19.39	35.562	28.24
Material cost[a] (Rs) Rs=Indian Rupees	644.5[a]	876.8[a]	5340.37[a]	6143.69[a]
TEC[b] (US$)	**11342**[b]	**10600**[b]	**324336**[b]	**309922**[b]
Stator bore diameter (m)	0.1636	0.1332	0.39364	0.34772
Stack length (m)	0.1204	0.13	0.41855	0.4242

[a] For comparison purpose, Rs. 14/kg for iron cost and Rs 42/kg for winding materials cost are considered as in [15],

[b] C_d = US $ 6.66/month and C_e = US $ 0.077/kWh

4.8   Induction Motor Design under Unbalanced Supply Voltage

In practice, induction machines experience overvoltages and undervoltages, depending on the location of the motor and the length of the feeder used. Furthermore, the supply voltage is not always balanced. Therefore, the motor will experience a combination of over- or undervoltages with unbalance voltages [132]. Any unbalance between the voltages in a three-phase system is equivalent to introducing a negative sequence voltage having a vector rotation opposite to that occurring with balanced voltages. These negative sequence voltages generate in the air gap a magnetic flux rotating against the rotation of the rotor, which requires a high input current. A small negative sequence voltage may produce currents in one or more phases of the stator and rotor conductors that considerably exceed those under balanced voltage conditions [54].

Due to voltage unbalance, induction motors face four kinds of problems [145]. First, the machine cannot produce its full torque as the inversely rotating magnetic field of the negative-sequence system causes a negative braking torque that has to be subtracted from the base torque linked to the normal rotating magnetic field. Secondly, the bearings may suffer mechanical damage because of induced torque components at double system frequency. Third, reduction in efficiency and finally, the stator and, especially, the rotor are heated excessively, possibly leading to faster thermal ageing. For example, a 5% voltage unbalance can lead to a 30–50% increase in current unbalance, accompanied by a 50% increase in motor temperature rise [164].

Table 4.9 Effect of Voltage Unbalance on a 200-hp Motor at Full Load [164]

Particulars		Voltage unbalance (%)			
		0	2.5	3.5	5.0
Increase in losses (%)		0	8	25	50
Temperature rise ($^\circ$C)	Class A	60	65	75	90
	Class B	80	86	100	120

The most effective way to solve the problems of motors overheating due to voltage unbalance is to eliminate the unbalance. The unbalance can be caused by unbalanced single-phase loads, faulty connections, or malfunctioning voltage regulators. It is not easily possible to eliminate the existence of voltage unbalance to the motors which are serving in remote villages for agriculture or other purposes.   If the voltage unbalance cannot be

eliminated, there are two ways to ensure long life of motor: (i) the motor must be derated as per the recommendation of NEMA [10] (shown in Fig. 4.35) or (ii) motor should be designed with the consideration of different levels of unbalanced voltages when manufacturing. To ensure consistent, efficient and reliable operation of motors, accounting unbalanced voltage in the stator terminals and optimizing the design of the motor will receive considerable attention from industry.
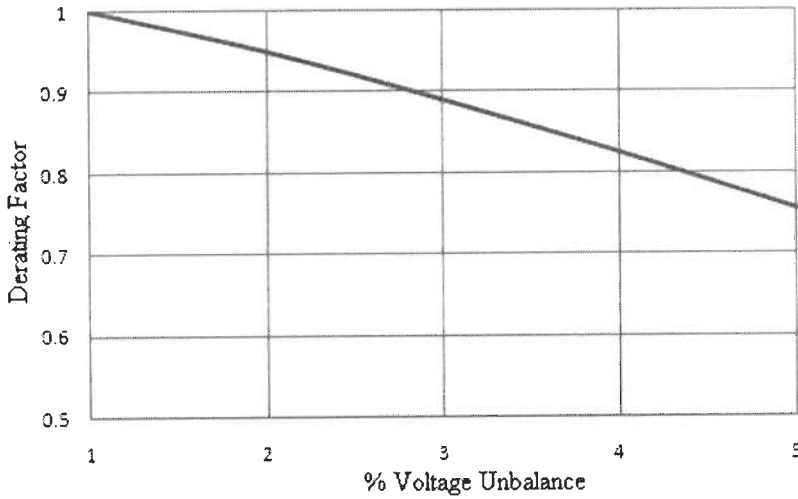
Fig. 4. 35. Derating factor of induction motor under voltage unbalance

The equations for output power (4.18), torque (4.19), positive and negative sequence currents, shown in Eqs. (4.20) and (4.21), of induction motor under unbalanced voltages are as follows [131]

$$P_{out} = I_p^2 * Rr(\frac{1-s}{s}) - I_n^2 * Rr(\frac{1-s}{2-s}) \tag{4.18}$$

$$T = \frac{3 * R_r * (\frac{I_p^2}{s} - \frac{I_n^2}{(2-s)})}{W_{syn}} \tag{4.19}$$

Positive sequence current (I_p) is given by;

$$I_p = \frac{V_p}{\sqrt{\left\{ \left[Rs + (\frac{Rr'}{s}) \right]^2 + (Xs + Xr')^2 \right\}}} \tag{4.20}$$

Negative sequence current (I_n) is given by;

$$I_n = \frac{V_n}{\sqrt{\left\{\left[\left(\frac{Rs + Rr'}{2 - s}\right)\right]^2 + (Xs + Xr')^2\right\}}}$$ (4.21)

The stator current per phase, which is the deciding factor of KVA power in the motor can be calculated as Eq. (4.21) when considering the voltage unbalance effect in the motor design;

$$I_{ph} = \sqrt{(I_p^2 + I_n^2)}$$ (4.22)

Therefore, the phase current will increase with the increasing level of voltage unbalance level. It is noted that the negative sequence current is zero in case of balanced supply.

The design results of sample motor 1 with the consideration of 5% unbalanced stator voltage are shown in Table 4.10. The operating cost and material cost of the motor increase with the increase of voltage unbalance by 14.8% and 2.9% respectively. The increase in material cost at voltage unbalance is due to the increase of ampere conductors/m to meet higher stator currents. Stator core depth is of higher value when the motor is optimized under voltage unbalance whereas stator slot depth to width ratio is lower. Stator temperature increases by 23.9% when considering voltage unbalance but much lower than the limiting value.

4.9 Effects of Harmonic Currents in Induction Motor Design

Several industrial and domestic loads comprising of static power converters, such as arc melting furnaces, induction heating devices, switch mode power supplies etc. inject current harmonics in the power system. Moreover, the development of the power electronic and inverter techniques, Induction motors fed by voltages source inverters are used in variety of industrial, residential and commercial applications, such as electric vehicle traction system, the paper-making and the steel-making system. The structure of the variable-frequency induction motor is same as the general asynchronous motor. However, due to the inverter fed supplies and requirements of the applications, such as electric vehicle traction systems, the performances of the variable frequency induction motor differ greatly from those of the general asynchronous motor, such as wide speed range, high efficiency, high power factor, high torque, high dependability and minimum size.

Table 4.10 Effects of Unbalanced Voltage in Sample Motor 1

Item	Balanced voltage			Unbalanced voltage (5%)		
	F(x)=A	F(x)=B	F(x)=D	F(x)=A	F(x)=B	F(x)=D
ampere conductor/m	19260	23847	15105	20012	23948	16926
stack length / pole pitch	0.937	1.32	0.904	1.112	1.325	1.76
stator slot depth to width	4.61	5.04	3.83	4.34	4.87	3.78
Stator core depth	30.79	35.19	20.99	33.49	37.80	26.12
air gap flux density	0.717	0.75	0.54	0.720	0.767	0.512
stator current density	13.08	5.47	6.38	14.66	6.243	8.406
rotor current density	7.55	5.2	9.9	6.99	5.01	7.886
Stator tooth flux density	1.68	2.0	1.56	1.673	2.0	1.26
Stator temperature rise, °C	40.66	48.4	32.74	48.46	51.54	40.58
Full load efficiency, pu	0.86	0.91	0.87	0.8	0.884	0.83
No load current, pu	0.5	0.5	0.49	0.42	0.46	0.37
Starting torque, pu	1.9	2..05	2.18	1.93	2.2	2.41
Maximum torque, pu	2.811	3.0	3.09	2.76	3.9	3.7
Full load Power factor	0.9	0.87	0.91	0.90	0.878	0.91
Full load slip	0.042	0.03	0.05	0.0411	0.03	0.048
Rotor temperature rise. °C	28	19.39	30.44	27.27	19.39	28.47
Material cost (Rs) Rs=Indian Rupees	644.5	876.8	774.17	740.3	953.7	944.5
TEC (US$)	11141	**10600**	10999	12083	**10911**	11548
Stator bore diameter (m)	0.1636	0.1332	0.197	0.163	0.1332	0.154
Stack length (m)	0.1204	0.13	0.14	0.120	0.13	0.134
Stator resistance / phase (Ω)	1.44	1.168	2.09	1.44	1.02	1.73
Rotor resistance / phase (Ω)	3.014	1.02	1.56	3.01	1.16	1.74

So the variable frequency induction motor design method is most different from those of general induction motor [101]. The main issue of inverter fed induction motor is the presence of harmonics which results more losses in the stator as well as in the rotor. The supply voltage harmonics have the following causes and effects on the performance of the cage induction motor [151]

- Current and flux harmonics results in additional copper and iron losses. Because of these additional losses the temperature rise is higher and the efficiency of the drive also tends to decrease.
- Driving and braking torques are produced in the motor, depending on the order of the harmonics, hence the overall available average torque is reduced.
- Torque pulsation due to interaction between the various harmonic currents and fluxes reduces the available speed range.

In addition with basic nine constraints which were used in the earlier sections one more constraint, harmonic rotor current, pu ≤ 0.01, is used as 10th constraint in this section to limit the harmonic current in the motor due to inverter supply.

Calculation of Harmonic Current:

Harmonic equivalent circuit [44] shown in Fig. 4. 36 is independent of the motor sped. Thus, harmonic currents are substantially constant and independent of the motor load and speed.

(a)   (b)
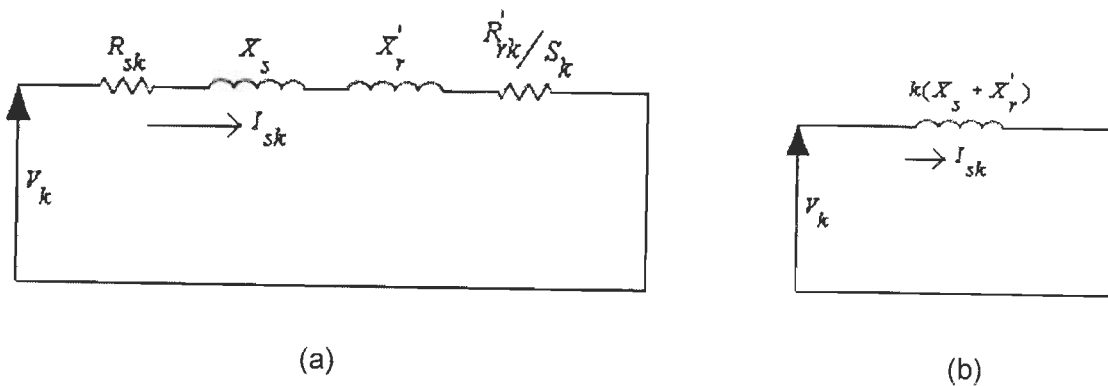
Fig. 4. 36 Harmonic equivalent circuit of the induction motor (a) full circuit,

(b) simplified circuit.

$$I_{sk} = \frac{V_k}{\sqrt{(R_{sk} + \frac{R'_{rk}}{S_k}) + k^2(X_s + X'^2_r)}}$$ (4.23)

where

V_k = harmonic rms phase voltage at a per unit frequency k.

I_{sk} = k^{th} harmonic current at a per unit frequency k.

R_{sk}, R'_{rk} = Stator and rotor resistance at k^{th} harmonic frequency

X_s, X'_r = Stator and rotor reactances at k^{th} harmonic frequency

S_k = Slip at k^{th} harmonic frequency

Since S_k is close to unity, the resistances have negligible values compared to the reactances. Now the Eq. (4.24) is simplified as

$$I_{sk} = \frac{V_k}{k(X_s + X'_r)}$$ (4.24)

In the present work, up to 13th order harmonics have been considered and the Eq. (4.24) can be rewritten as

$$I_{sk} = \frac{V_{ph}}{k(X_s + X'_r)} (\frac{1}{5^4} + \frac{1}{7^4} + \frac{1}{11^4} + \frac{1}{13^4})^{1/2}$$ (4.25)

where V_{ph} = Phase voltage of the motor.

Considering harmonic current as one of the constraints, the trends of the design variables, constraints and objective functions for the sample motor 3 are shown in Table 4.11-4.13. Depth of the stator slot is greater when starting torque is considered as objective function and the diameter of the stator bore is minimum. If the motor is designed with respect to its temperature rise minimization and limited harmonic current, width of the stator slot and tooth flux density are higher. The variations in the objective functions in between the optimized design of the motor when the limitation of harmonic current is considered and not considered are shown in Table 4.14. Results show that the harmonic current in the motor is successfully limited by modifying the design variables without affecting performance indices.

Table 4.11 Optimum Design Results for Efficiency Maximization

Items	Optimization algorithms					
	Normal [16]	SA [16]	Without harmonic constraint		With harmonic constraint	
			PSO	QIPSO	PSO	QIPSO
Width of the stator slot (m)	0.00132	0.0011	0.00487	0.00433	0.0044	0.0045
Depth of the stator slot (m)	0.021	0.0159	0.01962	0.01515	0.0242	0.018
Width of the rotor slot (m)	0.0068	0.005	0.00399	0.00355	0.0036	0.0037
Depth of the rotor slot (m)	0.0093	0.0091	0.00634	0.00660	0.0086	0.0081
Air gap flux density (wb/m^2)	0.6	0.521	2.000	2.00	1.722	1.471
Air-gap length (m)	0.0003	0.0003	0.0005	0.0005	0.0005	0.0005
Full load slip	0.0699	0.056	0.0488	0.0416	0.49	0.05
Stator bore diameter (m)	0.105	0.102	0.0902	0.0890	0.10	0.1014
Stator outer diameter (m)	0.181	0.177	0.208	0.1913	0.203	0.199
Stack length (m)	0.125	0.097	0.1269	0.109	0.094	0.12
Temperature rise, °C	46.8178	41.391	44.463	39.83	40.83	40.62
Efficiency	0.80309	0.82848	0.833	0.8356	0.812	0.813
Starting torque, pu.	1.2027	1.3444	1.426	1.730	1.49	1.51
Power factor	0.8041	0.8333	0.840	0.800	0.79	0.802

Table 4.12 Optimum Design Results for Starting Torque Maximization

Items	Optimization algorithms					
	Normal [16]	SA [16]	Without harmonic constraint		With harmonic constraint	
			PSO	QIPSO	PSO	QIPSO
Width of the stator slot (m)	0.00132	0.0012	0.00464	0.00555	0.0056	0.0048
Depth of the stator slot (m)	0.021	0.0187	0.02272	0.02118	0.0197	0.0247
Width of the rotor slot (m)	0.0068	0.0056	0.00379	0.00454	0.0046	0.0039
Depth of the rotor slot (m)	0.0093	0.0071	0.00537	0.00291	0.0050	0.0032
Air gap flux density (wb/m^2)	0.6	0.4713	1.1805	2.00	1.5065	2.00
Air-gap length (m)	0.0003	0.0004	0.0005	0.0005	0.0005	0.0005
Full load slip	0.0699	0.0645	0.046	0.0505	0.045	0.061
Stator bore diameter (m)	0.105	0.1028	0.111	0.0999	0.123	0.088
Stator outer diameter (m)	0.181	0.1733	0.252	0.2179	0.205	0.179
Stack length (m)	0.125	0.1162	0.164	0.114	0.097	0.113
Temperature rise, °C	46.8178	64.475	53.11	41.810	45.08	40.617
Efficiency	0.8030	0.79179	0.813	0.825	0.799	0.808
Starting torque, pu.	1.2027	1.3776	1.668	1.966	1.53	1.85
Power factor	0.8041	0.7938	0.863	0.813	0.809	0.811

Table 4.13 Optimum Design Results for Temperature Rise Minimization

Items	Optimization algorithms					
	Normal [16]	SA [16]	Without harmonic constraint		With harmonic constraint	
			PSO	QIPSO	PSO	QIPSO
Width of the stator slot (m)	0.00132	0.0013	0.00444	0.00457	0.0054	0.0051
Depth of the stator slot (m)	0.021	0.0236	0.01919	0.02258	0.0169	0.0174
Width of the rotor slot (m)	0.0068	0.005	0.00363	0.00374	0.0044	0.0041
Depth of the rotor slot (m)	0.0093	0.0093	0.00652	0.00499	0.0067	0.0074
Air gap flux density (wb/m^2)	0.6	0.439	2.000	1.632	1.680	2.00
Air-gap length (m)	0.0003	0.0004	0.0005	0.0005	0.0005	0.0005
Full load slip	0.0699	0.0684	0.05	0.0536	0.05	0.045
Stator bore diameter (m)	0.105	0.101	0.085	0.189	0.0953	0.0918
Stator outer diameter (m)	0.181	0.171	0.1919	0.099	0.1804	0.174
Stack length (m)	0.125	0.1216	0.124	0.114	0.147	0.1138
Temperature rise, °C	46.8178	40.0391	42.47	38.209	37.72	36.54
Efficiency	0.80309	0.803748	0.827	0.814	0.809	0.81
Starting torque, pu.	1.2027	1.117	1.098	1.133	1.01	1.07
Power factor	0.8041	0.7814	0.830	0.858	0.825	0.847

Table 4.14 Variations (actual) in the Objective Function Values when considering Harmonic Current

Objective Function	Sample motor 3	
	PSO	QIPSO
Efficiency	0.021	0.022
Starting torque	0.13	0.11
Temperature rise	4.75	1.67

4.10 Conclusion

This chapter investigated the optimal design of induction motors using Particle Swarm Optimization (PSO) and its variant, called Q IPSO, with five objective functions, active material cost, efficiency, starting torque, temperature rise and total energy cost. The effects of variables in the performance indices of the motor like efficiency, torque, material cost etc. were examined. Optimization techniques, both conventional and stochastic algorithms, used in motor design have been discussed in detail.

For minimum material cost, the tendency of the variable in obtaining an optimized design has been to have lower specific electric loading and higher values of stator and rotor winding current densities. Nearly 28% cost reduction was achieved in QIPSO based design of induction motor in comparison with Rosenbrock method.

For maximum efficiency and starting torque and minimum temperature rise, the tendency of the variable in obtaining an optimized design has been to have higher value of width of the stator slot, lower value of depth of the rotor slot and intermediate value of length of the stator stack. The values of these variables obtained from the different optimization algorithms and the corresponding objective function values were plotted.

Higher ampere conductors, stack length to pole pitch ratio, stator slot depth to width, stator core depth and average air gap flux density were required to achieve optimum operating cost or energy cost of the motor. Material costs slightly increased when the motor was designed with respect to optimizing its operating cost.

When voltage unbalance was considered at the motor design, material cost was increased due to the increase of ampere conductors per metre to meet higher stator currents Higher Stator core depth and lower stator slot depth to width ratio were required to get a good machine when subjected to voltage unbalance.

Greater depth of the stator slot for more starting torque, higher width of the stator slot and tooth flux density for minimum temperature rise were required when the motor was designed with limited harmonic current.

It is concluded that PSO and its improved version QIPSO gave good results in almost all the cases compared with Rosenbrock method, simulated annealing, basic PSO and normal design and therefore Particle Swarm Optimization is more suitable to the design optimization of induction motor.

Realisation of Induction Motor Design

[Present chapter realises the induction motor design results of chapter 4 which were obtained by Particle Swarm Optimization (PSO) and Quadratic Interpolation based Particle Swarm Optimization (QIPSO) via SPEED (Scottish Power Electronics and Electric Drives) software. The effects of variables (width of the stator slot, depth of the rotor slot and length of the stator stack), which are more dominant to give good design, in the performance indices are plotted with the help of ranging function in the SPEED. The variables required to get optimum design results of motor are reduced. Performance based optimal design of induction motor using SPEED is carried out and their results are analyzed. Theoretical justification is also given for the design with the minimum material cost.]

5.1 Introduction

The design of an induction motor involves a large number of variables which determine the electromagnetic performance and the temperature rise. A designer, using previous experience, selects a combination of variables which yields the desired performance. The designer will also investigate the possibility of generating designs which give better performance or designs which have reduced cost but at the same time satisfy the design requirements. The digital computer can run optimization algorithm easily and give number of possible solutions in the form of design sheets. But the problem is that the practical feasibility is very low to check all the alternatives [152]. Here, the induction motor design software, SPEED (Scottish Power Electronics and Electric Drive)/IMD (Induction Motor Drives) can be easily used to check its design sheets in terms of performance evaluation. It is also helpful to design engineers to select essential variables by performing initial work on it before starting the design procedure. Thus the presented work in this chapter considers minimum variables to design the motor with the help of SPEED software.

SPEED software is designed for modern motors. It caters to design of induction motors (poly-phase/single-phase), brushless permanent magnet motors (square wave/sinusoidal wave), switched reluctance motors, synchronous reluctance motors, and commutator machines. It run on the IBM PC platform, readily accessible to multiple users in one

company, including laptop users, It is easy to learn and use, and is provided with full documentation that include extensive information on the motor theory and design [107].

By using the ranging function, the effects of various design parameters are plotted against the objective function and some of the constraints. The constraints which are plotted are efficiency, starting torque and temperature rise. The other constraints are interrelated to these constraints hence these plots give sufficient information about the choice of the variables. As discussed in chapter 4, induction motor design problem becomes complicated if too many variables are involved. Therefore the present work is concentrated on reduction of such variables involved in motor design. With the help of SPEED/IMD, the number of variables required to get optimum design of motor are minimized though performance based optimization.

5.2 Need for Software Aided Design of Electric Motor

Techniques for designing, analysing, and driving electric motors have developed rapidly with thw advances in computers and power electronics. The role of numerical methods in electric machines is significant to analyse and optimize the electromagnetic, thermal, and mechanical performances of machines. Although numerical tools for electromagnetic analysis have been extensively developed in the last few years, the finite-element method is still one of the most powerful and popular tools for temperature analysis in electromagnetism. Some finite element analysis on brushless DC motor is available in [168], [169]. Design of electric machine requires imagination and judgment that go beyond the realm of mere computation. Software helps to design electric machine in many ways including the following tasks [137].

- Basic electrical and magnetic design
- Thermal management
- Control and system performance analysis
- Mechanical analysis (dynamics, stress, noise)
- Optimization
- Database management of designs, manufacturing details, inventory, etc.

Electric machines are usually designed by specialist engineers skilled in electrical and mechanical engineering. More and more, these specialists need knowledge of power electronics and system simulation. Also, separate specialists may be required for all the above tasks but this is a luxury beyond the reach of smaller companies. These factors make it increasingly important to have good communication between the various software tools, for example: interface between SPEED and MATLAB. Even when a computer program is

available to perform the performance calculations, the design engineer make all the decisions about parameter adjustments.

The SPEED software is a specialised calculating tool to assist the design engineer with initial sizing and preliminary design of motors by providing a simple intuitive interface and quick simulation. The programs include several common features [107]:

- Motor geometry is defined by parameterised models which allows both for quick data entry and modification, and for quick simulation.

- Simulation is based upon classical theory and equivalent circuit models

- Simulations vary with the program but include ideal, time-stepping, dynamic (including load characteristics and fault conditions), thermal and line-start in one package.

- Simulation includes the motor drive as well as the electromagnetic aspects.

- Output is in the form of textual design sheets listing the calculated parameters and graphical display of waveforms such as current, voltage, torque, back *emf* and flux-linkage.

- Material databases contain information about steels, magnets and brushes.

- Links to finite-element and system simulation programs are under constant development.

In the present work, ranging function is used to see the effectiveness of PSO and QIPSO search methods in the motor's design optimization. Ranging is the repetition of the performance calculation to determine the effect of variation in one or more parameters. It provides complete graphical representation of the torque/speed characteristic including the variation of current, efficiency, power-factor, etc., as the load and/or speed varies. Each of the ranging parameter can be varied in steps, starting with the initial value and ending up with the final value specified in the range.

5.3   Realization of Induction Motor Design Using SPEED Software

As discussed in chapter 4, the main conclusions of the obtained design results of minimum material cost are the tendency of the variable in obtaining an optimized design has been to have lower specific electric loading and higher values of stator and rotor winding current densities. However, maximum efficiency and starting torque and minimum temperature rise, the tendency of the variable in obtaining an optimized design has been to have higher value of width of the stator slot, lower value of depth of the rotor slot and intermediate value of length of the stator stack.

SPEED software is used in this section to check whether PSO or QIPSO has chosen best values of variables so that objective function is optimum. Ranging option of SPEED software is used for completing this goal. Ranging is the evaluation of a batch of designs, in which a number of parameters are stepped through a series of values. It assists in the selection of an optimal value for one or more parameters. The flow chart of SPEED realization is shown in Fig. 5.1. Ten steps was set in the ranging function throughout the realisation.
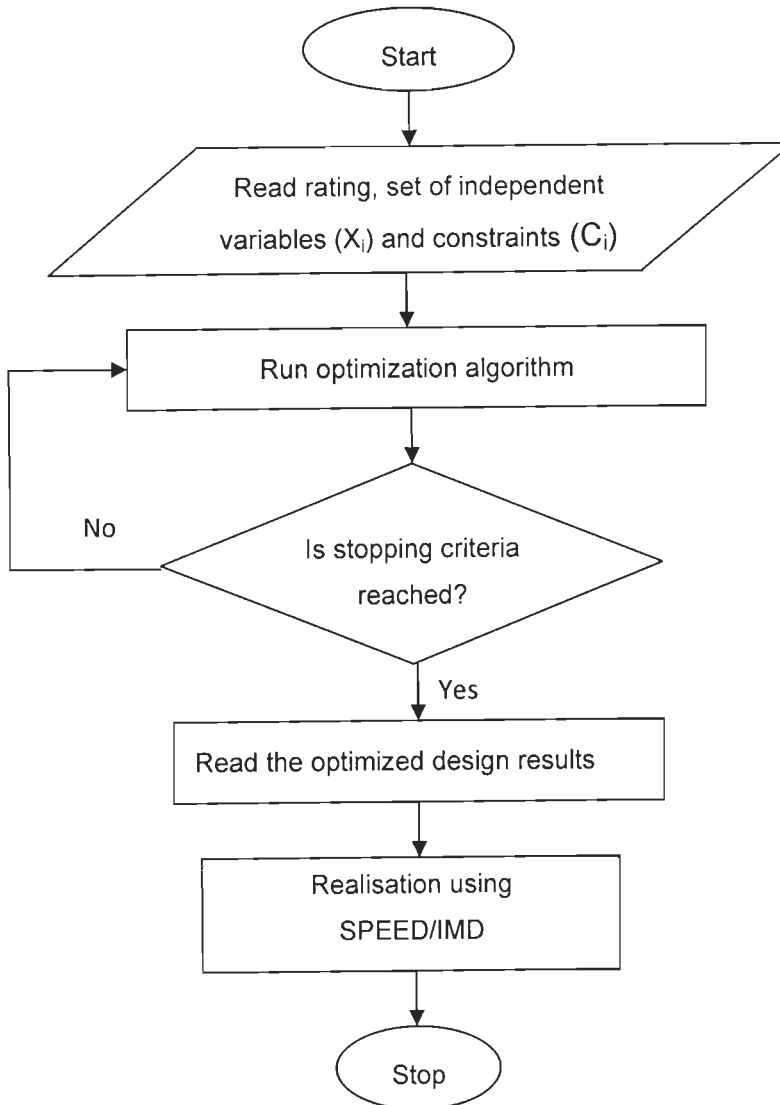
Fig. 5.1. Realization of induction motor design results using SPEED/IMD

5.3.1 Material Cost Minimization

From the design results presented in Tables 4.1 and 4.2 (chapter 4), the lower values of ratio of stator stack length to pole pitch offered by Particle Swarm Optimization (PSO) and QIPSO produced the optimized motor with minimum material cost. To realise this fact, the

trend of stator stack length versus material cost is plotted with the help of SPEED software. Length of stack in the optimized motors are calculated from the value of ratio of stator stack length to pole pitch (L/τ) and are shown in Table 5.1. The equation which governs their relationship is given below;

$$\tau = \frac{\pi D}{p}$$

(5.1)

where, D - Stator bore diameter and p – number of poles

Table 5.1 Values of Stack Length Obtained from Different Algorithms

Optimization algorithm	Sample motor 1			Sample motor 2		
	L/τ	L (mm)	Material cost (Rs)[a]	L/τ	L (mm)	Material cost (Rs) [a]
Rosenbrock	1.1877	150.10	847.7	0.9833	259.00	6459.66
PSO	0.937	120.33	644.5	0.961	197.97	5340.37
QIPSO	1.069	122.518	604.68	0.9801	200.08	5128.0

[a] For comparison purpose, Rs. 14/kg for iron cost and Rs 42/kg for winding materials cost are considered as in [15].

Figs. 5.2 – 5.4 give the variations in the weight of active materials with respect to length of the stator stack (L). Copper weight of stator windings and stator iron weight and finally total weight of active materials have increased with the increasing value of stator stack length. Since total material cost of the motor depends on weight of active materials the active material cost required to produce a motor increases with increase in the value of stator stack length. This is the reason to have less stack length in PSO and QIPSO based optimized motor.
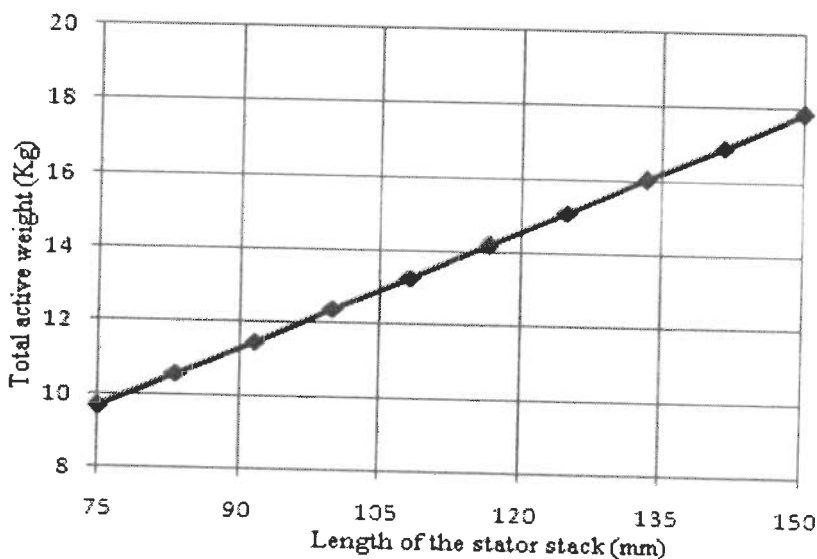
Fig. 5.2 Total active weight versus stator stack length in the optimized motor
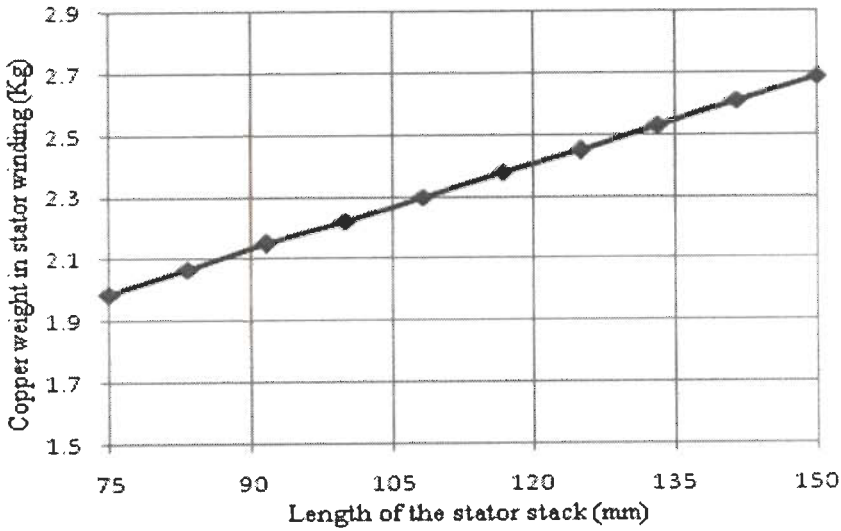
Fig. 5.3. Stator copper weight versus stack length in the optimized motor
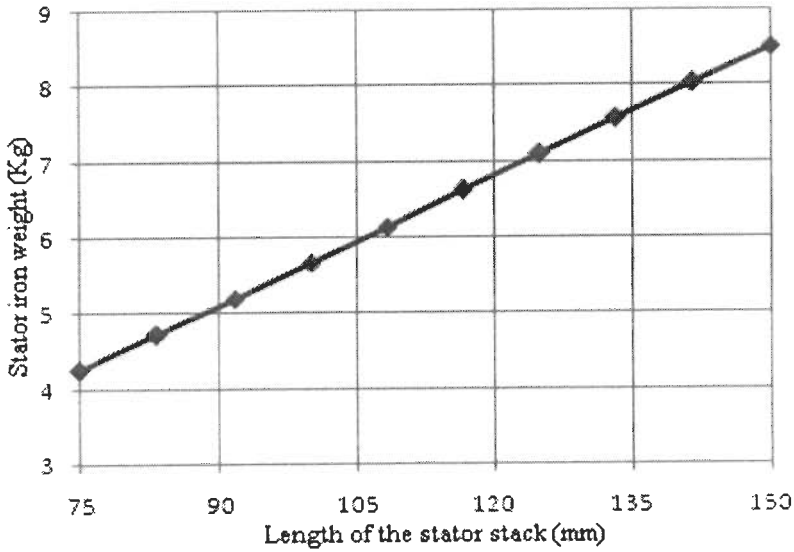
Fig. 5.4 Stator iron weight versus stack length in the optimized motor

The values of variables selected by PSO and its variant are effective in reducing the cost of active materials (iron and copper) and it is justified theoretically below. The total cost of active materials (TC) is classified in to two; one is total cost of iron (TC$_i$) which comprises the cost of stator teeth, core and rotor iron. Other one is the total cost of copper (TC$_c$) which comprises the cost of stator and rotor winding materials. The cost of active materials can be calculated by using the following equations (some equations reproduced here from the Appendix A).

Total material cost $\quad TC = TC_i + TC_c$ (5.1)

Cost of iron $\quad TC_i = C_i(W_t + W_c + W_r)$ (5.2)

$$W_t = \frac{\delta_i * S_1 * d_{ss} * t_s * L_i}{10^6}$$ (5.3)

$$W_c = \frac{\delta_i * L_i (OD - 0.001x_4)(x_4 * L_i)}{10^3}$$ (5.4)

$$W_r = \delta_i * L_i \left[\frac{(D^2 - ID^2)}{4} - \frac{(S^2 * a_{sr})}{10^6} \right]$$ (5.5)

$$t_s = \frac{\pi(D + 0.001d_{ss})}{S_1} - \frac{0.001d_{ss}}{x_3}$$ (5.6)

Cost of copper $TC_c = C_c(W_{sw} + W_{rw})$ (5.7)

$$W_{sw} = \frac{S * \delta_c (x_2 + 1.15 + 0.12)10^6}{2.22 * f * K_w * Y * x_2 x_5 x_6}$$ (5.8)

$$W_{rw} = \frac{S_2 a_b L_r^6}{10^6} + \frac{2\pi a_e D_e}{10^6} \delta_r$$ (5.9)

$$a_b = \frac{382.88 * S}{K_w * f * S_2 * Y^2 * x_2 x_5 x_7}$$ (5.10)

In PSO based design, the value of air gap flux density (x_5) is higher than other techniques. As in Eqs. (5.8) to (5.10), x_5 (average air gap flux density) is inversely proportional to the weights of stator and rotor winding materials (copper) and therefore the cost of active materials is lower. Similarly, the variable x_6 (stator winding current density) is also higher in PSO based design which results in lesser weight of stator winding materials according to (5.8) and finally less active material cost. The variable x_4 (stator core depth) is directly proportional to the weight of stator core (shown in Eq. 5.4) and therefore PSO selects minimum value for lower active material cost. Hence, the results produced by the algorithms used in this thesis are justified theoretically.

5.3.2 Efficiency, Starting Torque and Temperature Rise Optimization

The design results presented in Tables 4.4 - 4.6 (in chapter 4), show that the following variables dominate in PSO and QIPSO based design to achieve optimum value of efficiency, starting torque and temperature rise of the sample motor 3. The values of these variables are tabulated in Table 5. 2.

1. Width of the stator slot
2. Depth of the rotor slot
3. Length of the stator stack

Table 5.2 Values of Stator Slot Width, Rotor Slot Depth and Stack Length

Objective function	Algorithm	Variables		
		Stator slot width	Rotor slot depth	Stack length
Efficiency	SA	0.0011	0.0091	0.097
	PSO	0.00487	0.00634	0.1269
	QIPSO	0.00433	0.00660	0.109
Starting Torque	SA	0.0012	0.0071	0.1162
	PSO	0.00464	0.00537	0.164
	QIPSO	0.00555	0.00291	0.114
Temperature Rise	SA	0.0013	0.0093	0.1216
	PSO	0.00444	0.00652	0.124
	QIPSO	0.00457	0.00499	0.124

The effects of above variables on the objective functions or related parameters are realised by using ranging option in SPEED/IMD software and their results are shown in Figs. 5.5 - 5.13. Taking the width of stator slot (W_{ss}), its value in all the objective functions is higher in the PSO and QIPSO based optimization than in the SA and normal design. Efficiency and torque increase with the increase in the value of W_{ss}, shown in Fig. 5.5 and Fig. 5.6. Similarly total losses (indirectly temperature) offered by the motor are lower in case of higher W_{ss} and is shown in Fig. 5.7 and hence PSO and QIPSO algorithms selected higher value of stator slot width.

Taking the depth of the rotor slot (D_{sr}), motor offers higher torque and minimum losses at low D_{sr}, shown in Fig. 5.8 & 5.9. The value of D_{sr} chosen by PSO and QIPSO algorithms is smaller than all other algorithms such that it gave good performance in terms of higher torque and minimum temperature rise of the motor. Since lower D_{sr} offers lower efficiency, shown in Fig. 5.10, QIPSO takes higher D_{sr} in efficiency optimization compared to its values in other objective functions to produce maximum efficiency, keeping torque and temperature rise of the motor at an optimum.

Taking the length of the stator stack (L) in efficiency maximization, its value is higher in the QIPSO algorithm than SA and hence higher efficiency is offered by QIPSO, shown in Fig. 5.11. On the other hand, the value stator stack is lower for producing higher torque and lower temperature rise when the motor is designed with respect to optimizing its starting torque and temperature rise, shown in Fig. 5.12 and 5.13. Hence QIPSO has chosen intermediate value (neither higher nor lower) to produce all the objective functions optimally.
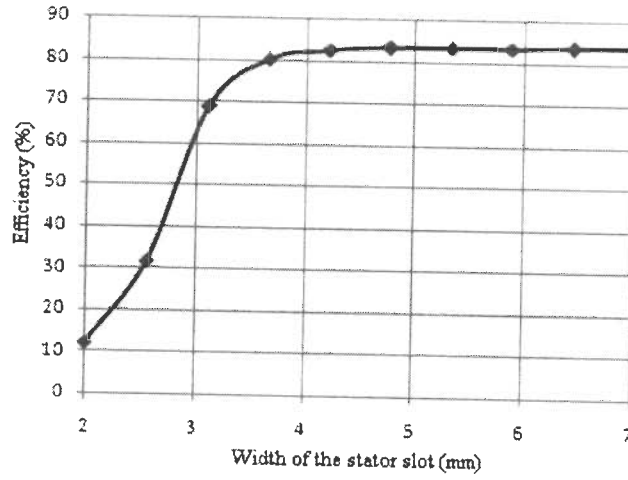
Fig. 5.5 Efficiency versus width of the stator slot in the optimized motor
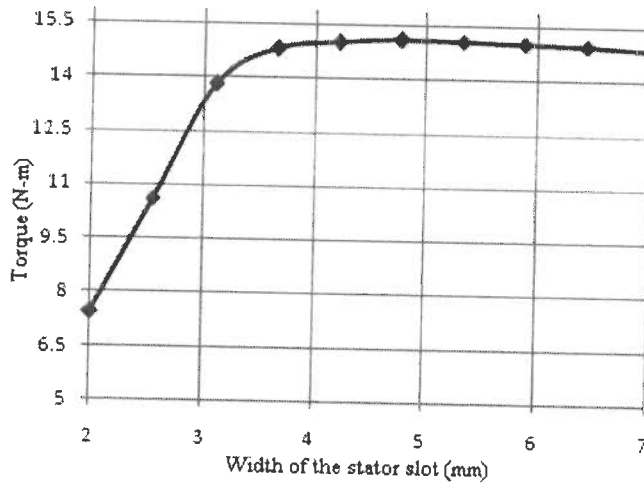
Fig. 5.6. Torque versus width of the stator slot in the optimized motor
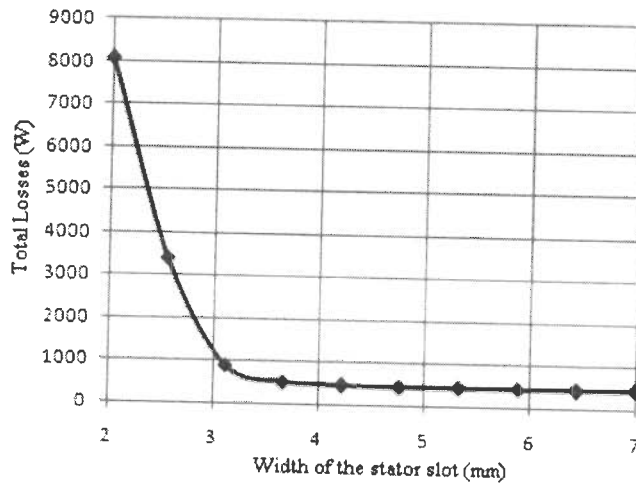
Fig. 5.7. Total losses versus width of the stator slot in the optimized motor
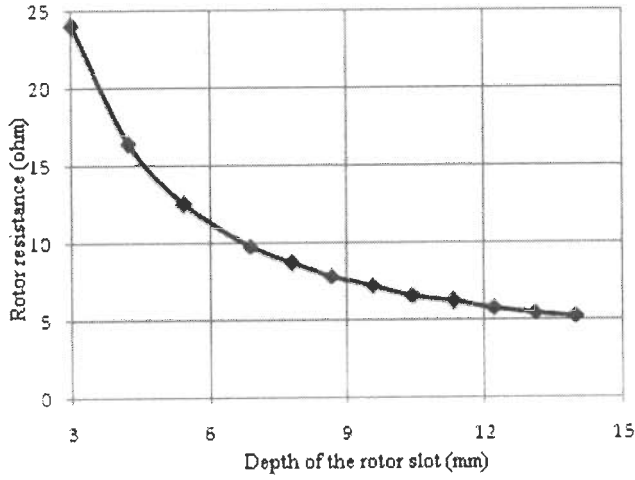
Fig. 5.8. Rotor resistance versus depth of the rotor slot in the optimized motor
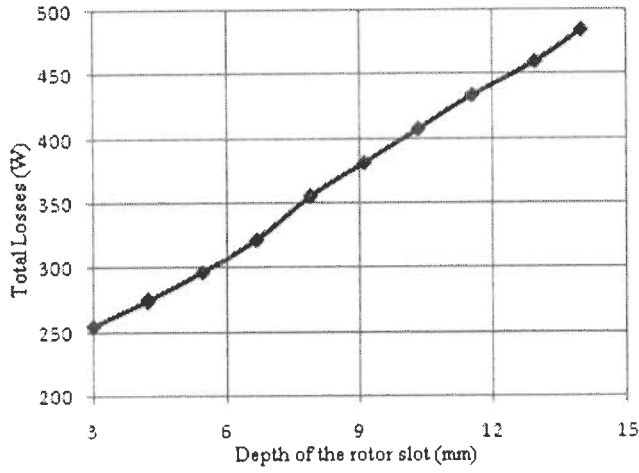
Fig. 5.9. Total losses versus depth of the rotor slot in the optimized motor
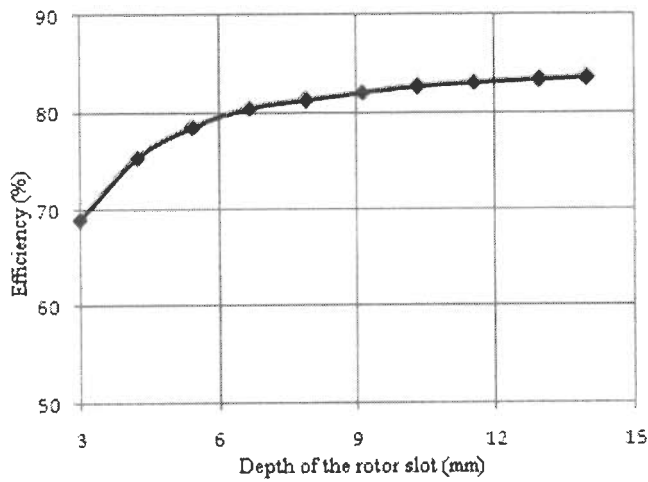
Fig. 5.10. Efficiency versus depth of the rotor slot in the optimized motor
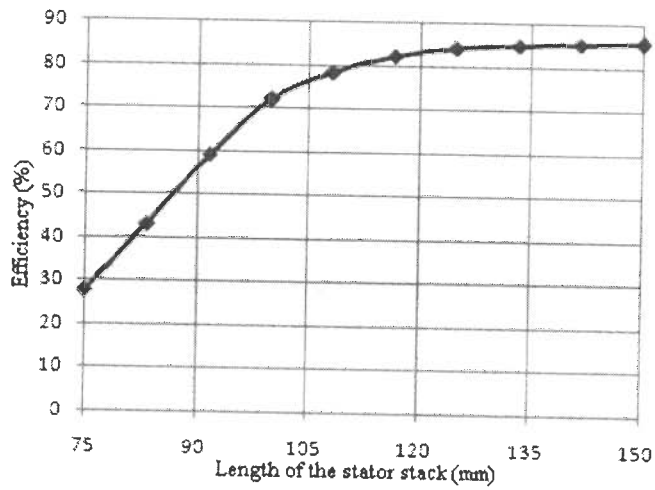
Fig. 5.11. Efficiency versus stator stack length in the optimized motor
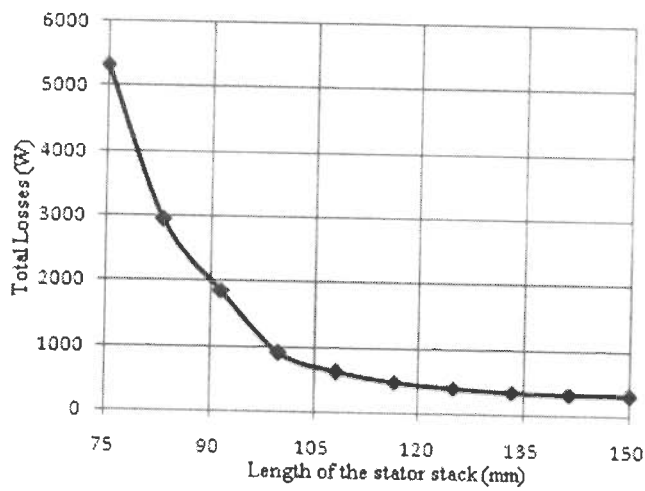
Fig. 5.12. Total losses versus stator stack length in the optimized motor
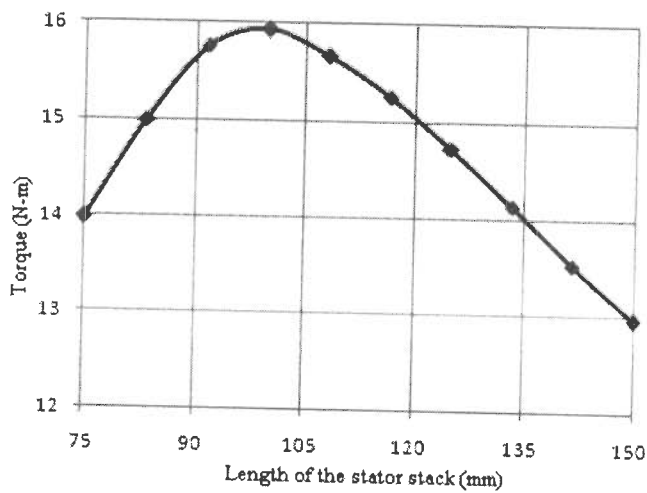
Fig. 5.13. Torque versus stator stack length in the optimized motor

5.4 Design of Induction Motor with Minimum Variables

In this section, SPEED software is used to reduce the required design variables. First, the motor design optimization is carried out by PSO and QIPSO algorithms with seven variables. Second, the optimized design results are realised with SPEED software to determine the effects of variables in the performance indices of the motor. Third, the variables (less number of variables than previously considered) are chosen which are affecting the performances of the motor in depth. Then the motor is again optimized by PSO and QIPSO with the reduced variables. Optimization algorithm in all the cases considers the efficiency, starting torque and temperature rise as objective function and nine performance indices as constraints. The results are compared with the Simulated Annealing (SA) technique and normal design. The flow chart of the above process is shown in Fig. 5.14.
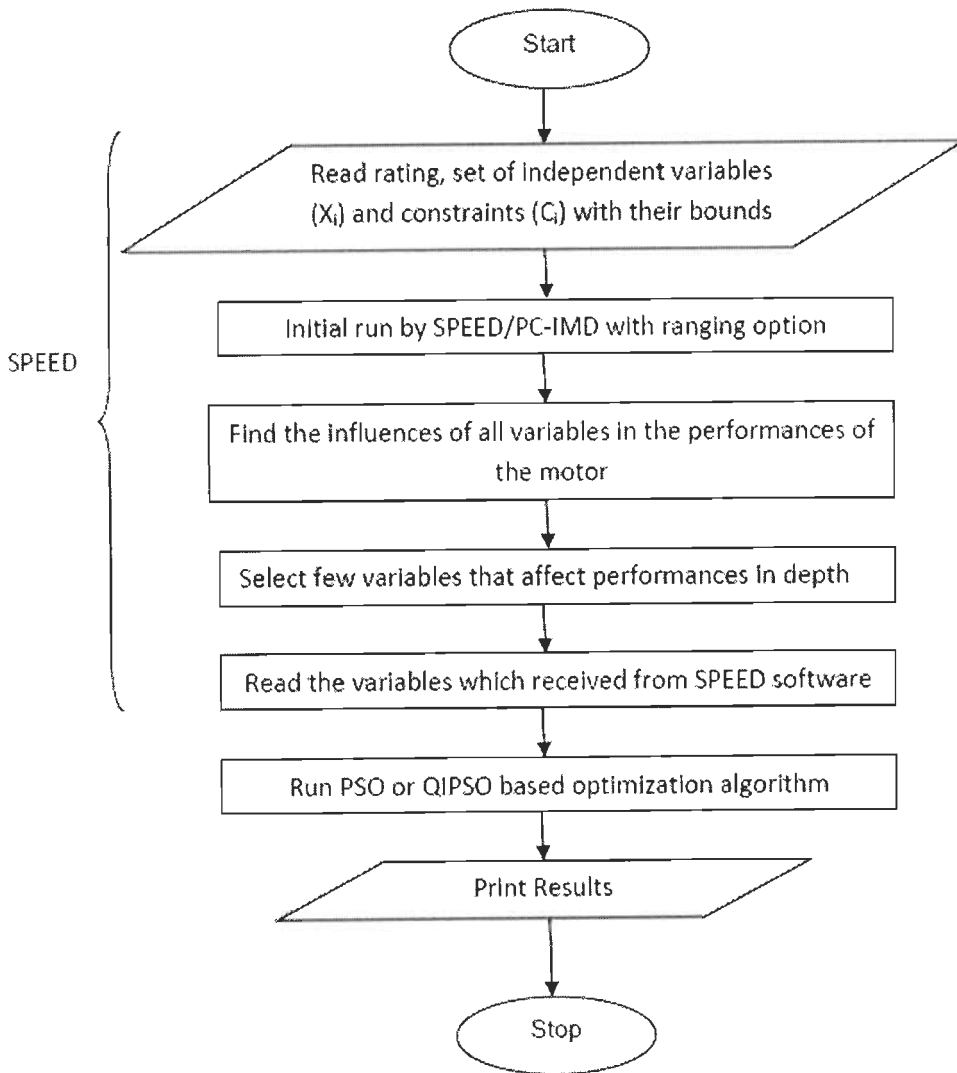
Fig. 5.14. Flow of induction motor design with minimum variables

The Figs. 5.5 – 5.13 which are plotted by SPEED software show that a particular value of stator slot width (=4mm) offers higher efficiency and torque and lower losses in the motor, shown in Figs. 5.5 – 5.7. Similarly, stator stack length (=120mm) offers good results which are shown in Figs. 5.11 – 5.13. These two values were fixed as constants and the remaining five variables are considered for design optimization of induction motor and the corresponding results of sample motor 3 are shown in Tables 5.3 – 5.5.

Table 5.3 Optimum Design Results of sample motor 3 for Efficiency Maximization

Items	Normal [14]	SA [14]	With 7 variables		With 5 variables	
			PSO	QIPSO	PSO	QIPSO
Width of the stator slot (m)	0.00132	0.0011	0.00487	0.00433	0.004	0.004
Depth of the stator slot (m)	0.021	0.0159	0.01962	0.01515	0.0172	0.0015
Width of the rotor slot (m)	0.0068	0.005	0.00399	0.00355	0.00415	0.0034
Depth of the rotor slot (m)	0.0093	0.0091	0.00634	0.00660	0.00232	0.006
Air gap flux density (wb/m^2)	0.6	0.521	2.000	2.00	2.00	1.729
Air-gap length (m)	0.0003	0.0003	0.0005	0.0005	0.0005	0.0005
Full load slip	0.0699	0.056	0.0488	0.0416	0.0492	0.04
Stator bore diameter (m)	0.105	0.102	0.0902	0.0890	0.0941	0.1013
Stator outer diameter (m)	0.181	0.177	0.208	0.1913	0.1919	0.2138
Stack length (m)	0.125	0.097	0.1269	0.109	0.120	0.120
Temperature rise, °C	46.8178	41.391	44.463	39.83	45.68	43.159
Efficiency	0.80309	0.82848	0.833	0.8356	0.8298	0.8398
Starting torque, pu.	1.2027	1.3444	1.426	1.730	1.320	1.712
Power factor	0.8041	0.8333	0.840	0.800	0.849	0.802

Variations in the objective function values when the motor is designed with limited variables (five instead of seven) are shown in Table 5.6. In efficiency and temperature rise optimization, less than 0.5% variation only occurred when the motor design was carried out with reduced variables. Variation in the torque values (upto 26%) is significant because the

trend in torque is of decreasing nature in the range of stack length from 105 mm to 150 mm. But this deviation does not affect the motor performances.

The computation time taken by different algorithms with seven and five variables is shown in Table 5.7. Particle Swarm Optimization with reduced variables has produced motor design results in a fraction of time in almost all the cases. Due to inherent nature of QIPSO (which calculate a new particle in every iteration and replace the worst particle by the new particle if new particle is better than the worst particle) it takes more time to converge. Even though QIPSO have taken more computation time but it produced better results in terms of objective function values i.e. high efficiency, high starting torque and low temperature rise.

Table 5.4 Optimum Design Results for Starting Torque Maximization

Items	Normal [14]	SA [14]	With 7 variables		With 5 variables	
			PSO	QIPSO	PSO	QIPSO
Width of the stator slot (m)	0.00132	0.0012	0.00464	0.00555	0.004	0.004
Depth of the stator slot (m)	0.021	0.0187	0.02272	0.02118	0.0222	0.0116
Width of the rotor slot (m)	0.0068	0.0056	0.00379	0.00454	0.0035	0.0034
Depth of the rotor slot (m)	0.0093	0.0071	0.00537	0.00291	0.0031	0.0061
Air gap flux density (wb/m^2)	0.6	0.4713	1.1805	2.00	1.286	1.729
Air-gap length (m)	0.0003	0.0004	0.0005	0.0005	0.0005	0.0005
Full load slip	0.0699	0.0645	0.046	0.050	0.0471	0.041
Stator bore diameter (m)	0.105	0.1028	0.111	0.0999	0.095	0.1013
Stator outer diameter (m)	0.181	0.1733	0.252	0.2179	0.2188	0.2138
Stack length (m)	0.125	0.1162	0.164	0.114	0.120	0.120
Temperature rise, °C	46.8178	64.475	53.11	41.810	52.54	44.15
Efficiency	0.8030	0.79179	0.813	0.825	0.79	0.83
Starting torque, pu.	1.2027	1.3776	1.668	1.966	1.283	1.44
Power factor	0.8041	0.7938	0.863	0.813	0.869	0.817

Table 5.5 Optimum Design Results for Temperature Rise Minimization

Items	Normal [14]	SA [14]	With 7 variables		With 5 variables	
			PSO	QIPSO	PSO	QIPSO
Width of the stator slot (m)	0.00132	0.0013	0.00444	0.00457	0.004	0.004
Depth of the stator slot (m)	0.021	0.0236	0.01919	0.02258	0.0107	0.0138
Width of the rotor slot (m)	0.0068	0.005	0.00363	0.00374	0.0028	0.0037
Depth of the rotor slot (m)	0.0093	0.0093	0.00652	0.00499	0.0063	0.0074
Air gap flux density (wb/m^2)	0.6	0.439	2.000	1.632	1.748	1.8914
Air-gap length (m)	0.0003	0.0004	0.0005	0.0005	0.0005	0.0005
Full load slip	0.0699	0.0684	0.05	0.050	0.05	0.0419
Stator bore diameter (m)	0.105	0.101	0.085	0.189	0.086	0.088
Stator outer diameter (m)	0.181	0.171	0.1919	0.099	0.173	0.1659
Stack length (m)	0.125	0.1216	0.124	0.114	0.120	0.120
Temperature rise, °C	46.8178	40.0391	42.470	38.20	42.632	38.38
Efficiency	0.80309	0.80374	0.827	0.814	0.810	0.82
Starting torque, pu.	1.2027	1.117	1.098	1.133	1.06	1.02
Power factor	0.8041	0.7814	0.830	0.858	0.8313	0.8343

Table 5.6 Percentage Deviations of Objective Function Values

Objective Function	Deviations	
	PSO	QIPSO
Efficiency	0.38	0.50
Starting torque	23.08	26.35
Temperature rise	-0.38	0.47

Table 5.7 Computation Time for PSO and QIPSO

Sl.No	Optimization Technique	Computation time (Second)		
		Efficiency maximization	Torque maximization	Temperature rise minimization
1	PSO with 5 variables	1	0	0
2	QIPSO with 5 variables	57	54	53
3	PSO with 7 variables	2	3	1
4	QIPSO with 7 variables	69	71	64

5.5 Conclusion

This chapter realised the induction motor design results of chapter 4 which was obtained by Particle Swarm Optimization (PSO) and Quadratic Interpolation based Particle Swarm Optimization (QIPSO) via SPEED software. Theoretical justification on the optimized results was given. The effects of variables (width of the stator slot, depth of the rotor slot and length of the stator stack) on efficiency, torque and temperature rise were plotted using the ranging function of SPEED software.

The performance based optimal design of induction motor using SPEED was also carried out to reduce number of design variables and hence, the convergence time to optimize the motor.

Optimal Energy Control of Induction Motor

[This chapter presents simulation studies on the optimal energy control of an inverter-fed three-phase induction motor. An overview of various controllers: loss model controller, search controller and their hybridization are given. Mine hoist drive of a mineral industry and the implementation of efficiency optimization controllers with the help of Particle Swarm Optimization (PSO) and fuzzy logic are given. The efficiency improvement of spinning drive of textile industry along with a case study in a medium scale industry is presented. Fuzzy Pre-Compensated Proportional Integral (FPPI) is used to improve motor's dynamic performances during the activation of optimal energy control. Motor is also simulated for the possible wide ranges of speed and torque in addition with industrial loads. Analysis shows that it is possible to conserve energy in Indian industries by choosing several possible ways of implementing optimal energy control.]

6.1 Introduction

Three-phase induction motors (IM) are the most frequently used machines in various electrical drives. About 70% of all industrial loads on a utility are represented by induction motors [103]. Recently oil prices, on which electricity and other public utility rates are highly dependent, are rapidly increasing. It, therefore, becomes imperative that major attention be paid to the efficiency of induction motors [183]. Process industries like textile and mineral industries are found to be energy-intensive (4% energy cost in total input cost) compared to other industries like chemical, food, computer manufacturing, etc., and hence extensive research has been focused on such industries in the past to reduce the energy cost and the total input cost [122].

Induction motors have a high efficiency at rated speed and torque. However, at light loads, iron losses increase dramatically, reducing considerably the efficiency [66], [80]. The efficiency and power factor can be improved by making the motor excitation a monotone increasing function of the load. To achieve this goal, the induction motor should either be redesigned or fed through an inverter [86]. Simply, the flux must be reduced, obtaining a balance between copper and iron losses [81].

In general, there are two different approaches to improve the induction motor efficiency under light-load conditions [60], namely, loss model controller (LMC) and search controller (SC). Many researchers have reported several strategies using different variables to

minimize losses in Induction Motor. Some algorithms use slip speed [66], [66], [27], rotor flux [85], [136], [98], power input [85], [63], and voltage [159] as variables. The present work considers flux producing current (indirectly flux) as a variable and searches its optimum through LMC, SC and their hybrid. Particle Swarm Optimization (PSO) is used to calculate the optimal value of variable when LMC is activated. PSO is similar to genetic algorithm (GA) in that the system is initialized with a population of random solutions. It is unlike a GA, however, in that each potential solution is assigned a randomized velocity, and the potential solutions, called particles, are then flown through the problem space [46].

Due to the adjustment in flux or flux producing current to achieve minimum input power, system suffers from stability problems in terms of ripples in torque and speed of the motor. Fuzzy Proportinal Integral (FPPI) controller is used in the present work to improve the stability of the drive when optimal energy controller is activated. The block diagram of the proposed efficiency optimization control in the induction motor drive is shown in Fig. 6.1. The proposed efficiency optimization controllers in induction motor are simulated by using MATLAB/SIMULINK.
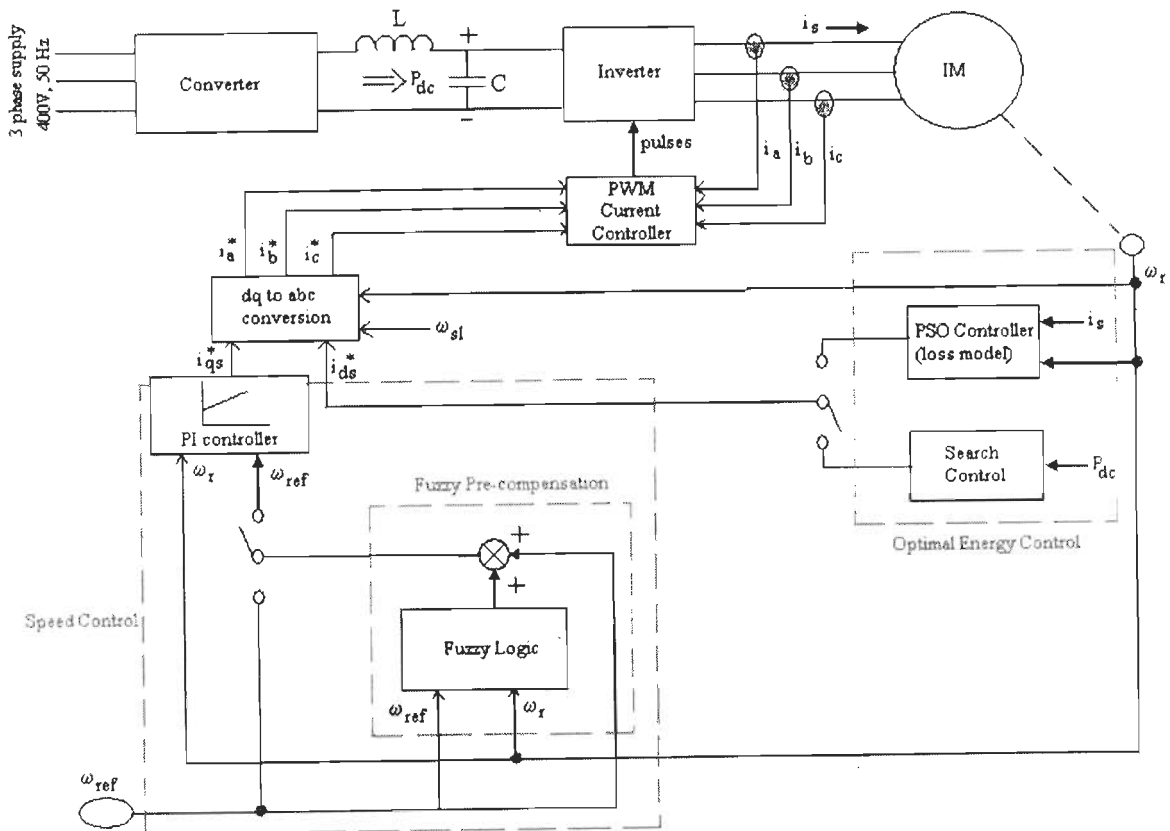
Fig. 6.1. Block diagram of optimal energy control using PSO and fuzzy logic

6.2 Optimal Energy Controllers

Three-phase induction motors consume more than 50% of industrial electricity and it takes considerable effort to improve their efficiency. This effort focuses mainly on the improvement of the materials, the design, and the construction techniques. However, in spite of the progress made in the fields mentioned above, there is significant margins for efficiency improvement, especially when the motor operates at light load [85]. Reduction in rotor flux results into efficiency improvement in the motor at light load. There are two distinct approaches available in the literature for the loss minimization in vector or scalar controlled induction motor drives. They are: loss model controller (LMC) and search controller (SC). Present work considers both LMC and SC. Hybrid controller is also designed by mixing of both LMC and search controller.

6.2.1 Loss Model Controller

The Loss Model Controller is a feed-forward approach, which calculates the optimum set of variables of the machine, depending on the optimization (maximize or minimize) of an objective function, defined using the machine parameters [29]. The objective function used in the present work is the total loss of induction motor drive. The loss model controller shown in Fig. 6.1, measures the speed and stator current and through the motor loss model determines the optimal air-gap flux (variable) which is involved in the loss model. The flow of loss model controller is shown in Fig. 6.2. The approach requires knowledge of the exact values of machine parameters which include core losses and main inductance flux saturation. Referring the loss model presented in chapter 3, LMC calculates the optimal flux from the Eq. 3.51. Equation 3.51 is a scalar loss model equation which is derived in chapter 3 and is reproduced here for convenience.

$$P_{loss} = R_s I_s^2 + \left(R_r' + K_{str}\omega^2\right)\frac{T_e^2}{\Phi_m^2} + \left[K_e\left(1+s^2\right)a^2 + K_h(1+s)a\right]\Phi_m^2 + C_{fw}\omega^2$$

$$+ R_s\left(S_1\Phi_m + S_2\Phi_m^3 + S_3\Phi_m^5\right) + I_h^2(R_s + R_r') + K_{inv1}I_s + K_{inv2}I_s^2 \qquad (6.1)$$

The flux producing current command (i_{ds}) at vector control of induction motor can be calculated from the optimal flux obtained from scalar model. PSO is used to find the optimum of flux in the above equation. Maximum levels of flux and stator currents are forced as constraints in the algorithm. It is noted that the motor's optimum operation is normally below the rated flux and hence flux constraint is not very important in the algorithm. Once optimal flux producing current is calculated as in Eq. (6.2), it is given to the stator reference

current generation block and generate appropriate pulses for PWM inverter which results optimal operation of induction motor in terms of minimum loss or maximum efficiency.

$$i_{ds}^* = \frac{(1+T_r s)}{L_m} \Phi_m^* \qquad (6.2)$$

Where T_r – rotor time constant.
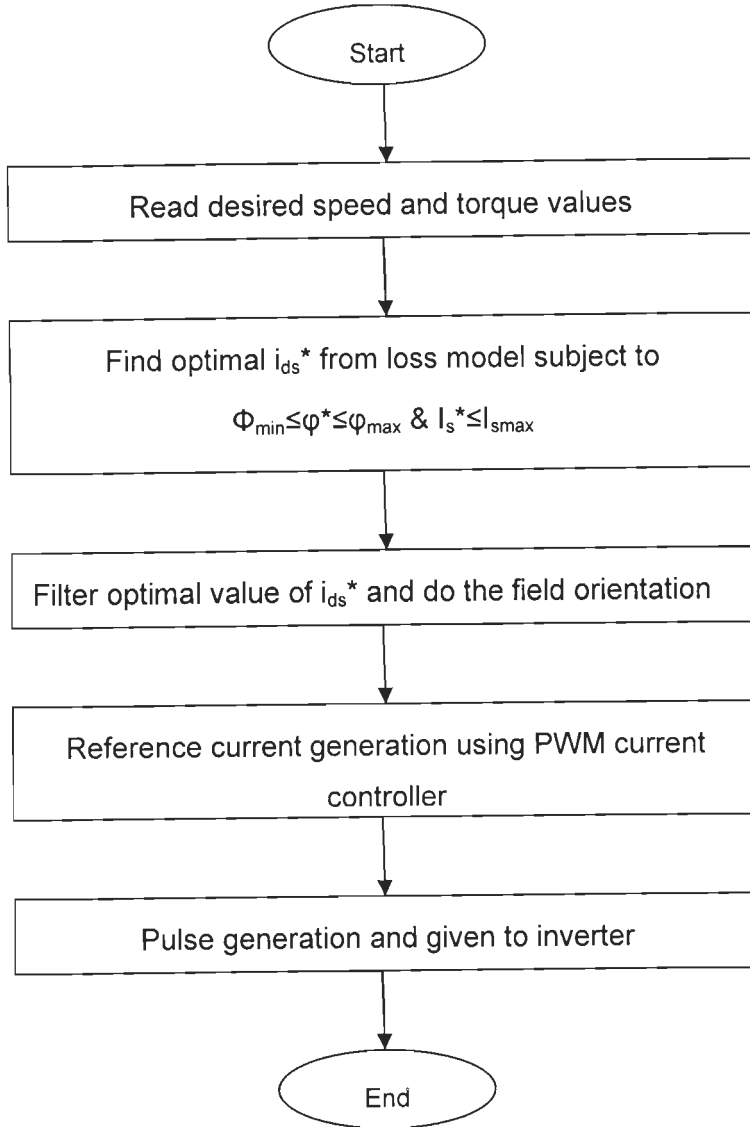
Fig. 6.2 Flow chart of loss model control

LMC approach is a fast method of efficiency optimization, however the demerits of this method are:

(i)   It is dependent on machine parameters and it may offer only sub-optimal solution when the parameter changes with respect to temperature and saturation effects are not accounted.

(ii)   Modeling of entire system including power electronic circuits, stray losses in the motor, accounting saturation effects are very complicated.

6.2.2 Search Controller

In search control method, which does not require the knowledge of the motor loss model, DC link or input power of the machine drive is measured regularly at fixed interval and optimal flux producing current or flux value is searched which results in minimum power input or stator current of the motor for the given values of speed and torque.
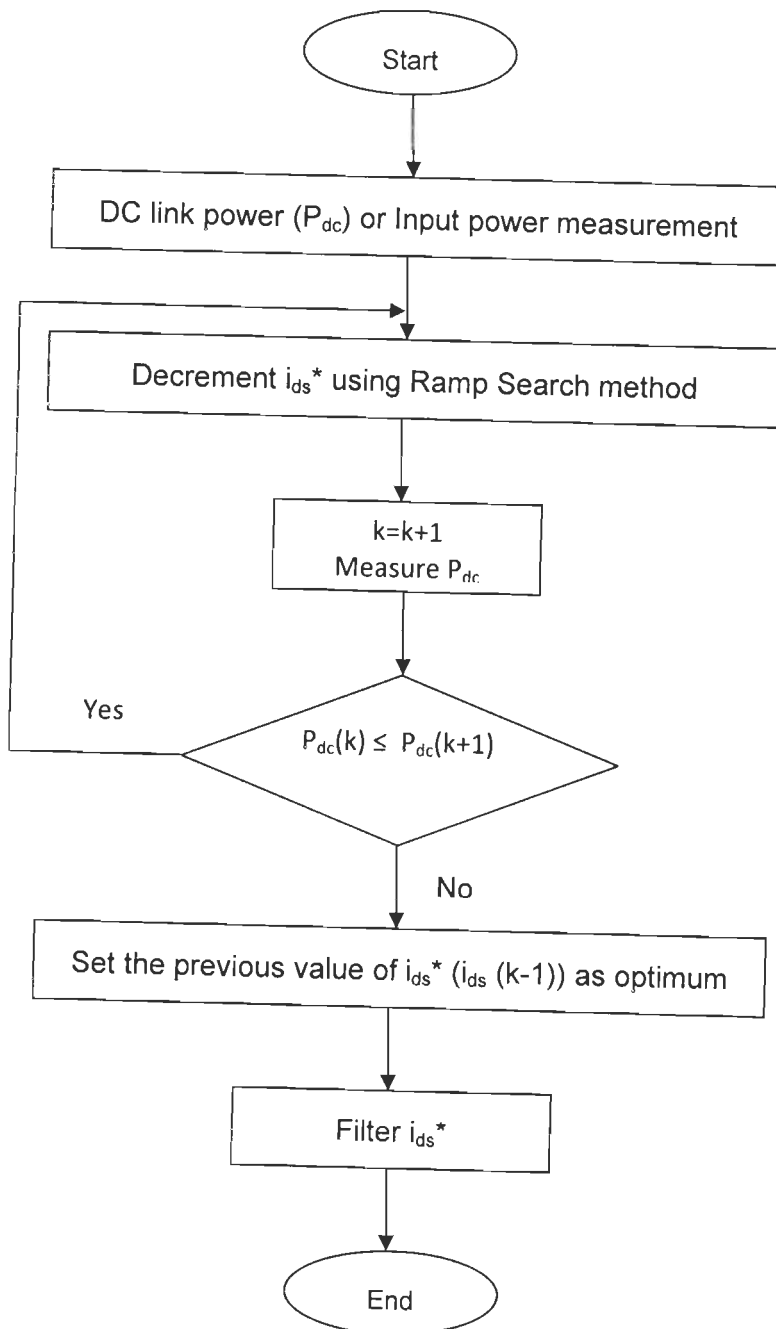
Fig. 6.3 Flow chart of search control

Once the DC link power is minimized the adjustment of flux is stopped and the current flux is maintained and given to the field oriented control as flux current command ($i_{ds}*$). Ramp search method is used to decrement $i_{ds}*$. The flow of search control is shown in Fig. 6.3.

a) *Ramp Search Method*

It is well known fact that oscillation in the flux producing current around its optimal value causes undesirable torque pulsations. Furthermore, many of the search techniques reported so far contain the risk of too much reduction in flux giving rise to stability problem. Usually, this is checked by putting a minimum limit of the flux. But, the problem remains is of reaching of the minimum limit during the process of search, may cause early termination of the search routine, if not properly taken care. To avoid such problems, ramp search can be used in the SC control which is shown in Fig. 6.4 [29]
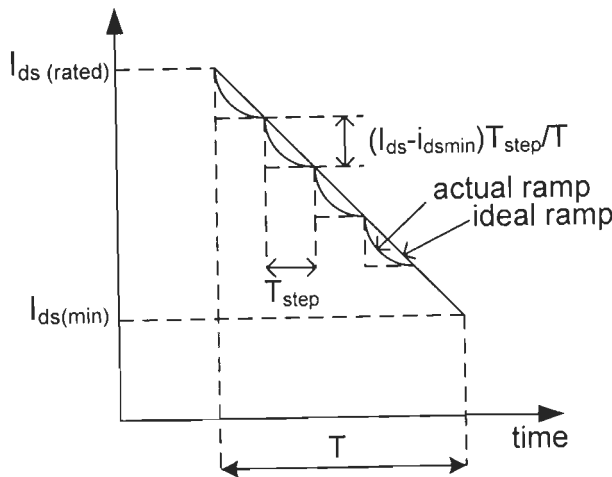
Fig. 6.4 Illustration of ramp search method

In this type of search control, variable (flux producing current command) is decreased from its rated value (1 pu) in small steps and corresponding dc link power or input power is increased. Decrement of the control variable is continued until the dc link power shows an upward trend. When subsequent magnitude of dc link power is higher, the search is stopped and the control variable is restored to the earlier step value and the optimum condition is thus reached.

Referring the Fig. 6.4 searching algorithm starts at rated value of $i_{ds(rated)}$ and proceeds with small step towards a preset minimum $i_{ds(min)}$ in a total time of T sec. Slope of the ramp is given by

$$(i_{ds(rated)} - i_{ds(min)}) / T \qquad\qquad (6.3)$$

Current reduction in each step is calculated by

$$(i_{ds(rated)} - i_{ds(min)}) \, T_{step} / T \qquad (6.4)$$

where T_{step} - step time and T – total time.

The main advantage of this method of search is that it is fairly independent of both the $i_{ds(min)}$ and step size [29].

Next step in the search control is filtering of $i_{ds}*$ to overcome torque pulsation during the search of $i_{ds}*$. Torque pulsation is normally compensated slowly by the speed control loop. This problem is undesirable, especially for the low-speed operation. To overcome this problem, second-order low pass filter can be used [166].

The DC link power, which contains ripples and noise, should be allowed to settle down to the steady value after each of step change of the flux current command. On the other hand, in this method the optimum magnitude of the flux current command is considered integral number of steps away from the initial (usually the rated) value. Thus, a large step size may not converge to the real optimal condition. All these indicate that a proper selection of step size is essential for better response of this method [29].

6.2.3 Hybrid Flux Controller

Hybrid flux controller (which consists both LMC and search control) is used to retain good features of individual controllers, while eliminating their major drawbacks [177], [29]. By this hybrid controller, slow convergence (drawback of search control) and parameter variation (drawback of LMC) due to saturation and temperature variations can be eliminated and good results can be achieved with rough knowledge of parameters. To implement this controller, activate loss model control first to find the initial estimate of the ids* and then activate search control to get more optimum value of control variable. In the present work, PSO is used to calculate optimal value of $i_{ds}*$ when LMC is activated and ramp search method is used when SC is activated. The flow of hybrid control is shown in Fig.6.5.

6.3   Optimal Control of Induction Motor: Mine Hoist Load Diagram

Induction motor is a large consumer of electrical energy in the industries and its influence is more in energy intensive industries as discussed earlier and, therefore, needs special attention. Industrial loads such as spinning drive in textile industry and hoist load in mining industry are considered in the present work. A motor, normally 2000 hp rated, is -
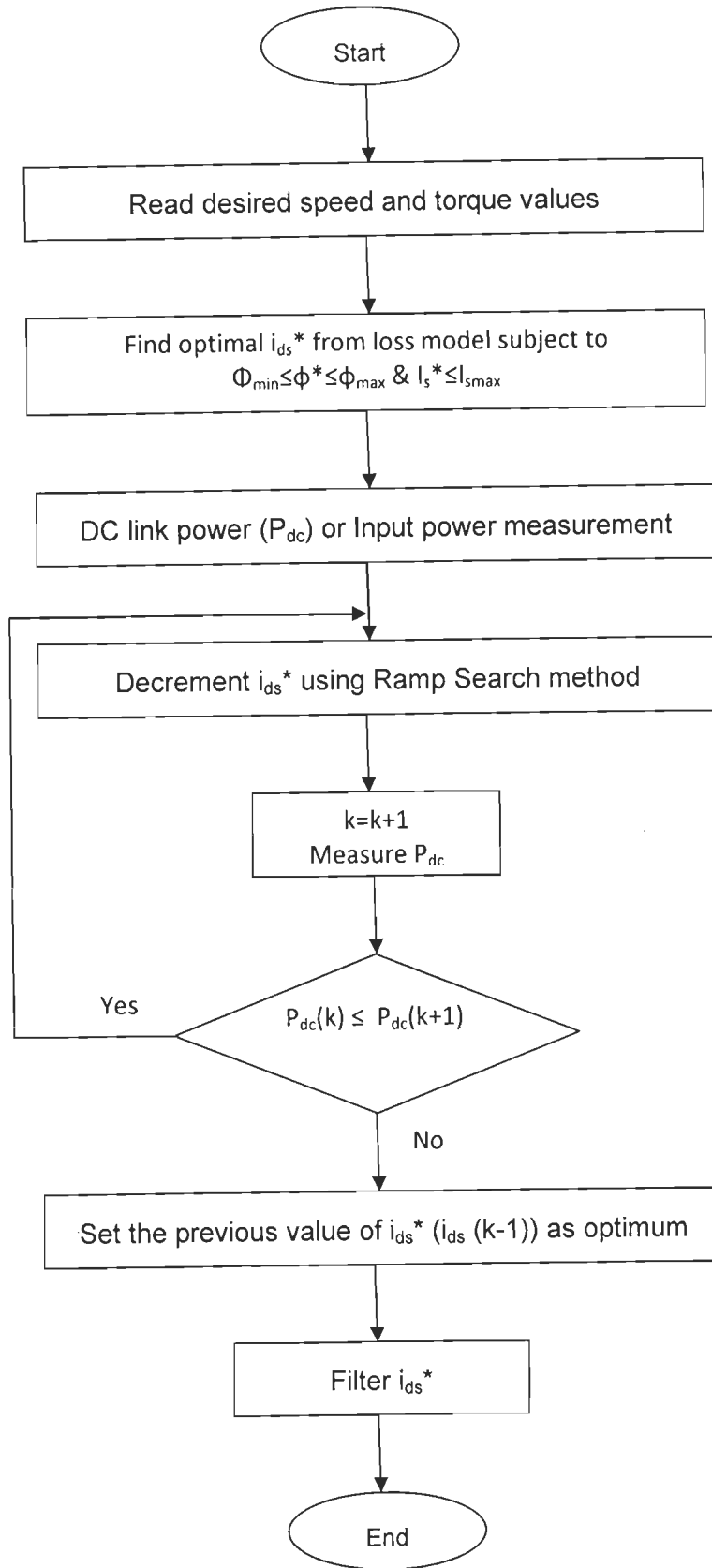
Fig. 6.5 Flow chart of hybrid flux control

- employing in mine hoist and is operated with variable load and speed as shown in Fig. 6.6 [32]. Region 't₃' of this load diagram offers light load (0.14 pu) and half the rated speed of the motor. Since the adjustment of flux level is mainly required at lightly loaded condition [98], [66], [85], [136], [27], [63],[159], [85], this region is focused in the present work for implementing optimal energy control with the help of three controllers; (i) LMC with PSO, (ii) search controller, (iii) hybrid controller. FPPI controller is used for improving the dynamic performances of the drive when optimal energy controllers are activated. Referring to mathematical models of motor, converter, inverter and loss models of entire drive system presented in chapter 3, optimal energy control of 1 hp induction motor drive for a mine hoist load diagram is simulated with MATLAB/SIMULINK. The detailed MATLAB/SIMULINK models of the entire drive system used in the present section are available in Appendix B.
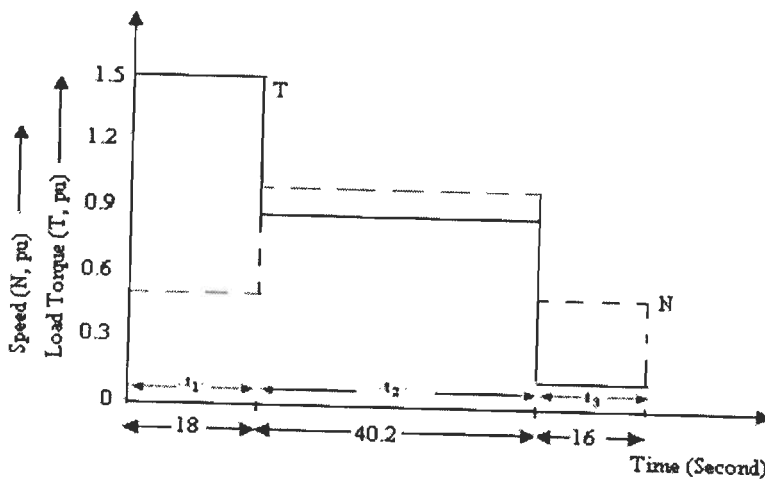
Fig. 6.6 Mine hoist load diagram

6.3.1 Simulation Results and Discussion

Although the mine-hoist drive motor is a large machine (normally in MW rating), 1 hp, 3 phase induction motor is used for simulation study in this section for easy analysis. The motor is operated with the given load diagram (Fig. 6.6) and its parameters are R_s =11.124 Ω, $R_r^{'}$ =8.9838 Ω, L_m = 490.45 mH, L_{ls} = $L_{lr}^{'}$ = 33.36 mH, k_e =0.0380, k_h =0.0380, C_{str} =0.0150, C_{fw} =0.0093, S_1=1.07, S_2=-0.69, S_3=0.45, K_1=0.000031307, K_2= 0.025. Rated load and speed of the motor are 2.5 Nm and 300 rad/s respectively. Simulation has been carried out for all the regions of the load diagram. But, the analysis is mainly focused from 3 to 5 seconds in the simulated results, where the partial load and speed occurs i.e. region t_3. A load torque of 0.35 Nm (0.14 pu) is applied at this region. The motor is accelerated to the step speed command of 0.5 p.u, 1.0 pu and 0.5 pu corresponding to three regions of-

Fig. 6.6 from start. Efficiency optimization techniques are initiated at 3 seconds. Figs 6.7 – 6.10 show the simulation results for the constant flux, LMC, SC and hybrid controllers respectively. The figures show flux, speed, developed torque and dc link power (P_{dc}) from top to bottom order.

a) Constant Flux Control

It is the conventional field oriented control, flux or flux producing current command $i_{ds}{}^*$ is always constant (1 p.u) irrespective of speed and torque shown in Fig. 6.7(a). At light load, there is no balance in between copper and constant losses, rather more core losses. Torque and speed overshoots occurred as 0.8 Nm and 150.05 rad/sec respectively. Motor consumes DC link power nearly 1170W during the operating region of t_3, shown in Fig. 6.7(d).

b) Loss Model Based PSO Controller

PSO is used to find optimal i_{ds} command from the loss model of induction motor in accordance with motor load and speed. This controller finds optimal i_{ds} instantly, shown in Fig. 6.8(a), instead of continuous adjustment in search control. Here, motor consumes 1075W, shown in Fig. 6.8(d), as dc link power which is higher than constant flux operation by 95 Watts. Torque and speed overshoots are occurred in the motor when activate this controller are 0.5 Nm and 150.1 rad/sec respectively, shown in Fig. 6.8(b) and (c). Speed overshoot is double in comparison with constant flux operation due to the sudden reduction in flux producing current. In view of these results, motor energy consumption can be reduced by selecting optimal value of flux current command.

c) Search Control

In search control, adjust (decrease) flux current command $i_{ds}{}^*$ step by step with small value and watch the dc link power at every adjustment as shown in Fig.6.9 (a). Search control is activated at 3s and searches the optimum value of $i_{ds}{}^*$. At 3.7s, minimum dc link power is reached and hence search is stopped. Using this controller, motor consumes DC link power nearly 1070W (Fig. 6.9(d)) which is lower by 100W and 5W in comparison with constant flux operation and LMC respectively. The difference in DC link power in between LMC and SC indicates the model error in LMC.
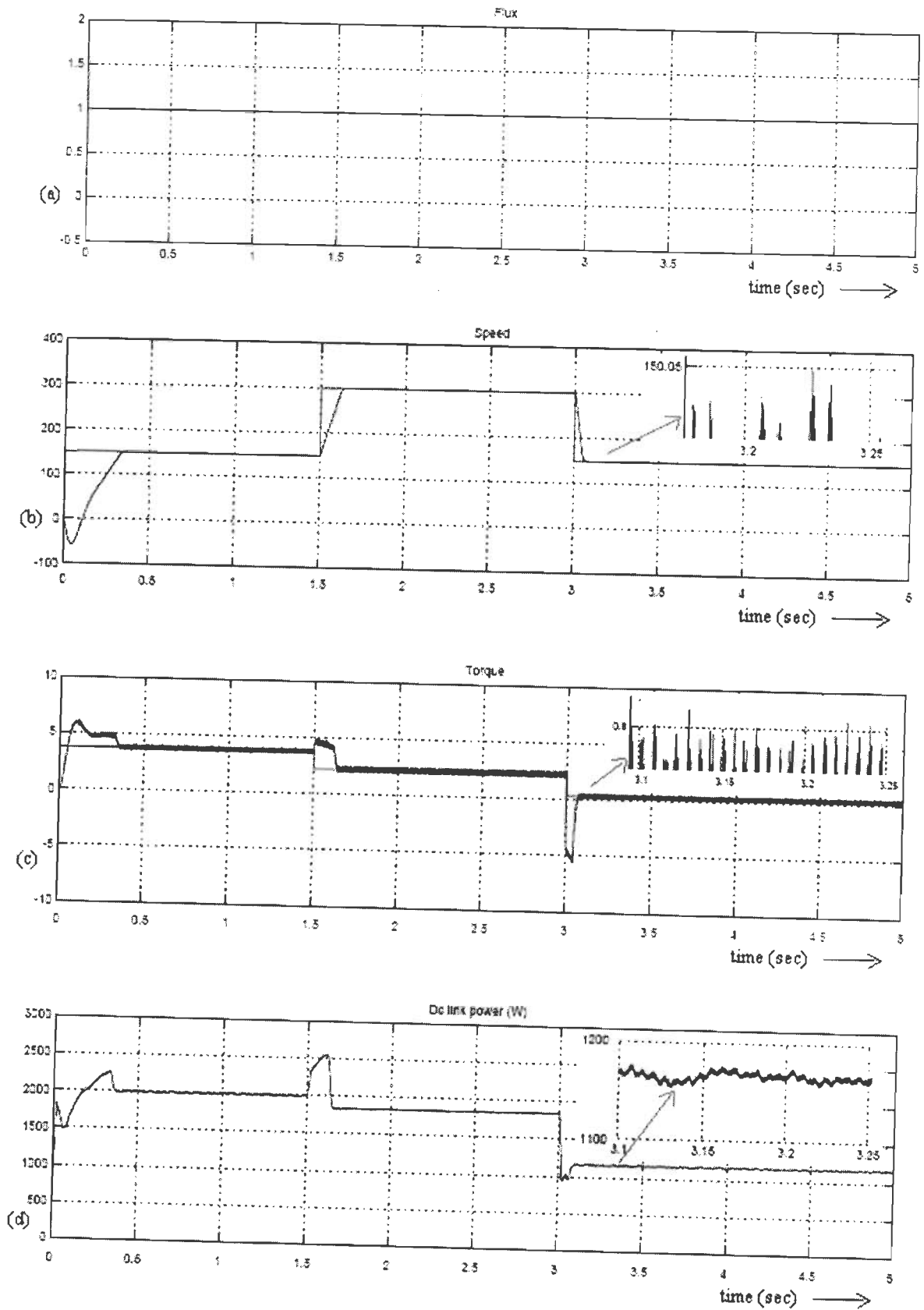
Fig. 6.7 Simulated results of constant flux operation of motor with PI controller: (a) Flux, (b) Speed, (c) Torque and (d) Dc link power
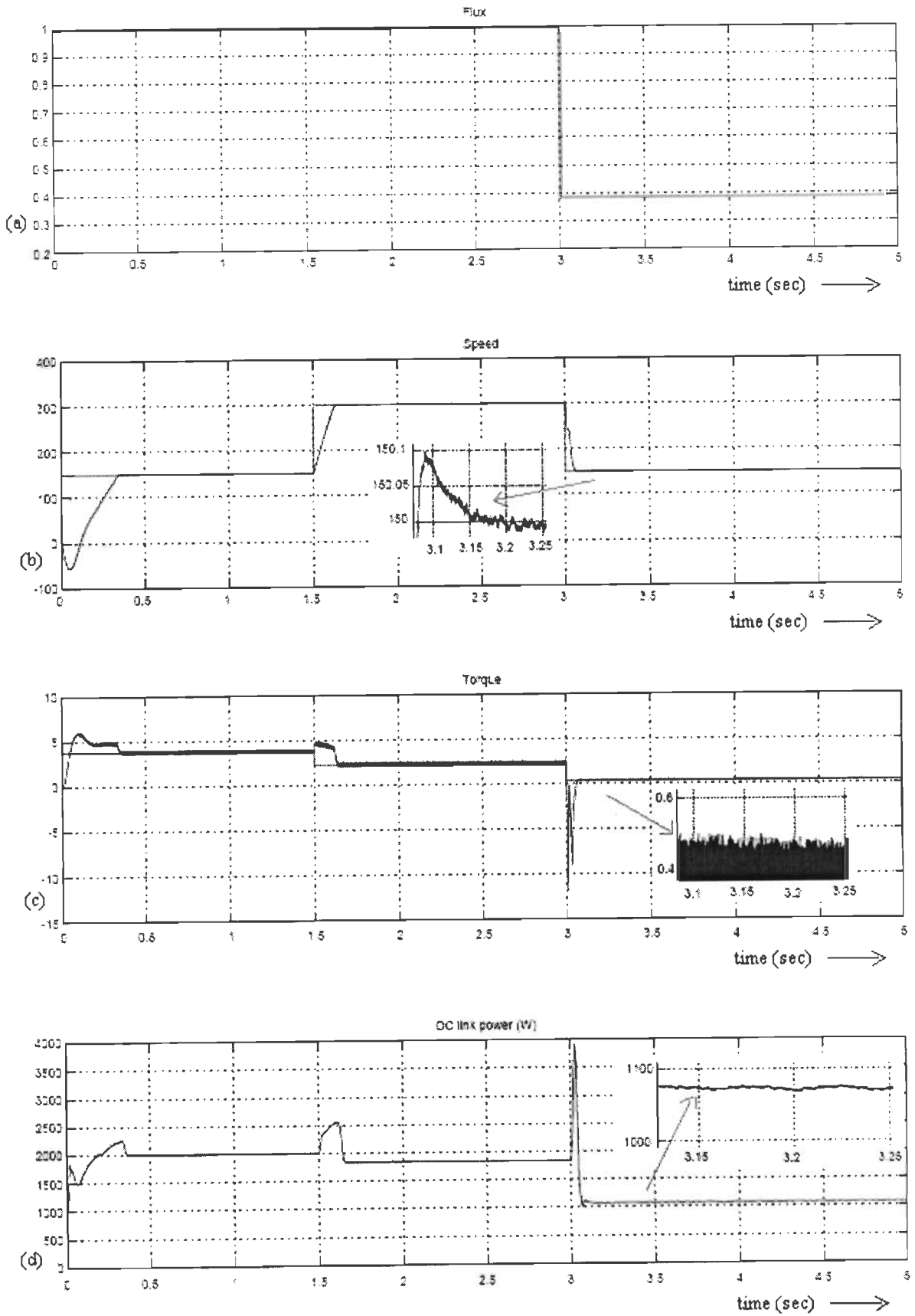
Fig. 6.8 Simulation results of loss model control with PI controller

Speed overshoot of 150.04 rad/sec occurred in the motor when this controller is activated which is lesser than LMC because of fine adjustment in flux current command whereas torque overshoot of 0.7 Nm is higher than LMC, due to continuous oscillation in motor flux, shown in Fig. 6.9(b) and (c).

d) Hybrid Controller

Simulated results of optimal energy control of induction motor using hybrid controller (which consists both LMC and search control) is shown in Fig. 6.10. LMC is activated at 3s and finds the sub-optimal ids* command for minimum DC link power and then SC is activated at 3.15s, which are shown in Fig. 6.10(a). As discussed earlier, this controller retains good features of both LMC and SC and hence offers minimum DC link power (1170W) like that of SC with less convergence time similar to LMC. In this controller, motor is reached its steady state within 0.1 second (shown in Fig. 6.10(d)) whereas 0.7 second in case of search control. Overshoots in speed and torque are similar to individual controller and hence not been zoomed them in Fig. 6.10(b) and (c).

e) Optimal Energy Controller with FPPI Speed Controller

Improvement in the dynamic performances of the motor by replacing PI speed controller in Fig. 6.1 with Fuzzy Pre-Compensated PI controller (FPPI) and then the drive was simulated. The corresponding results are shown in Fig. 6.11 and 6.12. Loss model control along with FPPI controller has the speed overshoot of 150.04 rad/sec, shown in Fig. 6.11(b), whereas this value in LMC with PI controller is 150.1 rad/sec. Similarly, SC with FPPI controller has less speed overshoot and settle down at 3.1s, shown in Fig. 6.11(b), whereas search control with PI controller did not settle down even at 3.25s. Thus the combination of PSO and FPPI controller helped much in the motor performances in terms of optimal energy consumption and less speed overshoot.

The simulated results presented in this section show that the hybrid control with FPPI controller outperformed the conventional controllers and saved 100 W power in the tested motor. Since the power rating of the mine hoist motor is very high, considerable amount of saving (in kW) is possible.
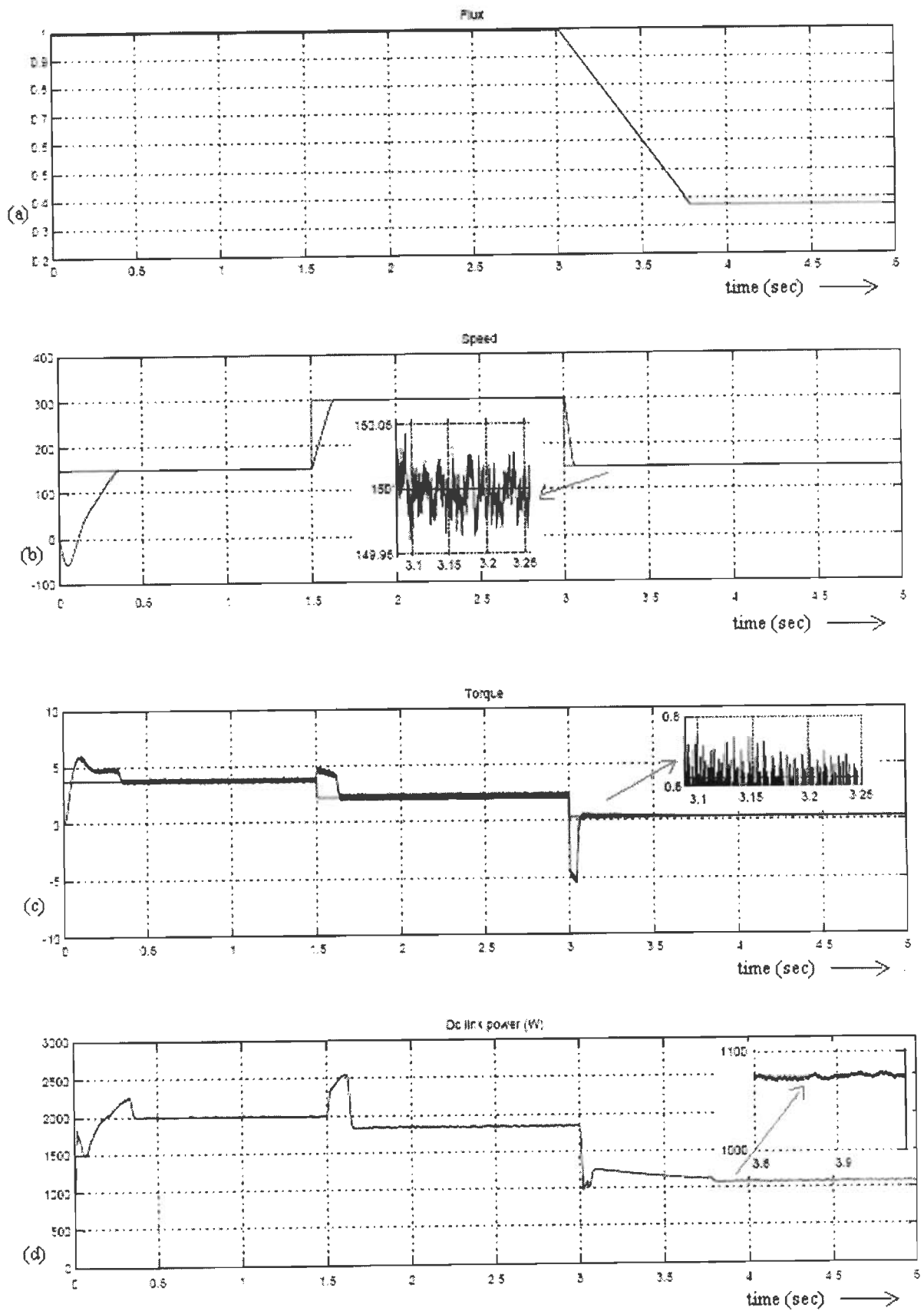
Fig. 6.9 Simulation results of search control with PI controller
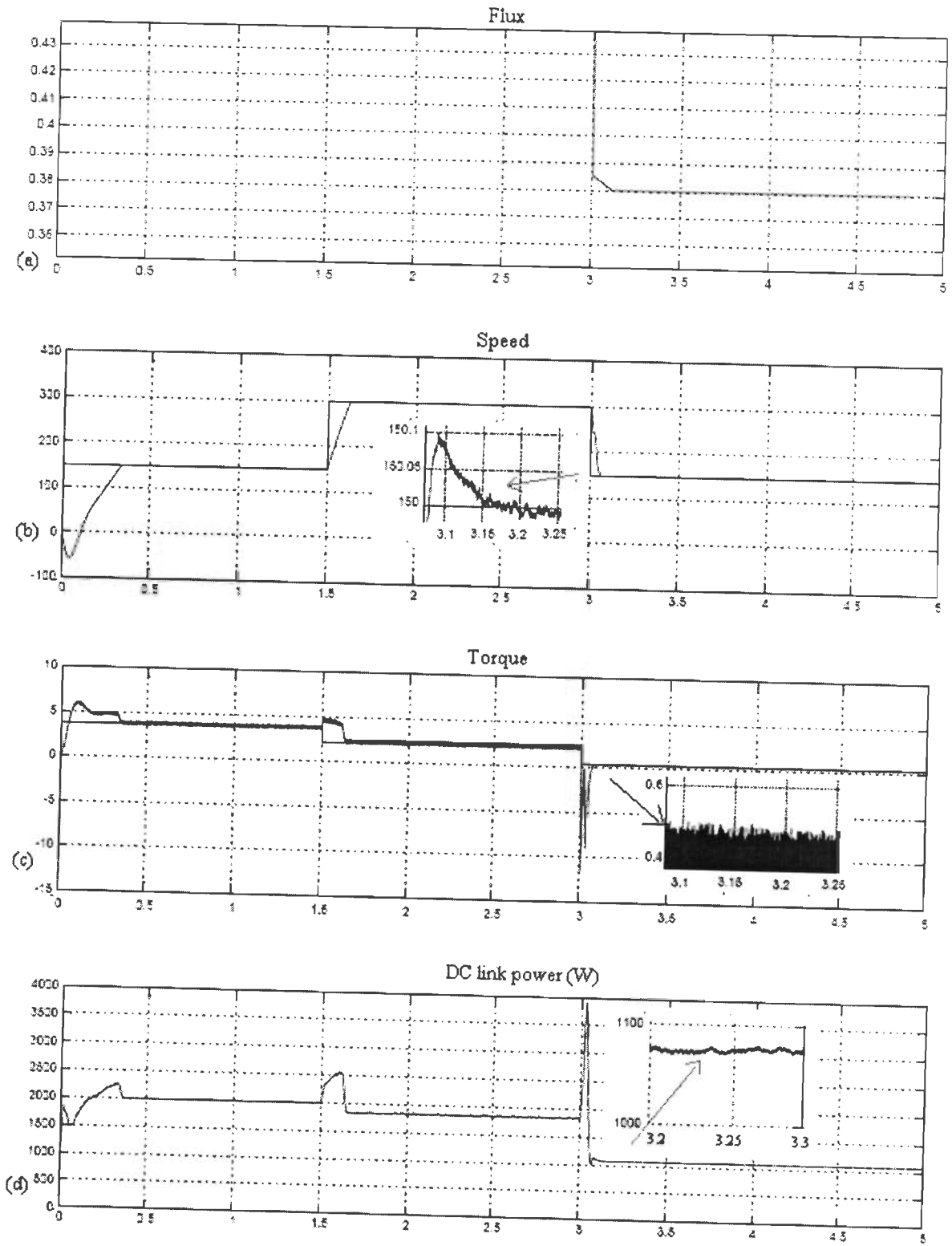
Fig. 6.10 Simulation results of hybrid control with PI controller
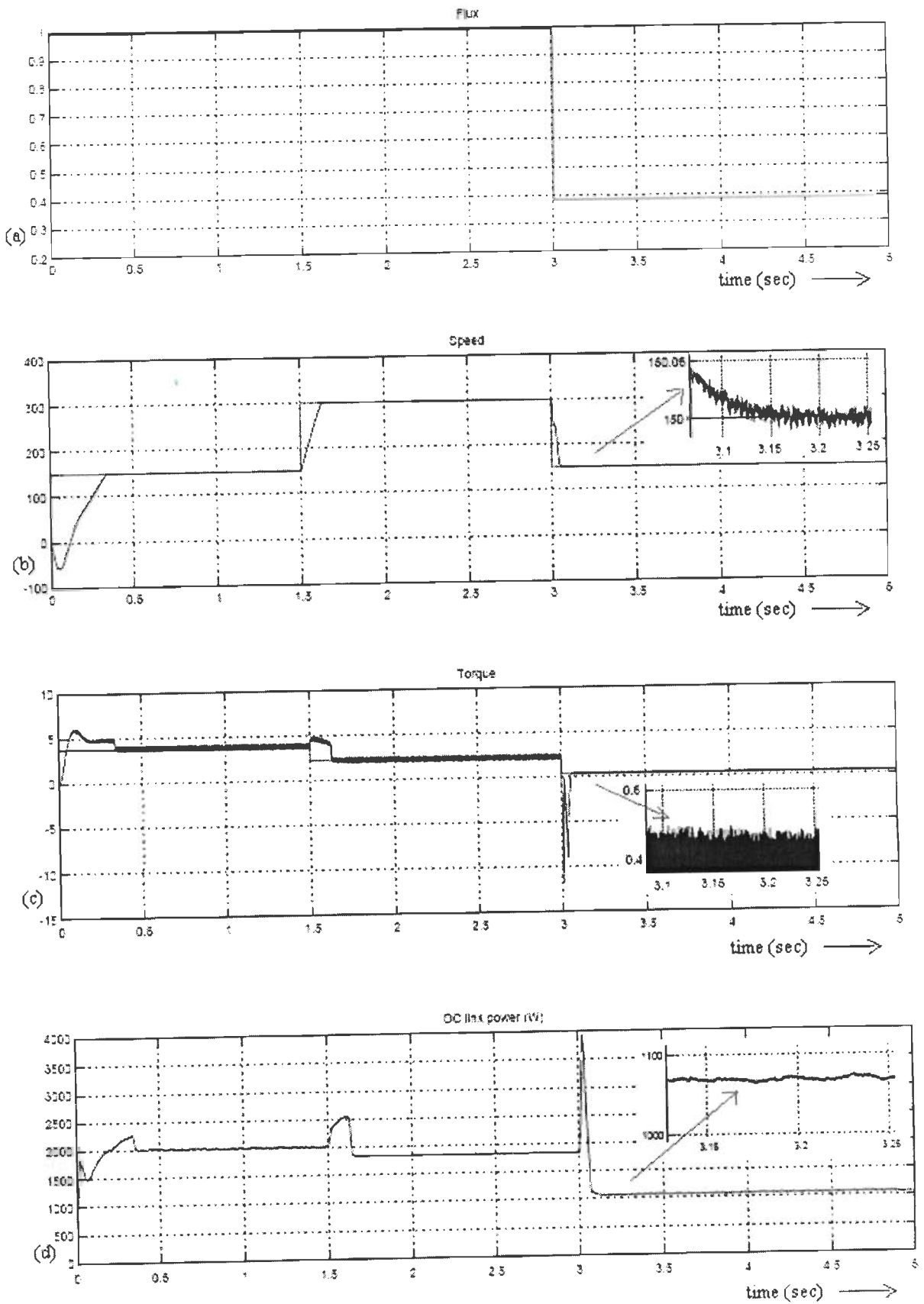
Fig. 6.11. Simulation results of loss model based control (PSO) with FPPI controller
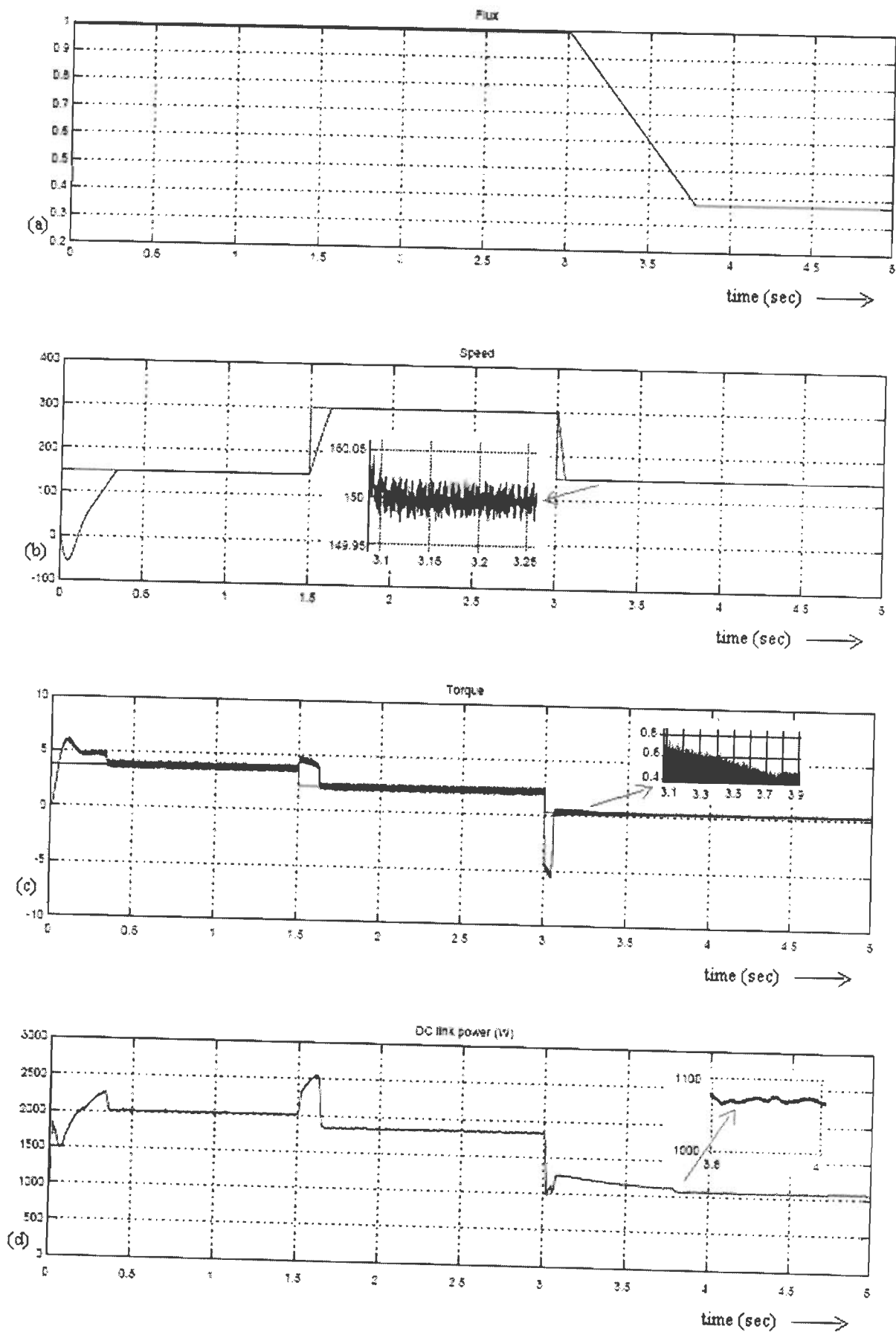
Fig. 6.12 Simulation results of search control with FPPI controller

6.4   Operating Cost Minimization of Induction Motor: Textile Industry

A ring spinning frame, shown in Fig. 6.13 (this figure is same as Fig. 1.1, repeated here for convenience) manufactures the cotton into yarn that wound on spindles and used to feed cone winding machine. Later, it can be used to make end products such as clothing with the help of weaving machine. The quantity of the yarn in the spindles varies from zero (when the process starts) to full (when process completes), hence the motor shaft load varies from zero to rated. The corresponding load diagram is shown in Fig. 6.14 which has taken from an industry located at Coimbatore, India. 'T' is the time consumption for the completion of one process.
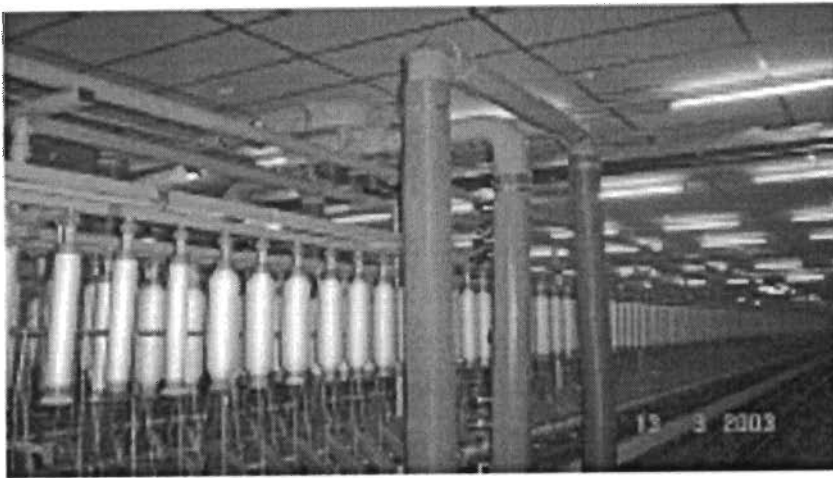
Fig. 6.13. Textile spinning ring frame
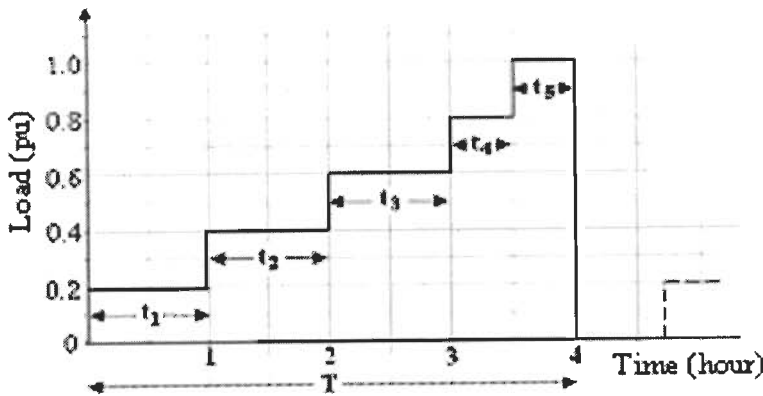
Fig. 6.14. Load diagram of a typical spinning ring frame drive motor

This section considers a 100 hp motor to study the importance of controllers on energy saving opportunity in textile mill (ring spinning frame) applications. The economics of the same motor is investigated with three topologies namely star-delta (S/D) connection, constant flux operation (V/f control) and loss model controller using PSO in steady-state conditions. The flux level in a machine has been considered to adjust to arrive minimum

operating cost of the motor. The configurations of these controller topologies are already presented in section 2.4 (chapter 2).

6.4.1   Simulation results and discussion

Referring to the induction motor (100 hp) parameters presented in [6], comparison of total energy cost is performed with three types of controllers. The motor parameters (per-unit) are R_s =0.029, R_r' =0.020, X_m =1.88, X_{lr} =0.067, k_e =0.006, k_h =0.006, C_{str} =0.025, C_{fw} =0.010, S_1=0.4, S_2=-0.30, S_3=0.45, K_1=0.000031307, K_2= 0.025, R_c = 0.000916

Total losses, energy cost, and stator current comparison of the constant speed (rated) induction motor for a textile mill load diagram with the following electricity tariff (Tamil Nadu Electricity Board, HT tariff I for the industries situated in rural areas) and assuming 5 processes repeated per day (motor running period = 20 hours per day), 355 days of operation/year and life time of the motor (N) is assumed as 15 years are summarized in Table 6.1 and 6.2. Individual losses comparison is shown in Table 6.3. The equations for operating cost calculation for the whole life of the motor are referred from chapter 4 (section 4. 7.3).

(i) Maximum demand (KVA) charges: US $ 6.66/month

(ii) Energy (kWh) charges: US $ 0.077/kWh (1 US $= Indian Rupees 45 approximately).

All the loads, star delta controller offered lower value of total energy cost due to the absence of converter losses. Although S/D offered minimum TEC compared to others, it cannot be applied over a wide range of variable load and speed applications. Loss model control which has Particle Swarm Optimization algorithm in its inner part performed much better than V/f control, in other words constant flux operation. For example, the load at t_1, LMC with PSO reduced the operating cost of the motor by 31% in comparison with constant flux operation, shown in Table 6.2. The difference in terms of operating cost of the motor at LMC and constant flux reduces with the increase in load which indicates the importance of LMC particularly at light load. Fig. 6.15 shows the variation of TEC (T is assumed as 8000) by adjusting flux level in the motor at three different load and speed points and it reveal that minimum TEC occurred at rated flux (1pu) for rated load and rated speed points and need to adjust the same at lightly loaded conditions.

Table 6.1 Total Losses, Flux and Stator Current in 100 hp Motor for Textile Mill Load

Time (hr)	Load (pu)	Φ_m (pu)			I_s (pu)			P_{loss} (KW)		
		S/D	V/f	LMC	S/D	V/f	LMC	S/D	V/f	LMC
t_1	0.2	0.557	1	0.669	0.408	0.587	0.387	1.82	3.64	2.51
t_2	0.4	1	1	0.842	0.688	0.688	0.599	3.25	4.53	4.07
t_3	0.6	1	1	0.940	0.830	0.830	0.802	4.41	5.96	5.86
t_4	0.8	1	1	1	0.995	0.995	0.998	6.03	7.89	7.89
t_5	1.0	1	1	1	1.175	1.175	1.175	8.13	10.32	10.32

Table 6.2 Operating Cost of 100 hp Motor for Textile Mill Load

Time (hr)	Load (pu)	S (US $)			D (US $)			TEC (US $)		
		S/D	V/f	LMC	S/D	V/f	LMC	S/D	V/f	LMC
t_1	0.2	3746	7480	5150	2190	4373	3011	5937	11854	8161
t_2	0.4	6666	9297	8352	3898	5436	4883	10565	14734	13236
t_3	0.6	9046	12218	12016	5289	7144	7026	14335	19363	19042
t_4	0.8	6189	8091	8090	7238	9463	9461	13427	17555	17551
t_5	1.0	8335	10581	10581	9748	12375	12375	18084	22956	22956

Table 6.3 Individual Loss Terms of 100 hp IM for Textile Mill Load

Load (pu)	P_c (KW)			P_i (KW)			$P_{str} + P_m + P_{conv}$ (KW)		
	S/D	V/f	DE	S/D	V/f	DE	S/D	V/f	DE
0.2	0.54	0.80	0.45	0.30	0.90	0.40	0.98	1.93	1.64
0.4	1.26	1.26	1.11	0.90	0.90	0.65	1.07	2.36	2.30
0.6	2.02	2.02	2.00	0.91	0.91	0.81	1.46	3.01	3.04
0.8	3.10	3.10	3.10	0.92	0.92	0.93	2.0	3.86	3.85
1.0	4.48	4.48	4.48	0.93	0.93	0.93	2.71	4.90	4.90
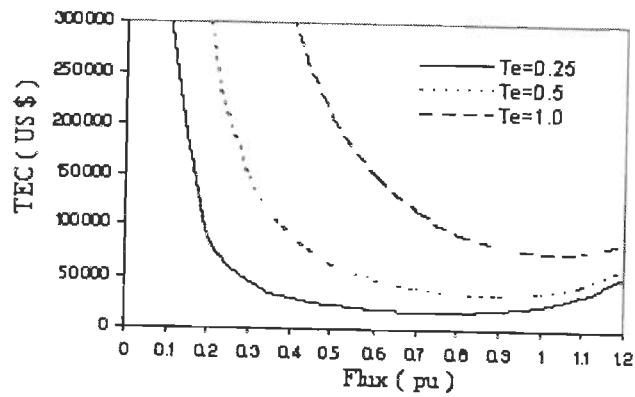
(a) $\omega_r = 0.25$
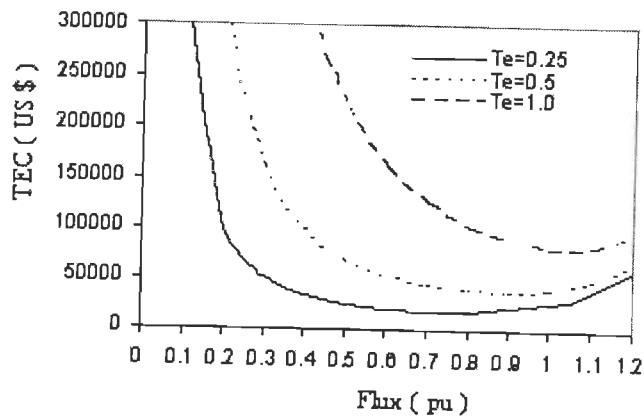
(b) $\omega_r = 0.5$
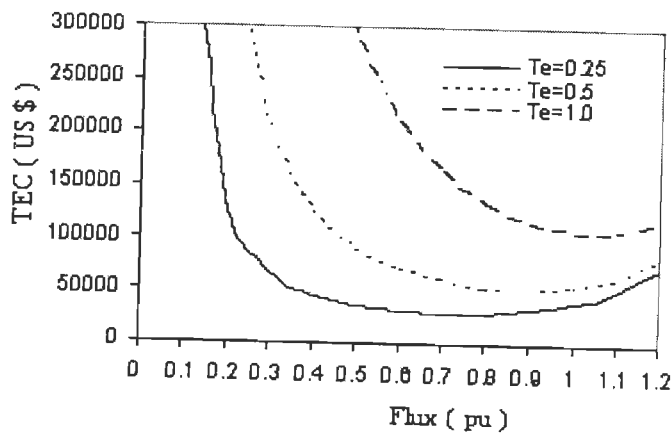
(c) $\omega_r = 1$

Fig. 6.15 TEC verses flux at variable speed and load of induction motor

(a) **Case Study at Medium Scale Textile Industry**

A privately owned medium size spinning and sewing thread industry in Tamil Nadu, producing 15 tons of yarn and 10 tons of sewing thread/day, having 96 ring frames [122]

has been considered for economic analysis. For this textile mill, the economical benefits of spinning drive motor by using LMC with PSO controller in comparison with constant flux operation are shown in Table 6.4. US$ 529536 can be saved in this industry for a whole life (15 years) of spinning drive motors.

Table 6.4 Case Study in a Typical Spinning Ring Frame for Economic Comparison

SI. No.	Controller	No. of Ring Frame	TEC (US $)	Savings (US $)
1	Constant flux	96	8300352	--
2	LMC with PSO	96	7770816	529536

6.5 Operating Cost Minimization for Wide Range of Load and Speed

The above section have focussed industrial loads whereas this section is focussed on minimization of operating cost in an induction motor operating over a wide range of variable load/speed application. The same motor (100 hp) is used for this analysis. Energy cost and demand cost are considered as mentioned in section 6.4.1 and the operating hour of the motor per year, T is assumed as 8000. Optimal flux, stator current and total losses of the motor for different set of load and speed are shown in Table 6.5. Operating cost and individual loss terms are available in Table 6.6 and Table 6.7 respectively. Results are also illustrated in graphical manner, shown in Figs. 6.16 – 6.22 for convenience. Fig. 6.16 - 6.19 show the variation of TEC by adjusting flux level in the motor at variable load and speed applications and it reveal that less TEC occurred in LMC at light loads. Thus flux adjustment is mainly required in the motor at lightly loaded condition for energy saving. Fig. 6.20 shows the LMC with PSO controller offers low losses as compared to V/f controller especially at light loads. Fig. 6.21 and 6.22 show the comparison of stator current drawn by the motor with both the controllers and reveals that LMC with PSO controller offers low stator current in the induction motor.

Table 6.5 Total Losses, Flux and Stator Current in 100 hp IM at Variable Load/Speed Operation

T$_e$ (pu)	ω$_r$ (pu)	Φ$_m$ (pu)		I$_s$ (pu)		P$_{loss}$ (KW)	
		V/f	LMC	V/f	LMC	V/f	LMC
0.2		1	0.727016	0.587755	0.388202	0.95161	0.535607
0.4		1	0.871034	0.688778	0.603797	1.423108	1.239523
0.6	0.2	1	0.951938	0.830457	0.805631	2.207203	2.167974
0.8		1	1.00901	0.995818	0.999094	3.305596	3.303695
1.0		1	1.053458	1.175187	1.186615	4.720697	4.633955
0.2		1	0.706158	0.587755	0.386814	1.194032	0.716817
0.4		1	0.863526	0.688778	0.602308	1.693127	1.485876
0.6	0.4	1	0.949336	0.830457	0.804828	2.522805	2.478416
0.8		1	1.008849	0.995818	0.999029	3.684867	3.682989
1.0		1	1.05475	1.175187	1.187249	5.181859	5.088372
0.2		1	0.686224	0.587755	0.386812	1.537911	0.984279
0.4		1	0.857183	0.688778	0.601301	2.082524	1.849765
0.6	0.6	1	0.948621	0.830457	0.804616	2.987695	2.94041
0.8		1	1.010984	0.995818	0.999912	4.25539	4.252374
1.0		1	1.058595	1.175187	1.189244	5.888386	5.776343
0.2		1	0.668948	0.587755	0.387819	1.983247	1.338009
0.4		1	0.852223	0.688778	0.600669	2.591297	2.331554
0.6	0.8	1	0.949618	0.830457	0.804912	3.601872	3.554089
0.8		1	1.015068	0.995818	1.001723	5.017165	5.011164
1.0		1	1.064544	1.175187	1.192653	6.840276	6.69595
0.2		1	0.655029	0.587755	0.389296	2.53004	1.778433
0.4		1	0.848672	0.688778	0.600299	3.219448	2.931567
0.6	1.0	1	0.952029	0.830457	0.80566	4.365336	4.319293
0.8		1	1	0.995818	0.995818	5.970191	5.970191
1.0		1	1	1.175187	1.175187	8.037531	8.037531

Table 6.6 Operating Cost of 100 hp at Variable Load/Speed Operation

Te (pu)	ωᵣ (pu)	S (US $)		D (US $)		TEC (US $)	
		V/f	LMC	V/f	LMC	V/f	LMC
0.2	0.2	8792.878	4949.006	1140.79	642.0853	9933.668	5591.091
0.4		13149.52	11453.19	1706.022	1485.94	14855.54	12939.13
0.6		20394.55	20032.08	2645.995	2598.967	23040.55	22631.05
0.8		30543.71	30526.14	3962.749	3960.469	34506.46	34486.61
1.0		43619.24	42817.74	5659.171	5555.185	49278.41	48372.93
0.2	0.4	11032.86	6623.385	1431.406	859.3197	12464.26	7482.705
0.4		15644.5	13729.5	2029.721	1781.269	17674.22	15510.77
0.6		23310.72	22900.56	3024.339	2971.125	26335.06	25871.69
0.8		34048.17	34030.82	4417.419	4415.167	38465.59	38445.99
1.0		47880.38	47016.55	6212.013	6099.94	54092.39	53116.49
0.2	0.6	14210.3	9094.743	1843.648	1179.954	16053.94	10274.7
0.4		19242.52	17091.83	2496.529	2217.499	21739.05	19309.33
0.6		27606.3	27169.39	3581.649	3524.964	31187.95	30694.36
0.8		39319.8	39291.94	5101.361	5097.746	44421.16	44389.68
1.0		54408.69	53373.41	7058.997	6924.68	61467.68	60298.09
0.2	0.8	18325.2	12363.2	2377.516	1604.005	20702.72	13967.21
0.4		23943.59	21543.56	3106.447	2795.067	27050.03	24338.63
0.6		33281.3	32839.78	4317.924	4260.642	37599.22	37100.43
0.8		46358.6	46303.15	6014.577	6007.383	52373.18	52310.54
1.0		63204.15	61870.58	8200.123	8027.105	71404.28	69897.68
0.2	1.0	23377.57	16432.72	3033.012	2131.986	26410.58	18564.71
0.4		29747.7	27087.68	3859.474	3514.363	33607.17	30602.04
0.6		40335.7	39910.26	5233.164	5177.968	45568.87	45088.23
0.8		55164.57	55164.57	7157.065	7157.065	62321.63	62321.63
1.0		74266.78	74266.78	9635.391	9635.391	83902.17	83902.17

Table 6.7 Individual Losses of 100 hp IM at Variable Load/Speed Operation

Te (pu)	ω_r (pu)	Pc (KW)		Pi (KW)		$P_{str} + P_m$ (KW)	
		V/f	LMC	V/f	LMC	V/f	LMC
0.2		0.80705	0.439011	0.111736	0.061106	0.032825	0.035489
0.4		1.265242	1.103748	0.116081	0.090183	0.041785	0.045592
0.6	0.2	2.029998	1.998034	0.120465	0.110405	0.05674	0.059535
0.8		3.102982	3.099998	0.124892	0.126831	0.077722	0.076866
1.0		4.486551	4.395542	0.129367	0.141105	0.104778	0.097308
0.2		0.80705	0.443466	0.255684	0.130037	0.131298	0.143313
0.4		1.265242	1.105381	0.260747	0.197025	0.167138	0.183471
0.6	0.4	2.029998	1.998508	0.265849	0.241114	0.226958	0.238794
0.8		3.102982	3.100019	0.270997	0.275446	0.310888	0.307524
1.0		4.486551	4.395471	0.276196	0.304335	0.419112	0.388566
0.2		0.80705	0.450533	0.435441	0.20811	0.295421	0.325637
0.4		1.265242	1.107531	0.44122	0.327277	0.376061	0.414957
0.6	0.6	2.029998	1.998675	0.447041	0.404042	0.510656	0.537693
0.8		3.102982	3.099848	0.45291	0.462393	0.699498	0.690132
1.0		4.486551	4.395896	0.458833	0.510599	0.943001	0.869848
0.2		0.80705	0.458869	0.651005	0.294911	0.525193	0.584228
0.4		1.265242	1.109696	0.657502	0.48111	0.668553	0.740748
0.6	0.8	2.029998	1.998446	0.664041	0.600751	0.907833	0.954891
0.8		3.102982	3.100124	0.670631	0.69019	1.243551	1.22085
1.0		4.486551	4.398462	0.677279	0.763091	1.676447	1.534398
0.2		0.80705	0.467097	0.902377	0.391299	0.820613	0.920037
0.4		1.265242	1.111503	0.909591	0.659185	1.044615	1.160879
0.6	1.0	2.029998	1.998021	0.916849	0.833044	1.418488	1.488228
0.8		3.102982	3.102982	0.92416	0.92416	1.943049	1.943049
1.0		4.486551	4.486551	0.931532	0.931532	2.619448	2.619448
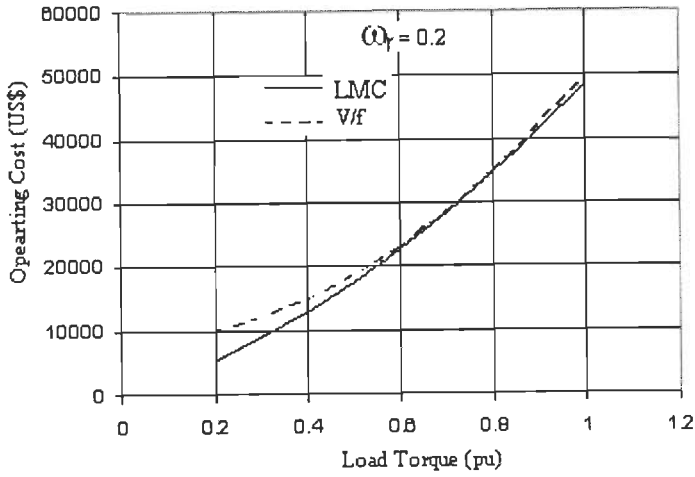
Fig. 6.16 TEC verses load torque at ω_r = 0.2
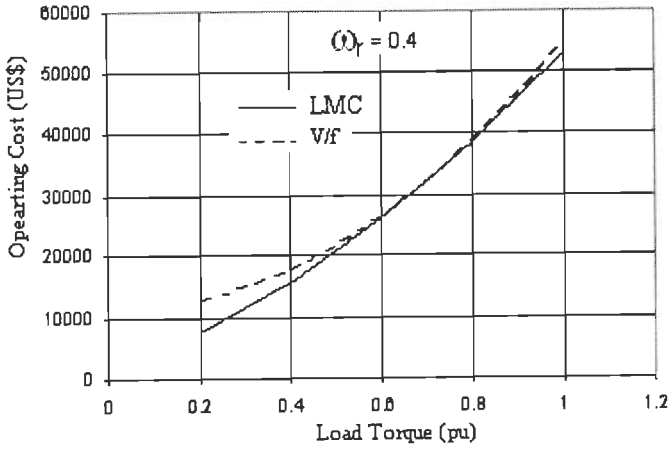
Fig. 6.17 TEC verses load torque at ω_r = 0.4
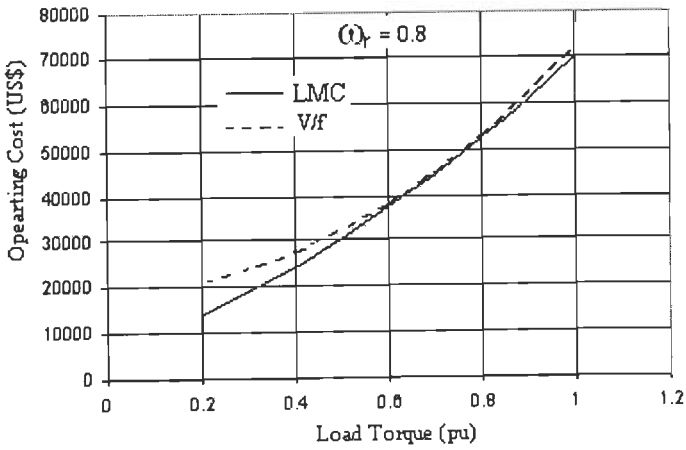
Fig. 6.18 TEC verses load torque at ω_r = 0.8
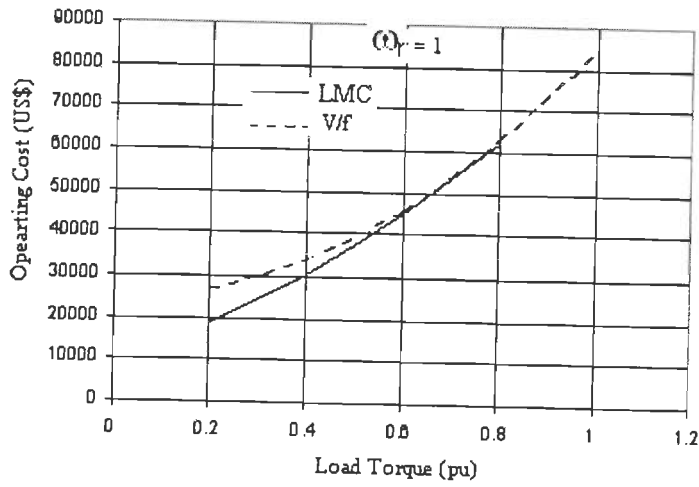
Fig. 6.19 TEC verses load torque at $\omega_r = 1$
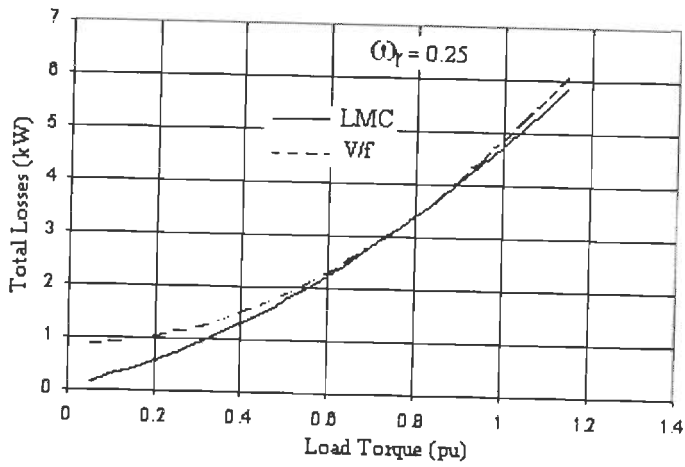
Fig. 6.20 Total losses load torque at $\omega_r = 0.25$
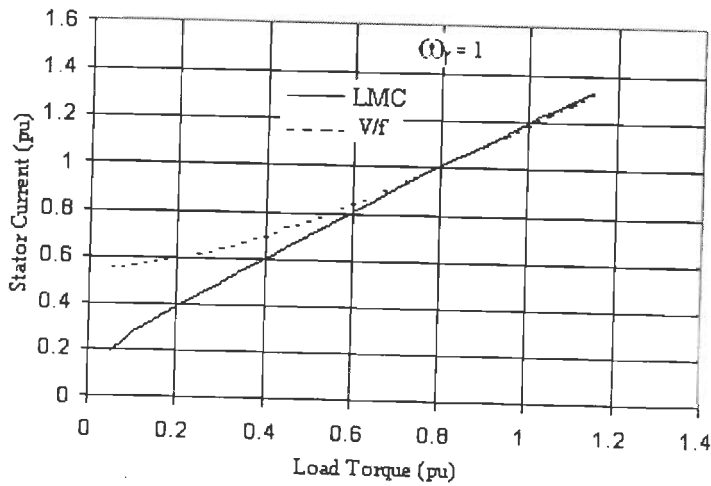
Fig. 6.21 Stator current verses load torque at $\omega_r = 1$
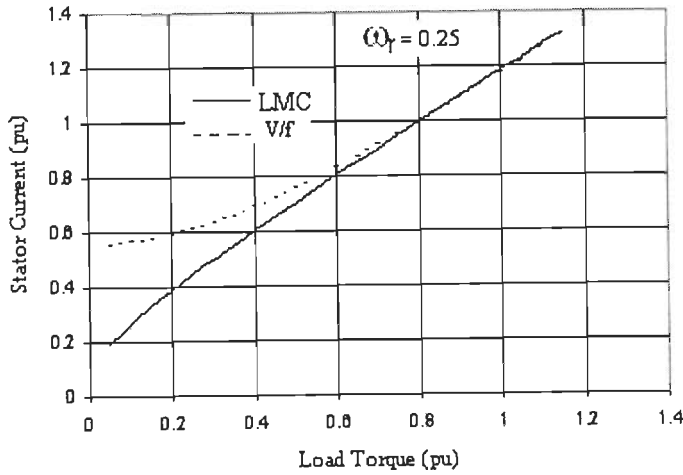
Fig. 6.22 Stator current verses load torque at $\omega_r = 0.25$

6.6   Conclusion

This chapter presented simulation studies on the optimal energy control of an inverter-fed three-phase induction motor using MATLAB/SIMULINK. Three types of efficiency optimization controllers: loss model controller, search controller and hybrid controllers have been successfully applied in mine hoist drive of mineral industry and minimum DC link or input power was achieved. Hybrid controller gave genuine optimum of DC link power and outperformed the loss model and search controllers. Operating cost minimization was applied in a spinning drive of textile industry and the case study in a medium scale textile industry was reported. US$ 529536 can be saved in a medium scale textile industry over its life, with the use of optimal energy controllers in spinning drive motors. Fuzzy Pre-Compensated Proportional Integral controller has been used to improve motor's dynamic performances in terms of speed overshoot during the activation of optimal energy controller. Motor was also simulated for the possible wide ranges of speed and torque in addition with industrial loads. The simulation results demonstrate that significant amount of energy can be conserved in Indian industries by choosing several possible ways of implementing optimal energy control. The drive system has been maintained satisfactory dynamic performance even when the motor operates at reduced flux.

Conclusion and Future Scope

7.1 Conclusion

A large part of electrical energy consumption goes to induction motor which is serving to industries and it is known that efficiency is drastically reduced in these motors at part-load operation. The part-load operation of induction motors cannot be avoided in many industrial applications like spinning drive in textile industry, hoist drive in mineral industry, pumps in all types of process industries, etc. The part load efficiency and power factor of the induction motor can be improved by adapting the magnetizing level in the motor in accordance with load and speed and, hence, motor should either be fed through an inverter or redesigned with optimization algorithms. Furthermore, a small increment in the efficiency of these motors by providing better control or optimum design can result in substantial saving in the long period. The research in the present work was carried out both in optimal design and control of induction motor to achieve maximum efficiency.

For optimal design, Particle Swarm Optimization (PSO) and its improved version, Quadratic Interpolation based Particle Swarm Optimization (QIPSO), have been applied for the fresh design of squirrel cage induction motors. Five objective functions namely, material cost, efficiency, starting torque, temperature rise and operating cost have been chosen with nine performance related indices as constraints. A set of design variables which are most sensitive to the objective functions have been judiciously chosen. They are: ampere conductors, ratio of stack length to pole pitch, stator slot depth to width ratio, stator core depth, average air gap flux densities, stator winding current density, and rotor winding current density. In order to facilitate the application of optimization algorithms the design and performance equations have been derived in terms of the chosen variables. The effects of variables in the performance indices of the motor like efficiency, torque, material cost, starting torque, power factor etc. were examined. The results of PSO and QIPSO have been compared with normal design, Rosenbrock and Simulated Annealing (SA) methods for exploring their superiority. It has been observed that QIPSO plays an important role in optimizing objective functions.

In the optimization of material cost, the tendency of the variable in obtaining an optimized design has been to have lower specific electric loading and higher values of

stator and rotor winding current densities. For maximum efficiency and starting torque and minimum temperature rise, the tendency of the variable has been to have higher value of width of the stator slot, lower value of depth of the rotor slot and intermediate value of length of the stator stack. Higher ampere conductors, stack length to pole pitch ratio, stator slot depth to width, stator core depth and average air gap flux density were required to achieve optimum operating cost or energy cost of the motor. Material costs slightly increased when the motor was designed with respect to optimizing its operating cost. Higher Stator core depth and lower stator slot depth to width ratio were required to get a good machine when subjected to voltage unbalance and the material cost was increased due to the increase of ampere conductors/m to meet higher stator currents. Greater depth of the stator slot for more starting torque, higher width of the stator slot and tooth flux density for minimum temperature rise were the effects when the motor was designed with the consideration of harmonic current.

Realisation of the induction motor design results obtained from Particle Swarm Optimization and Quadratic Interpolation based Particle Swarm Optimization has been done via SPEED (Scottish Power Electronics and Electric Drives) software. Theoretical justification on the optimized results was also given. The effects of variables (width of the stator slot, depth of the rotor slot and length of the stator stack) on efficiency, torque and temperature rise were plotted by the ranging function of SPEED software. The performance based optimal design of induction motor using SPEED software was also carried out and SPEED software helped in substantial reduction in convergence time to optimize the motor by reducing the design variables to five instead of seven.

For optimal control, flux level in a machine was adjusted to give minimum operating cost or maximum efficiency for the industrial load. Mathematical model of the entire induction motor drive system was presented. PWM inverter model was explained for every possible switching state. Sinusoidal pulse width modulated current controllers were modelled and used in the drive. Optimal energy controller was designed through the loss models of entire variable speed drive systems. Loss models of motor and converter for fundamental and harmonic frequencies were developed. Motor loss model has been performed with the help of single phase equivalent circuit and losses represented by stator, rotor, core and stray resistances. Transistor switching losses and the conduction losses of the diodes and chokes were considered for modelling the inverter losses. The Proportional Integral (PI) and Fuzzy Pre-compensated PI controllers were designed to produce torque command of the drive. The drive model was developed for the vector control scheme. Using the PWM

inverter, induction motor and associated controller models, the complete drive was simulated with MATLAB/SIMULINK and studied its performance.

Three types of efficiency optimization controllers: loss model controller, search controller and hybrid controllers have been successfully applied in mine hoist drive of mineral industry and achieved minimum DC link or input power. Hybrid controller gave genuine optimum of DC link power and outperformed the loss model and search controllers. Operating cost minimization was applied through Particle Swarm Optimization based loss model control in a spinning drive of textile industry and the case study in a medium scale textile industry was reported. US$ 563136 can be saved in a medium scale textile industry over the whole life when energy optimal controllers used in spinning drive motors. Dynamic performance of the motor in terms of speed overshoot during the activation of energy optimal controller was improved with the help of FPPI. Motor was also simulated for the possible wide ranges of speed and torque in addition with industrial loads. The simulation results demonstrate that significant potential of conservation in Indian industries by choosing several possible ways of implementing energy optimal control. The drive system has been maintained satisfactory dynamic performance even when the motor operates at reduced flux.

Two experimental studies were also performed for supporting the main objectives of this thesis. One study on voltage unbalance effects on induction motor performances and the other one was on the comparison of different efficiency measurement standards with the special attention to stray load losses in the motor. The first study has shown that US $ 188 additionally paid per year to the electricity supplier due to a small amount of voltage unbalance (less than 1%) in a 5 hp motor and hence industry personnel should not ignore voltage unbalance even its value is very less. Second study has revealed Indian Standard IS 325 estimated the motor efficiency of the motor accurately because it measured the stray load losses similar to that in IEEE 112- E.

To summarize, the loss models of induction motor drive systems were derived with the consideration of saturation effects. The broad approaches of induction motor loss minimization, namely loss model, search and hybrid controller were discussed with the special attention of their advantages and drawbacks. Design improvements of induction motor by selecting optimal values of variables and constraints using Particle Swarm Optimization and its variant, called QIPSO, were given. Optimized results given by PSO and QIPSO were validated by one of the electrical motor design softwares named SPEED/IMD and some benchmark problems. The performance based optimal design of induction motor using SPEED/IMD was also carried out and achieved reduction in number of required

design variables. Supply voltage unbalance and harmonics are taken into account while designing the motor. A detailed study along with simulation results of optimal control of induction motor for a mine hoist load was presented. FPPI controller was used to maintain good stability of the drive when the flux is adjusted. Case study in a medium scale textile industry for economical analysis was also presented. The results of both optimal design and control show excellent performance of the motor with the proposed optimization algorithm, in terms of efficiency, operating cost, manufacturing cost starting torque and temperature rise.

7.2 Future Scope

Research is a continuous process. An end of a research project is a beginning to a lot of other avenues for future work. Following aspects are identified for future research work in this area –

Optimal design:

1. The optimized deign results of the motor in terms of efficiency, torque, etc obtained from the algorithms are based on theoretical evaluations only. Hence, dynamic performances of the designed motor should be checked with the help of SPEED - MATLAB interface.

2. Many improved version of Particle Swarm Optimization other than QIPSO are available in the literature which can be applied in the design problem or further improvements in the optimization algorithms can be performed.

Optimal control:

1. The industrial loads considered in the present work are varying continuously with respect to time. Hence the design of efficiency optimization controllers with less convergence time will be useful to operate such drives with good dynamic performances. Further work can be focused to minimize convergence time in hybrid optimal energy controller.

2. Since the performance of loss model based controller is based on the accuracy of induction motor drive system loss models further work especially in converter losses and magnetic saturation is needed to get more accurate results.

Publications from this Work

A. OPTIMAL DESIGN OF INDUCTION MOTOR

JOURNALS

1   C. Thanga Raj, S. P. Srivastava, Pramod Agarwal, "Realization of Particle Swarm Optimized Design of Induction Motor Via SPEED/PC-IMD," *Engineering Letters*, vol. 16, no. 4, 2008, pp. 486-492.

2   C. Thanga Raj, S. P. Srivastava, Pramod Agarwal, "Energy Efficient Control of Three-Phase Induction motor- A Review," *Int. Journal of Computer and Electrical Engineering*, vol. 1, no. 1, 2009, pp. 61-70.

3   C. Thanga Raj, S. P. Srivastava, Pramod Agarwal, "Induction Motor Design with Limited Harmonic Currents Using Particle Swarm Optimization," *Int. Journal of Electrical Systems Science and Engineering*, vol. 1, no. 3, 2008, pp. 201-207.

4.   C. Thanga Raj, S. P. Srivastava, Pramod Agarwal, "Particle swarm optimized design of poly-phase induction motor with the consideration of unbalanced supply voltages," *Int. Journal of Mathematical Modeling, Simulation and Applications (India)*, vol. 1, No. 3, 2008, pp. 339-350.

5.   C. Thanga Raj, S. P. Srivastava, P. Agarwal, "Optimal design of poly-phase induction motor using particle swarm optimization," *i-manager Journal on Electrical Engineering (India)*, vol. 1, no. 4, April 2008, pp. 45-50.

6.   C. Thanga Raj, S. P. Srivastava, Pramod Agarwal, "Induction Motor Design with Ideal and Non-Ideal Supply Voltages using Particle Swarm Optimization," *IEEE Transaction on Magnetics* (Under Review).

7.   C. Thanga Raj, S. P. Srivastava, Pramod Agarwal, "Performance based Optimal Design of Induction Motor using SPEED/PC-IMD and PSO," *Int. Journal of Optimization and Engineering* (Under Review).

CONFERENCE PROCEEDINGS

8   C. Thanga Raj, S. P. Srivastava, Pramod Agarwal, "Cost Minimization and Its Realization on Induction Motor Design via SPEED/PC-IMD," in *Proc. IEEE Int. Conf. INDICON-2008*, IIT Kanpur, pp. 46-50.

9   C. Thanga Raj, S. P. Srivastava, Pramod Agarwal, "Realization on PSO based Induction Motor Design Via SPEED/PC-IMD," in *Proc.* Int. Conf. ICACC-2009, *IEEE* Computer Society Press, Singapore, Jan. 20-22, 2009 pp. 65-69.

B. OPTIMAL CONTROL OF INDUCTION MOTOR

JOURNALS

10.   C. Thanga Raj, S. P. Srivastava, Pramod Agarwal, "Particle Swarm and Fuzzy Logic Based Optimal Energy Control of Induction Motor for a Mine Hoist Load Diagram," *IAENG Int. Journal of Computer Science*, vol.36, no.1, 2009, pp. 17-25.

11.   C. Thanga Raj, S. P. Srivastava, Pramod Agarwal, "Differential Evolution based Optimal Control of Induction Motor Serving to Textile Industry," *IAENG Int. Journal of Computer Science*, vol. 35, no. 2, 2008, pp. 201-208.

12.   C. Thanga Raj, Pramod Agarwal, S. P. Srivastava, "Deviations in the Performance of a Three-Phase Induction Motor under Different Unbalanced Phase Voltages with Same Unbalance Factor," *i-manager Journal on Electrical Engineering (India)*, vol. 1, no. 3, Jan. 2008, pp. 7-12.

MAGAZINES

13.   C. Thanga Raj, Pramod Agarwal, S. P. Srivastava, "Indian Standard IS 325 – a Review," *Engineering Advances Magazine (India)*, vol. 19, no. 4, April, 2007, pp. 24-32.

14.   C. Thanga Raj, S. P. Srivastava, Pramod Agarwal, "Industrial Applications for Induction Motor-Situation Analysis," *Electrical India Magazine (India)*, vol. 48, no. 3, March 2008, pp. 70-73.

CONFERENCE PROCEEDINGS

15.   C.Thanga Raj, Pramod Agarwal and S.P.Srivastava, "Performance analysis of a three-phase squirrel-cage induction motor under unbalanced sinusoidal and balanced non-sinusoidal supply voltages" in *Proc. IEEE Int. Conf., PEDES*, IIT Delhi, India, Dec. 2006, pp. 1-4.

16.   C.Thanga Raj, Pramod Agarwal and S.P.Srivastava, "Particle Swarm Optimized Induction motor for a Textile mill load diagram", *in Proc. IET Int. Conf. ICTES 2007*, Dr. MGR University, India, 20-22, Dec. 2007, pp. 379-383.

Bibliography

[1]   Abbondanti A., "Method of flux control in induction motors driven by variable frequency, variable voltage supplies," Adjustable speed ac drives, IEEE press, B. K. Bose (Editor).

[2]   Abdin E. S., Ghoneem. G. A., Diab H.M.M., Deraz S.A., "Efficiency optimization of a vector controlled induction motor drive using an artificial neural network," in Proc. IEEE Int. conf. IECON 2003, pp. 2543-2548.

[3]   Abrahamsen F., Blaabjerg F., Pedersen J.K., Grabowski P.Z., Thogersen P. B., "On the efficiency optimized control of standard and high efficiency induction motor in CT and HVAC applications," IEEE Trans. Ind. Appl. vol. 34, no. 4, 1998, pp. 822-831.

[4]   Abrahamsen F., Blaabjerg F., Pedersen J.K., Thogersen P., "Efficiency-optimized control of medium size induction motor drives," IEEE Trans. Ind. Appl. vol. 37, no. 4, 2001, pp. 1761-1767.

[5]   Abrahamsen F. Energy Optimal Control of Induction Motor Drives. Ph.D Dissertation, Institute of Energy Technology, Aalborg University, 2000.

[6]   Ahmed F. I., Zaki A.M., Ali E. E., "Terminal-impedence control for energy-saving in induction motors at no and partial loads using microprocessor," in Proc. IEE Conf. Power Elect. And Variable Speed Drives, 1994, pp. 336-341.

[7]   Alger P. L., Angst G., Davies E. J., "Stray load losses in polyphase induction machine," AIEE Trans. Power App. And System, vol. 78, no.3, 1959, pp. 349-355.

[8]   Anderson O. W., "Optimum design of electrical machines," IEEE Trans. Power App. And Systems, vol. PAS-86, no. 6, 1967, pp. 707-711.

[9]   Angst G., "Saturation factors for leakage reactance of induction motors with skewed rotors," IEEE Trans. Power Apparatus and systems, vol. 82, no. 68, 1963, pp. 716-723.

[10]   "ANSI/NEMA Standard Publication no. MG1-1978," National Electrical Manufacturers Association, Washington, DC.

[11]   Award H., Bolen M. H. J., "Power electronics for power quality improvements," in Proc. IEEE Int. Symp. ISIE- 2003, vol. 2, pp. 1129- 1136.

[12]   Back Thamos, Evolutionry Algorithms in Theory and Practice. Oxford University Press, New York, 1996.

[13]   Bernal F. F., Cerrada A. G., "Model-based minimization for DC and AC vector-controlled motors including core satuartion," IEEE Trans. Ind. Appl. vol. 36, no.3, 2000, pp. 755-763.

[14]   Bharadwaj D. G, Venkatesan K., Saxena R.B., "Induction motor design optimization using Constrained Rosenbrock Method (Hill Algorithm)," Computer and Electrical Engineering, vol. 6, 1979, pp. 41-46.

177

[15] Bharadwaj D. G. Application of certain Optimization Techniques for Cage Induction Machine. Ph.D Thesis, University of Roorkee, India, 1979.

[16] Bhuvaneswari R., Subramanian S., "Optimization of three-phase induction motor design using simulated annealing algorithm", Electric Power Components and Systems, vol. 33, no. 9, 2005, pp. 947-956.

[17] Binns K.J., Rowlands G., "Simple rules for the elimination of cogging torque in squirrel cage induction motors," Proc. IEE, Electrical Power Appl., vol. 121, no.1, 1971, pp. 63-67.

[18] Blaabjerg F., Pedersen J.K., Rise S., Hansen H.H., Trynadlowski A.M., "Can soft-starters help save energy," IEEE Ind. Appl. Magazine, vol. 3, no. 5, 1997, pp. 56-66.

[19] Boglietti A., Cavagnino Andrea, Ferraris Luca, Lazzari Mario, Luparia Giorgio, "No tooling cost process for induction motors energy efficiency improvements," IEEE Trans. Ind. Appl., vol. 41, no. 3, 2005, pp. 808-816.

[20] Boldea I., Nasar S. A., Vector Control of AC Drives. Florida, CRC press, 1990.

[21] Bose B. K., Modern Power Electronics And AC Drives. Singapore: Pearson Education, 2003.

[22] Bose B. K., Patel N. R., Rajashekra K., "A neuro-fuzzy base on-line efficiency optimization control of a stator flux oriented direct vector controlled induction motor drive," IEEE Trans. Ind. Electron., vol. 44, no.2, 1997, pp. 270-273.

[23] Bounekhla M., Zaim M. E., Rezzoug A., "Comparative study of three minimization methods applied to the induction machine parameters identification using transient stator current," Electric Power Components and systems, vol. 33, 2005, pp. 913-930.

[24] Bowerfind J., Campbell S. J., "Application of solid-state ac motor starters in the pulp and paper industry," IEEE Trans. Ind. Appl. vol. IA-22, no. 1, 1986, pp. 109-114.

[25] Buck F. G. G., Gistelinck P., and Backer D., "A simple but reliable loss model for inverter supplied induction motors," IEEE Trans. Ind. Appl., vol. IA 20, no. 1, 1984, pp. 190-201.

[26] Bureau of Energy Efficiency, "Electric motors guide book," 2005, www.energymanagertraining.com/GuideBooks/3Ch2.p).

[27] Cacciato M., Consoli A., Scarcella G., Seelba G., Testa A., "Efficiency optimization technique via constant optimal slip control of induction motor drives," in Proc. IEEE Power Electronics, Electric Drives, automation, and Motion, 2006, pp. 32-42.

[28] Cao C., Zhou B., Min Li, Jing du, "Digital implementation of DTC based on PSO for induction Motors," in Proc. IEEE Conf. Intelligent Control and Automation, 2006, pp. 6349-6352.

[29] Chakraborty C., Minh C. Ta, Toshiyuki U., Yoichi H., "Fast search controllers for efficiency maximization of induction motor drives based on DC link power measurement", in Proc. IEEE conf. Power Conversion, PCC 2002, pp. 402-408.

[30] Chang J. H., Kim B. K., "Minimum-time and minimum-loss speed control of induction motors under field oriented control," IEEE Trans. Ind. Electron. vol. 44, no. 6, 1997, pp. 809-815.

[31] Chang Wook Ahn, Advances in Evolutionary Algorithms-Theory, Design and Practice. Springer Verlag, Netherlands, 2006.

[32] Chilikin M., 'Electric Drives," MIR Publishers, Moscow, 1976.

[33] Ching-Yin Lee, "The effects of unbalanced voltage on the performance of a 3 phase induction motor," IEEE Trans. Energy conversion, vol. 14, no. 2, 1999., pp. 202-208.

[34] Christian Koechli, Fussel .K., Prina S.R., James D.A., Perriard Y., "Design optimization of induction motors for aerospace applications," in Proc. IEEE Ind. App. Annual Meeting, 2004, pp. 2501-2505.

[35] Cleland J. G., Vance E. McCormick, Wayne Turner M., "Design of an optimization controller for inverter fed AC induction motors," in Proc. IEEE Ind. Appl. Conference, 1995, pp.16- 21.

[36] Clive Beggs, Energy Management, Supply and Conservation. Elsevier Science and Technology Book, 2002.

[37] Cunkas M., Akkaya R., "Design optimization of induction motor by genetic algorithm and comparison with existiong motor", Mathematical and Computational Applications, vol. 11, no. 3. 2006, pp. 193-203.

[38] Dabala K., "Analysis of mechanical losses in three-phase squirrel-cage induction motors," in Proc. Electrical Machines and Systems, ICEMS- 2001, pp. 39-42.

[39] De Wit C. C., Seleme S. I., "Robust torque control design for induction motors: the minimum energy approach," Automatica, vol. 33, no. 1, 1997, pp. 63-79.

[40] Deb K., Multi-objective Optimization Using Evolutionary Algorithm. Jhon Wiley, England, 2001.

[41] Deleroi W., Johan B. Woudstra, Azza A. Fahim, "Analysis and application of three-phase induction motor voltage controller with improved transient performance," IEEE Trans. Ind. Appl. vol. 25, no. 2, 1989, pp. 280-286.

[42] Dong Gan, Ojo O., "Efficiency optimizing control of induction motor using natural variables," IEEE Trans. Ind. Elect. vol. 53, no. 6, 2006, pp.1791-1798.

[43] Dubey G. K. Fundamentals of electric drives. Alpha Science International Limited, Second Edition, 2001.

[44] Dubey G. K. Power Semiconductor Controlled Drives. Prentice Hall, New Jesey, 1989.

[45] Eberhart R.C., Shi Y., Kennedy J., Swarm Intelligence. Academic Press, USA, 2001.

[46] Eberhart R. C., Shi Y., "Comparing inertia weights and constriction factors in particle swarm optimization", *IEEE* conference proceedings, 2000. pp 84-88.

[47] Eguilaz J. M., et al., "Induction motor optimum flux search algorithms with transient state loss minimization using fuzzy logic based supervisor," in proc. IEEE Conf. 1997, pp. 1302-1308 (DOI: 0-7803-3840-5/97).

[48] El-Laben O.S., "Particle Swarm Optimized direct torque control of Induction Motor," in Proc. IEEE Conf. IECON 2006, pp. 1586-1591.

[49] Emadi A., Energy Efficient Electric Motors. Marcel Dekker Inc, New York, 2005.

[50] Engelbrecht A.P., Computational Intelligence: An Introduction. Jhon Wiley, England, 2007.

[51] Eriction C. J., "Motor Design Features for Adjustable-Frequency Drives," IEEE Trans. Ind. Appl. vol. 24, no. 2, 1988, pp.192-198.

[52] Faiz J., Sharifian M.B.B., "Optimal design of three-phase Induction Motors and their comparison with a typical industrial motor," Computers and Electrical Engineering, vol. 27, no. 2, 2001, pp. 133-144.

[53] Faiz Jawad, Ebrahimpour H., Pillay P., "Influence of unbalanced voltage on the steady-state performance of a three-phase squirrel-cage induction motor," IEEE Trans. on Energy Conversion, vol. 19, no. 4, 2004, pp. 657-662.

[54] Faiz Jawad, Ehrahimpour H., Pillay P., "Influence of unbalanced voltage supply on efficiency of three phase squirrel cage induction motor and economic analysis," Energy Conversion and Management, vol. 47, 2006, pp.289-302.

[55] Faiz Jawad, Ghaneei M., Heyhani A., Proca A. B., "Optimal design of induction motor for electric vehicle," Electric Machines and Power Systems, vol. 28, 2000, pp. 1177–1194.

[56] Faiz Jawad, Sharifian M. B. B., "Optimum design of a three phase squirrel-cage induction motor based on efficiency maximization," International Journal of Computers and Electrical Engineering, vol. 21, no. 5, 1995, pp. 367-373.

[57] Famouri P., Cathey J. J., "Loss minimization control of an induction motor drive," IEEE Trans. Ind. Appl. vol. 27, No.1, 1991, pp. 32-37.

[58] Fei R., Fuchs E. F., Haung H., "Comparison of two optimization techniques as applied to three-phase induction motor design," IEEE Trans. Energy Conv., vol. 4, no. 4, 1989 pp. 651-660.

[59]   Galler D., "Energy efficient control of ac induction motor driven vehicles," in Proc. IEEE - IAS Annual Meeting, 1980, pp. 301-308.

[60]   Garcia G.O., "An efficient controller for an adjustable speed induction motor drive," IEEE Trans. Ind. Elect. vol. 41, no. 5, 1994, pp. 533-539.

[61]   Geng Y., Geng Hua, Wang Huangang, Guo Pengyi, "A novel control strategy of induction motors for the optimization of both efficiency and torque response," in Proc. Annual IEEE Conf. Ind. Electron. Society, 2004, pp. 1405-1410.

[62]   Ghijselen J. A. L., Van den Bossche A. P. M., "Exact voltage unbalance assessment without phase measurements," *IEEE Trans. Power Systems*, Vol. 20, No. 1, pp. 519-520, Feb. 2005.

[63]   Ghozzi S., Jelassi K., Roboam X., "Energy optimization of induction motor drives," in Proc. IEEE Conf. Industrial Technology (ICIT), 2004, pp. 602-610.

[64]   Gnacinski P., "Energy saving work of frequency controlled induction cage machine," Energy Conversion and Management, vol. 48, 2007, pp. 919-926.

[65]   Goldberg P.E., Genetic Algorithm in Search Optimization and Machine Learning. New-York, Addison-Wiley, 1989.

[66]   Hamid R. H. A., Amin A. M. A., Ahmed R. S., El-Gammal A., "New technique for maximum efficiency of induction motors based on PSO," in Proc. IEEE ISIE- 2006, pp. 2176-2181.

[67]   Hamid R. H. A., Amin A. M. A., Ahmed R. S., El-Gammal A., "Optimal operation of induction motors using artificial neural network based PSO," in Proc. IEEE conf. Industrial Tech., ICIT- 2006, pp. 2408-2413.

[68]   Han G. J, Shapiro S. S., Statiscal odels in engineering. Jhon Wiley and Sons, 1967.

[69]   Himmelblau D.M, Applied Non-Linear Programming. Mc.Graw Hill, 1972

[70]   http://faculty.ksu.edu.sa/Rizk_Hamouda/Induction%20Motor/inceasing%20eff%20AC%20MOTORS.pdf

[71]   Huijuan liu. Yihuang zhang, Qionglin zheng, Dong wang and Sizhou guo, "Design and Simulation of An Inverter-fed Induction motor for Electric Vehicles," in Proc. IEEE Vehicle Power and Propulsion Conference, 2007, pp.112-115.

[72]   Idir K., Liuchen Chang, Hepping Dai, "A new global optimization approach for induction motor design," in Proc. IEEE Canadian Conf. Electrical and Computer Engineering, 1997, pp. 870-873.

[73]   IEEE Power Engineering Society, IEEE Standard Test Procedure for Poly phase Induction Motors and Generators, IEEE Std: 112-2004, November 4, 2004.

[74]   India Core, "Overview of power sector in India," CD ROM, 2005.

[75] Jazdzynski W., "Multicriterial optimization of squirrel-cage induction motor design," IEE Proc., Elec. Power Appl., vol. 136 - Part B, no.6, 1989.

[76] Jian T. W., Schmitz N. L., and Novotny D. W., "Characteristic induction motor slip valuesfor variable voltage part load performance optimization," IEEE Trans. Ind. Appl., vol. PAS-102, no. 1, 1984, pp. 38-46.

[77] Jiyin Liu, "The impact of neighbourhood size on the process of simulated annealing: computational experiments on the flowshop scheduling problem," Computers & Industrial Engineering, vol. 37, 1999, pp. 285-288.

[78] Kennedy, J., "The Particle Swarm: Social Adaptation of Knowledge," in Proc. IEEE International Conference on Evolutionary Computation (Indianapolis, Indiana), IEEE Service Center, Piscataway, NJ, 1997, pg.303-308.

[79] Kennedy, J., Eberhart, R., "Particle Swarm Optimization", in Proc. IEEE Int. Conf. on neural networks (Perth, Australia), IEEE Service Center, Piscataway, NJ. 1995, pp. 1942-1948.

[80] Kim D. H., "GA-PSO based vector control of indirect three phase induction motor," Applied Soft Computing, vol. 7, no. 2, 2007, pp. 601-611.

[81] Kim G. S., In-Joong Ha, Myoung-Sam KO, "Control of induction motors for both high dynamic performance and high power efficiency," IEEE Trans. Ind. Electron., vol. 39, 1992, pp. 323-333.

[82] Kim J. H., Kim K. C., Chong E. K. P., "Fuzzy Pre-Compensated PID Controllers', IEEE Trans. Control System, Vol. 2, No. 4, 1994, pp. 406, 411.

[83] Kim J. W., Byung-Taek Kim, Byung II Kwon., "Optimal stator slot design of inverter-fed induction motor in consideration of harmonic losses," IEEE Trans. Magnetics, vol. 41, no.5, 2005, pp.2012-2015.

[84] Kim M. K., C.G. Lee, H.K. Iung, "Multi-objective optimal design of three-phase induction motor using improved evolution strategy," IEEE Trans. Magnetics, vol. 34, no.5, 1998, pp. 2980-2983.

[85] Kioskesidis I., Margaris N., "Loss minimization in induction motor adjustable speed drives," IEEE Trans. Ind. Elect., vol. 43, no.1, 1996, pp. 226-231.

[86] Kioskesidis I., Margaris N., "Loss minimization in scalar controlled induction motor drives with search controller," IEEE Trans. Power Electronics, vol. 11, no. 2, 1996, pp. 213-220.

[87] Kirkpatrick, S., Gellat C.D., Vecchi M.P., "Optimization by simulated annealing," Science Journal, vol. 220, 1983, pp. 671-680.

[88] Kirschen D. S., "Optimal efficiency control of induction machines," Ph.D dissertation, University of Wisconsin, 1985.

[89]   Kirschen D. S., Novotny D. W., Lipo T. A., "On-line efficiency optimization of a variable frequency induction motor drive," IEEE Trans. Ind. Appl. vol. 1A-21, no. 4, 1985, pp. 610-616.

[90]   Kirschen D. S., Novotny D. W., Suwanwisoot W., "Minimizing induction motor losses by excitation control in variable frequency drives," IEEE Trans. Ind. Appl. vol. 1A-20, no. 5, 1984, pp. 1244-1250.

[91]   Kirschen, N., Novotny W., Lipo T. A., "Optimal efficiency control of an induction motor drive," IEEE Trans. Energy Conv. vol. EC-2, no.1, 1983, pp. 561-570.

[92]   Krishnan R. Electric motor drives- Modeling, Analysis, and Control. Prentice Hall of India publication, 2003.

[93]   Krause P. C., Wasynczuk O., Sudhoff D. S. Analysis of Electric Machinery and Drive Systems. Second Edition, IEEE Press, Wiley Interscience, 2002.

[94]   Kusko A., Galler D., "Control means for minimization of losses in ac and dc motor drives," IEEE Trans. Ind. Appl. vol. 1A-19, no. 4, 1983, pp. 561-570.

[95]   Lee S. E, Jeong M. J., Jang B. I., Yoo C. H., Kim S. G., Park Y. S., "Fuzzy Pre-Compensated PI Controller for A Variable Capacity Heat Pump", Proc. IEEE Conf. Control Applications, Italy, 1998, pp. 953-957.

[96]   Li C., Rahman A., "Three-phase induction motor design optimization using the modified Hooke-Jeeves method," Electrical Machines and Power Systems, vol. 18, no. 1, 1990, pp. 1-12.

[97]   Li J., Xu L., Zhang Z., "A new efficiency optimization method on vector control of induction motor," in Proc. IEEE Conf. Electrical Machines and Drives, 2005, pp. 1995-2001.

[98]   Lim S., Nam K., "Loss minimization control scheme for induction motors," IEE proc. Electr. Power Appli., vol. 151, no. 4, 2004, pp. 385-397.

[99]   Lioyd T.C., Stone H.B., "Some aspects of poly-phase motor design-The design and properties of the magnetic circuit," IEEE Trans. Power Apparatus and systems, vol. 65, 1946, pp. 812-818.

[100]   Liu H., Abraham Ajith, Zhang W., "A Fuzzy Adaptive Turbulent Particle Swarm Optimization", International Journal of Innovative Computing and Applications, vol. 1, no. 1, 2007, pp. 39-47.

[101]   Liu H., Zhang Y., Zheng Q., Wang D., Guo S., "Design and Simulation of An Inverter-fed Induction motor for Electric Vehicles," in Proc. IEEE Vehicle Power and Propulsion Conference, 2007, pp.112-115.

[102] Liu J., "The impact of neighborhood size on the process of simulated annealing: computational experiments on the flowshop scheduling problem," *Computers & Industrial Engineering*, vol. 37, 1999, pp. 285-288.

[103] Maljkovic Z., Cettolo M., Pavlica M., "The Impact of the Induction Motor on Short-Circuit Current", *IEEE Ind. Application Magazine*, vol. 7, no. 4, 2001, pp.11-17.

[104] Marino J.C., Lipo T.A., Blasco V. B., "Simple efficiency maximize for an adjustable frequency induction motor drive," IEEE Trans. Ind. Appl. vol. 27, no. 5, 1991, pp. 940-946.

[105] Metwally H. M. B., Abdul-Kader F. E., El-Shewy H. M., El-Kholy M. M., "Proposed torque optimized behavior for digital speed control of induction motor," Energy Conversion and Management, vol. 43, 2006, pp. 1675-1685

[106] Michalewicz Zbigniew, Genetic Algorithms + Data Structures = Evolution programs. Springer Verlag, New York, 1992.

[107] Miller T. J. E., McGilp M., wearing A., "Motor design optimization using SPEED CAD software," in Proc. IEE Seminar, Practical Electromagnetic Design Synthesis, 1999, vol.2, pp. 1-5.

[108] Mohan Ned, Tore M. Underland and William P. Robbins, Power electronics converters, application, and design. John Wiley & Sons, Second edition, 1995.

[109] Moreno J., Cipolla M., Peracaula J., Da Costa Branco P.J., "Fuzzy logic based improvements in efficiency optimization of induction motor drives," in Proc. IEEE Fuzzy Systems, 1997, pp. 219-224.

[110] Muravlev O.,Muravleva O., Vekhter E., "Energetic parameters of induction Motors as the basis of energy saving in a variable speed drive," Electrical Power Quality and Utilization, vol. IX, no. 2, 2005, pp.99-106.

[111] Murphy J. M. D., Turnbull F. G., Power Electronic Control of AC Motors. Oxford Pergamon Press, 1988

[112] Murphy J. M. D., Honsinger V. B., "Efficiency optimization of inverter-fed induction motor drives," in Proc. IEEE-IAS Annual Meeting, 1982, pp. 544-552.

[113] Murthy S. S., Shridhar L., Singh Bhim, Jha C. S., Singh B. P., "Design of Energy Efficient Motor for Irrigation Pumps Operating under realistic Conditions", Proc. IEE, Electrical Power Appl., vol. 141, no. 6, Nov. 1994, pp. 269-274.

[114] Murthy S.S., Singh Bhim, Singh B.P., Jha C.S., "Experience in Design Optimization of Induction Motors using SUMT Algorithm", IEEE Trans. on Power Apparatus and Systems, vol. PAS-102, 1983, pp. 3379-3384.

[115] Nabae A., Otsuka K., Uchino H., Ryoichi K., "An approach to flux control of induction motors operated with variable frequency power supply," IEEE Trans. Ind. Appl., vol. IA-16, no. 3, 1980, pp. 342-349.

[116] Nayan R Samal, Amit Konar, Swagatam Das, Ajith Abraham, "A closed loop stability analysis and parameter selection of the Particle Swarm Optimization dynamics for faster convergence," in Proc. IEEE Congress on Evolutionary Computation, 2007, pp. 1769-1776.

[117] Nevelsteen J., Aragon H., "Starting of larger motors-methods and economics," IEEE Trans. Ind. Appl. vol. 25, no. 6, 1989, pp. 1012-1018.

[118] Novotny W. D., Nasar, S. A. High frequency losses in induction motors. NASA Contractor Report (NAG3-940), 1991.

[119] Ojo O., Bhat I., Sugita G., "Steady-state optimization of induction motor drives operating in the field weakening region," in Proc. IEEE Power electronics Specialist Conf. 1993, vol. 2, pp. 979-985.

[120] Pacific Gas and Electric Company, "*Efficiency Improvements for AC Electric Motors, application note, 1997. pp 1-14.*

[121] Padma S., Bhuvaneswari R., Subramanian S., "Application of soft computing techniques to induction motor design", Computation and Mathematics in Elec. and Electronics Engg., vol 26, no. 5, 2007, pp. 1324-1345.

[122] Palanichamy C., Nadarajan C.,.Naveen P., Babu N. S., Dhanalakshmi , "Budjet constrained energy conservation- An experience with a textile industry," IEEE Trans. Energy Conversion, Vol. 16, No. 4, 2001, pp. 340-345.

[123] Palit B. B., "Energy saving operation at induction motors by voltage reduction at no-and low partial load," in Proc. IEEE Ind. Appl. Annual Meeting, 1989, pp. 147-151.

[124] Pant M., Thangaraj R., Abraham Ajith, "A New Particle Swarm Optimization Algorithm Incorporating Reproduction Operator for Solving Global Optimization Problem", in Proc. of Hybrid Intelligent System (HIS), IEEE Computer Society Press, 2007, pp. 144-149.

[125] Pant M., Thangaraj R., Abraham Ajith, "A New PSO Algorithm with Crossover Operator for Global Optimization Problems", Advances in Soft computing Series, Springer Verlag, Germany, E. Corchado et al. (Eds.): Innovations in Hybrid Intelligent Systems, vol. 44, 2008, pp. 215-222.

[126] Pant M., Thangaraj R., Singh V. P., "A New Particle Swarm Optimization with Quadratic Interpolation", Proc. of Int. Conf. on Computational Intelligence and Multimedia Applications (ICCIMA'07), India, IEEE Computer Society Press, vol. 1, 2007, pp. 55 – 60.

[127] Pant M., Thangaraj R., Singh V. P., "A New Particle Swarm Optimization with Quadratic Crossover", Proc. of Int. Conf. on Advanced Computing and Communications (ADCOM'07), India, IEEE Computer Society Press, 2007, pp. 81 – 86.

[128] Parag R. Upadhyay and K. R. Rajagopal, "FE Analysis and CAD of Radial-Flux Surface Mounted Permanent Magnet Brushless DC Motors", IEEE Trans. Magnetics, vol. 41, no.10, Oct. 2005, pp. 3952-3954.

[129] Park M. H., Sul S. K., "Microprocessor based optimal efficiency drive of an induction motor, " IEEE Trans. Ind. Elec. vol. IE-31, no. 1, 1984, pp. 69-73.

[130] Perron M., Huy H. L., "Full load range neural network efficiency optimization of an induction motor with vector control using discontinuous PWM," in Proc. IEEE Symposium Ind. Electronics, vol.1, 2006, pp. 166-170.

[131] Pillay P., Hofmann P., Manyage M., "Derating of induction motor operating with a combination of unbalanced voltages and over or under voltages," IEEE Trans. Energy Conversion, vol. 17, no. 4, 2002, pp. 485-491.

[132] Pillay P., Manyage M., "Loss of life in induction machines operating with unbalanced supplies," IEEE Trans. Energy Conversion, vol. 21, no. 4, 2006, pp. 813-822.

[133] Poirer Eric, Ghribi Mohsen and Kaddouri A., "Loss minimization control of induction motor drives based on genetic algorithm," in Proc. IEEE Conf. Electrical machines and Drives, IEMDC-2001, pp. 475-478.

[134] Pottebaum J. R., "Optimal characteristics of a variable frequency centrifugal pump motor drive," IEEE Trans. Ind. Appl. vol. IA-20, no. 1, 1984, pp. 23-31.

[135] Price K.V., Storm R.M., Lampinen J.A., Differential Evolution: A Practical Approach to Global Optimization," Springer Verlag, New York, 2005.

[136] Pryymak B., Moreno-Eguilaz, J.M., Peracaula J., "Neural network flux optimization using a model of losses in induction motor drives," Mathematics and Computers in Simulation, vol. 71, no. 4, 2006, pp. 290-298.

[137] Pyrhonen J., Jokinen T., Hrabovcova V. Design of rotating electrical machines. John Wiley and Sons, Ltd., 2008.

[138] Ramarathnam R., Desai B. G., "Optimization of polyphase induction motor design: a nonlinear programming aproach", IEEE Trans. Power Apparatus and Systems, vol. PAS-90, no. 2, Mar./Apr. 1971, pp. 570-578.

[139] Rezek A. J. J, Coelho C. A. D., Cortez J. A., Vicente J. M. E., "Energy conservation with use of soft starter," In Proc. IEEE Int. Conf. Harmonics and Quality of Power, 2000, pp. 354-359. DOI: 0- 7833-6499-6/00.

[140] Rosenbrock H. H., An automatic method of finding the greatest or least value of function," Computer Journal, vol. 3, 1960, pp. 175-184.

[141] Rowan T. M., Lipo T. A., "A quantitative analysis of induction motor performance improvement by SCR voltage control," IEEE Trans. Ind. Appl. vol. 1A-19, no. 4, 1983, pp. 545-553.

[142] Say, M.G., The Performance and Design of Alternating Current Machines. CBS Publishers and Distributors, 3rd Edition, New York, NY, 1983.

[143] Sawhney A. K. A course in electric machine design. Danpat Rai and Co., 1998.

[144] Schittkowski K., "NLPQL: A Fortran subprogram solving constrained nonlinear programming problems," Annals of Operation Research, vol. 5, 1985, pp. 485-500.

[145] Seleme S. I., Mendes E., Canudas de wit C., Razek A., "Experimental validation of the minimum energy approach for induction motor control," in Proc. IEEE Conf. Systems, Man and Cybernetics, vol. 5, 1993, pp. 78-83.

[146] Sen S., Yeh S. N., "Optimal efficiency analysis of induction motors fed by variable-voltage and variable-frequency source," IEEE. Trans. Energy Conv., vol. 7, no. 3, 1992, pp.537-543.

[147] Sen P. K., Landa H. A., "Derating of induction motor due to waveform distortion," IEEE Trans. Ind. Appl., vol. 26, no. 6, 1990, pp. 1102-1107.

[148] Shi Y., Eberhart R.C., "A Modified Particle Swarm Optimizer", In. Proc. IEEE Congress on Evolutionary Computation, 1998, pp. 69-73.

[149] Siddique Arfat, Yadava G.S., Singh Bhim, "Effects of voltage unbalance on induction motors," in Proc. IEEE Int. Symp. Electrical Insulation, 2004, pp. 26-29.

[150] Singh B him, Ghatak Choudhuri, "Fuzzy Logic Based Speed Controllers for Vector Controlled Induction Motor Drive," IETE Journal of Research, 2002, vol.48, no.6, pp.441-447.

[151] Singh Bhim, Singh B. N., "Experience in the design optimization of a voltage source inverter fed squirrel cage induction motor", Electric Power Systems Research, vol. 26, 1993, pp. 155-161.

[152] Singh C., Sarkar D., "Practical considerations in the optimization of induction motor design," IEE Proc-B, vol. 139, no.4, 1992.

[153] Singh G. K., "A research survey of induction motor operation with non-sinusoidal supply waveforms," Electric Power System Research, vol. 75, no. 2-3, pp. 200-213.

[154] Sousa G. C. D., Bose B. K., Cleland J. G., "Fuzzy logic based on-line efficiency optimization control of an indirect vector controlled induction motor drive," IEEE Trans. Ind. Elec. vol. 42, no. 2, 1995, pp.192-198.

[155] Spiegel R. J., Turner M. W., McCormick V. E., "Fuzzy-logic-based controllers for efficiency optimization of inverter-fed induction motor drives," Fuzzy Sets and Systems, vol. 137, no. 3, 2003, pp. 387-401.

[156] Srinivasan D., Hoole S.R.H., "Fuzzy multiobject optimisation for the starting design of a magnetic circuit," IEEE Trans. on Magnetics, vol. 32, no. 3, 1996, pp. 1230-1233.

[157] Sujitjorn S., Areerak K. L., "Numerical approach to loss minimization in an induction motor," Applied Energy, vol. 79, no. 1, 2004, pp. 87-96.

[158] Sul S. K., Park M. H., "A novel technique for optimal efficiency control of a current-source inverter-fed induction motor," IEEE Trans. Power. Elect. vol. 3, no. 2, 1988, pp. 192-199.

[159] Sundareswaran K, Palani S., "Artificial neural network based voltage controller for energy efficient induction motor drives," in Proc. IEEE Conf. Global Connectivity in Energy, Computer, Communication and Control, 1998, pp 410-413.

[160] Sundareswaran K., and Palani S., "Optimal Efficiency Control Of Induction Motor Drive Using Neural Networks", AMSE Journal on Advances in Modeling and Analysis, vol. 41, no.1,2, pp.9-21, 1999.

[161] Sundareswaran K., Palani S., "Fuzzy logic approach for energy efficient voltage controlled induction motor drive," in Proc. IEEE Power Electronics and Drives PEDS-1999, pp. 552-554.

[162] Syed A. Nasar, Handbook of Electrical Machines. McGraw-Hill Book Company, New Delhi, 1987.

[163] Thanga Raj C. Power Electronics based Electrical Energy Conservation in Industries. *M. Tech. Dissertation*, Anna University, Chennai, 2005.

[164] Toliyat H. A., Kliman G. B (Editors). Handbook of Electric Motors. CRC Press, Second Edition, 2004.

[165] Tsouvalas N., Xydis I., Tsakirakis I., Papazacharopoulos Z., "Asynchronous motor drive loss optimization," Material Processing and Technology, vol. 181, no. 1-3, 2007, pp. 301-306.

[166] Ta C. M., Hori Y., "Convergence improvement of efficiency-optimization control of induction motor drives," IEEE Trans. Ind. Appl., vol. 37, no. 6, 2001, pp. 1746-1753.

[167] Udaigiri M. R., Lipo T. A., "Simulation of inverter ed induction motors including core losses," in Proc. IEEE Ind. Electr. Conf., 1989, pp. 232-237.

[168] Upadhyay P. R., Rajagopal K. R., "FE Analysis and CAD of Sandwiched Axial-Flux Permanent Magnet Brushless DC Motor", IEEE Transactions on Magnetics, vol. 42, no. 10, 2006, pp. 3401-3403

[169] Upadhyay P. R., Rajagopal K. R., "A novel Integral-force technique for the analysis of an axial-field permanent-magnet brushless DC motor using FE method," IEEE Trans. Magnetics, vol. 41, no. 10, 2005, pp. 3958–3960.

[170] Upadhyay P. R., Rajagopal K. R., "Genetic Algorithm Based Design Optimization of a Permanent Magnet Brushless DC Motor", Journal of Applied Physics, vol. 97, 2005, pp. 10Q516.

[171] Vaez-Zadeh S., Hendi F., "A continuous efficiency optimization controller for induction motor drives," Energy Conversion and Management, vol. 46, no. 5, 2005, pp. 701-713.

[172] Valdenebro L.R., Bim E., "A Genetic algorithm approach for adaptive field oriented control of induction motor drives," in Proc. IEEE Conf. Electrical machines and drives, IEMD, WA, USA, 1999, pp. 643-645.

[173] Vamvakari, A. Kandianis, A. Kladas, S. Manias and J. Tegopoulos, "Analysis of Supply Voltage Distortion Effects on Induction Motor Operation, Proc. IEEE, 360-362. 1999. DOI- 0-7803-5293-9/9.

[174] Vas P., Sensorless Vector and Direct Torque Control. Oxford University Press, New York, 1998.

[175] Vas P., Vector Control of AC Machines. Oxford University press, 1990.

[176] Vickers H., "The induction motor," Second Edition, Pitman Publishing Corporation, New York.

[177] Vulosavic S. N., Levi E., "A method for transient torque response improvement in optimum efficiency induction motor drives," IEEE Trans. Energy Conv., vol. 18, no. 4, 2003, pp. 484-493.

[178] Vukosavic S. N., Levi E., "Robust DSP-Based efficiency optimization of a variable speed induction motor drive," IEEE Trans. Ind. Elect., vol. 50, no. 3, 2003, pp. 560-570.

[179] Wallace A.K., Van Jouanne A.R., Wiedenbrug E.J., Andrews P.S., "The measured effects of under-voltage , over-voltage and unbalanced voltage on the efficiency and power factor of induction motors over wide ranges of load," in Proc. IEE Conf., EMD 97, pp. 258-262.

[180] Wang Fang, Qiu Yuhui, "A modified particle swarm optimizer with Roulette selection operator," in Proc. IEEE Conf. Natural Language Processing and Knowledge Engineering, NLP-KE-2005, pp. 765-768.

[181] Wieczorek J. P., Gol O., Michaewicz Z., "An evolutionary algorithm for the optimal design of induction motors," IEEE Trans. Magnetics, vol. 36, no. 6, 1998, pp. 3882 – 3887.

[182] Xu D., Zhu D., Wu Bin, "High performance induction motor drive with optimized excitation current control," in Proc. IEEE IAS Annual Meeting, 2001, pp. 1673-1678.

[183] Yoon M. K., Jeon C. S., Kauh S. K., "Efficiency increase of an induction motor by improving cooling performance," IEEE Trans. Energy Conversion, vol. 17, no. 1, 2002, pp. 1-6.

[184] Zenginobuz G., Cadirci I., Ermis M., Barlak C., "Performance optimization of induction motors during voltage –controlled soft starting," IEEE Trans. Energy Conv., vol. 19, no. 2, 2004, pp. 278-288.

Appendix-A: Optimal Design

Test Motors, Assigned Parameters and Design Expressions

A.1 Specification of Test Motors

Sample motor 1

Capacity	7.5 kW
Voltage per phase	400 volts
Frequency	50 Hz
Number of poles	4
Number of stator slots	36
Number of rotor slots	44

Sample motor 2

Capacity	110 kW
Voltage per phase	3300 volts
Frequency	50 Hz
Number of poles	6
Number of stator slots	90
Number of rotor slots	93

Sample motor 3

Capacity	2.2 kW
Voltage per phase	400 volts
Frequency	50 Hz
Number of poles	4
Number of stator slots	36
Number of rotor slots	44

A.2 Assigned Parameters

Table A.1 Assigned Values of Parameters used in Motor Design

Parameter	Assigned values		
	Test motor 1	Test motor 2	Test motor 3
Winding factor	0.96	0.96	0.96
Stator slot opening, mm	3.0	3.0	3.0
Rotor slot opening, mm	2.0	2.0	2.0
Stator slot wedge height, mm	3.0	3.0	3.0
Rotor slot wedge height, mm	2.0	2.0	2.0
Stator slot fullness factor	0.35	0.3	0.35
Rotor slot fullness factor	1.0	1.0	1.0
Radial air gap length, mm	0.5	1.0	0.5
Cooling coefficient	0.03	0.03	0.03

A.3 Lower and Upper Bounds of Variables and Constraints

Table A.2 Lower and Upper Bounds of Variables and Constraints

Variables (implicit) or Constraints (explicit)	Lower	Upper
ampere conductors/m	15000	25000
ratio of stack length to pole pitch	0.9	2.0
stator slot depth to width ratio	3.0	5.5
stator core depth (mm)	2.0	5.0
average air gap flux densities (wb/m^2)	0.4	0.8
stator winding current densities (A/mm^2)	4.0	15.0
Rotor winding current densities (A/mm^2)	4.0	15.0
maximum stator tooth flux density,wb/m^2	0.5	2.0
stator temperature rise, °C	20.0	70.0
full load efficiency, %	80.0	100.0
no load current, pu	0.02	0.5
starting torque, pu	1.5	10.0
maximum torque, pu	2.2	10.0
slip, pu	0.01	0.05
full load power factor	0.8	1.0
rotor temperature rise, °C	10.0	70.0

A.4   Design Expressions

There are two basic expressions needed for deriving the design formulae of induction or any electric motors. They are: E.M.F and output equations. The derivations in present work of optimal design pertain to polyphase induction motors in terms of the variables chosen [15], [142].

The E.M.F equation for a motor is given by

$$E_{ph} = 4.44 K_w f\phi \; T_{ph}$$

(A.1)

The output equation for a three-phase induction motor is written as

$$S = 3E_{ph}I_{ph} *10^{-3} \; \text{KVA}$$

(A.2)

The term specific electric loading is defined as the number of r.m.s ampere conductors per unit length of gap surface circumference. The present work considers ampere conductors per meter as a variable (x_1) and can be expressed as

$$x_1 = \frac{6T_{ph}I_{ph}}{\pi D}$$

(A.3)

The term specific magnetic loading is the average magnetic flux density over the whole surface of the air-gap and can be expressed as follows. It is also considered as a variable in the present work.

$$x_5 = \frac{\phi p}{\pi D L}$$

(A.4)

Use of expressions (A1) – (A4), the volume of the motor is

$$D^2 L = \frac{1000 S P}{2.22 K_w \pi^2 f x_1 x_5} \qquad \text{m}^3$$

(A.5)

The separation of main dimensions D and L can be done from the expression (A.5) by approximately choosing the ratio of core length to pole pitch, which in the present case is considered as a variable. Thus,

$$D = \frac{1}{\pi} \sqrt[3]{\frac{1000 S P^2}{2.22 K_w f x_1 x_2 x_5}}$$

(A.6)

and
$$L = x_2 \frac{\pi D}{p} = x_2 Y$$

(A.7)

The calculation of net length of the core which considers the stacking factor for sheets as well as the allowance for the ventilating ducts is given by

$$L_i = K_i(L - 0.001 n_d w_d) \qquad \text{(A.8)}$$

Total number of conductors per slot can be derived from the equations (A.1) – (A.4) which is always an integer and is to be rounded off)

$$Z_{1s} = \frac{6E_{ph}}{4.44 f K_w S_1 Y^2 x_2 x_5} \qquad \text{(A.9)}$$

The area of stator slot can be calculated with the assigned slot fullness factor as

$$a_{ss} = \frac{1000S}{2.22 K_w f Y^2 S_f x_2 x_5 x_6} \qquad \text{(A.10)}$$

the stator slot depth to width ratio facilitates the separation of slot area into depth and width. Hence the depth of slot can be expressed as

$$d_{ss} = \sqrt{\frac{1000 S x_3}{2.22 K_w f Y^2 S_1 S_f x_2 x_5 x_6}} \qquad \text{(A.11)}$$

Stator core outside diameter can be expressed as

$$OD = D + 0.002 D_{ss} + 0.002 x_4 \qquad \text{(A.12)}$$

Using the equations (A.2), (A.3), (A.7), the rotor bar current and area can be expressed with the assumption that the rotor ampere turns at full load are 85% of stator ampere turns at full load as

$$I_b = \frac{850S}{2.22 K_w f Y^2 S_2 x_2 x_5} \qquad \text{(A.13)}$$

and $$\qquad a_b = \frac{382.88S}{K_w f Y^2 S_2 x_2 x_5 x_7} \qquad \text{(A.14)}$$

Cage induction motors normally use the rotors with skewed slots (normally by one slot pitch) and give better performance. The length of the bar is slightly more than the core length , ususlly by 0.03m. The rotor slot area with the assigned value of rotor slot fullness factor can be calculated as

$$a_{sr} = \frac{a_b}{S_{fr}}$$
(A.15)

for cast iron $S_{fr} = 1$

The depth and width of the rotor slots can be expressed in terms of stator slot depth

$$d_{sr} = \frac{a_{sr}S_2 x_3}{S_1 d_{ss}}$$
(A.16)

$$W_{sr} = \frac{S_1 d_{ss}}{S_2 x_3}$$
(A.17)

The mean end ring diameter can be expressed as

$$D_e = D - 0.002 I_g - 0.002 d_{sr}$$
(A.18)

The rotor end ring current in terms of rotor bar current is given by

$$I_e = \frac{S_2 I_b}{\pi p}$$
(A.19)

End ring cross section (in mm²) can be calculated as

$$a_e = \frac{I_e}{x_7} = \frac{S_2 a_b}{\pi p}$$
(A.20)

With the assumption of same core flux density on stator and rotor side the depth of stator and rotor core behind the slot will remain same, the rotor inner diameter can be expressed as

$$ID = D - 0.002 I_g - 0.002 d_{sr} - 0.002 x_4$$
(A.21)

A.4.1 Expressions for Cost of Active Material

The cost of active materials consists of the cost of laminations and winding materials on stator and rotor. Hence, the first step is to calculate separately the weight of stator teeth, stator core and iron and are expressed (in kg) as

$$W_t = \frac{\delta_i S_1 d_{ss} t_s L_i}{10^6}$$
(A.22)

$$W_c = \frac{\delta_i \pi (OD - 0.001 x_4)) x_4 L_i}{10^3}$$
(A.23)

$$W_r = \delta_i L_i \left[\frac{(D^2 - ID^2)}{4} - \frac{(S^2 a_{sr})}{10^6} \right] \qquad (A.24)$$

where t_s = mean stator tooth width in mm which is expressed as

$$t_s = \frac{\pi(D + 0.001 d_{ss})}{S_1} - \frac{0.001 d_{ss}}{x_3} \qquad (A.25)$$

With the help of iron cost per kg, Total cost of iron in stator and rotor laminations can be calculated as

$$TC_i = C_i (W_t + W_c + W_r) \qquad (A.26)$$

There are two types of windings in motor: stator and rotor windings and hence there is a need to calculate individual costs. They are expressed as

$$W_{sw} = \frac{S \delta_c (x_2 + 1.15 + 0.12) 10^6}{2.22 f K_w Y x_2 x_5 x_6} \qquad (A.27)$$

$$W_{rw} = \frac{S_2 a_b L_r^{\,6}}{10^6} + \frac{2 \pi a_e D_e}{10^6} \delta_r \qquad (A.28)$$

where,

$$a_b = \frac{382.88 S}{K_w f S_2 Y^2 x_2 x_5 x_7} \qquad (A.29)$$

Now the cost of winding materials can be calculated as

$$TC_c = C_c (W_{sw} + W_{rw}) \qquad (A.30)$$

From the Eqn. (A.26) and (A.30), total cost of active materials is given by

$$TC = TC_i + TC_c \qquad (A.31)$$

A.4.2 Equivalent Circuit Parameters

Motor's performance related items such as efficiency, power factor, current and speed at different load torque can be calculated from the equivalent circuit. The parameters involved in the equivalent circuit are derived in terms of variables [142], [9], [15], which are:

A.4.2.1 Stator and rotor resistance:

The resistance of the stator winding can be calculated with the known value of specific resistivity of the winding materials by

$$R_s = \frac{\rho_c E_{ph} x_6}{2.22 K_w f I_{ph} Y x_5} + (1 + \frac{1.15}{x_2} + \frac{0.12}{x_2 Y}) \tag{A.32}$$

Total resistance (sum of the bar and end-ring resistance) in cage induction motor with reference to stator side can be expressed as

$$R_r' = \frac{12 \rho_r T_{ph}^2}{S_2 a_b}(L_r + \frac{2D_e}{p}) \tag{A.33}$$

The RMS magnetizing current in terms of excitation ampere turns for B_{30} is given by [142], [15]. The detailed expression for ampere turn (AT) is avillable in [15].

$$I_m = \frac{p}{1.17 K_w T_{ph}} AT \tag{A.34}$$

Magnetizing inductance is given by

$$X_m = \frac{E_{ph}}{I_m} = \frac{E_{ph} * 1.17 K_w T_{ph}}{pAT} \tag{A.35}$$

The resistance of no-load component (R_m) can be calculated through total iron losses. The iron loss/kg for the teeth and core are calculated corresponding to maximum tooth flux density and core flux density.

The expression for maximum tooth flux density is given by

$$B_{t(max)} = \frac{1.57 \pi DL x_5 * 10^5}{S_1 t_{13} L_i} \tag{A.36}$$

Where, $t_{13} = \dfrac{\pi(1000D + 2^{d_{ss}}\!/\!3)}{S_1} - \dfrac{d_{ss}}{x_3} \tag{A.37}$

If the loss per kg corresponding to tooth portion and core is taken as W_{tk} and W_{ck} espectively, then the total iron loss can be expressed as

$$SIL = W_t * W_{tk} + W_c * W_{ck} \tag{A.38}$$

The equivalent magnetizing resistance is given by

$$R_m = \frac{3 E_{ph}^2}{SIL} \tag{A.39}$$

The core loss component of no-load current is calculated in terms of friction, windage and iron losses and is given in Eq. (A.40). These losses are proportional to the peripheral speed, length and diameter of the motor [176], [15]. The present work assumes friction and windage losses as one percent of the output.

$$I_c = \frac{W_F + SIL}{3E_{ph}} \tag{A.40}$$

Usings the equations (A.34) and (A.40), total no-load current of the motor is expressed as

$$I_o = \sqrt{I_m^2 + I_c^2} \tag{A.41}$$

A.4.2.2 Leakage Reactance

(i) Stator slot leakage reactance

Fig. A.1 shows a parallel sided semi-closed slot used in the present work and the empirical relations on slot are given by [99]. Semi-closed slots are normally used in the induction motors to get smaller magnetizing current in addition with less tooth pulsation loss and noise levels.
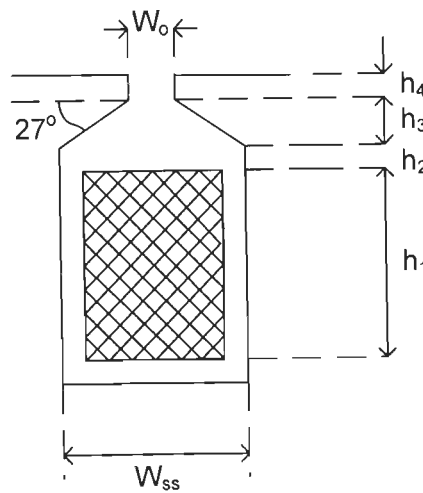

Fig. A.1 Schematic of semi-closed slot arrangement

Total area occupied by the conductors in the slot is calculated by

$$a_{sc} = S_f a_{ss} = \frac{S_f d_{ss}^2}{x_3} \tag{A.42}$$

To get maximum value of slot fullness factor the conductors in the slots must be arranged in such a way that the depth to width ratio of conductor and slot should remain same. The value of h_1 in the Fig. A.1 is

$$h_1 = \sqrt{a_{sc}x_3}$$ (A.43)

Substitute the equation (A.11) in (A.43) and gives

$$h_1 = \sqrt{\frac{1000Sx_3}{2.22fK_wS_1Y^2x_2x_5x_6}}$$ (A.44)

and $\qquad h_2 = d_{ss} - h_1 - h3 - h4$ (A.45)

stator slot permeance can be written as

$$P_{ss} = \mu_o\left(\frac{h_1}{3W_{ss}} + \frac{h_2}{W_{ss}} + \frac{2h_3}{W_o + W_{ss}} + \frac{h_4}{W_o}\right)$$ (A.46)

where, slot width, $W_{ss} = \dfrac{d_{ss}}{3}$ (A.47)

The stator slot leakage reactance can be expressed as

$$X_{ss} = 8\pi fT_{ph}^2 L\left(\frac{3P_{ss}}{S_1}\right)$$ (A.48)

(ii) Rotor Slot Leakage Reactance

Semiclosed slots give better performance in terms of starting torque and over load capacity in squirrel cage rotors also. Rotor slot permeance can be calculated from the rotor slot dimensions similar to stator slot permeance.

$$P_{rs} = \mu_o\left(\frac{h_{1r}}{3W_{sr}} + \frac{h_{2r}}{W_{sr}} + \frac{2h_{3r}}{W_o + W_{sr}} + \frac{h_{4r}}{W_o}\right)$$ (A.49)

When referred to stator side rotor slot permeance can be written as

$$P'_{rs} = P_{rs}K_w\,{S_1}\big/{S_2}$$ (A.50)

Therefore the rotor slot leakage reactance is calculated as

$$X_{rs} = 8\pi fT_{ph}^2 L\left(\frac{3P'_{sr}}{S_1}\right)$$ (A.51)

Overhang leakage reactance of the full pitch coil can be calculated by [15]

$$X_o = \frac{3.4E_{ph}^2 x_1 *10^{-9}}{K_w S x_2 x_5}$$ (A.52)

Zig-zag leakage reactance depends on relative widths of teeth, slot openings and air gap and is expressed by [15]

$$X_z = \frac{5}{6} X_m p^2 \left(\frac{1}{S_1^2} + \frac{1}{S_2^2}\right)$$ (A.53)

Referring the Eqns. (A.42) – (A.53), total phase reactance of an induction motor refered to stator side can be expressed by

$$X_1 = X_s + X_r'$$ (A.54)

where, $X_s = X_{ss} + 0.5X_o + X_z$ = stator leakage reactance

$X_r' = X_{rs} + 0.5X_o$ = rotor leakage reactance referred to stator side.

A.4.3 Expressions for Constraints and Objective Functions

(1)   Maximum stator tooth flux density

Maximum stator tooth flux density which is expressed in (A.36) and is repeated here for convenience

$$B_{t(max)} = \frac{1.57\pi DL x_5 *10^5}{S_1 t_{13} L_i}$$

(2)   Stator Temperature Rise:

For continuously rated machines, the final stator temperature rise θ_{ms} is the determining factor and with the assumption that the cooling by convection, conduction and radiation is proportional to temperature rise [15]. The temperature rise is directly proportional to the heat developed due to losses and indirectly proportional to cooling surface area.

$$\theta_{ms} = \frac{\tau_c (SCL + SIL)}{S_s}$$ (A.55)

Where, cooling coefficient $\tau_c = \dfrac{0.03 - 005}{1 + 0.1u}$; $u = \dfrac{2\pi fD}{P}$

Total effective cooling surface area $S_s = S_i(1 + 0.1u) + S_0$. S_i, S_o are the inside and outside cylindrical surface area of the motor.

3)   Full Load Efficiency:

The full load efficiency of an induction motor is written as

$$\eta = \frac{1000P_o}{1000P_o + SCL + W_{RCL} + SIL + W_F} * 100 \tag{A.56}$$

Where copper loss $SCL = 3I_{ph}^2(R_s)$

Rotor copper loss $W_{RCL} = \frac{\rho_r S_2 I_b^2}{a_b}(L_r + \frac{2D_e}{p})$

(4)   No-Load to Full Load Current Ratio

Expression for no-load current is given by equation (A.41). The ratio of no-load to full load current can be written as

$$CR = \frac{I_o}{I_{ph}} \tag{A.57}$$

(5)   Full Load Slip

Full load slip can be written as

$$s = \frac{W_{RCL}}{1000P_o + W_{RCL} + W_F} \tag{A.58}$$

Rotor copper loss W_{RCL} is given in Eqn. (A.56). The summation of friction and windage losses are assumed to be 1% of output as mentioned in (A.40).

(6)   Starting torque to full load torque ratio

The equation for starting torque of the motor is

$$T_{fl} = \frac{3E_{ph}^2 \frac{R_r'}{s}}{[R_s + C_1(\frac{R_r'}{s})]^2 + [X_s + C_1 X_r']^2} \tag{A.59}$$

At starting slip s=1, then the starting torque can be written as

$$T_{st} = \frac{3E_{ph}^2 R_r'}{[R_s + C_1 R_r']^2 + [X_s + C_1 X_r']^2} \tag{A.60}$$

Where $C_1 = 1 + \frac{R_s}{R_m} + \frac{X_s}{X_m}$

Now, starting to full load torque ratio $TRT_1 = \dfrac{T_{st}}{T_{fl}}$ (A.61)

(7)   Maximum torque to full load torque ratio

The slip for maximum torque is obtainable by differentiating Eqn. (A.59) with respect to s and equating it to zero thus yielding to

$$S_{maxT} = \frac{R_r'}{\sqrt{R_s^2 + (X_s + X_r)^2}}$$ (A.62)

Maximum torque produced in the motor can be expressed by substituting the Eqn. (A.62) in (A.59)

$$T_{max} = \frac{3E_{ph}^2}{2C_1[R_s + \sqrt{R_s^2 + (X_s + C_1 X_R')^2}]}$$ (A.63)

Now, the ratio of maximum torque to full load torque (in other words p.u maximum torque) can be expressed as

$$TRT_2 = \frac{T_{max}}{T_{fl}}$$ (A.64)

(8)   Full load power factor

Determining full load power factor of the motor requires impedances of stator, rotor and magnetizing circuits and are expressed as below [15]

$$Z_s = R_s + jX_s$$ (A.65)

$$Z_r = \frac{R_r'}{s} + jX_r'$$ (A.66)

$$Z_m = \frac{jR_m X_m}{R_m + jX_m} = \frac{R_m X_m^2 + jR_m^2 X_m}{R_m^2 + X_m^2} = G_1 + jG_2$$ (A.67)

The impedance at the parallel combination of rotor and magnetizing circuit can be expressed as

$$Z_{rm} = \frac{(\frac{R_r'}{s} + jX_r')(G_1 + jG_2)}{(\frac{R_r'}{s} + G_1) + j(X_r' + G_2)} = G_4 + jG_5$$ (A.68)

Where,
$$G_5 = \frac{(\frac{R'_r}{s}+G_1)(\frac{R'_r}{s}G_2 + X'_r G_1) - (X'_r + G_2)\frac{R'_r}{s}G_1 - (X'_r G_2)}{G_3}$$

$$G_4 = \frac{(\frac{R'_r}{s}G_1 - X'_r G_2)(\frac{R'_r}{s}+G_1) + (\frac{R'_r}{s}G_2 - X'_r G_1)(X'_r + G_2)}{G_3}$$

$$G_3 = (\frac{R'_r}{s}+G_1)^2 + (X'_r + G_2)^2$$

$$G_2 = \frac{R_m^2 X_m}{R_m^2 + X_m^2}$$

$$G_1 = \frac{R_m X_m^2}{R_m^2 + X_m^2}$$

The total series impedance of the equivalent circuit referred to stator side can then be expressed as

$$Z_1 = R_s + jX_s + G_4 + jG_5 = (R_s + G_4) + j(X_s = G_5) \tag{A.69}$$

Full load power factor is then given by

$$PF = \frac{R_s + G_4}{\sqrt{\{(R_s + G_4)^2 + (X_s + G_5)^2\}}} \tag{A.70}$$

(9)   Full load rotor temperature rise

The calculations of rotor temperature rise are based on similar considerations as that of stator temperature rise. The cooling surface is calculated from the rotor dimension. Thus the full load rotor temperature rise is calculated as

$$\theta_{mr} = \frac{\tau_c W_{RCL}}{S_r} \tag{A.71}$$

Where, S_r – total rotor cooling surface area.

A.5 Validation of Optimization algorithms with Some Benchmark Problems

Four standard benchmark problems (shown in Table A.3) namely: Rastringin, Sphere, Griewank and Rosenbrock are used to validate the performance of QIPSO and compared with

basic PSO. From the numerical results shown in Table A.4 and convergence graphs shown in Fig. A.2 and A.3, QIPSO gave better results in all the test problems and hence it was validated successfully.

Table A.3 Standard Benchmark Problems for Validating QIPSO

Benchmark Problems	Range	Mini. Value
$f_1(x) = \sum_{i=1}^{n}(x_i^2 - 10\cos(2\pi x_i) + 10)$	[-5.12,5.12]	0
$f_2(x) = \sum_{i=1}^{n} x_i^2$	[-5.12,5.12]	0
$f_3(x) = \dfrac{1}{4000}\sum_{i=0}^{n-1} x_i^2 + \sum_{i=0}^{n-1}\cos(\dfrac{x_i}{\sqrt{i+1}}) + 1$	[-500,500]	0
$f_4(x) = \sum_{i=0}^{n-1} 100(x_{i+1} - x_i^2)^2 + (x_i - 1)^2$	[-30,30]	0
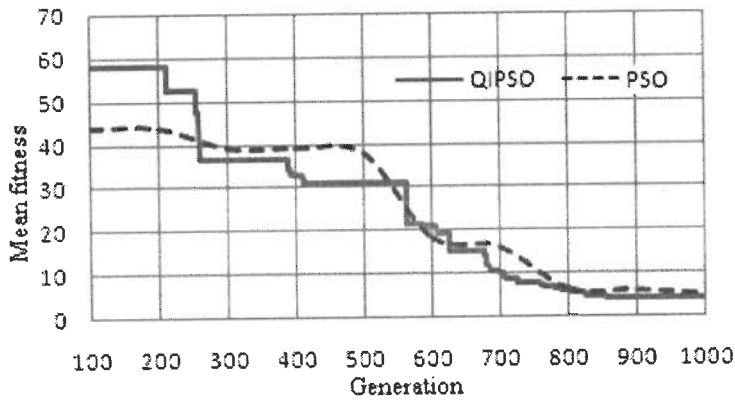
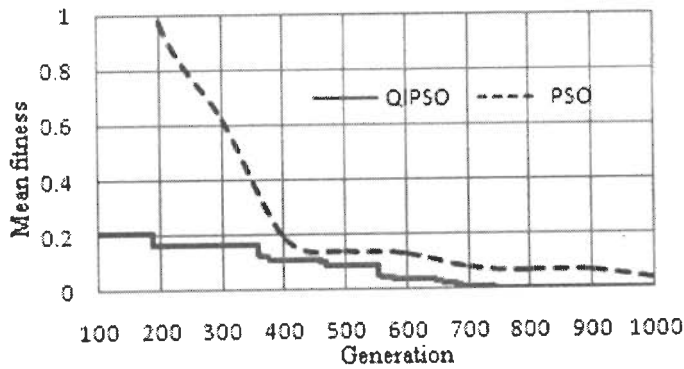Fig. A.2 Convergence graph for function f_1

Fig. A.3 Convergence graph for function f_2

Table A.4 Results of QIPSO and Its Comparison with PSO in Benchmark Problems (Mean fitness/Standard Deviation)

Function	Dim	PSO	QIPSO	No. of times QI activated in QIPSO
f_1	2	5.57913e-015 1.63684e-014	0.00000 0.00000	469
	10	4.75341 3.07381	4.01845 1.37636	85
f_2	2	3.02769e-022 5.93778e-022	5.7574e-049 1.72705e-048	898
	10	7.27335e-005 2.88549e-004	1.09812e-007 2.58381e-007	784
f_3	2	1.11077e-012 3.3323e-011	2.46617e-016 1.99805e-016	241
	10	0.0197954 0.153591	0.0024669 0.00977076	210
f_4	2	0.00115649 0.00219637	2.72628e-011 4.97405e-011	767
	10	90.1189 26.9975	8.24632 0.755432	797

Appendix-B: Optimal control

MATLAB/SIMULINK Models used for Simulation

B.1 MATLAB/SIMULINK Models for Energy Optimal Control of Induction Motor

The complete MATLAB/SIMULINK model of energy optimal control is shown in Fig. B.1. These models mainly consist of speed controller, energy optimal controller, flux angle calculation, vector control and current controller and are integrated individually, shown in Figs B.2 – B.9.
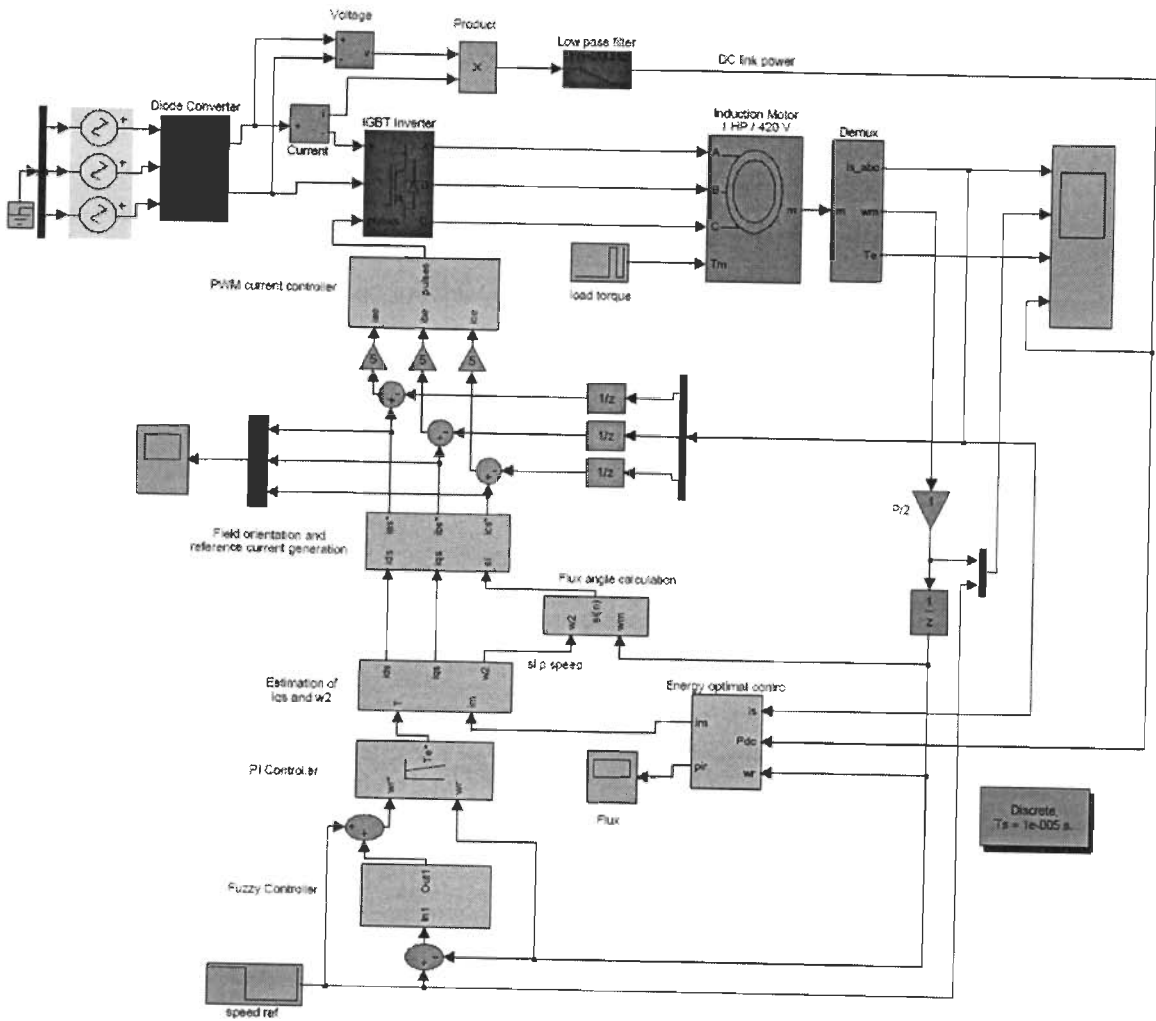

Fig. B.1 MATLAB/SIMULINK model of optimal energy control of induction motor

B.1.1   PI Speed Controller

The MATLAB/SIMULINK model diagram of the PI controller in discrete time is shown in Fig. B.2. As seen in figure, using the proportional and integral gain parameters namely, k_p and k_i respectively along with the limiter, the reference torque is calculated in accordance to the motor rating used.
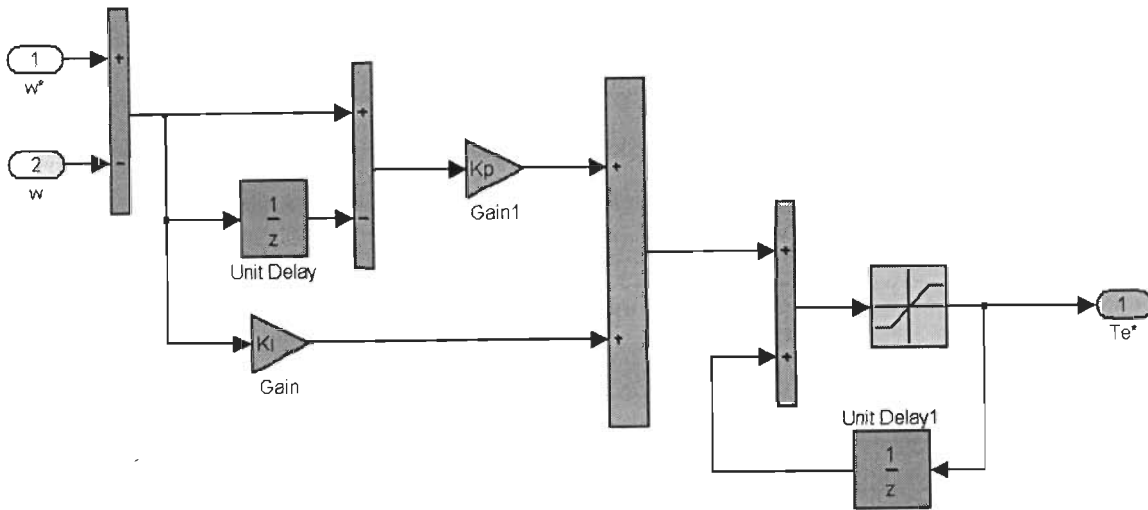

Fig. B.2 MATLAB model for Proportional Integral (PI) Controller

B.1.2   FPPI Speed Controller

Fig. B.3 shows the MATLAB model of the Fuzzy Pre-compensated PI controller. As shown in figure the FL controller produces the modified reference speed signal by which the speed error is calculated and is fed as a reference signal for the PI controller.
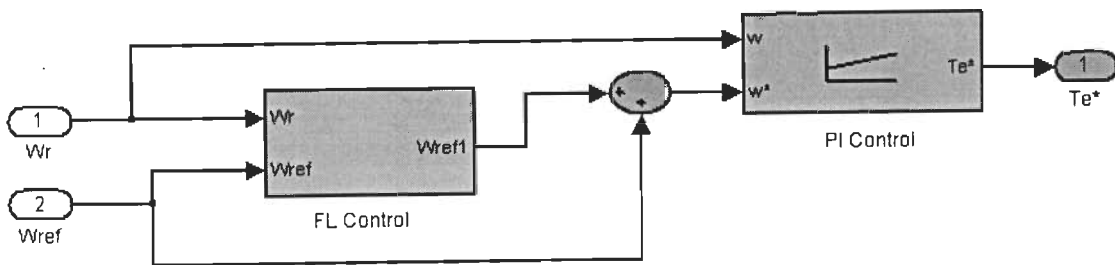

Fig. B.3 MATLAB model for Fuzzy Pre-compensated Proportional Integral (FPPI) speed controller.

B.1.3 Energy Optimal Controller

Fig. B.4 shows the MATLAB model of optimal energy controller which consists of three controllers and the output is magnetizing current i_m. Switch is used for selecting required controllers, say loss model control (LMC) or search control or their combination. In LMC, PSO program is stored in s-function to calculate optimum value of magnetizing current. In case of SC, magnetizing current is decreased from its rated value with the concentration on DC link power. Magnetizing current is then transformed into q-axis current with the help of rotor time constant and magnetizing reactance.
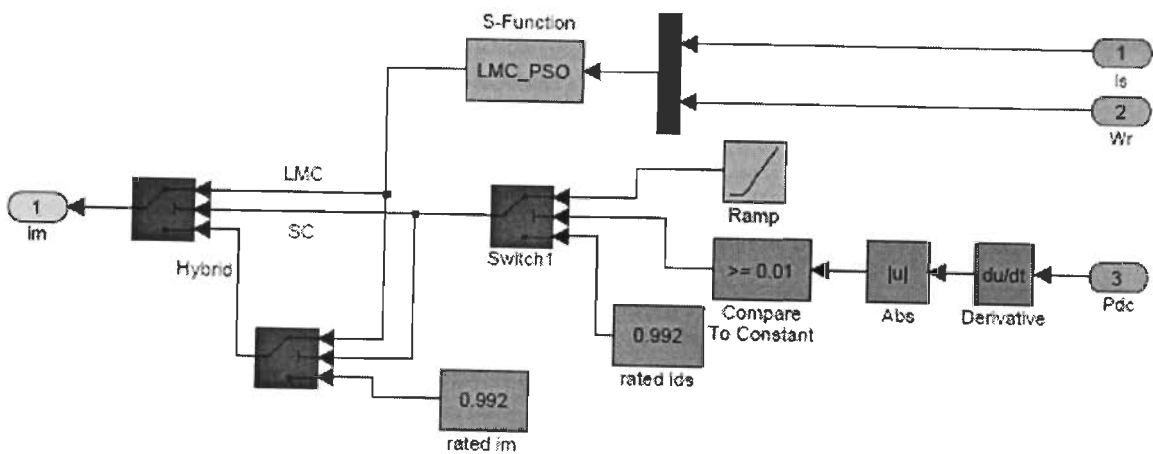

Fig. B.4 MATLAB model for energy optimal controller

B.1.4 Vector Controller [Estimator for i_{ds}*, i_{qs}* and ω_2*]

This section calculates the direct and the quadrature axis stator current components (i_{ds}* and i_{qs}*). Mathematically, the equations for calculating these two components of the current in the discretised form are stated as follows [93], [111]:

$$i_{ds}^*(n) = i_m(n) + \tau_r \frac{di_m^*}{dt} \qquad (B.1)$$

$$i_{qs}^*(n) = \frac{T^*(n)}{k\, i_m^*(n)} \qquad (B.2)$$

$$\omega_2^*(n) = \frac{i_{qs}^*(n)}{\tau_r i_{mr}^*(n)} \qquad (B.3)$$

where τ_r is the rotor time constant defined as

$$\tau_r = L_r / R_r \tag{B.4}$$

$$k = \left(\frac{3}{2}\right)\left(\frac{P}{2}\right)\left(\frac{M}{1+\sigma_r}\right) \tag{B.5}$$

P is the number of poles, $i_{ds}^*(n)$ and $i_{qs}^*(n)$ refer to flux and torque components of stator current at n^{th} instant, $\omega_2^*(n)$ refer to n^{th} instant reference slip speed of rotor, M is the mutual inductance, σ_r is the rotor leakage factor and L_r is the rotor self inductance and are defined as below

$$L_r = L_{lr} + L_m \quad \text{or} \quad L_r = (1+\sigma_r)M \tag{B.7}$$

$$\sigma_r = \frac{L_r}{R_r} = \frac{L_{lr} + L_m}{R_r} \tag{B.8}$$

R_r is the rotor resistance and L_m is the magnetizing inductance. The MATLAB model for the estimation of i_{ds}^*, i_{qs}^* and ω_2^* is shown in Fig.B.5
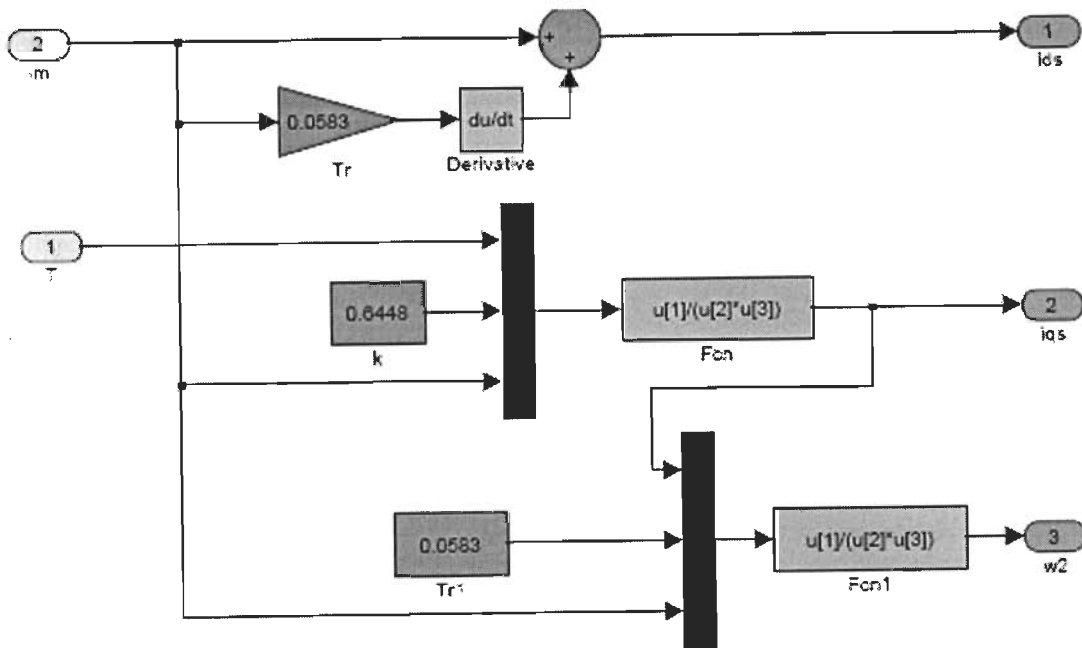

Fig. B.5 MATLAB model for the estimation of i_{ds}^*, i_{qs}^* and ω_2^*

B.1.5 Field orientation and Reference current generation

This block converts the two phase reference currents (i_{ds}^* and i_{qs}^*) in rotating frame into three phase reference currents (i_{as}^*, i_{bs}^* and i_{cs}^*) in stationary reference frame (SRF). In this section, the flux angle (ψ) at which the synchronously rotating reference frame (SRRF) is to be inclined is also calculated as given below. First the reference slip frequency of the rotor

$(\omega_2\dot{}_{(n)})$ is added to the sensed rotor speed $(\omega_{r(n)})$ and then a discrete integration is carried out to calculate the flux angle at the nth instant. The flux angle (ψ) is defined at the nth instant as:

$$\Psi_{(n)} = \Psi_{(n-1)} + (\omega_2\dot{}_{(n)} + \omega_{r(n)}) \Delta T \tag{B.9}$$

where ΔT is the sampling time

After calculating the flux angle and d-q components of the reference stator current in the SRRF, calculate the required three phase reference current $(i_{as}\dot{}, i_{bs}\dot{}$ and $i_{as}\dot{})$ in the stationary reference frame. The required transformation from d-q components to abc components is given as below:

Two-Phase rotating to three phase stationary reference frame converter can be modeled as follows:

$$i_{as}\dot{} = -i_{qs}\dot{} \; Sin \; \psi + i_{ds}\dot{} \; Cos \; \psi \tag{B.10}$$

$$i_{bs}\dot{} = [(-Cos \; \psi + \sqrt{3} \; Sin \; \psi) \; i_{ds}\dot{}(\frac{1}{2})] + [(Sin \; \psi + \sqrt{3} \; Cos \; \psi) \; i_{qs}\dot{}(\frac{1}{2})] \tag{B.11}$$

$$i_{cs}\dot{} = -(i_{as}\dot{} + i_{bs}\dot{}) \tag{B.12}$$

where $i_{ds}\dot{}$ and $i_{qs}\dot{}$ refer to decoupled components of the stator circuit $i_s\dot{}$ in two-phase system with respect to rotor reference frame and $i_{as}\dot{}$, $i_{bs}\dot{}$ and $i_{cs}\dot{}$ are three phase currents in stator reference frame.

Fig. B.6 shows the calculation of flux angle in the discrete frame in which the sampling time is taken as $10e^{-6}$ sec. Similarly the MATLAB model for calculating the three phase reference currents is shown in Fig. B.7.
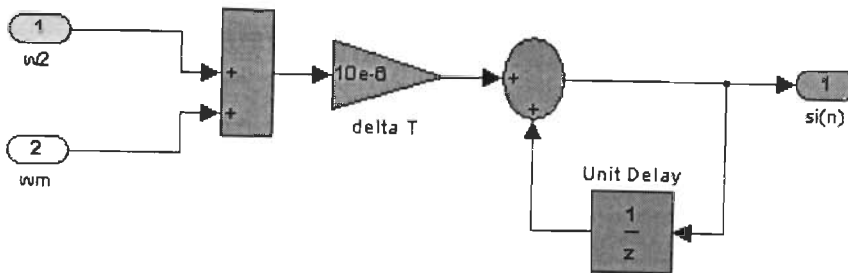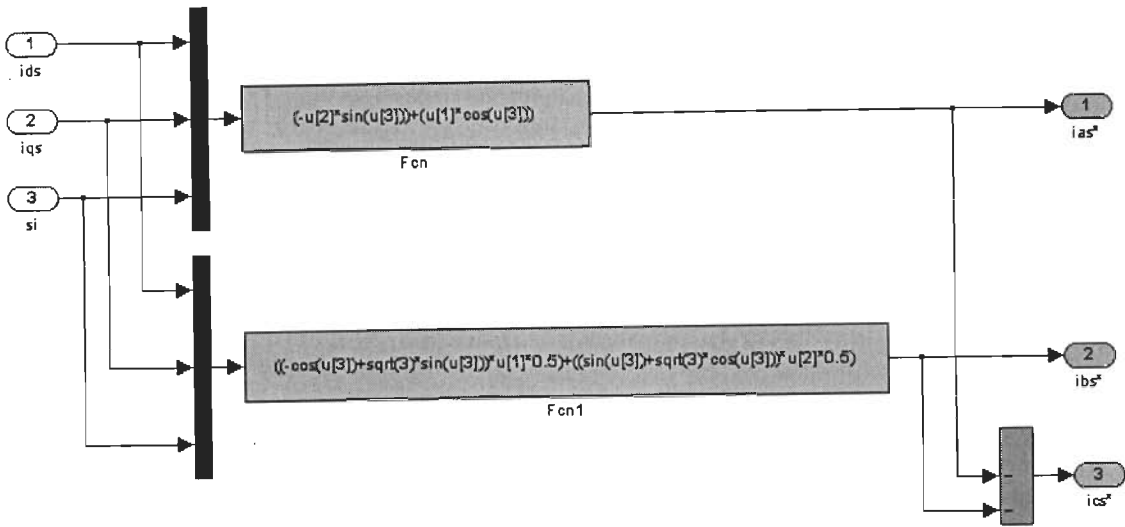

Fig. B.6 MATLAB model for calculating the flux angle

Fig. B.7 MATLAB model for the three phase reference current generation

B.1.6 PWM Current Controller

As there are three phases, there will be three current errors. The current error for a particular phase is defined as the difference between the reference current and the sensed (actual) winding current for that phase only. Hence the current errors in the three phases at the nth instant are modeled as below:

$$i_{aes}^{*}{}_{(n)} = i_{as}^{*}{}_{(n)} - i_{as(n)} \qquad\qquad (B.13)$$

$$i_{bes}^{*}{}_{(n)} = i_{bs}^{*}{}_{(n)} - i_{bs(n)} \qquad\qquad (B.14)$$

$$i_{ces}^{*}{}_{(n)} = i_{cs}^{*}{}_{(n)} - i_{cs(n)} \qquad\qquad (B.15)$$

These current errors in each phase are processed through a proportional controller to generate a modulating signal for each phase. This modulating signal is then compared with a triangular carrier waveform to generate a switching signal. The frequency of the modulating signal is the fundamental frequency of the inverter output voltage and the frequency of the carrier wave is the switching frequency of the inverter. The MATLAB model for calculating the current errors required for the PWM current controller is shown in Fig B.8. The model of pulse generation for PWM inverter is shown in Fig. B.9.
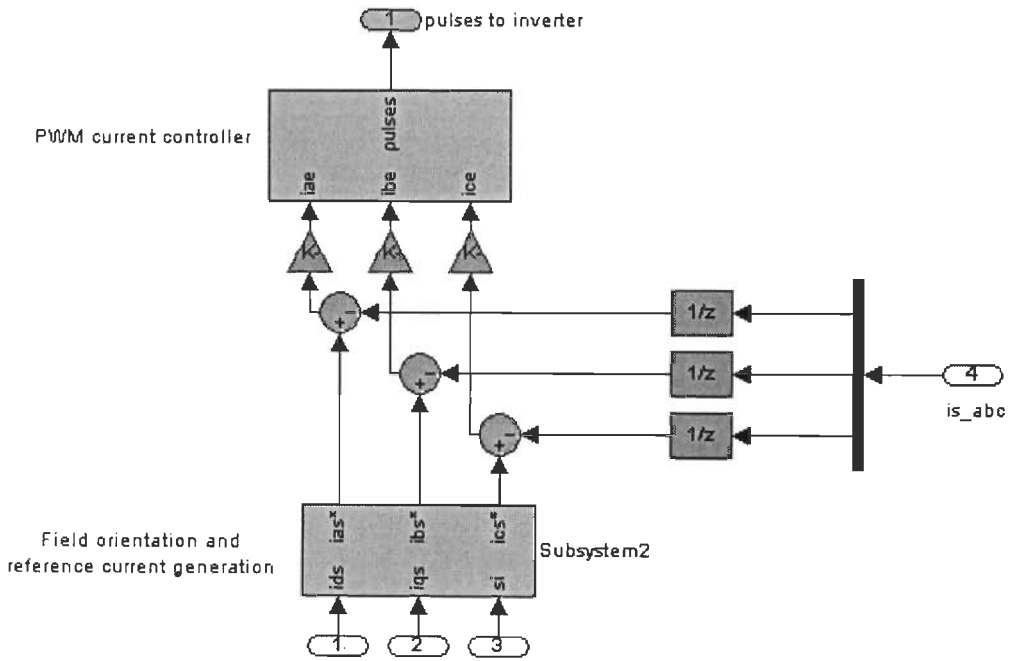
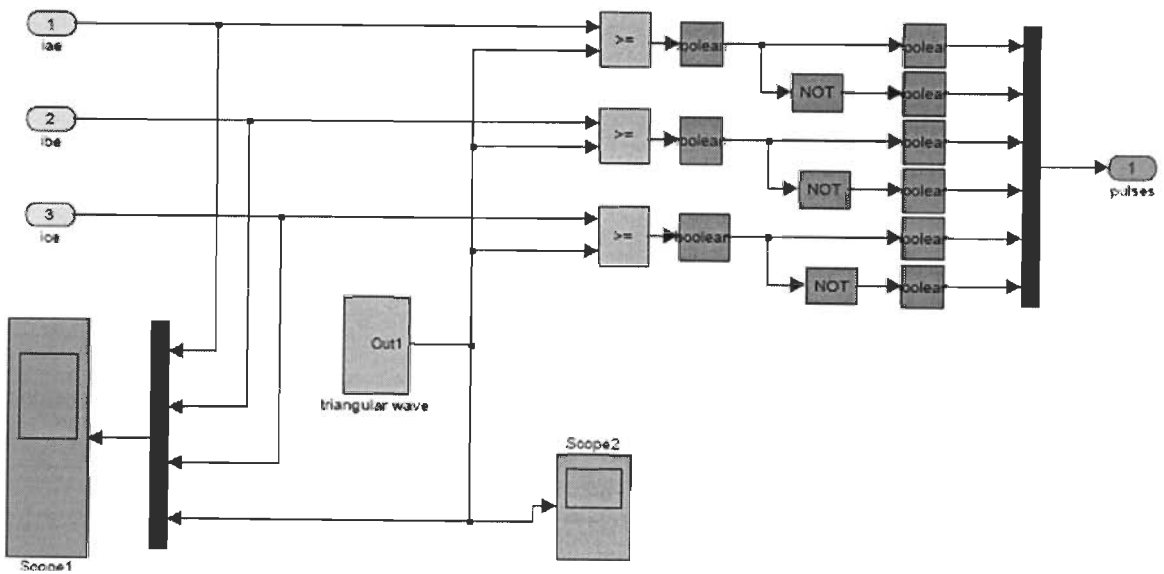Fig. B.8 MATLAB model for the three phase reference current generation

Fig. B.9 Pulse generation for PWM inverter

Appendix-C

Standards for Efficiency Measurement – An Experimental Study

C.1 Introduction

The IEC 34-2 (European), IEEE 112 (USA) and the JEC 37 (Japanese) international standards and the Indian standard IS 325, represent the most important references for the three-phase induction motor efficiency measurements. These standards recommend different measurement procedures, in particular for the stray losses determination and the temperature corrections of the copper losses. This section analyses the relative features of IS 325 over the international standards with the special consideration of stray-load losses. The main differences in the stray-load losses calculation are highlighted and that, of course, is the goal of this section.

C.2 Experimental results

The motor (5 HP) used in experimental study is again used in this study. The motor was first operated in no load condition to establish the baseline for normal performance. The next test to be undertaken was the load tests by varying applied load to the motor up to full load. Motor is indirectly loaded with the help of DC generator and lamp load. Measurements were taken for the entire range of loading i.e. from no-load to full load. At the end of the variable load test, the motor has been reported in thermal steady state conditions using the rated load. Then, the stator resistance at the voltage shutdown has been measured. Reverse rotation test was performed for measuring stray load losses in the motor.

C.2.1 Stray Load Losses

Following the procedures given in the previous sections, the stray load losses have been measured and corrected as stipulated by the standards. The results are shown in Table C.1 and Fig. C.1. This figure shows that the stray losses of IS 325 and IEEE 112 are very close up to 75% of full load. In IEC 34-2, stray loss assumption is significantly smaller than measured value.

Table C.1 Stray Load Losses (in Watts) of 5 HP Motor at Different Standards

Motor Load	Stray load losses			
	IS 325	IEEE 112-E$_1$	IEC 34-2	JEC
¼ load	12	14.57	7.3	0
½ load	23	20.17	10.5	0
¾ load	57	53.26	19.5	0
Full load	110	70.92	23.3	0

C.2.2 Efficiency

The standards IEC and JEC over estimate the motor efficiency as shown in Fig. C.1 because they define instead of measurement of the stray load losses. The IS 325 estimates motor efficiency correctly because it measures stray load losses. The IEEE 112- E$_1$ slightly over estimate the motor efficiency.
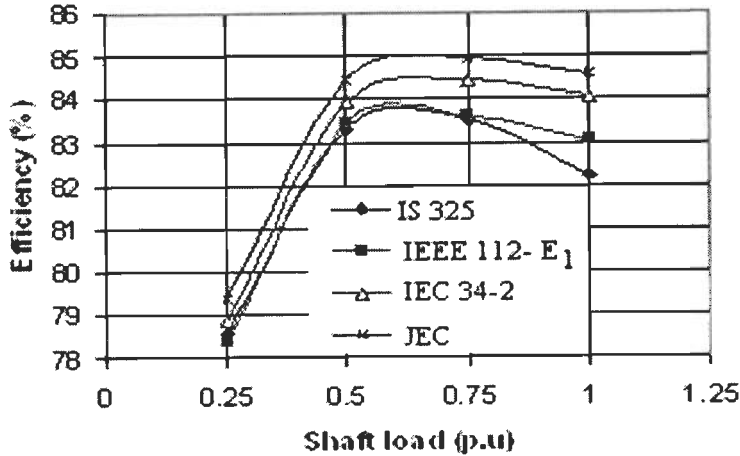

Fig. C 1. Efficiency of 5 HP motor at different standards

The main conclusions from this study are the following:

- As IEEE 112- E, the IS 325 estimates the motor efficiency accurately because it measures the stray load losses.
- The IEEE 112- E$_1$ slightly over estimates the motor efficiency because it assumes stray load losses with respect to motor load.
- The IEC 34-2 and JEC 37 over estimate the motor efficiency because they define instead to measure the stray load losses.